Novel Process Strategies for the Stabilization of Biopharmaceuticals for Parenteral Use

PhD Thesis

Submitted for the degree of PhD

at

South East Technological University (SETU),

Waterford, Ireland

by

Ashutosh Sharma, MEngSc

(20082168)

Pharmaceutical and Molecular Biotechnology Research Centre (PMBRC),

South East Technological University (SETU),

Ireland

&

Manufacturing Science (MSAT),

Sanofi, Waterford,

Ireland

Under the direction and supervision of

Prof. Dr. Helen Hughes, SETU, Waterford

Dr. Dikshitkumar Khamar, Sanofi, Waterford

Ambrose Hayden, SETU, Waterford

2023

Table of Contents

Declaration

This is to certify that the work compiled in this thesis is my own and has not been submitted for another degree, either at SETU Waterford or elsewhere. All external references and sources are clearly acknowledged and identified within the content. I have read and understood the regulations of SETU Waterford concerning plagiarism.

Ashutosh Sharma

Acknowledgements

I thank everyone who has been a part of or somehow contributed to the completion of this thesis. First and foremost, I would like to express my sincere gratitude to my supervisors, Prof. Dr. Helen Hughes and Ambrose Hayden at SETU Waterford and industry mentors, Dr. Dikshitkumar Khamar, Sean Cullen and Timothy McCoy at Sanofi, Waterford, for giving me this opportunity to pursue a PhD at PMBRC, SETU in collaboration with MSAT, Manufacturing Science Department (formerly Technical Development) and for guiding me in the process of completion of my thesis. They have been amazing mentors to me and have given their valuable time ensuring that I had all the needed help and support at all times. I extend my gratitude to the entire Manufacturing Science Team, including all former members, and to the staff at PMBRC, SETU for their support in providing me the right guidance and advice when needed. Moreover, I would like to thank Dr. Abina Crean and Dr. Niall O'Reilly for giving me the opportunity to continue my research for the degree of PhD post transfer examination. All their review and feedback has been truly acknowledged. A huge thank you to Prof. Dr. Damien Thompson and Dr. Pierre Cazade at the Bernal Institute, University of Limerick for collaborating in this project and for all their contributions, specifically in Chapter 3 and 4 of this thesis. Special thanks to Dr. Jason Beirne and Dr. Ciaran Maguire for all their guidance and contributions in the completion of Chapter 5 of this thesis.

To my Mom (Aarti Sharma), Dad (Ajay Sharma) and Brother (Vaibhav Sharma) without whom I wouldn't have been able to reach this far. I cannot thank them enough for all the unconditional love, support and encouragement in all times and throughout.

Thank you!

ॐ नमः शिवाय, ॐ नमो भगवते वासुदेवाय। 🙏

A List of Publications

Peer-Reviewed Papers

1. Sharma, A., Khamar, D., Cullen, S., Hayden, A., Hughes, H. (2021). 'Innovative Drying Technologies for Biopharmaceuticals', International Journal of Pharmaceutics. Elsevier, p. 121115. doi: https://doi.org/10.1016/j.ijpharm.2021.121115.
2. Sharma, A., Beirne, J., Khamar, D. et al. Evaluation and Screening of Biopharmaceuticals using Multi-Angle Dynamic Light Scattering. AAPS PharmSciTech 24, 84 (2023). https://doi.org/10.1208/s12249-023-02529-4.
3. Sharma, A., Cazade, P., Thompson, D., Khamar, C., Hayden, A., Hughes, H. 'Molecular Insight on the Stability of Spray-dried Therapeutic Enzyme' (in-preparation).

Oral Presentations

1. Sharma, A., Beirne, J., Khamar, D., Hayden, A., Hughes, H. (2021) 'Novel Process Strategies for the Stabilization of Biopharmaceuticals for Parenteral Use'. 73rd Irish Chemistry Research Colloquium, University College Dublin, Ireland, June 2022.
2. Sharma, A., Khamar, D., Cullen, S., Hayden, A., Hughes, H. (2021) 'Novel Process Strategies for the Stabilization of Biopharmaceuticals for Parenteral Use'. University Hospital Waterford Research Meeting, Waterford, Ireland, January 2021.
3. Sharma, A., Beirne, J., Khamar, D., Cullen, S., Hayden, A., Hughes, H. (2021) 'Novel Process Strategies for the Stabilization of Biopharmaceuticals for Parenteral Use'. Waterford Institute of Technology Postgraduate Conference, Waterford, Ireland, January 2021.
4. Sharma, A., Khamar, D., Cullen, S., Hayden, A., Hughes, H. (2019) 'Spray-drying of Biologics: A Process Alternative to Lyophilization'. LyoTalk, Dublin, Ireland, June 2019.

Poster Presentations

1. Sharma, A., Beirne, J., Khamar, D., Maguire, C., Hayden, A., Hughes, H. (2022). 'A correlation between Multi-Angle Dynamic Light Scattering (MADLS) and Size Exclusion Chromatography (SEC) for the Characterization of Biopharmaceuticals'. Sanofi Analytical Science Symposium, USA, September 2022.
2. Sharma, A., Khamar, D., Cullen, S., Hayden, A., Hughes, H. (2019) 'Spray-drying of Biologics: A Process Alternative to Lyophilization'. BPCI ITG Research Showcase, Dublin, Ireland, April 2019.

A List of Figures

A List of Tables

A List of Equations

A List of Abbreviations

ADH	Alcohol dehydrogenase
API	Active Pharmaceutical Ingredient
ATR	Attenuated Total Reflectance
AUC	Analytical Ultra Centrifuge
BCA	Bicinchoninic Acid
BET	Brunauer-Emmett-Teller Theory
BfARM	Bundesinstitut für Arzneimittel und Medizinprodukte
BSA	Bovine Serum Albumin
CD	Circular Dichroism
CFD	Computational Fluid Dynamics Modelling
cGMP	Current Good Manufacturing Practices
CHO	Chinese Hamster Ovary
CQA	Critical Quality Attributes
DAD	Diode Array Detector
DCR	Drive Mean Count Rate
DLS	Dynamic Light Scattering
DMA	Dynamic Mechanical Analysis
DNA	Deoxyribonucleic acid
DoE	Design of Experiments
DSC	Differential Scanning Calorimetry
DTA	Differential Thermal Analysis
EMA	European Medicines Agency
EU	European Union
FDA	Food and Drug Administration
FDM	Freeze Drying Microscopy
FMS	Frequency Modulated Spectroscopy
FTIR	Fourier Transform Infrared Spectroscopy
HDX-MS	Hydrogen Deuterium Exchange - Mass Spectrometry
rhGH	Recombinant Growth Hormone
HMWS	High Molecular Weight Species
HPLC	High Performance Liquid Chromatography
HPRA	Health Products Regulatory Authority
HSA	Health Safety Authority
ICH	The International Council for Harmonisation of Technical Requirements for Pharmaceuticals for Human Use
IFT	Interfacial Tension Measurement
IR	Infrared
ISO	International Organization for Standardization
KF	Karl Fischer
LC	Liquid Chromatography
LDH	Lactate dehydrogenase
mAb	Monoclonal Antibody
MALDS	Multi-angle Dynamic Light Scattering

MDS	Molecular Dynamics Simulations
MS	Mass Spectrometry
NIBS	Non-Invasive Back-Scatter
NIR	Near Infrared Spectroscopy
NMR	Nuclear Magnetic Resonance
NRMSD	Normalized Root Mean Square Deviation
OKT3	Orthoclone
PAGE	Poly Acryl Amide Gel Electrophoresis
PAT	Process Analytical Technology
PDB	Protein Data Bank
PDI	Polydispersity Index
PDMS	Polydimethylsiloxane
pI	Isoelectric Point
PSD	Particle Size Distribution
PTM	Post Translational Modification
QC	Quality Control
RABS	Restricted Barrier Access Control
RMC	Residual Moisture Content
RSD	Relative Standard Deviation
SAXS	Small Angle X-Ray Spectroscopy
SDS	Sodium Dodecyl Sulphate
SEC	Size Exclusion Chromatography
SEM	Scanning Electron Microscopy
SFD	Supercritical Fluid Drying
SRCD	Synchrotron Radiation Circular Dichroism
SSA	Specific Surface Area
TPGS	D-α-tocopherol polyethylene glycol 100 succinate
UHPLC	Ultra High Performance Liquid Chromatography
VISF	Vacuum-Induced Surface Freezing
VUV	Vacuum Ultraviolet region
WAXS	Wide Angle X-Ray Spectroscopy
XRD	X-Ray Diffraction
ZS	Zetasizer

Abstract

In the past two decades, biopharmaceuticals have provided a breakthrough in improving the quality of lives of patients with various cancers, autoimmune and genetic disorders etc. With the growing demand of biopharmaceuticals, the need for reducing manufacturing costs is essential without compromising on the safety, quality, and efficacy of products. Freeze-drying is the primary commercial means of manufacturing solid biopharmaceuticals. However, Freeze-drying is an economically unfriendly means of production with long production cycles and heavy capital investment, resulting in high overall costs. This thesis reviews several alternative drying technologies such as continuous Freeze-drying, Spray-drying, Active-freeze-drying, Spray-freeze-drying, PRINT® Technology etc. that have not yet gained popularity for manufacturing parenteral biopharmaceuticals and focuses on assessing the stability of two proteins i.e., Lysozyme by Freeze-drying and Spray-drying, and a commercial therapeutic enzyme by Active-freeze-drying and Spray-drying. The key findings of this thesis showed that lysozyme was a robust protein, and its efficacy was enhanced in the presence of excipients such as sucrose and trehalose post Freeze-drying and Spray-drying. To substantiate experimental results, molecular dynamics simulations were performed that elucidated a conformation change (without unfolding) may have resulted in increased flexibility of the active sites. Furthermore, Enzyme 'A', a commercial therapeutic enzyme, was susceptible to process-induced stress post Active-freeze-drying and Spray-drying, thereby, resulting in increased protein aggregation. However, the inclusion of Arg-HCl in the formulation of Enzyme 'A' significantly improved the reconstitution time by 63 % and turbidity by 83 % and promoted the suppression of insoluble aggregates post Spray-drying. In agreement with experimental results, molecular dynamics simulations showed that while Arg-HCl was capable of acting as the main stabilizer, it interacted the most with the positively and negatively charged residues on the surface of Enzyme 'A' and also acted as a neutral crowder resulting in reduced protein-protein interactions. The last segment of this thesis thoroughly evaluates and discusses the potential of Multi-Angle Dynamic Light Scattering (MADLS)

as a 3-in-1 screening tool for the determination of particle size, product concentration and protein aggregation of three proteins including Bovine Serum Albumin (BSA), a commercial monoclonal antibody (mAb) and a therapeutic enzyme. A good calibration curve with an R^2 of > 0.95 was obtained between the particle number concentration by MADLS and protein concentration by UV-Vis spectroscopy for the 3 proteins whereas an excellent quadratic correlation ($R^2 = 0.9938$) was observed between MADLS and SEC for the quantitative estimation of protein aggregation in the enzyme. Therefore, the approach provided using MADLS can be employed as a rapid screening method for the analysis of aberrations in different formulations and products prior to other Quality Control (QC) tests to speed up the batch release process.

Overall, some of these alternative drying technologies offer a paradigm shift towards continuous manufacturing and allow controlled dry particle characteristics. The potential impact of these novel technologies can significantly reduce time, energy and costs associated with the manufacturing of biopharmaceuticals. The inclusion of Process Analytical Technology (PAT) and offline characterization techniques (described in Chapter 1), in tandem, provide additional information on the on the Critical Process Parameters (CPPs) and Critical Quality Attributes (CQAs) of biopharmaceutical products. Moreover, molecular modelling is a powerful tool that can reveal atomic-scale details to study the mechanisms of interactions of excipients with biologics. These technologies together can be envisaged to increase the manufacturing capacity of biopharmaceuticals at reduced costs as well as open avenues for further research and development.

Chapter 1:

Literature Review

1.1 Introduction to Biopharmaceuticals

Emerging from Pharmaceuticals and the application of Biotechnology, biopharmaceuticals differ from conventional drugs (Crommelin *et al.*, 2003; Li, 2015). The terms "Biopharmaceuticals", "Biotechnology medicines", "Biologics" etc. are used interchangeably by different authors (Crommelin *et al.*, 2003; Walsh, 2010; Li, 2015). Biologics or biopharmaceuticals are biotechnology-derived active drug substances produced using recombinant DNA technology and controlled gene expression techniques from living host cells (Declerck, 2012). Biopharmaceuticals are composed of either peptides, proteins, glycoproteins and nucleic acids or composite combinations of biomolecules. They are produced and isolated from a variety of natural sources including animals, humans, microbes etc. (Declerck, 2012; Li, 2015). Monoclonal and polyclonal antibodies, antibody-drug conjugates, recombinant proteins, nanobodies, enzymes, hormones, vaccines and gene therapy products are a few examples of biopharmaceuticals that are being currently manufactured (Walsh, 2010; Gervasi *et al.*, 2018). The first biologic peptide hormone – Humulin was developed and marketed by Genentech and Eli Lilly in 1982 (Junod, 2007; Conner *et al.*, 2014) and the first commercial therapeutic monoclonal antibody, Orthoclone OKT3, was approved in 1986 (Ecker *et al.*, 2015). In contrast to conventional pharmaceuticals, it is difficult to identify, isolate and characterize therapeutic proteins produced from mammalian cells. The activity of biologics can be negatively affected by temperature, moisture, prolonged storage, denaturants, organic solvents, shear stress, oxygen and changes in pH (Arakawa *et al.*, 2001; Wang *et al.*, 2007; Declerck, 2012; Li, 2015; Milne, 2016; Wang and Roberts, 2018). The Pharmaceutical and Biopharmaceutical industry describe manufacturing, research and development, testing and distribution of medicines based on: 1) Safety; medicines must be safe to use in terms of potential risks such as carcinogenicity, reprotoxicity and genotoxicity, 2) Quality; high quality product must be achieved using cGMP (Current Good Manufacturing Practices) as specified by the International Council for Harmonisation (ICH) Q7 guidelines, 3) Efficacy; drugs must be effective to produce desired output, particularly a therapeutic response in patients (ICH, 2000). The Food and Drug Administration (FDA) in the USA, European Medicines Agency (EMA) and National

Competent Authorities (NCA) in the EU, Health Products Regulatory Authority (HPRA) in Ireland, Bundesinstitut für Arzneimittel und Medizinprodukte (BfARM) in Germany and Health Canada are a few agencies concerned with licensing, registration, development, manufacturing, marketing approval and labelling of pharmaceuticals and biopharmaceuticals. According to ICH, it aims to achieve greater harmonization in all aspects of pharmaceuticals including product registration, interpretation of technical guidelines, testing and research and development of new drugs.

A major class of biopharmaceuticals are recombinant proteins with therapeutic significance. These proteins are derived using biotechnological processes. Major biological sources include microbes, mammalian cells, genetically modified cells, organs, tissues etc. from which mammalian cell lines are used for large scale production of monoclonal antibodies. (Valderrama-Rincon *et al.*, 2012; Durocher and Butler, 2009). A lot of advancements are being developed to improve the production of biologics (Jozala *et al.*, 2016). Glycosylation is one of the most common post-translational modifications (PTM) that takes place in the endoplasmic reticulum and Golgi apparatus (Planinc *et al.*, 2016). This is an important area of research as stability, solubility, clearance, immunogenicity and structure of the protein product are affected by changes in the patterns of glycosylation (Kobata, 2008; Kaneko *et al.*, 2006). Table 1.1 differentiates between pharmaceuticals and biopharmaceuticals.

Table 1.1: Differences between Pharmaceuticals and Biopharmaceuticals (adapted from Declerck, 2012; Li, 2015).

Characteristic	Pharmaceuticals	Biopharmaceuticals
Size	Small, low molecular mass.	Large, high molecular mass.
Structure	Simple and well-defined.	Complex, heterogeneous.
Manufacturability	Easy, reproducible API by chemical reactions.	Complex, not fully reproducible through living systems.
Characterization	Completely characterized.	Difficult to characterize.
Stability	Stable, less sensitive to stress.	Unstable, sensitive to stress.
Immunogenicity	Mostly nonimmunogenic.	Immunogenic.

Proteins are usually highlighted and represent a major class of biopharmaceuticals due to their high versatility, having varied physiological functions in the human body. Proteins typically function as catalysts, receptors, membrane channels, macromolecular carriers, cellular defence agents etc. (Zawaira *et al.*, 2012). Table 1.2 shows a few examples of commercially manufactured biopharmaceuticals.

Table 1.2: Selected commercial Biopharmaceutical Products (FDA, 2022).

Product Name	**Manufacturer**	**Product Type**	**Therapeutic Indication**
Comirnaty® (BNT162b2)	BioNTech / Pfizer	m-RNA Vaccine	Immunization for COVID-19
Prevenar 13® (Pneumococcal 13-valent Conjugate Vaccine)	Pfizer	Conjugate Vaccine	Immunization for *Streptococcus pneumoniae.*
Humira® (Adalimumab)	AbbVie	Monoclonal Antibody	Rheumatoid, Psoriatic Arthritis, Ankylosing Spondylitis, Crohn's disease, Plaque Psoriasis.
Keytruda® (Pembrolizumab)	Merk	Humanized Antibody	Melanoma, various Lung Cancers, Lymphoma, Carcinoma etc.
Stelara® (Ustekinumab)	Janssen	Monoclonal Antibody	Plaque Psoriasis, Active Psoriatic Arthritis, Crohn's disease.
Kadcyla® (Transtuzumab emtansine)	Roche	Antibody-Drug Conjugate	Breast Cancer
Jemperli® (Dostarlimab)	GSK	Monoclonal Antibody	Endometrial Cancer
Vimzim® (Elosulfase alfa)	BioMarin	Enzyme	Mucopolysaccharidosis Type IVA
Zolgensma® (Onasemnogene abeparvovec-xioi)	Novartis	Gene therapy	Spinal muscular atrophy (SMA)

1.2 Manufacturing Process: Upstream, Downstream and Fill Finish Technology

It is anticipated and asserted that biopharmaceuticals will constitute up to 50 % of all drugs in development within the next 5 to 10 years (Jozala *et al.*, 2016). Bioprocessing, a crucial part of biotechnology for biologics, includes a wide range of techniques. Bioprocessing is broken into three major processes known as upstream, downstream and fill finish processing. A typical schematic of a biopharmaceutical production process is shown in Figure 1.1.

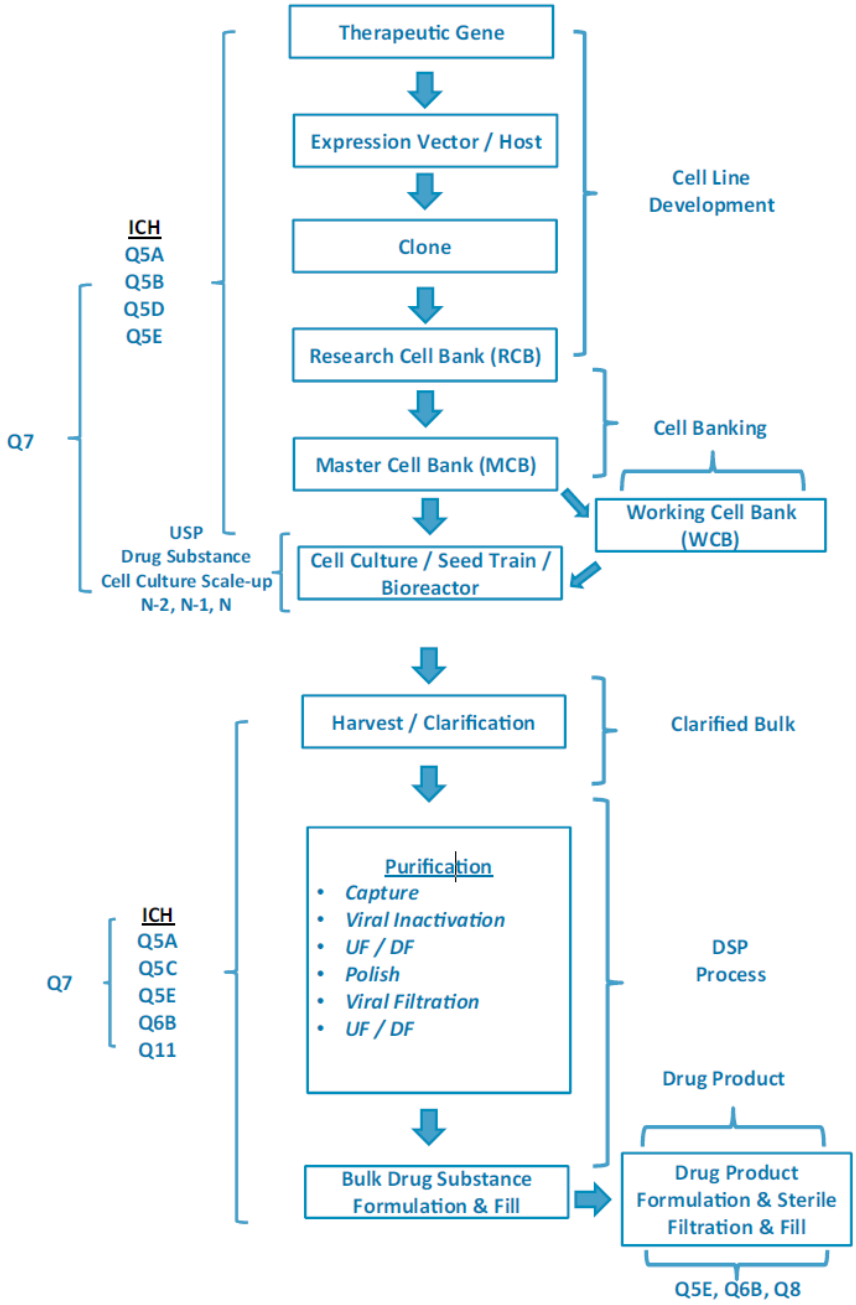

Figure 1.1: Schematic of a Biopharmaceutical Production Process. Adapted from (Conner *et al.*, 2014).

1.3 Biopharmaceutical Drying Technologies

Biopharmaceuticals are relatively unstable molecules and susceptible to stresses by a number of factors. Nevertheless, 66 % of biologics are formulated and marketed as liquid doses, while 34 % of biologics are lyophilized in the European market (Gervasi *et al.*, 2018). The removal of water or solvents offers numerous benefits compared to formulated liquid products. Some benefits include improved shelf-life and stability, ease of handling and storage, reduced transportation costs and energy consumption (Jain *et al.*, 2012; Walters H. *et al.*, 2014; Cicerone *et al.*, 2015; Langford *et al.*, 2017; Sebastião *et al.*, 2019). Several drying technologies reported in literature for pharmaceutical applications include Freeze-drying, Active-freeze-drying, Spin-freeze-drying, Spray-drying, Spray-freeze-drying, Microglassification, Vacuum Foam Drying, Electrospinning, Supercritical Fluid Drying, Microwave-assisted-freeze-drying and other hybrid drying techniques. Some of these drying techniques have been summarized in Table 1.3 and discussed in the following sub-sections.

Table 1.3: Potential drying technologies for biopharmaceutical application.

Drying Technology	Key Features	Molecule / Biomolecule Processed	Batch / Continuous processing	Product Yield	Achievable RMC (w/w)	Dry Product Characteristics	Potential Process-induced Stress	Aseptic Equipment Manufacturer	References
Single Dose Drying Technologies									
Batch Freeze-drying	Gentle drying, improved shelf-life, reduced cold chain requirement.	A wide range of enzymes, antibodies, hormones, vaccines, gene therapy products etc.	Batch.	≥ 98 %	≤ 1 %	• Intact, porous cake. • Cake surface area ~ 300 – 400 mm^2.	• Cold denaturation. • Ice-liquid interfacial denaturation.	SP Scientific, IMA Life, GEA Lyophil, Optima Pharma, MillRock Technology.	(Tang and Michael J. Pikal, 2004; De Beer *et al.*, 2009; Nail *et al.*, 2017; Ganguly *et al.*, 2018; Gervasi *et al.*, 2018; Harguindeguy and Fissore, 2021).
Spin-freeze-drying	Spinning on longitudinal axis, large surface area and heat/mass transfer, no shear stress.	Alcohol dehydrogenase, IVIG.	Continuous.	Not available.	≤ 1 %	• Intact dry layer along the inner surface of vials. • Dry layer surface area ~ 2500 mm^2.	• Cold denaturation. • Ice-liquid interfacial denaturation.	Prototype available by RheaVita.	(Corver, 2012; De Meyer *et al.*, 2015; Lammens *et al.*, 2018; Vanbillemont, Carpenter, *et al.*, 2020).
Continuous Freeze-drying of suspended vials	Controlled nucleation via VISF and homogeneous heat transfer, continuous flow of vials.	Aqueous solutions of sucrose and mannitol.	Continuous.	Not available.	~ 1 %	• Intact, porous cake.	• Cold denaturation. • Ice-liquid interfacial denaturation.	Not available.	(Capozzi *et al.*, 2019)
Foam drying in vials	Rapid evaporation/boiling at low vapour pressure and ambient temperature, no freezing required, lower energy consumption.	Vaccines, rhumAb, bacteria.	Batch.	Not available.	> 1 – 3 %	• Dry foam structure. • Lower specific surface and lower water desorption rate.	• Stress due to surface tension and cavitation.	Not available.	(Abdul-Fattah *et al.*, 2007; Ohtake, R. A. Martin, *et al.*, 2011; Ohtake, R. Martin, *et al.*, 2011).
Microwave vacuum drying	Rapid dehydration, reduction in freeze-drying cycle time by ≥ 80 %, comparable product appearance and enzyme activity.	Haemoglobin, catalase, live virus vaccine.	Semi-continuous.	Not available.	~ 1.8 %	• Dried cake with an average SSA of 1.52 m^2/g comparable to the SSA of freeze-dried (1.61 m^2/g) counterpart.	• Cold denaturation during flash freezing. • Thermal denaturation due to plasma discharge at high electromagnetic field intensity. • Heterogenous heating and arcing may cause burning of product.	EnWave.	(Durance *et al.*, 2020; Bhambhani *et al.*, 2021; EnWave, 2021).
Bulk Drying Technologies									
Active-freeze-drying	Bulk processing of product, free flowing powder, small particle size, improved properties with continuous stirring for certain products.	Ketoconazole.	Batch.	85 – 94 %	< 0.5 %	• Free-flowing powder • Particle size: 1 – 100 µm.	• Stress due to continuous stirring by impeller. • Ice-liquid interfacial denaturation. • Cold denaturation.	Hosokawa Micron B.V.	(Van Der Wel, 2012; Touzet *et al.*, 2018; Hosokawa Micron B.V., 2019).
Spray-drying	Continuous and rapid drying, particle engineering, free-flowing powder, low energy, and equipment cost.	Raplixa®, Exubera®, Lysozyme, BSA, mAbs, siRNA and other biomolecules listed in Table 1.5.	Continuous.	> 50 – 95 %	≳ 1 – 2 %	• Free-flowing powder. • Particle size: 300 nm – 100 µm.	• Shear due to atomization. • Air-liquid interfacial denaturation. • Thermal denaturation due to residence time at high outlet temperatures.	SPX Flow Technologies - Anhydro, GEA Niro, Fluid Air, Ohkawara Kakohi Co. Ltd.	(White *et al.*, 2005; Vehring, 2008; Bowen *et al.*, 2013; Silva *et al.*, 2013; Walters H. *et al.*, 2014; FDA, 2015; Wang *et al.*, 2018; Wu *et al.*, 2019; Ziaee *et al.*, 2020; Vehring *et al.*, 2020; Uddin *et al.*, 2021).

Drying Technology	Key Features	Molecule / Biomolecule Processed	Batch / Continuous processing	Product Yield	Achievable RMC (w/w)	• Dry Product Characteristics	• Potential Process-induced Stress	Aseptic Equipment Manufacturer	References
Spray-freezing and Dynamic Freeze-drying	Uses frequency driven prilling nozzle. Primary, secondary drying occurs in rotary freeze drying chamber.	mAb.	Continuous.	> 97 %	< 1 %	• Free-flowing powder. • Particle size: < 300 µm – 1000 µm.	• Shear due to frequency nozzle and atomization. • Cold denaturation.	Meridion Technologies.	(Struschka *et al.*, 2016; Lowe *et al.*, 2018; Luy *et al.*, 2018).
Lynfinity® Technology	Uses piezoelectric spray nozzle to produce dried spheres. Primary, secondary drying occurs on cascading vibratory shelves.	Not available.	Continuous.	Not available.	≤ 1 %	• Free-flowing powder. • Particle size: ~ 600 µm.	• Shear due to piezoelectric nozzle and atomization. • Cold denaturation.	IMA Life.	(DeMarco and Renzi, 2015; IMA Life, 2019b).
PRINT®	Tunable shape, size, and morphology of nano and microparticles, enhanced surface properties and API bioavailability, large-scale production is possible.	Lysozyme, BSA, DNase, IgG, siRNA, ribavirin, vaccines.	Continuous.	Not available.	Not available.	• Free-flowing powder. • Particle size: 2 – 200 µm. • Customizable particle shape and morphology.	• Cold denaturation. • Roller pressure may induce shear stress.	Liquidia Corporation.	(Kelly and DeSimone, 2008; Garcia *et al.*, 2012; Galloway *et al.*, 2013; Xu *et al.*, 2013; DeSimone, 2016; Wilson *et al.*, 2018).
Microglassification™	Controlled particle size, morphology, release and dissolution, no excipients used.	BSA, lysozyme, α-chymotrypsin, catalase, horseradish peroxidase, ELP.	Batch.	Not available.	Assumed comparable to Freeze-drying by the authors.	• Particle beads. • Particle size: 1 - > 10 µm.	Not available.	Not available.	(Aniket *et al.*, 2014; Aniket, Gaul, *et al.*, 2015; Aniket, Tang, *et al.*, 2015).
Electrospinning	Gentle, rapid drying (~ 0.1 s) and reconstitution due to high surface area. Ultra-fine particles by electrical atomization. Requires viscous solutions. Comparable product stability.	Infliximab, zein, siRNA, inulin, β-galactosidase, lysozyme.	Continuous.	~ 80 %	~ 6.5 %	• Dry particles size: < 10 µm.	• Shear due to electrical atomization.	Bioinicia.	(Jain *et al.*, 2014; Karthikeyan *et al.*, 2015; Wagner *et al.*, 2015; I. Abraham *et al.*, 2019; Domján *et al.*, 2020).
Supercritical Fluid drying	Rapid drying, drying can occur via Spray-drying in the presence of supercritical fluid (e.g., CO_2) at low temperatures (> 32° C) and pressure (~ 103 Bar) or via supercritical antisolvent precipitation. Particle engineering possible, no freezing required.	Albumin, alkaline phosphatase, catalase, chymotrypsin, insulin, lactase, rhDNase, trypsin, urease, lysozyme, myoglobin, IgG, LDH.	Continuous.	Not available.	≳ 1 %	• Free-flowing powder. • Micron-sized particles (≥ 200 nm – 50 µm).	• Shear due to atomization. • Fluid-fluid interfacial denaturation. • High pressure denaturation.	Extratex, Natex, Separex.	(Sellers *et al.*, 2001; Jovanović *et al.*, 2004; Bouchard *et al.*, 2007; Jovanović, Bouchard, Hofland, *et al.*, 2008; Jovanović, Bouchard, Sutter, *et al.*, 2008; Long *et al.*, 2019).

API, Active Pharmaceutical Ingredient; BSA, Bovine Serum Albumin; DNase, Deoxyribonuclease; ELP, Elastin-like Polypeptide; IgG, Immunoglobulin G; LDH, Lactate dehydrogenase; mAb, monoclonal antibody; rhDNase, recombinant human Deoxyribonuclease; siRNA small interfering Ribonucleic Acid; SSA, Specific Surface Area

1.3.1 Single Dose Drying Technologies

1.3.1.1 Conventional Batch-freeze-drying

The earliest mention of the possibility of drying a frozen product under moderate vacuum was reported and demonstrated by Bordas and Jacques-Arsene d'Arsonval in Paris in 1906 (Rey and May, 2004). It was asserted that products such as sera and vaccines would remain stable and could be preserved for a long time (Rey and May, 2004). This led to the introduction of the term 'Freeze-drying'. Earl W. Flosdorf *et al.* 1935, published their work on lyophilisation. The term is derived from Greek literature, 'lyophile'; which describes the ability of the product to rehydrate again (E. W. Flosdorf *et al.*, 1935). Significant work on the mass production of lyophilised human plasma was carried out by Earl Flosdorf, Ronald Greaves and Francois Henaff (Flosdorf and Mudd, 1935, 1938; Rey, 1935; Ke *et al.*, 1942; Greaves, 1946; Jenke, 2014). Furthermore, Ernst Boris carried out notable work on the preparation of antibiotics and sensitive biochemicals through freeze-drying (Rey and May, 2004). Moreover, this technique has been an effective way of recovering water-damaged books and documents by removing water from them (Waters, 1993). In the 21st century, freeze-drying is being used extensively in the pharmaceutical and biopharmaceutical industry and holds great significance for further exploring its suitability along with other drying techniques.

Several advantages of freeze-drying have been identified in the past making it one of the most extensively used techniques for the manufacturing of biologics. Lyophilization allows improved shelf-life of heat-sensitive and labile protein therapeutics along with easy handling and transport (Carpenter and Chang, 1996; Tang and Michael J. Pikal, 2004). Chemical decomposition is reduced at very low temperatures, keeping the product stable (Harrison, 1994). Also, the high specific surface area of the freeze-dried cake provides fast and complete reconstitution of the product (Harrison, 1994). Moreover, this technique can be used to concentrate products with low molecular weight and those that are too small in size to be filtered (Shalaev *et al.*, 2008). To date, lyophilization has been the gold standard for stabilising a wide range of biomolecules including antibodies, hormones, enzymes, fusion proteins etc. (Gervasi *et al.*, 2018).

However, several drawbacks associated with lyophilization have been reported. Firstly, processing times could vary from days in optimized cycles to weeks in the case of poorly developed cycles (Nail and Gatin, 1993; Tang and Michael J. Pikal, 2004). Secondly, along with high operational and maintenance cost (Walters H. *et al.*, 2014), exergy analyses have shown major energy losses during primary drying leading to reduced efficiency in the overall process (Liapis and Bruttini, 2008; Liu *et al.*, 2008). Thirdly, concerns related to heat and mass transfer and scaling up the process have been discussed which depend on the dryer design, container closure and load condition etc. (Patel and Pikal, 2011; Ohori *et al.*, 2021). Moreover, many biologics are sensitive to freeze-drying related stresses such cold denaturation and denaturation at the air-liquid interface (Chang *et al.*, 1996; Jonas, 1997; Kunugi and Tanaka, 2002). Also, issues of vial to vial and within vial heterogeneity caused due to phase separations studied by Raman and FTIR spectroscopy during the process of freeze-drying have been discussed (Salnikova *et al.*, 2015).

Vial-based batch freeze-drying is limited to processing small volumes of product which increases the requirement for a large number of vials. The intervention of manual labour during the process can increase the risk of contamination despite GMP cleanroom practices (Varshney and Singh, 2015). Moreover, being a static process, it increases the risk of failure of the entire batch during process failure. Heterogeneous heat transfer allows vials situated on the edge of the shelves to dry faster than vials present in the centre due to better heat transfer from the walls of the chamber (Lammens *et al.*, 2018). In addition, certain high concentration lyophilised protein cakes can take very long to reconstitute compared to free-flowing powders produced by alternate drying techniques (Dani *et al.*, 2007; Cao *et al.*, 2013). Free-flowing powders are also beneficial in terms of their distribution and filling into different types of containers (Varshney and Singh, 2015). To combat various challenges associated with batch type freeze-drying, a few modifications to the conventional lyophilization process and approaches towards continuous manufacturing have been discussed in sections 1.3.1.2, 1.3.1.3 and 1.3.1.4.

1.3.1.1.1 Principle and Process of Freeze-drying

Freeze-drying or lyophilization typically involves removal of the solvent from the solution. It is based on the principle that frozen water from the product is sublimed to obtain a dried solid product (Smith *et al.*, 2017). Antibiotics, bacteria, vaccines, sera, cells, tissues, proteins, and biotechnological products are a few examples of freeze-dried products. Freeze-drying consists of three major steps: 1) Freezing of the product which involves solidification of the product at very low temperatures. The product is solidified until it reaches its crystalline and/or amorphous state (Harrison, 1994), 2) Primary drying involves vaporisation of water directly from its solid to gaseous state at low temperature and pressure (Nireesha *et al.*, 2013). This is known as sublimation of water. 3) Secondary drying which involves desorption of bound water to obtain the appropriate residual moisture level. This is carried out at elevated temperatures and low pressure (Harrison, 1994). The final step involves conditioning and storage of the dried product at optimum conditions. The steps involved in the process of vial-based pharmaceutical freeze-drying technology are further elaborated as follows: -

a. Pre-treatment of the product is a sample preparation method required prior to its freezing. Concentrating or diluting the product, addition of substances that confer stability and improve its processing and increasing the surface area are some methods used during pre-treatment. It is carried out to preserve product appearance, stabilize reactive products and to decrease high vapour pressure solvents (Wang, 2000; Nireesha *et al.*, 2013). The formulated drug substance is filled in glass vials with the required fill volume. All the vials in a batch are partially stoppered and equilibrated to the shelf temperature of 5 °C prior to freezing (Figure 1.2).
b. Freezing of the product is carried out at very low temperatures between – 40 °C and – 80 °C (Rey and May, 2004). This is done to solidify the product completely as most components freeze below their eutectic/melt point (T_m) or the frozen-state glass transition temperature (T_g'). The product is ramped down to – 40 °C to ensure complete solidification of amorphous and crystalline components (Figure 1.2). The product must be adequately frozen since it requires a change in the state of matter directly from solid to vapour phase to successfully carry the process of drying.

Small ice crystals are produced as a result of rapid cooling which leads to faster sublimation but slower secondary drying, whereas large ice crystals are formed when the temperature is dropped slowly allowing less restriction in the secondary drying process (Roy and Gupta, 2004).

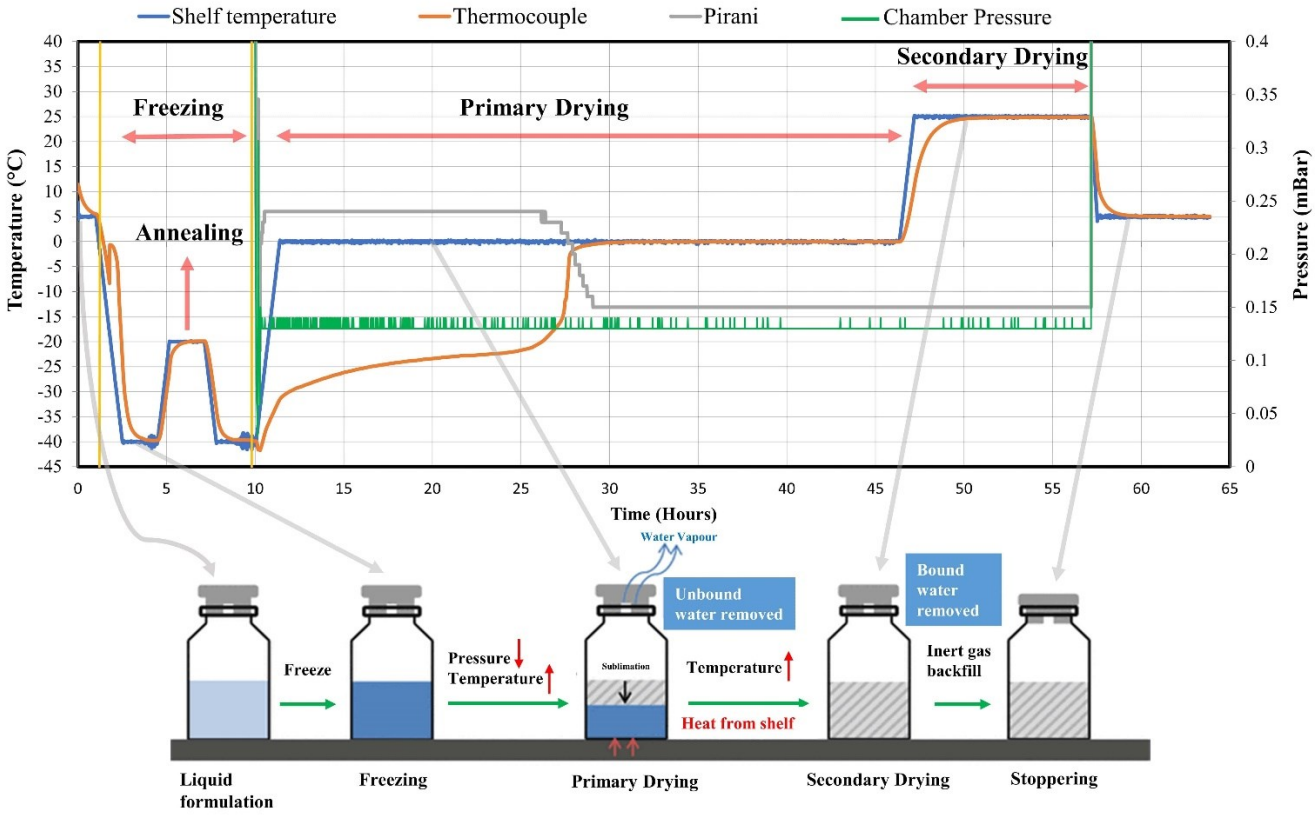

Figure 1.2: Schematic evolution of a Freeze-drying cycle. Adapted from (LyophilizationWorld, 2020).

The two ways in which freezing may occur are: Firstly, product in which water is the solvent is subjected to temperatures below their eutectic point. In this case, the solute concentration changes and water is separated in the form of ice as the temperature is lowered. It is important to completely freeze the product by lowering the temperature below their eutectic point, which may otherwise lead to the formation of small gaps of unfrozen material in the lattice that could interfere with the structural stability of the product and the drying process. Annealing is an optional additional step performed to completely crystallize crystalline or amorphous

components and to study the impact of crystallization in the formulation (Hawe and Frieß, 2006; Dixon *et al.*, 2009; Al-Hussein and Gieseler, 2012). During the annealing step, the shelf temperature is ramped up to – 20 °C and held for 2 h (Figure 1.2). The product temperature at this point is kept below its eutectic melt. Post 2 h, the shelf temperature is ramped down to – 40 °C. Secondly, a solution could undergo glass formation during freezing. In this case, the viscosity of the entire product solution increases as high as $10^{12\text{-}14}$ Pa·s with decreasing temperature (Sun and Davidson, 1998). The product freezes at the glass transition point to form a solid (Nireesha *et al.*, 2013; Khairnar *et al.*, 2013). Thermo analytical techniques such as DSC (Differential Scanning Calorimetry) (Hatley, 1992) can be used to determine the freezing point and the solid-state glass transition temperature (T_g).

c. Primary drying is based on the principle of sublimation wherein the solid state is directly transformed into gas without forming any liquid. The sublimation of water occurs at temperatures and pressures below its triple point (Figure 1.3) i.e. 0.0099°C (~ 273.16 K) and 6.117 mBar (4.579 mm Hg or 611.7 Pa), respectively (Nireesha *et al.*, 2013). Partially stoppered vials allow the migration of water vapor from the vials to the condenser. The primary drying phase constitutes the largest fraction of a freeze-drying cycle (Figure 1.2). During this step, an adequate balance has to be established between heat input (heat transfer) and sublimation of water (mass transfer) to ensure successful drying of the product (Rey and May, 2004). The temperature is certainly increased to speed up the process of sublimation keeping the pressure low. The rate of sublimation increases with a decrease in chamber pressure. Very low pressures less than 0.0066 mBar (50 mTorr) hamper the sublimation process and limit the rate of heat transfer to the product (Khairnar *et al.*, 2013). It is important that the pressure in the chamber must be lower than the vapour pressure of the product to allow the molecules to migrate from high to low pressure to facilitate the process of sublimation. Increased temperature at lower pressure is ideal for sublimation, however, the product temperature must remain below its T_g' or melting point (T_m) as shown in Figure 1.2 (Rey and May, 2004; Tang and Michael J Pikal, 2004). An increase in the

temperature above T_g' or T_m may result in decreased product stability as a consequence of increased flexibility and mobility in the molecular structure. It has been reported that a rise in temperature of 1°C makes the drying process 13% faster (Craig *et al.*, 1999).

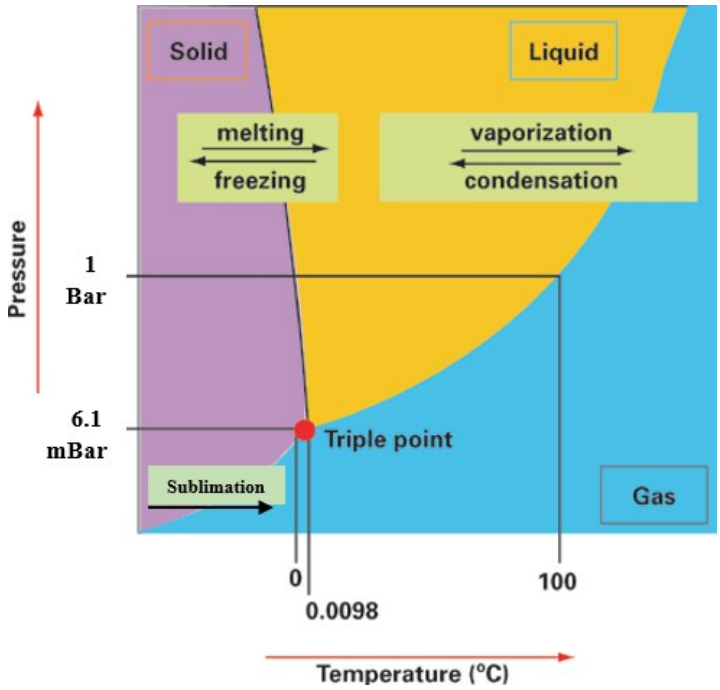

Figure 1.3: Phase diagram of water. Adapted from (Barley, 2020).

d. Secondary drying is also known as the desorption phase. This phase is carried out to reach the optimum residual moisture level. Moisture content of less than 1% can be achieved during secondary drying (Khairnar *et al.*, 2013). At this stage, the water molecules bound to the protein molecules and the trapped water molecules in the glass phase are removed at much higher temperatures (Roy and Gupta, 2004). As shown in Figure 1.2, the temperature is increased to the maximum allowed temperature for the dried product which is typically between 20 °C to 40 °C (Khairnar *et al.*, 2013) and the process requires one third to one half of the time required for primary drying (Nireesha *et al.*, 2013). This temperature is maintained below the T_g of the product. This also implies that the shelf temperature is increased many fold, keeping the chamber pressure at its minimum. Desorption is independent of the sample thickness, but is a function of the porosity of the sample product (Craig *et al.*, 1999).

e. Final storage and reconstitution is also a critical step which must be carried out with great care and diligence to ensure maintained product stability and efficacy that has been achieved in the preceding steps (Rey and May, 2004). Stoppering of vials under adequate vacuum conditions is considered to be safe. Moreover, for products in bulk or in ampules, the extraction of the product from the equipment is carried out in a tight gas chamber by remote operation. The moisture level, water, light and other contaminants level must be controlled (Rey and May, 2004). Typically, freeze-dried biologics are stored between – 20 °C to 4 °C. Water, salt solutions or solvents are ways to restore the initial concentration of the product. This is also used to either dilute or concentrate the product.

1.3.1.1.2 Types of Freeze-dryers and Equipment

The three broad categories of freeze-dryers reported in the literature include Manifold freeze-dyers, Rotary freeze-dryers and the Tray style freeze-dryers (Nireesha *et al.*, 2013). The difference between the three types of freeze-dryers lies in the method by which the dried substance is interfaced with a condenser. A short circular tube is used to connect multiple containers with the dried product to a condenser in a manifold dryer (Wang, 2000). Ambient conditions are required to provide heat for the product to sublime. Manifold dryers are typically used to dry liquid products in small containers in a laboratory setting. Rotary dryers are used for drying pellets and pourable substances. Uniform drying is achieved through a cylindrical reservoir that is rotated in a rotary dryer during the process of drying (Korey and Schwartz, 1989). Tray style dryers consist of shelves on which vials are placed on trays. They are larger than manifold dryers and are used for products for long-term storage. These dryers are capable of performing both primary as well as secondary drying (Nireesha *et al.*, 2013).

The lyophilisation chamber must allow thermal conductivity and should be capable of being tightly sealed at the end of the cycle. The chamber must also minimize the amount of moisture that could permeate its walls. The essential components of a freeze-dryer consist of a refrigeration system,

chamber, process condenser, vacuum system, and a control system. These are briefly discussed as follows:

a. Refrigeration System: The initial freezing process is carried out here. It cools the ice condenser present inside the freeze-dryer (SP Scientific, 2018). The compressor is also employed to cool the shelves in the product chamber. Significant energy is required for the freezing step which is aided by liquid nitrogen (Nireesha *et al.*, 2013).
b. Chamber: Also known as the lyophilisation chamber, it is a vacuum tight box containing stainless steel shelves that are insulated on the outside. Shelves are used to hold product present in vials, flasks etc. Shelves act as heat exchangers which facilitate the removal of energy during freezing and provide energy during the process of drying.
c. Vacuum System: It is employed to remove the vaporised solvent during the drying process. Operational pressures below the eutectic point are reached during freeze-drying (Jordi Palau, 2018). The vacuum pressure is typically between 50 – 100 µbar (Nireesha *et al.*, 2013) and multiple pumps are connected for large chambers.
d. Process Condenser: A condenser is known as the cold trap which accumulates the vapours being sublimed which are then condensed into ice. The condensed solid ice is then removed at the end of the drying process.
e. Control System: It provides an automated system to control the freeze-dryer. Time, shelf temperature and pressure are the parameters programmed during the cycle.

1.3.1.1.3 Effects of Freeze-drying on Protein Stability

Proteins, being the most abundant biological macromolecules in the living system and cells, are highly complex structures which accounts for their diverse biological functions (Nelson & Cox, 2012). Amino acids are the building blocks of proteins, typically consisting of a carboxyl group, an amino group, a hydrogen atom, and R-groups. Each amino acid joins to another amino acid covalently

forming a peptide, consequently, many peptides join to form a polypeptide chain. A native protein present in its folded conformation having the lowest Gibbs free energy, is thermodynamically stable (Nelson and Cox, 2012). The stability of proteins, typically biopharmaceuticals, is expressed in terms of their storage, transportation and operationability (Roy and Gupta, 2004). Biologics, being highly sensitive to external stress in terms of temperature, sheer, pH, and denaturing agents, are deemed suitable if they are pharmaceutically and thermodynamically stable.

Pharmaceutical stability of biologics is of utmost concern as it refers to the ability of the protein to be processed, stored and distributed without any irreversible change in its primary structure, conformation or its state of aggregation. This instability is also known as degradation of the protein (Pikal, 2004). Protein inactivation can be either reversible or irreversible (Mozhaev, 1993). An unfolded protein can go back into its native state if the denaturing agent is removed during a reversible change, whereas irreversible changes due to prolonged heat treatment can denature the protein permanently (Roy and Gupta, 2004). Pharmaceutical instability may occur on a short time scale or on a long-time scale during processing or storage, respectively. On the other hand, thermodynamic stability refers to a shift in the position of equilibrium between the native and the unfolded conformations. A stable protein would require high temperatures or high concentrations of chemical denaturant to shift the equilibrium towards the unfolded state. Proteins may show thermodynamic instability during the process of freeze-drying, but may be pharmaceutically stable upon its reconstitution (Pikal, 2004). Unfolded and partially folded protein conformations may lead to degradation through irreversible aggregation (Brems *et al.*, 1985). Aggregation occurs when hydrophobic residues of an unfolded protein are exposed, leading to intermolecular hydrophobic interactions.

The process of drying is employed to remove free and bound water to minimize the moisture content available to the protein present. The removal of water is important as it is a destabilizing agent for the long-term preservation of the desired protein product. The presence of water allows hydrophobic interactions with the native protein conformation, thereby, destabilizing it. In the absence of water,

the amino acid side chains interact with each other, thereby, locking up the conformation, preventing it from further interactions. This rigid conformation is devoid of its catalytic activity leading to a stable conformation in its dry state (Ahern *et al.*, 1987; Poole and Finney, 1983). It has also been stated (Pikal, 2004) that the process of freeze-drying leads to the phenomenon of freeze concentration which refers to an increase in the protein and any potential reactant's concentrations, leading to an increase in the rate of biomolecular degradation reactions. Thus, in spite of the decrease in the temperature, the reaction rate would increase. Moreover, deviations and perturbations in the protein conformation may be as a result of protein adsorption to surfaces. This is because liberation of dissolved air during thawing may generate numerous bubbles that provide a significant area for protein adsorption (Pikal, 2004).

1.3.1.2 Spin-freeze-drying of Unit Doses

The method of Spin-freezing was first patented by Becker in 1957, patent no. DE967120 (Becker, 1957). This method was then employed for Freeze-drying and patented by Broadwin in 1965, patent no. US3203108A and Oughton et al. in 1999, patent no. US5964043 (Broadwin, 1965; Oughton *et al.*, 1999). With modifications to the patents and to the conventional freeze-drying process, authors invented a novel continuous freeze-drying process for unit doses (Corver, 2012; De Meyer *et al.*, 2015). A major characteristic of this continuous freeze-drying technology is the rotation of vials containing the liquid product of interest along their longitudinal axis, therefore, this is known as Spin-freeze-drying (Figure 1.4).

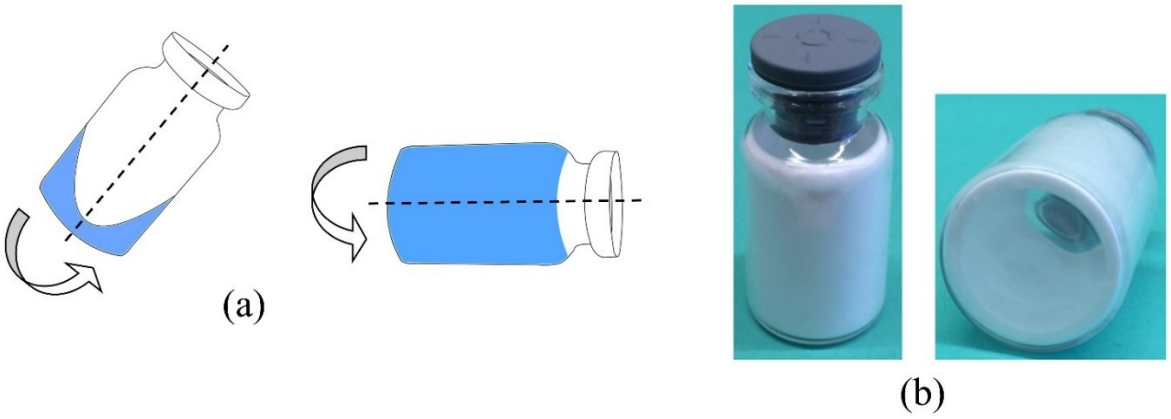

Figure 1.4: Spin-freezing of a vial along its longitudinal axis and (b) Spin-freeze-dried vials. Reprinted from (De Meyer *et al.*, 2015).

The process begins with the continuous Spin-freezing step wherein vials containing the liquid product of interest are spun rapidly, typically at 2500 – 3000 rpm, along their longitudinal axis for a period of time. The axial rotating motion results in the formation of a dispersion layer on the inner walls of the vial with a relatively uniform thickness of 1 mm (Corver, 2012). Subsequently, the rotating vials are exposed to a flow of sterile cryogenic gas, such as nitrogen or carbon dioxide, which is temperature controlled. This further results in a large surface area, as the frozen product is spread all over the inner walls of the vial, thereby, allowing fast and homogenous freezing/heating of the dispersion layer (De Meyer *et al.*, 2015). The process of solidification takes about 1 – 2 min and the product is typically subjected to a temperature between – 40 °C and – 60 °C for another 10 – 20 min (Corver, 2012). To achieve crystallization and the desired morphology of the excipients, further modifications are made to the cooling process conditions in a temperature-controlled chamber. Following the cooling step, the vials are transferred to the primary drying chamber through a conveyor belt system. Each vial is held in a heat conducting jacket or a pocket in the chamber with the desired pressure and temperature conditions. The jacket surrounds the outer surface of the vials to facilitate homogenous distribution of heat through conduction or radiation. Subsequently, the vials are transferred to the secondary drying chamber for desorption of residual water content. Figure 1.5 depicts a schematic for the continuous drying system. The drying step lasts for about 30 min to 2 h

(Corver, 2012). It was reported that the total processing time is reduced by 10 – 40 times depending on the vial dimensions and the product formulation (De Meyer *et al.*, 2015). Moreover, by adding multiple parallel lines, the continuous freeze-drying process can be easily scaled up, unlike the conventional method of lyophilization.

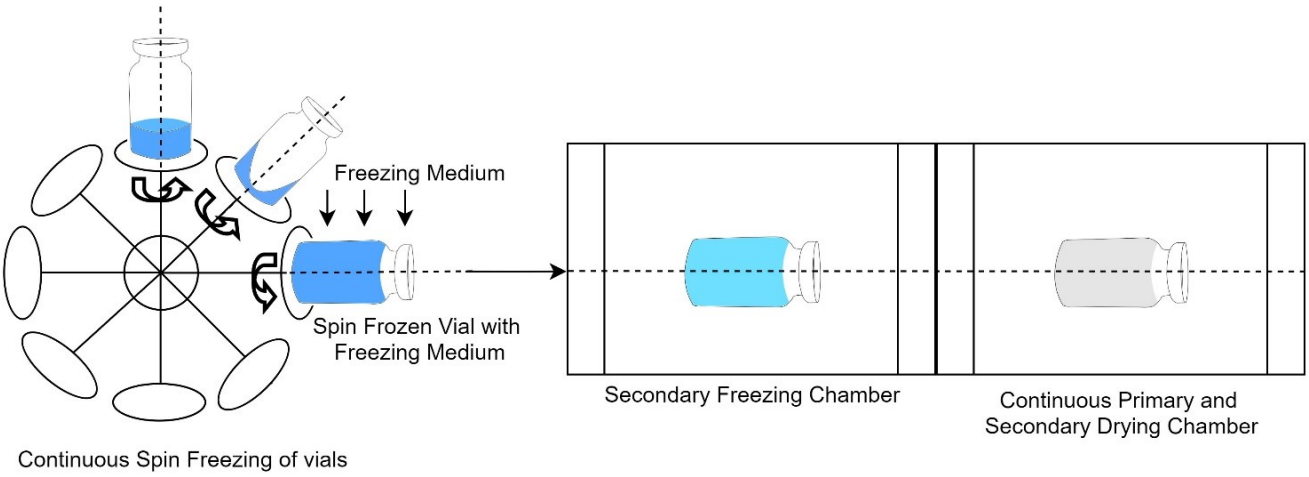

Figure 1.5: A schematic of the continuous Spin-freezing-drying system. Adapted from (De Meyer *et al.*, 2015).

De Meyer *et al.* through their study, compared and evaluated spin-freeze-drying and conventional freeze-drying in terms of their sublimation rates and the total drying time (De Meyer *et al.*, 2015). Using Equation 1.1, the calculated optimum rotation speed was 2500 rpm resulting in a uniform layer of the liquid product. They elucidated the effect of five different formulations with different dry product resistance, fill volume, freezing method, freezing rate, shelf temperature and chamber pressure on the amount of sublimed water after two hours of drying using a full factorial design of experiments. Data analysis showed that the freezing method significantly contributed to the amount of sublimed water after a period of 2 h on the spin frozen vials compared to batch freezing. This was due to the fact that the presence of a thinner product layer and large surface area in the inner walls of the vials contributed to much higher sublimation rates. The sublimation rates were calculated using Equation 1.2.

$$\omega = \sqrt{\frac{\Delta h * 2g}{r_1^2 * r_2^2}} \qquad \textbf{Equation 1.1}$$

Where ω is the angular velocity in rad/sec, Δh is the height of the spin frozen product layer, g is the gravitation constant and r_1 and r_2 are the layer thickness at the bottom and the top of the vial

$$\frac{dm}{dt} = \left[\frac{A}{R_p}\right](P_P - P_c) \qquad \textbf{Equation 1.2}$$

where dm/dt is the sublimation rate in g/h, A is the surface area of the frozen product layer in cm^2, R_p is the area-normalized dried product resistance in cm^2 m Torr h g^{-1}, P_p is the vapour pressure of ice in m Torr and P_c is the chamber pressure in m Torr.

Amongst the other factors studied, increasing the shelf temperature and the chamber pressure increased the sublimation rates. However, the freezing rate and the fill volume did not have a significant impact on the sublimation rates during spin freeze-drying and batch freeze-drying (De Meyer *et al.*, 2015). Furthermore, through another full factorial design, they studied the effect of the five formulations and pressure upon the total drying time. The chamber pressure was observed to have an unexpectedly greater effect on the spin frozen vials due to inadequate contact between the vial and the holder, whereas the effect of chamber pressure on the batch frozen vials was relatively smaller than the shelf temperature itself. This was again due to the fact that the product surface area on the inner walls of the vial was much greater for spin frozen vials (2533 mm^2) than the traditionally frozen vials (373 mm^2) (De Meyer *et al.*, 2015). Shelf temperature was reported to be the most influential factor on the rate of sublimation of the spin and the batch frozen vials. Higher values of sublimed water obtained for spin frozen vials were due to a much higher rate of sublimation. Innovatively, an NIR probe coupled to a Nicolet Antasris II FT-NIR analyser was connected to the vial holder to demonstrate the primary and secondary drying endpoint in the spin frozen vials. The NIR probe had a spot size of 28 mm^2 and the collected spectra was in the range 10000 cm^{-1} to 4500 cm^{-1}. Results showed a decrease in the intensity of ice peaks around 5000 cm^{-1} and 6700 cm^{-1} after

58 min, before which no change in the spectra were observed. This was because of the poor penetration depth of the NIR beam into the inner side of the frozen layer. The disappearance in the ice crystal bands and increase in the spectra signal of the formulation marked the end of the primary drying phase. Similarly, the disappearance of the free water band at 5160 cm^{-1} with no further spectral changes after 152 min marked the end of the secondary drying phase.

Through another study, the effect of shear stress, sedimentation and diffusion velocity was studied by Lammens *et al.* on the activity and aggregation of alcohol dehydrogenase (ADH) during Spin freeze-drying (Lammens *et al.*, 2018). Using Equation 1.3 (modified Equation 1.1), they elucidated that a smaller relative deviation in the frozen product layer between the top and bottom of the vial was obtained with a higher rotation velocity. Secondly, a lower rotation velocity was required for high fill volume and vice-versa. The shear stress and the shear rate were calculated using Equation 1.4 and Equation 1.5.

$$\omega = \sqrt{\frac{h * g}{2\pi * \Delta L * r_{p,i}}} \qquad \textbf{Equation 1.3}$$

Where ω is the rotation velocity and ΔL is the difference in the layer thickness between the top and the bottom (similar to Equation 1.1).

$$\tau = \nu \frac{\omega}{L} \qquad \textbf{Equation 1.4}$$

Where τ is shear stress in Pa, ν is viscosity of the solution in Kg m^{-1} s^{-1} and L is fluid layer thickness in m.

$$\gamma = \frac{\tau}{\nu} \qquad \textbf{Equation 1.5}$$

Where γ is shear rate in s^{-1}, τ is shear stress in Pa and ν is viscosity of the solution in Kg m^{-1} s^{-1}.

The calculated shear rates at 2900 rpm, 800 rpm and 400 rpm for 2 – 4 min were 2145 s^{-1}, 591 s^{-1} and 295 s^{-1} respectively. These values were comparatively lower than the shear rates (4000 s^{-1} – 20,000 s^{-1}) generated during some processes such as cross-flow filtration and lobe pumping (Gomme *et al.*, 2006; Stroev *et al.*, 2007; Bee, Stevenson, *et al.*, 2009; GE, 2014) indicating that Spin-freezing would not negatively impact ADH. It is worthwhile understanding that the liquid in the vial experiences maximum shear when the vial is accelerated from rest. As the vial attains the maximum desired rotational velocity, the relative rotational velocity of the vial with respect to the liquid reduces, thereby, reducing the shear rate. This is analogous to a person sitting in a moving aircraft experiencing negligible force with respect to the aircraft. However, further product-specific evaluation is required to study the effect of Spin-freezing on labile biopharmaceuticals. No significant loss in the activity of spin frozen ADH was observed. Moreover, no permanent aggregates were seen in the DLS results of the spin frozen samples as compared to the original sample. This confirmed that the shear rate experienced during Spin-freezing did not affect the stability of ADH. Furthermore, inhomogeneity associated with sedimentation velocity (6.59×10^{-9} m s^{-1}) and stress experienced due to diffusion velocity (diffusion coefficient = 6.10×10^{-11} m^2 s^{-1}) during spin freezing were shown to have negligible effects on proteins within 10 min of spin freezing (Lammens *et al.*, 2018). Two of these factors become inapplicable at the end of freezing as a decrease in the temperature will reduce the sedimentation and diffusion velocity. In addition, the sedimentation velocity of viruses and bacteria were evaluated. It was found that the sedimentation velocity of viruses was 5730 times higher and that of bacteria was up to 20,000 times higher compared to the sedimentation velocity of proteins. This meant that viruses and bacteria are more prone to inhomogeneity in the frozen product layer due to sedimentation.

More recently, the impact of Spin-freeze-drying was studied on the stability of a commercial polyclonal antibody, human intravenous immunoglobulin (IVIG), manufactured by Baxter Healthcare Corporation (Vanbillemont, Carpenter, *et al.*, 2020). The authors concluded that the stability of the Spin-freeze-dried protein was comparable to its conventionally freeze-dried

counterpart. Since low shear rates and no major air-liquid interfaces were generated, Spin-freezing did not impact the stability of the protein. These results were consistent with results shown previously (Lammens *et al.*, 2018).

In terms of aseptic manufacturing, a GMP-like engineering prototype for Spin-freeze-drying has been developed by RheaVita and Ghent University (Corver *et al.*, 2018). The authors propound that this technology can be scaled-up by adding 5 parallel lines within an area of 25 m^2 to produce 10,000 Spin-freeze-dried vials per day. In comparison to the throughput delivered by the Spin-freeze-drying prototype, a commercial batch freeze-dryer, within an area of 30 m^2, can deliver 100,000 vials with a capacity of 2 mL over a 3-day cycle. In conclusion, Spin-freeze-drying technology has shown to be a potential competitor to batch freeze-dying in terms of process associated stresses and PAT, though the feasibility of implementing more than 5 parallel lines to generate a higher throughput along with the associated costs in a cGMP environment would be an interesting area of study.

1.3.1.3 Continuous Freeze-drying of suspended vials

More recently, Capozzi *et al.* developed a new concept of continuous freeze-drying known as continuous freeze-drying of suspended vials (Capozzi *et al.*, 2019). As shown in Figure 1.6, the freeze-drying setup consists of a sequence of modules for different unit operations connected together to ensure a continuous flow of vials. The vials are suspended over a track with multiple rows that allow the transfer of vials through chambers with different temperature and pressure conditions. Each chamber is separated by a load-lock system that facilitates the transfer of vials between different modules. As the vials are continuously being loaded into the lyophilizer, they are filled and partially stoppered. After filling, the vials enter the freezing zone where freezing occurs either through spontaneous or controlled nucleation using vacuum-induced surface freezing (VISF). Heat transfer during freezing is achieved by cooling gas through forced air convection or radiation. A significant reduction in temperature gradients within the product results in the formation of larger and uniform pores which is achieved by the suspended-vial configuration. This further results in a faster

sublimation rate, thereby, reducing the total drying time compared to conventional freeze-drying. In addition, VISF reduces vial-to-vial ice crystal inhomogeneity which results in a homogenous porous structure amongst vials. Following the process of freezing, the vials subsequently move into the primary and secondary drying chamber. The desired pressure is applied to initial sublimation. Controlled heat transfer is achieved through circulating heat transfer fluid in the radiating surfaces. This feature helps to overcome the drawback of heterogeneous heat and mass transfer during conventional freeze-drying. It was shown that this type of configuration reduced the primary drying time by 3 – 4 times and the total drying time was reduced by a factor of 6 with an approximated total drying time of 6 h (Capozzi *et al.*, 2019; Pisano *et al.*, 2019). Moreover, the size of this continuous freeze-drier would be 6 – 8 times smaller compared to a conventional batch lyophilizer (Capozzi *et al.*, 2019). Further insights on continuous lyophilization are available in their recently published chapter (Pisano *et al.*, 2022).

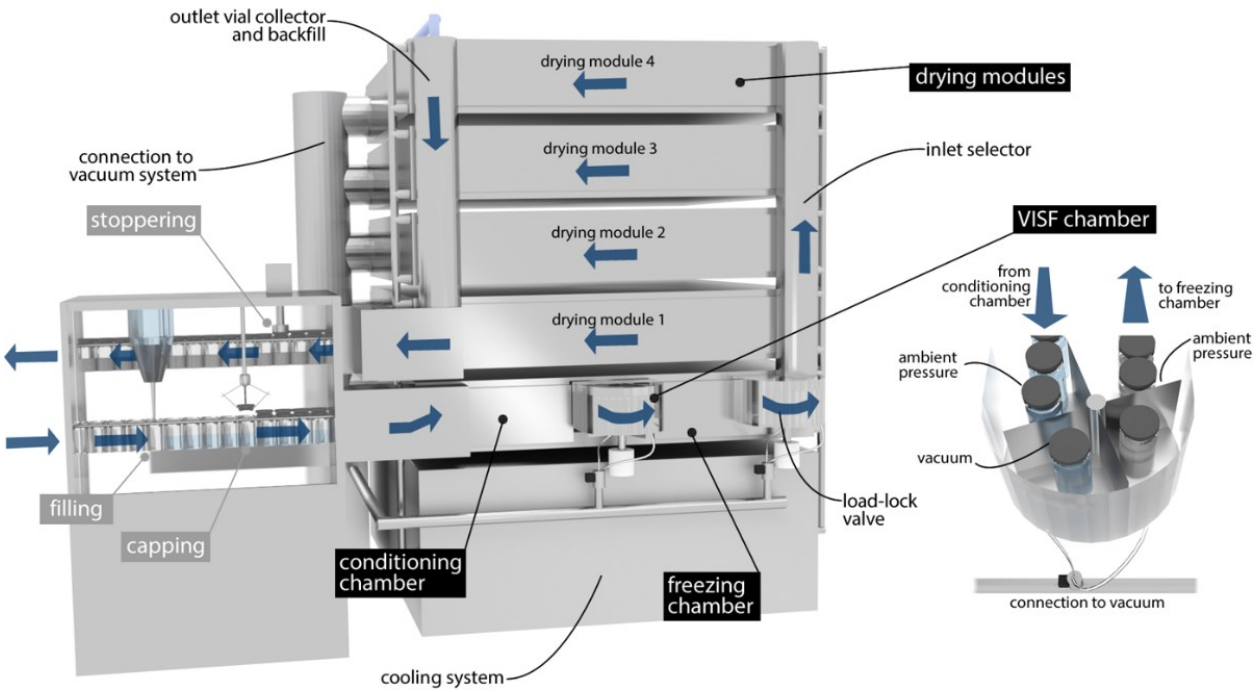

Figure 1.6: Continuous freeze-drying of Suspended Vials (Capozzi *et al.*, 2019).

1.3.1.4 Other Concepts for Continuous Freeze-drying Technology

A few other patents for continuous shell/spin freeze-drying were filed. As stated in Patent No. DE967120, Becker's concept of continuous freeze-drying includes a guide capsule that carries each vial inside the drying chamber (Becker, 1957). The vial containing liquid is rapidly rotated and frozen under vacuum. Next, the guide capsule transfers the vial into a drying chamber and this process is subsequently repeated with other vials. Under the influence of gravity, the vials are rolled down inside the drying chamber, which consists of a long, winding heated conduit (Becker, 1957; Pisano *et al.*, 2019). Furthermore, Broadwin developed a continuous freeze-drying concept based on shell-freezing as described in Patent No. US3202108A (Broadwin, 1965). This design consists of a vacuum chamber with a rotating shaft that holds bottles containing the product to be dried. As a result of centrifugation, the liquid mass is spread all along the internal surface of the bottle assuming a shell shape. This increases the available surface area of the liquid, thereby, increasing the rate of sublimation or heating. The liquid is frozen, and vacuum is applied. Dehydration is achieved by reducing the temperature to – 15°C. At this point, the centrifuge is stopped, and heat is applied to evaporate any unfrozen liquid. Subsequently, the temperature is reduced to – 50°C to allow complete dehydration of the frozen shell (Broadwin, 1965; Pisano *et al.*, 2019). To allow a relatively higher throughput, Oughton *et al.* described a continuous freeze-drying process in their Patent No. US5964043 titled "Freeze-drying process and apparatus" (Oughton *et al.*, 1999). The apparatus comprised of qui-spaced apertures of a magazine in which vials were placed for drying. The vials were transported to different zones during the process using a conveyor. The vials filled with the desired product were removed from the magazine and frozen with the help of an inert gas while being rotated horizontally. The rotation velocity was controlled to allow the formation of shell with a relatively uniform thickness. After the completion of the freezing step, the vials were placed in the magazine and transferred into the vacuum tunnel that contains heating blocks. The heating blocks present provide heat energy to the vials, thus, speeding up the rate of drying. The vials are then transported to a plugging zone for capping and labelling (Oughton *et al.*, 1999; Pisano *et al.*, 2019).

1.3.2 Bulk Drying Technologies

1.3.2.1 Active-freeze-drying

In contrast to tray-based bulk freeze-drying, Hosowaka Micron B.V. developed stirred bulk freeze-drying known as “Active-freeze-drying” based on Patent No: EP1601919A2 (Van Der Wel, 2012). The Active-freeze-drying process allows lyophilization of heat-sensitive bulk materials ranging from solutions, suspensions and pastes to wet solids with minimal handling (Touzet *et al.*, 2018; Capozzi *et al.*, 2019; Hosokawa Micron B.V., 2019; Pisano *et al.*, 2019). The final dried product is obtained as a free-flowing powder, unlike lyophilized cakes. As an additional feature, the characteristics of certain products can be improved by stirring or agitation (Hosokawa Micron B.V., 2019). Moreover, a higher rate of heat transfer and reduced drying times can be achieved (Touzet *et al.*, 2018). This technology can be applied to foods, pharmaceuticals, nanomaterials, polymers, ceramics, catalysts and glass powder (Hosokawa U.K., 2019). The process flow includes a jacketed conical vacuum dryer, an impeller, a collection filter, a product collector and a vacuum pump as shown in Figure 1.7 (Touzet *et al.*, 2018; Hosokawa Micron B.V., 2019).

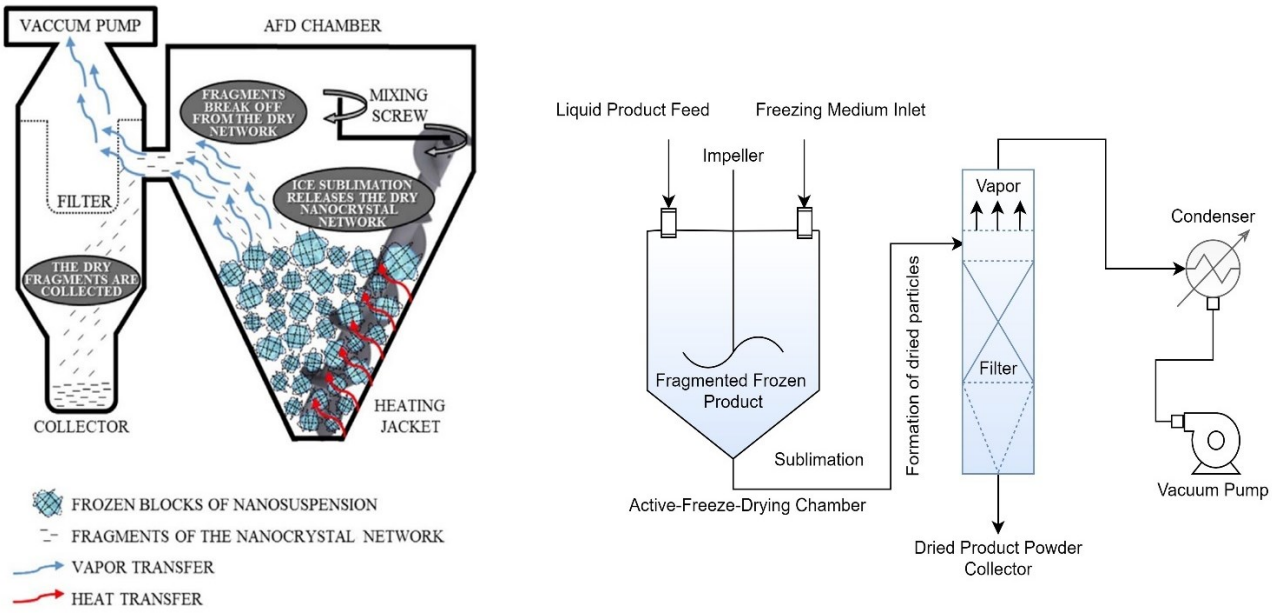

Figure 1.7: (a) A pictorial representation and (b) a process flow diagram of the Active-freeze-drying process. Adapted from (Touzet *et al.*, 2018).

The working principle involves dynamic freezing of the product in a conical stirred drying chamber with the help of a freezing medium. The chamber is surrounded by a controlled heating/cooling jacket. Frozen granules of different sizes and shapes are obtained as a result of a Vacuum Induced Surface Freezing technique (VISF) and stirring motion (Touzet *et al.*, 2018). Subsequently, sublimation takes place at a suitable pressure and heat is distributed through the jacket along with the stirring motion. Mixing provides a large surface area for sublimation leading to a higher rate of heat transfer, thereby, reducing the drying time (Touzet *et al.*, 2018). Sublimation starts at the outer layers eventually moving towards the inner layers of the frozen granules. Due to stress induced by the stirring motion, the dried layer is continuously disintegrated into fragments which reduces resistance to vapour flow. These fragments are driven into the collector by vacuum. The drying process is finished when the product temperature is in equilibrium with the chamber wall temperature.

Touzet *et al.* conducted a pilot-scale study on Active-freeze-drying of nanocrystal-based ketoconazole drug showing that the technique efficiently produced reconstitutable nanocrystal

powder (Touzet *et al.*, 2018). The effect of four different process parameters namely, freezing method (fast and slow), nanocrystal concentration (10 % w/w and 20 % w/w), the jacket temperature (0 °C and 30 °C) and the screw rotation speed (minimal and maximal) were studied on the process performance and product characteristics using a two-level fractional factorial design. The process performance was studied in terms of the average rate of vapour transfer, yield and drying time, whereas the CQAs of the product examined were particle size and re-dispersibility of the dried fragments. Out of the four process parameters, the jacket temperature significantly contributed to the rate of sublimation and the yield. An increase in the jacket temperature approximately doubled the rate of sublimation (Touzet *et al.*, 2018). The majority of the dried fragments were obtained in the collector at a critical rate of vapour flow below which no migration of the dried fragments was observed. Moreover, an increase in the jacket temperature resulted in the collection of significantly larger fragments due to the corresponding increase in the vapour flow rate allowing the transfer of large fragments from the chamber into the collector, thereby, leading to a higher yield. Secondly, large fragments, as shown by SEM (Figure 1.8), were also obtained by increasing the nanocrystal concentration as a result of a stronger nanocrystal network structure as compared to the lower nanocrystal concentration.

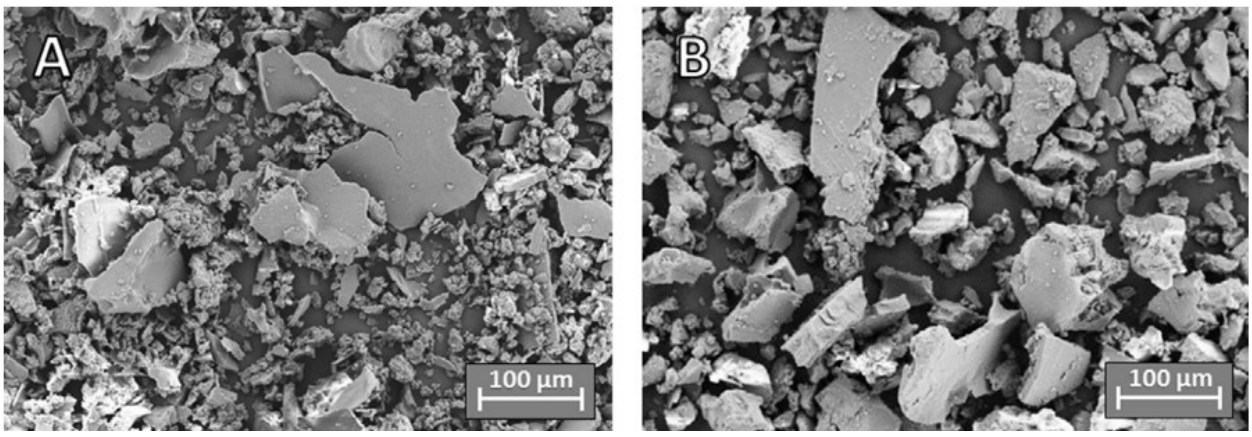

Figure 1.8: (A) SEM picture of 10 % w/w ketoconazole drug crystals (B) SEM picture of 20 % w/w ketoconazole drug crystals (Touzet *et al.*, 2018).

Furthermore, particle size analyses of the nanocrystal suspensions were carried out using wet laser diffraction on a Mastersizer® 2000. All reconstituted Active-freeze-dried powders showed the presence of aggregates between 1 – 100 µm, along with reduced presence of the original population by volume compared to the initial nanocrystal suspension. The presence of aggregates induced by freeze-drying reduced the surface area available for rehydration by 45 – 50 % (Touzet *et al.*, 2018). It was stated that no surface loss was observed over the period of 2 weeks of storage post freeze-drying and the nanocrystal suspensions were physically stable. In order to overcome the challenge of aggregation, the concentration of D-α-tocopherol polyethylene glycol 100 succinate (TPGS) in the formulation was increased by three-fold. A significant reduction in the fraction of aggregates was observed, thereby, leading to an increased availability of the surface for re-dispersion. However, this did not reduce the reconstitution time of the dried nanocrystals. Lastly, they also demonstrated that lowering the freezing temperature from – 19 °C to – 33 °C led to reduced aggregation (Touzet *et al.*, 2018).

While this technology employs the principle of freeze-drying to produce bulk powder, it is still a batch process. Continuous operation and automated recovery of the dried product is yet to be addressed. Moreover, the continuous stirring motion throughout the freezing and drying process can be detrimental to the stability of proteins. Continuous stirring can lead to increased foaming in the liquid product, thereby, exposing the protein to interfacial denaturation and aggregation (Duerkop *et al.*, 2018). During the freezing step, breaking up of ice crystals by continuous stirring can interfere with ice nucleation and the cooling rate which may lead to instability at the ice-liquid interface (Authelin *et al.*, 2020). Furthermore, continuous stirring in an insulated vessel can lead to a relative increase in temperature and so, it is crucial to accurately monitor the product temperature during sublimation. Sublimation above the T_g' may lead to product collapse (Meister and Gieseler, 2009; Meister *et al.*, 2009; Ohori and Yamashita, 2017). Active-freeze-drying technology may be more suited for small molecules and stable biopharmaceuticals, though the feasibility of this technique needs investigation for commercially manufactured parenteral biopharmaceuticals.

1.3.2.2 Spray-drying

Spray-drying is a technique with potential applications in the pharmaceutical industry. It is one of the few techniques used to produce dried powder formulation from liquid, slurry or low-viscosity paste (Celik and Wendell, 2010). The earliest description of spray-drying of products was stated in a patent in 1872, titled "Improvement of Drying and Concentration Liquid Substances by Atomizing" (Percy SR, 1872). It has been reported that spray-drying has been employed across a wide variety of fields including food products, chemicals, fabrics, electronics and cosmetics (Masters, 1985; Jain *et al.*, 2012). Enzymes (amylase, trypsin, lipase, protease) (Samborska *et al.*, 2005; Namaldi *et al.*, 2006; Forbes *et al.*, 2007; Costa-Silva *et al.*, 2014; De Jesus and Maciel Filho, 2014; Abdel-Mageed *et al.*, 2019), antibiotics (Kho *et al.*, 2010; Chan *et al.*, 2013; Park *et al.*, 2013), APIs (Lee *et al.*, 2013; Oliveira and Poco, 2013; Paudel *et al.*, 2013), vitamins (vitamin B12, ascorbic acid) (Uddin *et al.*, 2001; Ahmed *et al.*, 2010; Sarti *et al.*, 2012; Estevinho *et al.*, 2016) and excipients (lactose, mannitol) (Chandrapala and Vasiljevic, 2017; Mönckedieck *et al.*, 2017; Martins *et al.*, 2019) are a few examples of pharmaceutical products that have been spray-dried (Celik and Wendell, 2010). The production of nanomaterials including nanoparticles, nanocatalysts and nanodrugs is another possible application of spray-drying (Wisniewski, 2015).

Several advantages of spray-drying have been reported. Firstly, it eliminates the need for a large number of unit operations which makes it cost-effective and improves production efficiency (Jain *et al.*, 2012). The manufacturing cost associated with spray-drying is only 20 % of the manufacturing cost associated with freeze-drying (Roser, 1991; Santivarangkna *et al.*, 2007). Secondly, it is said to be a rapid, continuous one-step process which means that the drying equipment will keep producing the spray-dried product as long as the slurry / liquid feed is being constantly fed into the equipment (Celik and Wendell, 2010; Walters H. *et al.*, 2014). Properties such as particle size and shape can be controlled and engineered by spray-drying (Vehring, 2008). Thirdly, this technique can take thermolabile products into consideration. The evaporation process takes approx. milliseconds to a few seconds and the process is very instantaneous, thereby, minimizing exposure to high temperatures

(Celik and Wendell, 2010). The production of millions of small droplets provides a large surface area for heat and mass transfer allowing rapid evaporation. Moreover, it increases the dissolution rate and bioavailability of APIs that are not easily soluble in water and a uniform particle size can be achieved using a suitable atomizer during the process (Aulton, 2007). SPX Flow Inc. has had aseptic spray-dryers that have been inspected by the FDA and produced clinical supplies for phase 3 pivotal studies. The authors have demonstrated the use of Anhydro MS-35 spray-dryer to successfully produce dry powder-based mAbs (Bowen *et al.*, 2013; Gikanga *et al.*, 2015).

1.3.2.2.1 Principle and Process of Spray-drying

The process of spray-drying involves the conversion of liquid feed into solid product (Celik and Wendell, 2010). It is based on the principle that sprayed liquid medium droplets containing the desired product are introduced into a hot gas stream allowing evaporation of the droplet, thereby, producing solid particles which are then separated from the gas stream and collected as dry powder (Wisniewski, 2015; Jain *et al.*, 2012). Each droplet exposed to the hot gas stream is dried to form an individual solid particle. The phenomenon of drying and particle formation both occur in this process (Vehring, 2008). The drying process is continued until the desired moisture content is achieved in the dried particle. As mentioned earlier, the evaporation process rapidly decreases the temperature of the gas, keeping the droplet temperature low, allowing the drying of thermo-sensitive products. This is a very fast process and the contact of the product with the gas is quite short (Wisniewski, 2015). It has been noted that thermolabile products such as vaccines can be spray dried at 150°C (Roser, 2005). The process of spray drying typically consists of four major steps (Wisniewski, 2015; Jain *et al.*, 2012; Mezhericher, 2011): 1) Atomization of the liquid feed, 2) introduction of the sprayed droplets into the hot gas stream, 3) drying and particle formation, and 4) separation and collection of the dried powder product from the hot gas stream. Figure 1.9 depicts a typical spray-drying schematic.

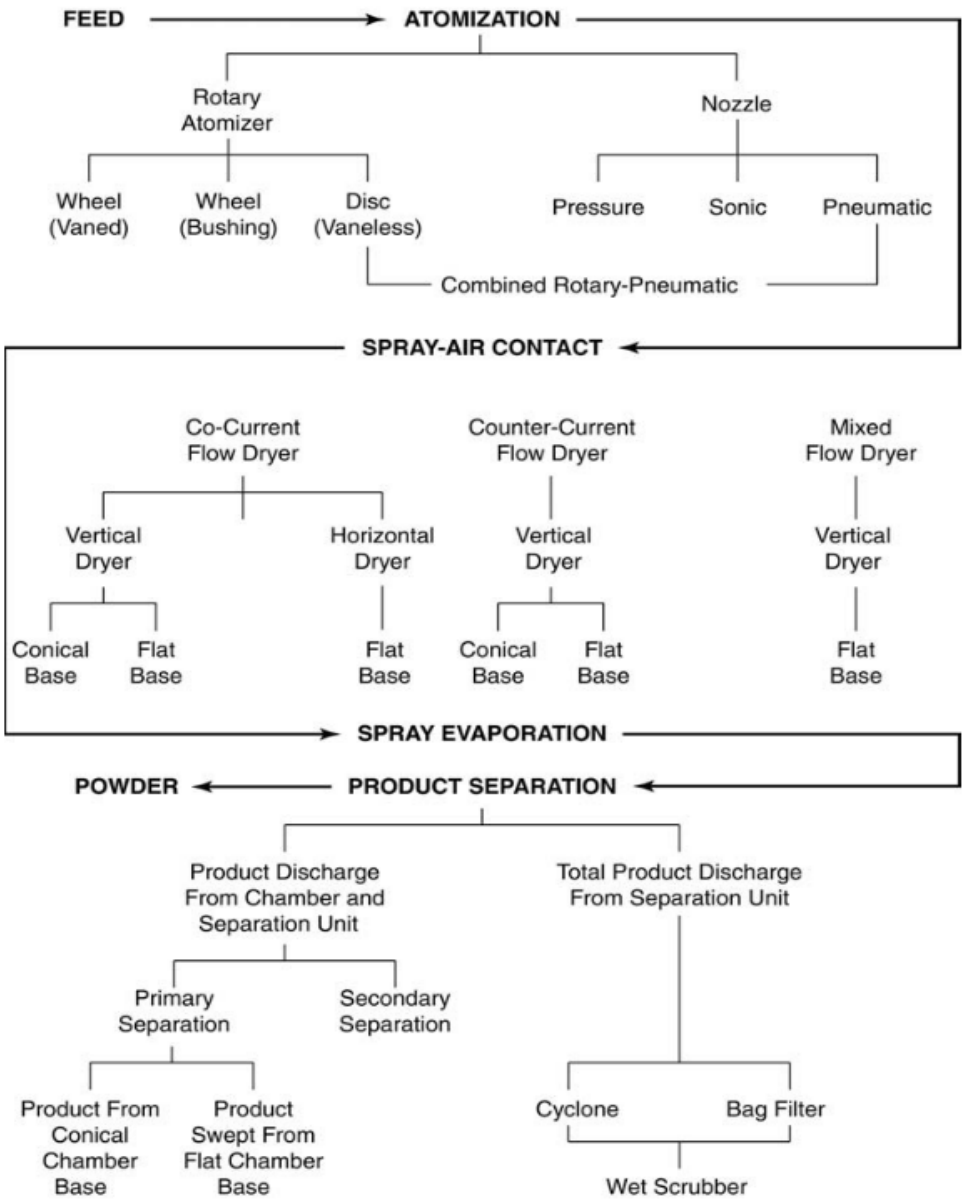

Figure 1.9: Schematic of spray-drying process (Celik and Wendell, 2010).

The spray-drying process begins with atomization of the liquid feed containing the product. Atomization, also known as droplet generation, involves the disintegration of the liquid feed into numerous fine droplets. Figure 1.10 depicts the critical process parameters for the spray-drying process. The liquid feed is sprayed by a peristaltic pump through the nozzle. At this point, the process parameters of interest include feed flow rate (pump speed), air inlet temperature, spray flow rate, nozzle size and nozzle pressure (Figure 1.10). A higher pump rate corresponds to high inlet mass which requires higher energy to evaporate the droplet to particles. This leads to an increase in the difference between the air inlet temperature and outlet temperature resulting in a product with high

residual moisture content (RMC) (Büchi Labortechnik AG, 2002) (Figure 1.10). The atomising air flow rate is the amount of compressed air required to disperse the solution/suspension through the nozzle. Higher atomising flow rates result in smaller particle size. The particle size of the product is directly proportional to the feed concentration (Büchi Labortechnik AG, 2002).

For optimum evaporation of the liquid and to achieve the desired properties of the particle, the atomized droplet must exhibit a high surface to mass ratio (Celik and Wendell, 2010; Masters, 1985). Larger surface area is one of the factors that hastens the evaporation process. Particle character is one of the important factors controlled by the droplet size which brings in the importance of the choice of atomizer (Aulton, 2007). The different types of atomizers are discussed in section 1.3.2.2.2.1. It has also been reported that higher thermal efficiency of a dryer could be achieved by using a high concentration of solutes in the liquid feed (Wisniewski, 2015). This is because low amounts of solvent would be available for evaporation. Moreover, to confront high temperatures during drying, the liquid medium (solvent) should be thermostable (Wisniewski, 2015).

The atomization process follows introduction of the sprayed droplets into the heated gas stream to allow evaporation of the solvent. This takes place in the drying chamber. An air dispenser uses perforated plates or channels that allows the flow of gas into the chamber, ensuring the flow of gas evenly to all parts of the chamber. The position of the atomizer and the spraying pattern play a critical role in the way in which the sprayed droplets interact with the heated stream of gas (Celik and Wendell, 2010; Wisniewski, 2015). The atomizer and the air disperser, usually fixed into the roof of the chamber, are present adjacent to each other to ensure even mixing. Also, the air entering through the air disperser is devoid of any temperature gradients which would otherwise lead to uneven drying of the product (Celik and Wendell, 2010).

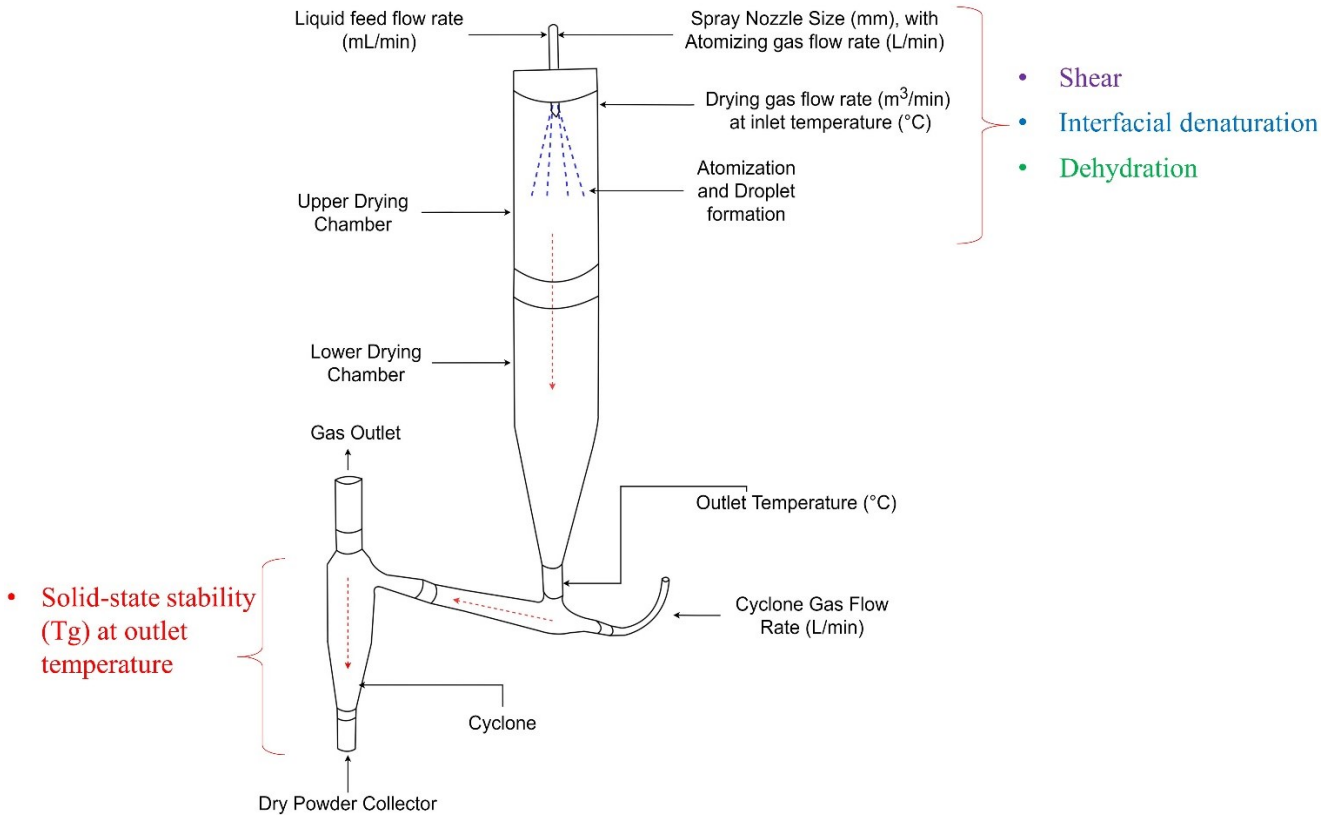

Figure 1.10: A schematic diagram of the spray-drying process with a cyclone separator and possible sites for protein denaturation. Blue dotted lines represent the sprayed droplets. The red dotted lines represent the trajectory of the particles.

There are three distinct types of air flow patterns and spray droplet movements that take place inside the drying chamber depending upon its design (Jain *et al.*, 2012; Aulton, 2007). 1) The co-current flow pattern involves the flow of the atomized spray droplets and drying air in the same direction as depicted in Figure 1.11 (a). It allows rapid evaporation to take place and the dry air cools in a short duration. This configuration is suitable for thermolabile products such as enzymes, peptides and proteins (Celik and Wendell, 2010). The product is not subject to thermal degradation. 2) The counter-current flow involves movement of sprayed droplet and air in exactly opposite directions as shown in Figure 1.11 (b). Each of them enters from the two opposite ends of the drying chamber. This configuration has been reported to result in increased powder flowability and is described to be suitable for non-heat-sensitive products (Celik and Wendell, 2010). 3) Lastly, the mixed flow arrangement is a combination of the co-current and the counter-current air flow patterns (Figure 1.11

(c)). This type of configuration can be implemented in a relatively small sized drying chamber. The product powder is exposed to higher particle temperature as it reaches the low drying chamber (Celik and Wendell, 2010).

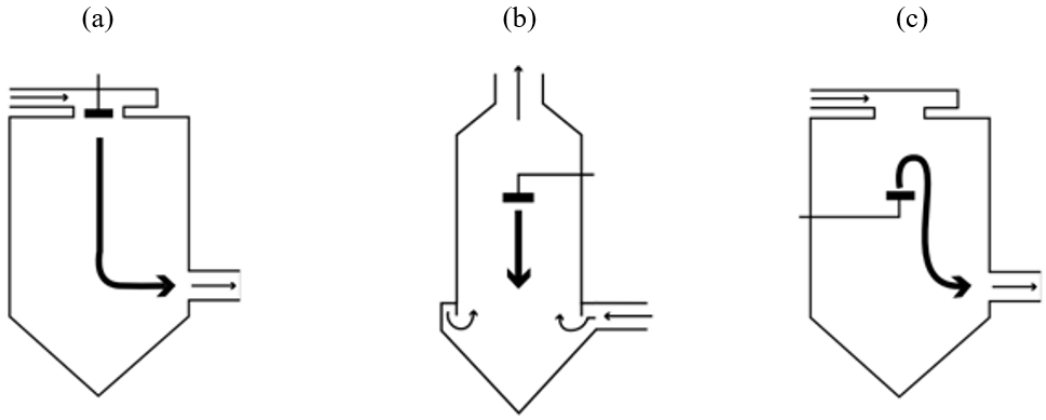

Figure 1.11: Spray-air contact patterns: (a) co-current flow, (b) counter-current flow, (c) mixed flow (Büchi Labortechnik AG, 2002).

The following step 'drying', also known as droplet evaporation, occurs in the drying chamber. As discussed by Celik and Wendell, the drying vessel could either have a large cylinder height and a short diameter or short height and a large diameter (Celik and Wendell, 2010). The spray-drying process is a convective process under the influence of a heated carrier gas. This convective process involves heat and mass transfer when the atomized liquid droplets are in contact with the heated stream of gas. Heat is transferred from the gas to the droplet and mass is transferred from the droplet to air when the droplet is vaporized. The three main phases of the drying rate curve have been depicted in Figure 1.12 (Celik and Wendell, 2010).

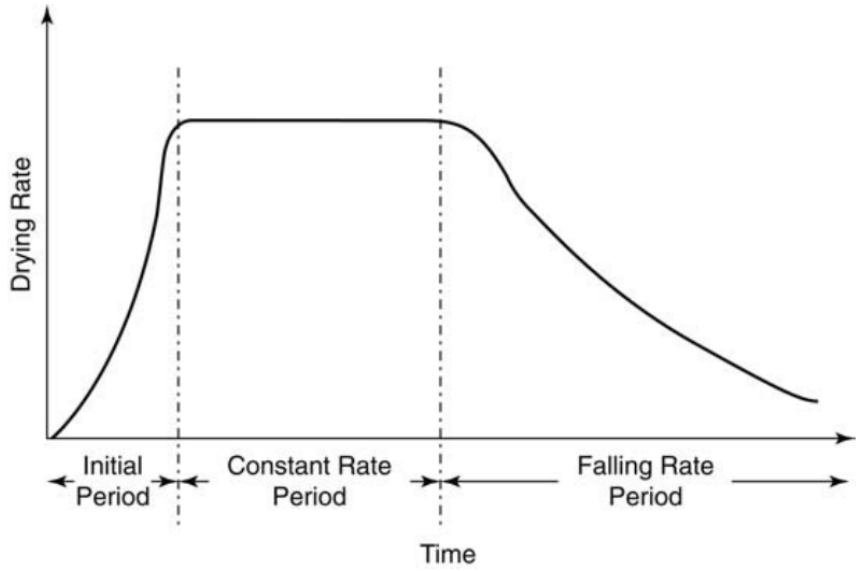

Figure 1.12: Typical Drying Rate Curve (Celik and Wendell, 2010).

These include: 1) the initial drying phase in which the droplet evaporation rate is constantly accelerating. During this phase, the temperature of the drying air is decreased rapidly, and the droplet surface temperature rises slightly. It takes about 1.5 s to achieve the majority of the evaporation (Celik and Wendell, 2010). This phase continues until an equilibrium is established between the droplet surface and surrounding air; the droplet evaporation rate becomes constant. 2) During the constant rate of the drying phase, the majority of the droplet moisture content is removed. The temperature and partial pressure of the droplet surface is nearly constant and is represented as the wet bulb temperature (Snyder, 2012). When the moisture removal rate becomes rate-limiting to the drying rate, the drying process enters into the falling-rate phase. 3) The final phase, also known as the falling-rate phase, depicts the retarding drying rate. Retardation occurs due to the exposed solid layer of the spray-dried particle that acts as a rate-limiting factor in the drying process, as most of the moisture content is removed in the earlier stages. Until there is an equilibrium established between the droplet moisture content and the surround air stream, the evaporation rate continues to deaccelerate.

Grisso *et al.* showed solution droplet data using free fall, evaporation and drying. Initial droplet diameter and final drop diameter and demonstrated evaporation time were compared as shown in Table 1.4 (Grisso *et al.*, 2013).

Table 1.4: Evaporation of Pesticide Solution Droplet in Free Fall (Grisso *et al.*, 2013).

Droplet Diameter (μm)	Terminal Velocity (m/s)	Final Drop Diameter (μm)	Time to Evaporate (s)
20	0.012	7	0.3
50	0.075	17	1.8
100	0.273	33	7.0
150	0.510	50	16
200	0.720	67	29

The final step in the process of spray-drying is the separation of the dried powder from the drying air. At this point, the two important process parameters are the outlet temperature and the aspirator flow rate (Figure 1.10). The outlet temperature is the maximum temperature that the product experiences during spray-drying (Büchi Labortechnik AG, 2002). The aspirator air flow rate is an important parameter that impacts the degree of migration/separation in the cyclone and the residual moisture content (RMC) in the product. A higher aspirator rate results in a higher degree of separation in the cyclone, whereas a lower aspirator rate results in lower RMC (Büchi Labortechnik AG, 2002). This is because the residence time of the particles in the spray-dryer is increased, experiencing outlet temperature for a longer duration, thereby, leading to lower RMC (Büchi Labortechnik AG, 2002).

Two different methods of separation have been discussed, namely, cyclone separation and baghouse filtration (Snyder and Lechuga-Ballesteros, 2008). Both of these methods arose from dust pollution control and chemical processing industries with the motive of reducing particles (Heumann, 1997). Choosing the appropriate separation system depends on the formulation stability and powder characteristics of the product. The cyclone separation method follows the principle of the difference in density of the dispersed phase and the continuous medium (Snyder, 2012). When both phases are subjected to acceleration within a vortex, the smaller particles deviate from the continuous phase due to velocity lag and migrate to the outer wall of the cyclone which is then collected. Cyclone design, particle size distribution and the operating conditions are factors that determine the efficiency of the cyclone separation method. On the other hand, the baghouse particle separation system employs a

depth filter or a size-exclusion membrane filter to filter out the powder particles from the flowing gas stream (Snyder, 2012). As the gas flows through the filter, the powder particles are restricted to flow through, forming a layer on the filter media. The filters are normally geometrically cylindrical (Heumann, 1997). The final product is collected via a high pressure back-pulse mechanism wherein the powder is removed off the filter media.

1.3.2.2.2 Spray-drying Equipment

1.3.2.2.2.1 Atomizer

Based on the source of energy, three types of atomizers, namely, 1) centrifugal atomizers (rotary atomizers), 2) kinetic energy nozzle (pneumatic nozzle atomizers) and 3) pressure nozzle atomizers have been discussed and implemented (Aulton, 2007; Jain *et al.*, 2012). Rotary atomizers have replaced simple jet atomizers that prevent blockage due to deposition of residual solid on the nozzle (Aulton, 2007). Rotary atomizers comprise of a rotating wheel or a disc onto which the liquid feed is fed. The liquid stream is disintegrated into tiny droplets. It has been reported that the disc rotates in the range of 5000 to 25,000 rpm, with wheel diameter of 5 to 50 cm (Celik and Wendell, 2010). The liquids feed rate and viscosity are directly proportional to the mean size of the droplet, whereas the disc speed is inversely proportional to the mean size of the droplet. These atomizers are reliable, easy to use and can incorporate high feed rate and feed rate fluctuations (Jain *et al.*, 2012). A rotary atomizer is shown in Figure 1.13.

Figure 1.13: Rotary Atomizer (GEA Pharma Systems).

Pneumatic nozzle atomizers or two-fluid nozzles generate high frictional forces over the liquid's surface through compressed air, thereby, disintegrating the liquid feed into tiny spray droplets. Typically pressure in the range of 200 to 350 kPa is required (Celik and Wendell, 2010). A typical two-fluid nozzle is shown in Figure 1.14.

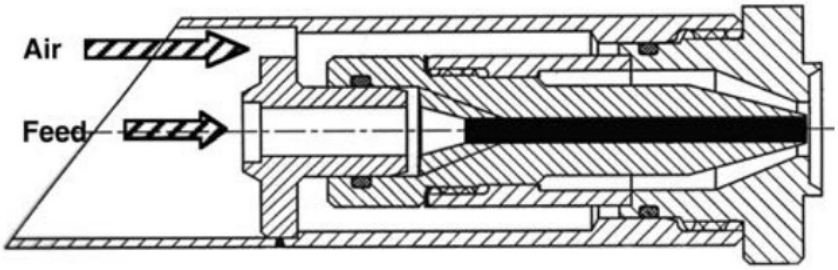

Figure 1.14: Cross-sectional representation of a two-fluid nozzle (GEA Pharma Systems).

Pressure nozzles typically involve a pressurized liquid stream forced by a pump through a nozzle orifice. The disintegrated fine droplets emerge in a cone-shaped spray pattern as a result of the rotatory motion of the liquid feed inside the nozzle. Spiral grooved or swirl inserts within the nozzle facilitate the rotatory motion. While pressure nozzles can handle high concentration feeds at high feed rates, the sprayed powders are less homogeneous and coarser with the size of 120 – 300 μm (Celik and Wendell, 2010). Figure 1.15 shows a cross-sectional view of pressure nozzles.

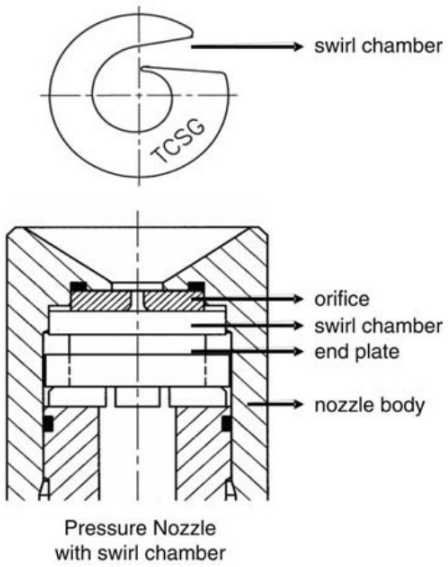

Figure 1.15: Cross-sectional view of pressure nozzles (GEA Pharma Systems; Celik and Wendell, 2010).

1.3.2.2.2.2 Chamber

In a typical spray-drying chamber, the drying droplets are rotated by the tangentially entering air stream to increase the residence time, thereby, increase the time for drying (Aulton, 2007). In a pharmaceutical clean room environment, a filter and heat exchanger are employed to filter and heat the clean air. A separate filter bag or cyclone filter is used to recover the dust carried by the outlet air stream. Just like in a few pharmaceutical manufacturing sites, 80% recycled air is used as it is cost effective and the efficiency of the drying process is increased if 60% of the exhaust air is recycled to the air inlet of the spray-dryer (Aulton, 2007).Three different sizes of spray-dryers have been reported in the literature. With the laboratory-scale spray-dryer, having a volume of 100 – 200 mL, product weighing up to a few grams can be spray-dried using an aqueous or organic solution. The pilot-scale spray-dryer is capable of evaporating 7 kg of water per hour with geometrical dimensions of the chamber diameter and height being 800 mm and 3 m respectively (Aulton, 2007). Lastly, the industrial-scale model could have a chamber diameter and height of 3.5 m and 6 m respectively, being capable of evaporating 50 – 100 kg of water per hour (Aulton, 2007).

1.3.2.2.2.3 Product

For the final spray-dried product, in terms of the particle's characteristic shape, hollow spheres with a small hole in the centre have been reported (Aulton, 2007). This is because evaporation occurs first on the outer surface of the droplet leaving behind residual liquid in the centre. Later, this internal liquid evaporates leaving a hole in the centre of the sphere. This leads to the formation of a spherical product (Aulton, 2007).

1.3.2.2.3 Stability of Spray-dried Proteins

Studies focusing on the effect of spray-drying on the stability and shelf-life of monoclonal antibodies have been carried out. Excipients such as trileucine are reported to effectively protect the protein from sheer stress caused during the transformation of the liquid droplet into a dried particle (Lechuga-Ballesteros *et al.*, 2008). During this time, the droplet viscosity is low enough to allow conformational mobility within the protein which makes the molecule more likely to undergo potential unfolding, subsequently leading to protein aggregation (Snyder, 2012). Non-reducing sugar excipients such as sucrose, raffinose and trehalose have also been reported to stabilize proteins in their amorphous state at low moisture levels (Snyder, 2012). Another commonly spray-dried pharmaceutical excipient is lactose (Gohel & Jogani, 2005; Jain *et al.*, 2012). Moreover, spray-drying has been implemented on proteins and antibodies for pulmonary drug delivery (Schüle *et al.*, 2008). Exubera™, an inhaled insulin product developed by Pfizer Inc., is an example of a spray-dried product (discontinued) (White *et al.*, 2005). Exubera's formulation components include sodium citrate, sodium hydroxide, glycine and mannitol (FDA, 2006). Raplixa™, a Human Fibrin Sealant developed by ProFibrix (The Medicines Company), is manufactured by Nova Laboratories Ltd. via spray-drying technology (FDA, 2015). The product contains 824 mg/g trehalose, 11 mg/g calcium chloride, human albumin, sodium chloride, sodium citrate and L-Arginine hydrochloride (FDA, 2015).

Initially, anti-IgE antibody formulations with mannitol were reported to show better flowability for inhalation applications, but then it was stated that formulations with trehalose resulted in higher protein stability compared to mannitol due to its tendency to recrystallize (Costantino *et al.*, 1998; Andya *et al.*, 1999). Later on, protein stabilizers such as trehalose, sorbitol and sucrose were preferred in spray-drying formulations and were demonstrated to show their efficacy on antibodies (Maury *et al.*, 2005; Dani *et al.*, 2007). Dani *et al.* tested a 1: 0.8 mAb : trehalose ratio by weight and concluded that this formulation was enough for the stabilization of spray-dried IgG antibody (Dani *et al.*, 2007). Additionally, Maury *et al.*, carried out different mAb : trehalose (ratio by weight) formulations at 130 °C inlet air and 90 °C outlet air temperatures with 5 % residual water content in the spray-dried powders. They concluded that 20 – 30 % of sugar content was sufficient to safe guard the antibody in terms of its stability (Maury *et al.*, 2005).

In spite of studies carried out on the stability of antibodies, the effect of elevated temperature stress (>180 °C) on monoclonal antibodies due to high inlet temperatures of large-scale spray-dryers was still a concern (Bowen *et al.*, 2013). Bowen *et al.* conducted further studies by testing different mAb : trehalose formulations (2:1 and 1:2 ratio by weight, respectively) (Bowen *et al.*, 2013). Their study focused on the physical stability of these mAbs by deducing the percentage of monomers present after storing the spray-dried product at 40 °C for a couple of months. In conclusion, they stated that aggregation was observed in both spray-dried and freeze-dried product due to a decrease in the percentage of monomers, but more importantly the percentage of monomers was lower in the freeze-dried product even though the residual water content in the freeze-dried product was quite low compared to the spray-dried product (Bowen *et al.*, 2013).

More recently, Ajmera and Scherließ screened a large number of amino acids and their combinations to study their stabilizing effect on spray-dried Catalase, lysozyme and Pandemrix influenza vaccine containing Haemagglutinin in the ratios 1:1 and 2:1 (amino acid : protein) (Ajmera and Scherließ, 2014). Standard catalase and lysozyme and their formulations were spray-dried at an air inlet temperature of 180 °C and the outlet air temperature between 90 – 95 °C. The feed flow rate was kept

between 5 – 7.5 mL/min, nozzle size was 1.5 mm, air speed was 470 L/h and the aspirator flow rate was kept at 35 m^3/min. The vaccine containing haemagglutinin and its formulations were spray-dried at an air inlet temperature of 120 °C and the air outlet temperature was between 50 – 55 °C. Through experimental results, they showed that arginine, glycine and protein in the ratio [(1+1) +1] resulted in a very good stabilizing effect post spray-drying compared to the non-formulated protein itself. They elucidated their results through bioactivity, FTIR, XRD, particle size and accelerated storage stability analysis on relatively large proteins, catalase and haemagglutinin, as well as a small protein lysozyme (Ajmera and Scherließ, 2014).

In comparison to spray-drying, drug administration methods such as nebulization and nasal spray expose proteins to air-liquid interfaces, shear and temperature, which may cause deterioration in the CQAs of biopharmaceuticals (Niven *et al.*, 1995, 1996; Albasarah *et al.*, 2010; Hertel *et al.*, 2015; Bodier-Montagutelli *et al.*, 2020; Fröhlich and Salar-Behzadi, 2021). Examples of some commercial and clinical dry powder-based biopharmaceuticals administered via the parenteral route, inhalation or nebulization are collated in Table 1.5. The stability and composition of such products can provide more insight while studying the impact of the atomization process during spray-drying or spray-freeze-drying.

Table 1.5: Some commercial / clinical powder-based biopharmaceuticals and some biopharmaceuticals administered via spraying or nebulization.

Biopharmaceutical and Manufacturer	Biomolecule API	Formulation Excipients	Manufacturing Process (Administration Method)	Reference
Exubera® by Pfizer / Nektar (Discontinued).	Insulin (Hormone)	Sodium citrate dihydrate, mannitol, glycine, sodium hydroxide.	Spray-dried powder. (Inhaled for diabetes)	(FDA, 2006; White et al., 2005)
Raplixa® by Profibrix, The Medicines Company (Commercial).	Fibrin and Thrombin.	Trehalose, calcium chloride, human albumin, sodium chloride, sodium citrate, L-arginine hydrochloride.	Spray-dried powder. (Powder applied on surface of bleeding tissue for uncontrolled bleeding)	(FDA, 2015a; Manufacturing Chemist, 2015)
Afrezza® / Technosphere insulin (TI) by Mannkind (Commercial).	Recombinant Human Insulin.	FDKP, Polysorbate 80.	Technospheres® by precipitation, adsorption and freeze-drying. (Inhaled for diabetes)	(McElroy et al., 2013; Sarala et al., 2012; Tsai-Turton, 2014)
Inbrija® by Acorda Therapeutics (Commercial).	Levodopa (aromatic amino acid).	DPPC and sodium chloride.	Arcus® Technology – spray-dried powder. (Inhaled for off episodes in patients with Parkinson's disease).	(Acorda Therapeutics, 2021; FDA, 2018)
Somatuline® LA by Ipsen (Commercial).	Lanreotide acetate (octapeptide analogue of somatostatin hormone).	PLGA, mannitol, carmellose sodium, polysorbate 80.	Phase separation and spray-dried microspheres. (Powder and solvent for prolonged-release suspension for injection against multiple conditions).	(EMA, 2013; HPRA, 2019; Pinto et al., 2021)
Trelstar® LA by Verity Pharmaceuticals (Commercial).	Triptorelin pamoate (synthetic decapeptide analogue of GnRH hormone).	PLGA, mannitol, carboxymethycellulose sodium, polysorbate 80.	Phase separation and spray-dried microspheres. (Powder and solvent for prolonged-release suspension for injection for the treatment of prostate cancer)	(Pinto et al., 2021; Vhora et al., 2019)
Sandostatin® by Novartis (Commercial).	Octreotide acetate (cyclic octapeptide).	Mannitol, D,L-lactic and glycolic acids copolymer, carboxymethylcellulose sodium.	Dry powder prepared by Phase separation and spray-drying. (Injectable suspension for the treatment of acromegaly etc.)	(FDA, 1988; Hou et al., 2018; Vhora et al., 2019)
TOBI® Podhaler™ by Novartis (Commercial).	Tobramycin (Antibacterial aminoglycoside).	DSPC, calcium chloride, and sulfuric acid.	PulmoSphere™ by spray-drying. (Orally inhaled for cystic fibrosis against *Pseudomonas aeruginosa*).	(FDA, 2015b; Weers and Tarara, 2014)
Fludase® by Ansun Biopharma (NexBio) (Clinical Trial Phase 2).	DAS181 sialidase (recombinant neuraminidase).	Histidine, trehalose, citric acid, magnesium sulphate, acetate buffer.	TOSAP. (Dry powder for oral inhalation against influenza like illness)	(Bodier-Montagutelli et al., 2018; ECRI, 2011; Mack et al., 2012; Moss and Li, 2015)
CSJ117 by Novartis (Clinical Trial Phase 2)	Anti-TSLP antibody fragment.	Leucine, trileucine, mannitol and trehalose.	PulmoSol™ engineered powder. (Dry powder inhaled for asthma).	(Fröhlich and Salar-Behzadi, 2021; Liang et al., 2020; NCT04410523, 2021)

Biopharmaceutical and Manufacturer	Biomolecule API	Formulation Excipients	Manufacturing Process (Administration Method)	Reference
Aerovant® by Aerovance / Bayer (Clinical Trial Phase 2).	Cytokine – Pitrakinra.	Different formulations including sucrose, mannitol or trehalose, leucine or poly (amino acid) and citrate, acetate or lactate buffer were evaluated.	Spray-dried powder. (Inhaled for asthma)	(Bodier-Montagutelli et al., 2018; Liang et al., 2020; Otulana, 2011; Vehring et al., 2020; Wenzel et al., 2007)
Abrezekimab (VR942) by UCB Pharma, Vectura. (Clinical Trial Phase 2).	CDP7766 (IL-13 mAb fragment).	Trehalose dihydrate, L-leucine and phosphate buffer.	Spray-dried powder. (Inhaled for asthma)	(Burgess et al., 2018; Giles Morgan et al., 2017; Liang et al., 2020; Vectura Limited, 2015; Vehring et al., 2020)
Pulmozyme® by Genentech / Roche (Commercial).	Deoxyribonuclease I.	Calcium chloride dihydrate, sodium chloride.	Liquid formulation. (Inhaled through jet nebulizer against cystic fibrosis to improve pulmonary function).	(Bodier-Montagutelli et al., 2018; FDA, 2014b)
Miacalcin® by Novartis / Mylan (Commercial).	Polypeptide hormone (Calcitonin).	Sodium chloride, benzalkonium chloride, hydrochloric acid.	Liquid formulation. (Nasal spray for the treatment of postmenopausal osteoporosis).	(FDA, 2017; Ozsoy et al., 2009)

Authors have also demonstrated approaches to identify CPPs and formulation components for spray-drying proteins (Batens *et al.*, 2018; Grasmeijer *et al.*, 2019; Ziaee *et al.*, 2019). The outlet temperature was found to be the most critical factor that affected the enzymatic activity of lysozyme. High outlet temperatures, ultrasonic vibrations and mechanical stress produced from ultrasonic nozzles had a negative impact on the activity of lysozyme (Ziaee *et al.*, 2020).

While the impact of spray-drying on proteins has been studied in terms of temperature, the effect of shear and interfacial denaturation during atomization and spraying is also crucial as some proteins are susceptible to such stresses (Broadhead *et al.*, 1993; Mumenthaler *et al.*, 1994; Y. F. Maa and Hsu, 1997; Y. F. Maa *et al.*, 1998; Koshari *et al.*, 2017; Grasmeijer *et al.*, 2019; Wilson *et al.*, 2019; Ziaee *et al.*, 2020). Understanding the impact of spraying conditions prior to dehydration, can provide more insight while developing and choosing excipients for spray-drying proteins. Typically, the liquid feed is drawn into a two-fluid nozzle at velocity, ν_{liq} and exits the nozzle tip with a diameter, d_i (Figure 1.16). A resultant velocity, ν_{av} is generated at the mixing zone with the help of an atomizing gas flow rate, ν_{gas}. The shear rate generated from a two-fluid spray nozzle has been estimated using Equation 1.6 (Hede *et al.*, 2008; Ghandi *et al.*, 2012).

$$\gamma = \frac{\left[2\left(\nu_{av} - \nu_{liq}\right)\right]}{d_i} \qquad \textbf{Equation 1.6}$$

Where γ is the shear rate in s^{-1}, ν_{av} is the average velocity at mixing point in m/s, ν_{liq} is the velocity of liquid in m/s and d_i is the inner diameter of the nozzle tip in mm. ν_{av} is a function of the mass flow rates (kg/s) of the gas and liquid and must not be confused with the arithmetic mean of their velocities.

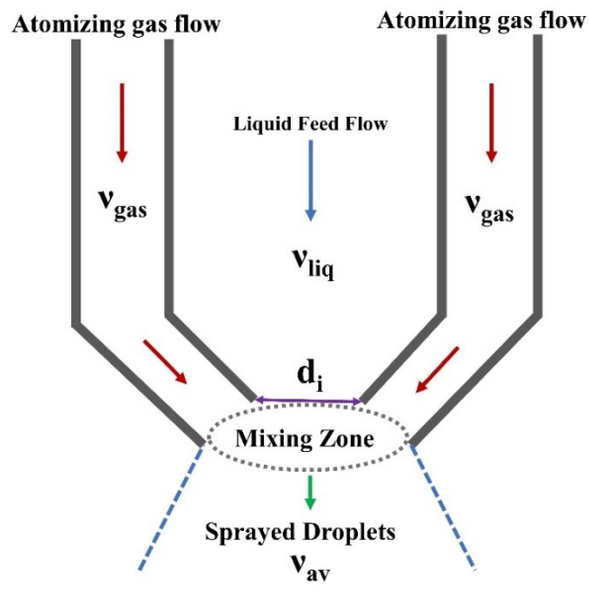

Figure 1.16: A schematic representation of external mixing in a two-fluid nozzle.

Using Equation 1.6, authors have shown that the shear rates generated from a two-fluid nozzle at different atomizing flow rates and liquid densities can range from 97,000 s^{-1} to 992,000 s^{-1} (Ghandi *et al.*, 2012; Morgan *et al.*, 2020). Shear-induced inactivation for some proteins can occur at < 2000 s^{-1} for ≥ 20 min (Charm and Wong, 1981; Ashton *et al.*, 2009), while some proteins may remain stable up to a shear rate of > 250,000 s^{-1} for > 30 min (Bee, Stevenson, *et al.*, 2009; Duerkop *et al.*, 2018). Bekard *et al.* elucidated that the α-helical content in poly-L-lysine was inversely proportional to the square root of shear strain and the extent of unfolding decreased with increasing molecular weight due to greater cohesive forces (Bekard *et al.*, 2011). Such shear levels can be experienced during similar drying methods such as spray-freeze-drying and so, it is crucial to study the stability of biopharmaceuticals as a function of shear and atomization.

In conclusion, spray-drying is one of the most popular industrial drying technologies and has been studied over a wide range of products over the past few decades. The challenges associated with the CPPs of spray-drying of labile parenteral biopharmaceuticals, choice of formulation excipients and their molecular mechanism of interactions with biopharmaceuticals during spray-drying require further product-specific study.

1.3.2.2.4 Microencapsulation via Spray-drying

Microencapsulation is the process of producing tiny particles or droplets embedded in a matrix or surrounded by a coating for numerous applications. It can provide a physical barrier between the core analyte of interest and other components present (Gharsallaoui *et al.*, 2007). A few reported benefits of microencapsulation to the food industry are easier handling, controlled release of the core material and reduced reactivity and transfer rate of the core with environmental factors (Shahidi and Han, 1993; Gharsallaoui *et al.*, 2007). As described by Gharsallaoui *et al.*, a microcapsule is a small uniformly coated sphere that comprises of the core, internal phase/fill and the wall (also known as shell, coating or membrane) (Gharsallaoui *et al.*, 2007). The morphology of the microcapsule produced can be of various types such as simple, irregular, multi-core and multi-wall etc. (Gibbs *et al.*, 1999; Gharsallaoui *et al.*, 2007). Spray-drying is one of the commonly used processes for microencapsulation applications primarily in the food industry (Gouin, 2004). Other microencapsulation techniques include spray-cooling, spray-chilling, air suspension coating, centrifugal extrusion, coacervation, lyophilization, liposome entrapment, molecular inclusion, interfacial polymerization etc. (Shahidi and Han, 1993; King, 1995; Gibbs *et al.*, 1999; Gouin, 2004; Desai and Park, 2005; Gharsallaoui *et al.*, 2007). Microencapsulation through spray-drying typically involves four stages: 1) preparation of the emulsion or dispersion, 2) homogenization of the prepared dispersion, 3) atomization of the dispersion and 4) dehydration of the particles (Dziezak, 1988; Shahidi and Han, 1993). The process involves preparation of an emulsion or dispersion of the core substance in the wall solution. The core material which is usually hydrophobic is heated and homogenized in the solution of an immiscible coating agent. This emulsion must be stable over a period of time. The viscosity and droplet size of the emulsion are important factors to be considered before spray-drying. Low viscosity and droplet size are desirable (Drusch, 2007). Atomization of high viscosity dispersions can lead to formation of large and elongated particles that negatively affect the drying time (Rosenberg and Sheu, 1996). Lastly, spray-drying the emulsion leads to the formation of microcapsules.

In terms of the spray-drying operating conditions, the feed temperature, air inlet and outlet temperature are important parameters to be considered (Liu *et al.*, 2004). An increase in the feed temperature decreases the viscosity and the droplet size, however, high temperatures can also degrade heat-sensitive components in the feed. Even though higher air inlet temperatures can induce cracks in microcapsule membrane and degradation and loss of volatile components, lower air inlet temperatures can lead to reduced evaporation rates which results in the formation of high density membrane microcapsules with high water content, poor fluidity and increased agglomeration (Zakarian and King, 1982; Gharsallaoui *et al.*, 2007). This implies that optimization of spray-drying parameters is necessary to obtain good microencapsulation efficiency. As summarised and reported by Gharsallaoui *et al.*, 50°C – 80°C is the optimum outlet temperature for the microencapsulation of food products (Gharsallaoui *et al.*, 2007). Moreover, the addition of lactose to whey protein improved the formation of crust during spray-drying. This was because lactose formed a continuous glass phase which also increased the hydrophilic nature of the wall material, thereby, limiting the diffusion of solvent through the wall (Moreau and Rosenberg, 1996; Rosenberg and Sheu, 1996). The efficiency of microencapsulation can be improved by using a suitable wall coating material based on physico-chemical properties, molecular weight, thermal properties, diffusibility, crystallinity and emulsifying properties (Gharsallaoui *et al.*, 2007). The presence of a limited number of materials with good water solubility and the need for post processing of fine microcapsules are two drawbacks of microencapsulation via spray-drying (Gharsallaoui *et al.*, 2007).

1.3.2.2.4.1 Microencapsulation of Proteins

Amara *et al.*, demonstrated encapsulation of the model protein lysozyme by coacervation via spray-drying (Amara *et al.*, 2016). They prepared 7.142 g/L lysozyme and 30 g/L low methoxyl amidated pectin suspensions in 5 mM imidazole-acetate buffer at pH 7. The lysozyme suspensions containing 20 % maltodextrin were spray-dried at an air inlet temperature of 180 °C and air outlet temperature of 90 °C. The nozzle size was 0.5 mm and the feed flow rate was 0.5 L/h (Amara *et al.*, 2016). Turbidity measurements indicated lower maximum turbidity of spray-dried lysozyme-pectin

complexes compared to the unprocessed samples at the same concentration. As shown in Figure 1.17, the turbidity of the spray-dried samples and unprocessed samples decreased as the concentration of pectin was increased from 0.4 – 1 g/L after which a plateau was achieved. It was elucidated that reduced electrostatic interactions between anionic pectin and cationic sites on lysozyme resulted in dissociation of aggregates when the concentration of pectin was increased. On the other hand, the turbidity of the spray-dried samples was relatively higher in this region than the original material due to strong electrostatic repulsions induced, making the complexes more prone to thermal aggregation during spray-drying. Secondly, bioactivity results showed a decrease in the activity of rehydrated spray-dried lysozyme by 36.5%. A significant decrease in the bioactivity of untreated and spray-dried lysozyme was observed at the highest and lowest pectin concentrations, however, the bioactivity of lysozyme was protected at intermediate pectin concentrations as shown in Figure 1.18. Moreover, fluorescence spectroscopy results indicated that the tertiary structure of lysozyme was preserved. Low lysozyme aggregates were also observed at intermediate pectin concentrations (Amara *et al.*, 2016). In conclusion, the activity of lysozyme can be effectively preserved using this technique though further study is required to elucidate its secondary and tertiary structure using FTIR and CD spectroscopy.

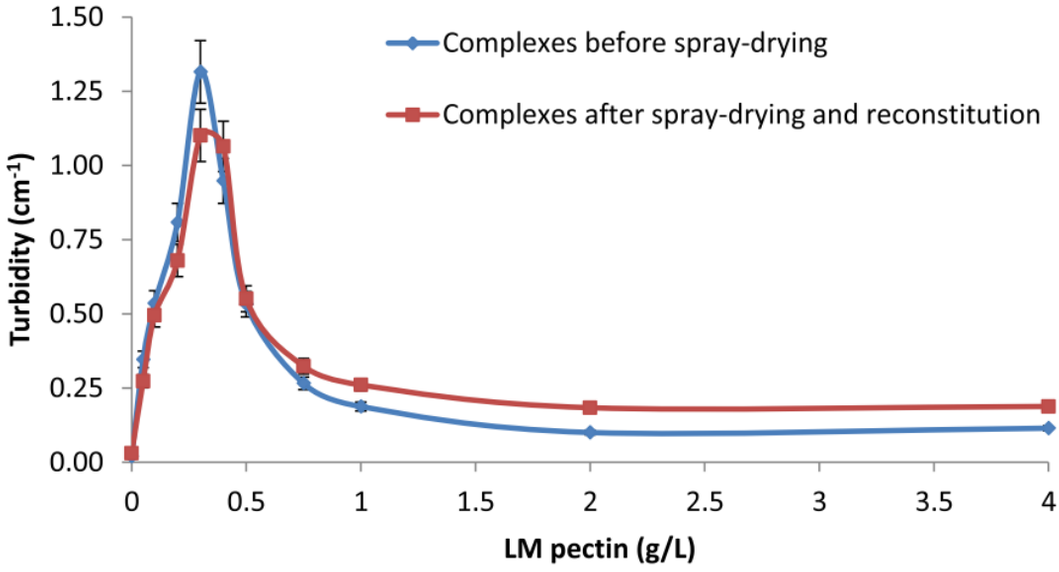

Figure 1.17: Turbidity of unprocessed and spray-dried lysozyme-pectin samples measured using UV-vis spectroscopy at 600 nm (Amara *et al.*, 2016).

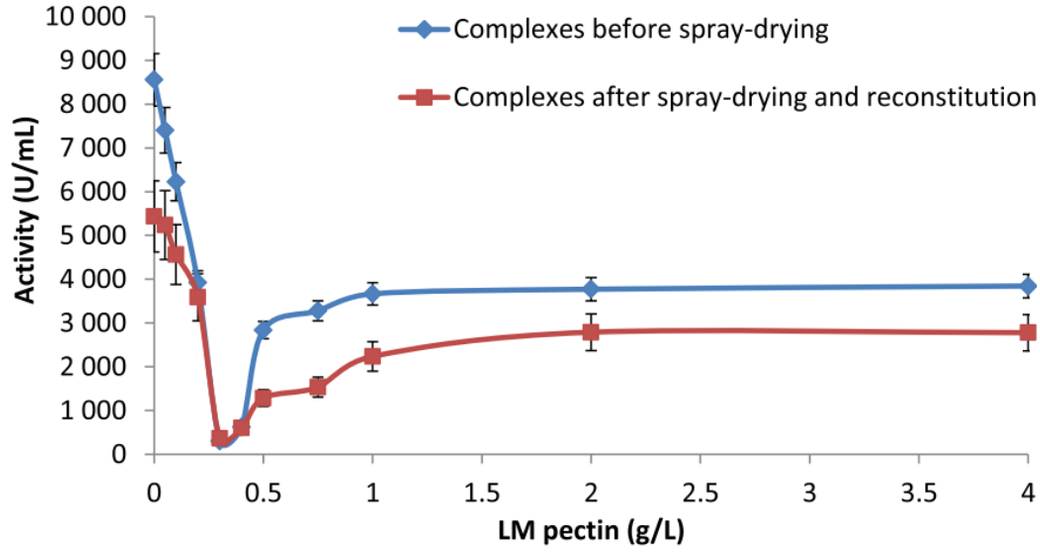

Figure 1.18: Bioactivity of unprocessed and spray-dried coacervated lysozyme at different pectin concentrations (Amara *et al.*, 2016).

Microencapsulation of nisin, a peptide synthesised by *Lactococcus lactis* was also demonstrated (Amara *et al.*, 2017). 10 g/L Nisin suspensions were prepared with 30 g/L pectin and 30 g/L alginate in 5 mM imidazole acetate buffer at pH 5. The prepared suspensions were spray-dried at an air inlet temperature of 180 °C and air outlet temperature being 90 °C. The nozzle size was 0.5 mm and the

feed flow rate was 0.5 L/h (Amara *et al.*, 2017). Turbidity and particle size measurements of nisin-pectin and nisin-alginate showed an increase and decrease, respectively, in the turbidity and particle size post spray-drying as shown in Figure 1.19. This indicated that spray-drying promoted and demoted aggregation in nisin-pectin and nisin-alginate complexes, respectively. Moreover, Figure 1.20 showed that the antimicrobial activity of nisin was the highest and that of nisin-alginate was the lowest. This result was in agreement with the data obtained from UV-Vis spectroscopic analysis showing that alginate could effectively protect the bioactivity of nisin post spray-drying.

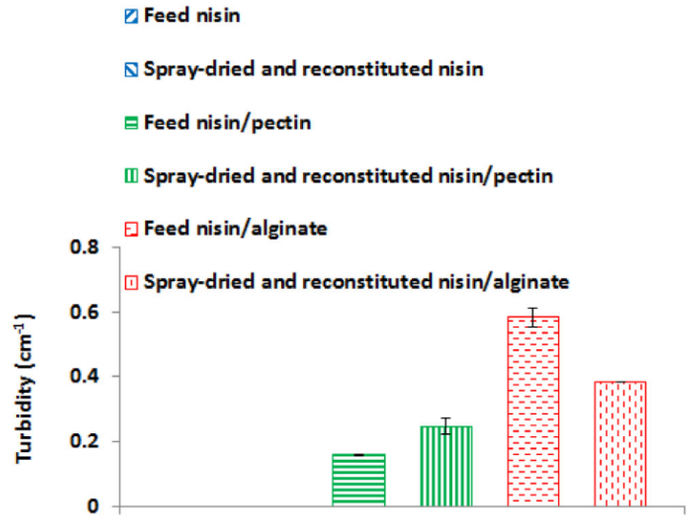

Figure 1.19: Turbidity of unprocessed and spray-dried nisin-pectin and nisin-alginate complexes (Amara *et al.*, 2017).

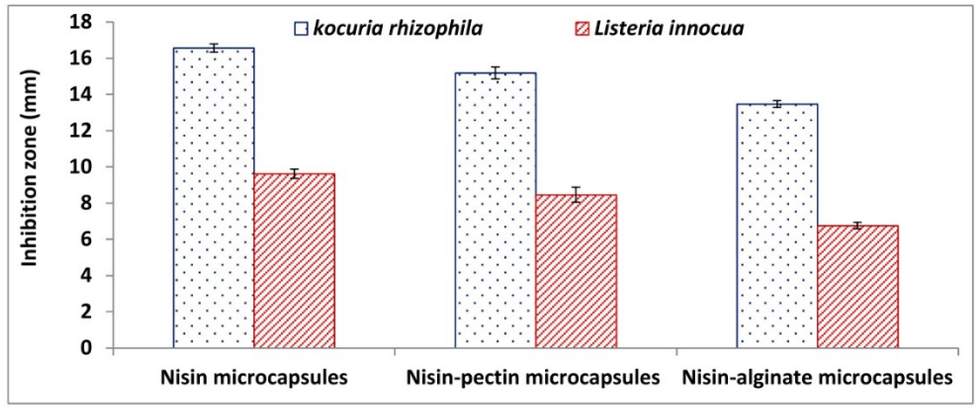

Figure 1.20: Antibacterial activity of spray-dried nisin, nisin-pectin and nisin-alginate complexes against Kocuria rhizophila and Listeria innocua (Amara *et al.*, 2017).

1.3.2.3 Spray-freeze-drying

The development of drying technologies over decades has shown vast implications in the food and the pharmaceutical industries. These techniques have been considered to exhibit promising results in terms of time, cost, efficiency, ease of use and reliability in the biopharmaceutical industry as well. Another such technique having potential applications in the area of bioproducts, and biologics is Spray-freeze-drying (SFD). Spray-freeze-drying was first introduced by Werly and Baumann in 1964 in their paper titled "Production of Submicronic Powder by Spray-freezing" (Werly and Bauman, 1964). Whilst being an unconventional drying technique, it produces distinctively powdered products and incorporates the benefits associated with conventional freeze drying as well (Ishwarya *et al.*, 2015). SFD is considered superior over other drying techniques in terms of product quality, structure and the retention of volatile and bioactive products (Ishwarya *et al.*, 2015).

Several advantageous of SFD have been mentioned. Firstly, SFD provides enhanced solubility of newly developed APIs that are not readily soluble in water (Vo *et al.*, 2013). Secondly, the ultra-fast freezing process allows the drug product to be amorphously distributed in the excipient material. This minimizes the phase separation between the excipient and the drug substance (Wanning *et al.*, 2015). Thirdly, along with producing flowable powder, SFD allows controlled particle-size distribution and is considered advantageous over conventional freeze-drying (Wanning *et al.*, 2015). Moreover, it is considered that SFD can process thermally sensitive products, which was a concern of spray-drying, (Cheow *et al.*, 2011) and provides improved reconstitution characteristics of polymeric nanoparticles (Ali and Lamprecht, 2014). Furthermore, SFD is favourable in terms of time, cost and energy consumption over conventional drying techniques (Claussen *et al.*, 2007).

1.3.2.3.1 Principle and Process of Spray-freeze-drying

SFD is typically understood as three major steps involving atomization of the liquid feed into droplets, freezing or solidification of the droplets in the presence of a cold fluid and sublimation of the droplets at low pressure and temperature (Leuenberger, 2002). SFD is a unique combination of freeze-drying

and spray-drying (Filkova *et al.*, 2007). Further application of SFD in encapsulation of sensitive active compounds has been mentioned (Ishwarya *et al.*, 2015). This technique has been specifically attractive for its ability to encapsulate sparingly soluble drugs in water, producing particles with unique aerodynamic properties for pulmonary delivery (Leuenberger, 2002; Sweeney *et al.*, 2005; D'Addio *et al.*, 2012; Y. Wang *et al.*, 2012). The spray-freezing step can occur by either spraying the liquid feed into a cold dry gas, by spraying into cryogenic liquid or by spraying the feed into cryogenic liquid in a gaseous headspace region (Ishwarya *et al.*, 2015). Likewise, it has also been mentioned that the freeze-drying step can be carried out under vacuum, at atmospheric pressure, at sub-atmospheric pressure or in a fluid bed under atmospheric or sub-atmospheric pressure (Ishwarya *et al.*, 2015).

The three major steps in the process of SFD are as follows:

1) Atomization of liquid feed, just like in the process of spray-drying, generates numerous tiny droplets by disintegrating the liquid feed containing the drug substance. Here the liquid stock could be either a solution or a suspension. SFD drying employs a variety of nozzles just as in the spray-drying process. These include hydraulic (one fluid) nozzles, pneumatic (two fluid) nozzles and ultrasonic nozzles. One fluid nozzle and two fluid nozzles are commonly worked with on SFD (Al-Hakim *et al.*, 2006). In the case of SFD, freezing may occur inside the nozzle due to the low temperatures in the spray-freezing step. Plastic nozzles or nozzle heaters are used to avoid this (Ishwarya *et al.*, 2015). The droplet size is determined by the atomization step and is not altered by the freezing or spray-freezing steps. In terms of obtaining economic production of high quality products, the choice of atomizer is important (Fellows, 2009).
2) Freezing of liquid droplets follows the atomization step. Thermal energy is transferred from the liquid droplet to the cold gas or cryogen to form ice particles. The effects of solutes and suspended particles on freezing and nucleation were studied. Hoffer reported that soluble salts caused depression in the freezing point of droplets, whereas insoluble salts increased the freezing point of the droplets (Hoffer, 1961). It was concluded that the depression in the freezing point was a function of solute concentration (Hoffer, 1961). The freezing phenomenon has been

explained in a number of steps (Figure 1.21) (Hindmarsh *et al.*, 2003; MacLeod *et al.*, 2006; Hindmarsh *et al.*, 2007): (a) Liquid cooling and supercooling; wherein the liquid droplets are cooled from an initial state to a supercooled state below the normal freezing point. (b) Nucleation; involving sufficient supercooling to allow formation of ice crystals. (c) Recalescence; at this step, supercooling permits further growth of the crystal. This results in an abrupt rise in temperature as latent heat of fusion is liberated during crystal growth. This phase terminates as the droplets reach an equilibrium freezing temperature.

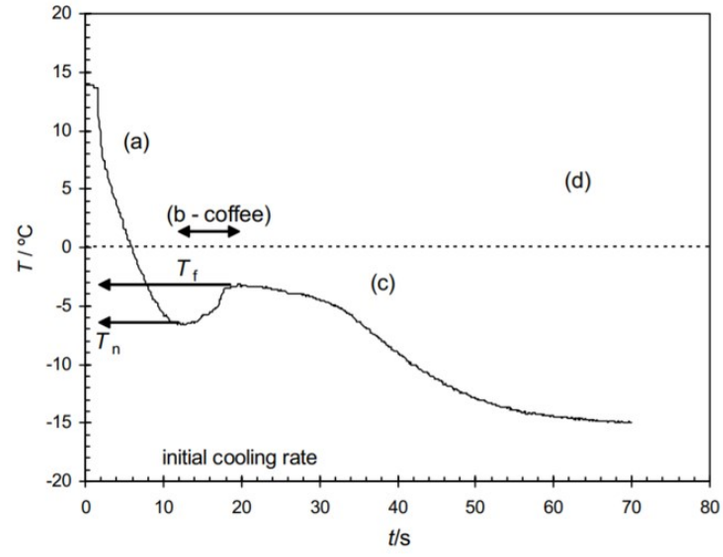

Figure 1.21: Time - Temperature data during spray-freezing of a droplet of coffee solution (MacLeod *et al.*, 2006).

(d) The freezing phase continues until further growth of the crystal is restricted by the rate of heat transfer to the surrounding atmosphere from the droplet. During this phase, the freezing point may be further lowered due to an increase in the solute concentration. This phase leads to a steady state wherein the temperature of the droplets falls near to that of the ambient air temperature.

3) The final step in the SFD process is similar to that of a conventional freeze-drying (lyophilisation) process. It involves primary drying which is followed by secondary drying as discussed in section 1.3.1.1.1.

1.3.2.3.2 Spray-freezing and Dynamic-freeze-drying Technology by Meridion Technologies

Meridion Technologies developed the SprayCon Lab® spray-freeze-dryer based on two patents by Sanofi Pasteur SA, Patent No: US10006706B2 (Luy *et al.*, 2018) and US9347707B2 (Struschka *et al.*, 2016). A schematic of the production-scale spray-freeze-drying process by Meridion Technologies is shown in Figure 1.22 (a). The transfer liquid vessel and the spray-freezing chamber are positioned over the rotary freeze-dryer connected through a cooled tube and a flap that tightly separates both process areas. The dried product is transferred from the drying chamber through a transfer tube into filling vessels Figure 1.22 (b) (Luy and Stamato, 2020).

This process is divided into two broad steps, namely, spray-freezing and dynamic freeze-drying. The spraying process employs a frequency-driven prilling nozzle. The liquid feed disintegrates into round droplets at the resonance frequency and are guided by gravity into the freezing chamber. The flow rate, nozzle frequency, viscosity and orifice diameter influence the droplet size. It has been reported that approximately 1000 – 5000 droplets/s can be generated (Mishra, 2015; Luy and Stamato, 2020). The freezing chamber is a double-walled, cylindrical vessel into which the droplets are frozen using a cryogenic medium (liquid N_2 and gas N_2). The droplets are not directly in contact with N_2 (l). Sterile N_2 (g), at an operating temperature in the range of – 80 °C to – 150 °C is filled inside the chamber where heat exchange occurs by convention. Several parameters such as gas temperature, droplet size, T_g, total solid content and the height of the freezing chamber impact the rate of freezing of the droplets. Typically, uniform frozen spheres of a size of 300 – 1000 µm can be generated in 1 – 3 s of travelling 1.5 m – 3.5 m (Luy and Stamato, 2020).

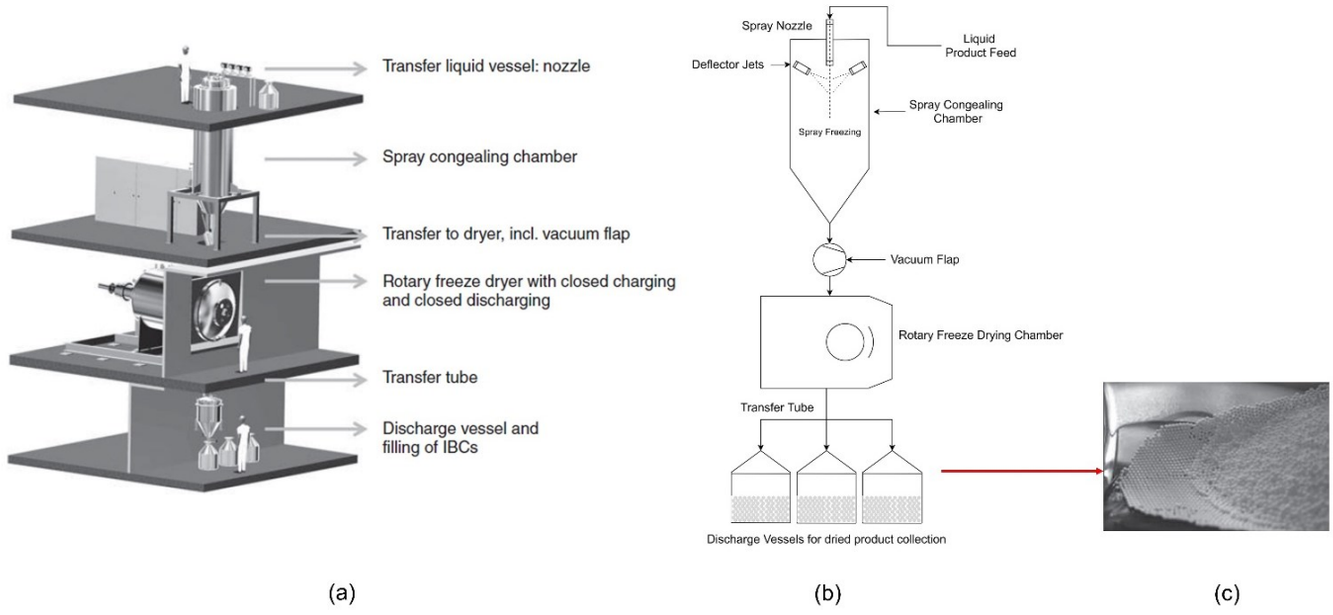

Figure 1.22: (a) A pictorial representation, (b) process flow diagram of the Spray-freeze-Drying process and (c) Spray-freeze-dried microspheres by Meridion Technologies. Adapted from (Luy and Stamato, 2020).

Post spray-freezing, the dynamic freeze-drying process involves a rotary freeze-dryer made of a cylindrical drum located inside a double-walled vacuum drum. For sterile operation, the freezing chamber and rotary freeze-dryer are connected through an isolation valve. The rate of sublimation is increased as a result of the constant rotary motion of the drum along its longitudinal axis and increase in temperature. Conductive heat transfer to the product is achieved by silicon oil that flows through the double-walled surface and by IR radiators installed inside the drum. The vacuum is set to 100 µbar or lower. Moreover, the cross-sectional area for the flow of water vapour is significantly increased through the opening located at either ends of the drum. By reverse rotation of the drum, the dried bulk product spheres are taken up by discharge scoops that are directed downwards through a funnel for final collection or filling Figure 1.22 (a) (Luy and Stamato, 2020).

Free-flowing, homogeneous spray-freeze-dried spheres generated using SprayCon Lab® technology by Meridion Technologies and Lynfinity® technology by IMA Life are shown in Figure 1.23 (a) and (b) respectively. Lynfinity® technology is described in section 1.3.2.3.3.

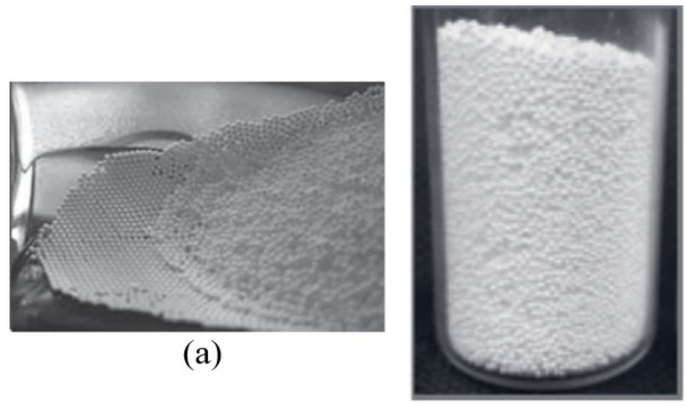

Figure 1.23: Spray-freeze-dried spheres by (a) Meridion Technologies (Luy and Stamato, 2020) and (b) IMA Life (IMA Life, 2019b).

Reported benefits of this technology are described here. Unlike conventional lyophilization, the large surface area of the frozen spheres confers increased heat and mass transfer, thereby, reducing the total drying time. Reduction in the water vapour diffusion length is achieved in a spray-frozen microsphere with a diameter of 1 mm and maximum diffusion length 500 µm compared to a 10 mm thick freeze-dried cake with a maximum diffusion length of 10000 µm (Luy and Stamato, 2020). Heat transfer is achieved by both the rotating drum surface as well as the IR radiators. Residual moisture content of the dried microspheres of ≤ 1 % can be achieved. While a recommended total solid content of 5 – 10 % in the product feed allows strong spherical structures, drying of the product feed with higher solid content of up to 40 % can be achieved in a short drying time. Moreover, even though particle size of < 300 µm is achievable during spray-freezing, the presence of high solid content reduces the risk of loss of particles due to a high rate of sublimation. The risk of particle loss for product feed with low solid content can be reduced by generating larger particle sizes i.e. 2 – 3 mm (Luy and Stamato, 2020). It has been reported that the time required for spray-freezing a 100 L bulk with 20 % solid content is ~ 10 to 20 h and the time required for dynamic freeze-drying is ~ 24 h with > 97 % yield (Luy and Stamato, 2020).

1.3.2.3.3 Continuous Aseptic Spray-freeze-drying Technology by IMA Life

IMA Life America INC. invented and patented a bulk freeze-drying process design using a combination of Spray-freezing and Stirred drying, Patent No: US9052138B2 (DeMarco and Renzi, 2015). The process flow begins with the freezing step involving spraying of the bulk product along with an aseptic freezing medium into an aseptic freezing vessel. This is followed by introduction of a vacuum to the frozen powder to initiate sublimation. The frozen material is stirred using a spiral blade agitator at a low speed. Subsequently, the frozen powder is heated to increase the rate of sublimation. Lastly, the vacuum is released to obtain the final freeze-dried product.

With modifications to the patent, IMA Life developed the Lynfinity® spray-freeze-dryer. A schematic diagram of the Lynfinity® process is depicted in Figure 1.24. The spraying process begins with the generation of uniform droplets under the influence of frequency vibrations as the product feed is made to flow through a temperature-controlled droplet zone. The disintegrated product feed passes through the nozzle into the freezing column where the freezing process begins. The stainless-steel freezing column is lined with a double walled jacket that utilizes liquid nitrogen and silicone oil for controlling the temperature in the chamber. The cooling gas is maintained at temperatures below – 130 °C. As the droplets are sprayed into the column, they are instantaneously (in less than 5 feet from the point of ejection with an average volumetric diameter of 500 µm) frozen allowing them to maintain their shape (Figure 1.24 (b)) (IMA Life, 2019c). The frozen spheres are collected at the base of the freezing chamber (Figure 1.24).

Before entering the drying module, an intermediate chamber allows the product to be transferred from the freezing column at atmospheric pressure to the drying chamber under vacuum conditions without disrupting the continuous process. The movement of frozen spheres inside the drying chamber is carried out at a controlled rate on cascading shelf stacks using gentle vibratory agitation. Agitation through vibration along with heat through heat transfer fluid initiates rapid sublimation and prevents agglomeration of the spheres inside the drying chamber. Post drying, the dried spheres are collected as bulk in the collection chamber (Figure 1.24) (IMA Life, 2019c). Unlike a conventional freeze-dryer, the Lynfinity® contains dual ice condensers allowing continuous operation (IMA Life, 2019c).

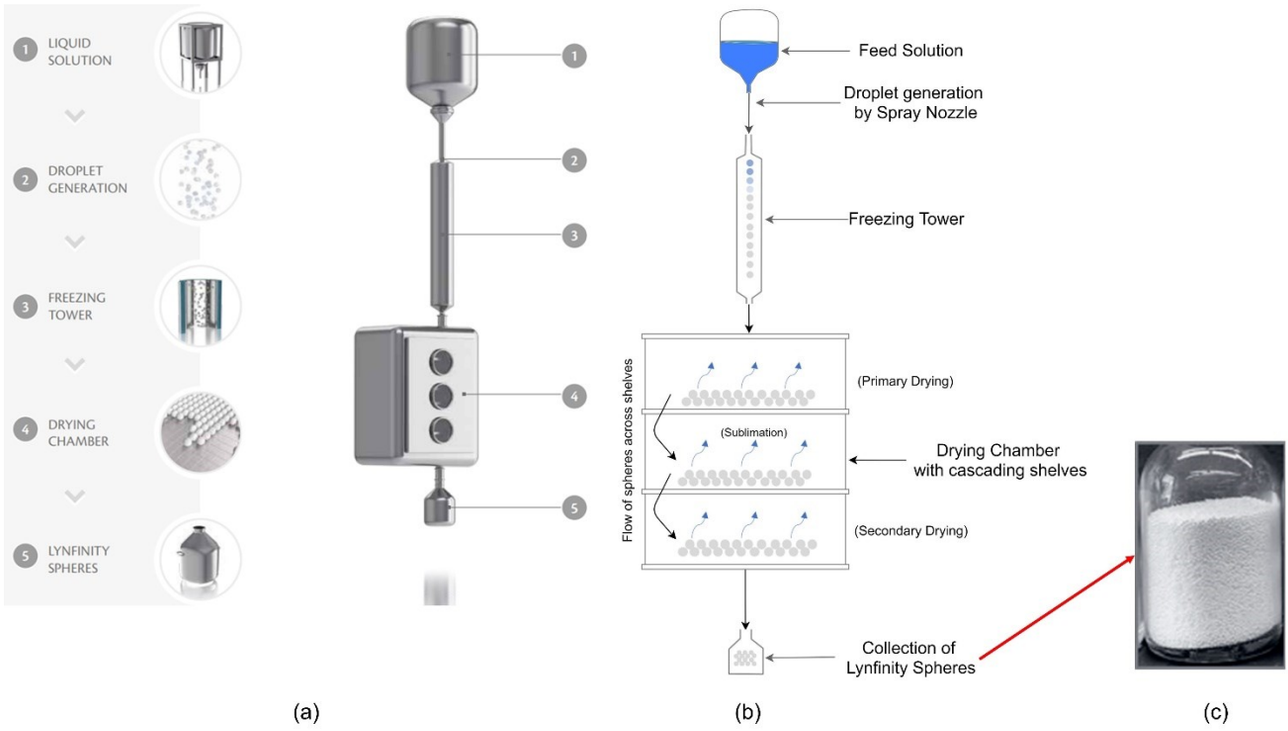

Figure 1.24: (a) A pictorial representation, (b) process flow diagram of the LYnfinity® Spray-freeze-drying process and (c) Spray-freeze-dried spheres by IMA Life. Adapted from (IMA Life, 2019a).

The Lynfinity® production-scale spray-freeze-dryer is show in Figure 1.25. Anticipated benefits of this technique over conventional freeze-drying include bulk processing with minimal handling of trays without the need for post-processing operations such as granulation and milling (Siow *et al.*, 2018) along with higher productivity and lower downtime (IMA Life, 2019c). Secondly, it confers increased efficiency of heat and mass transfer between the product, trays and shelves (IMA Life, 2019c). Thirdly, it may establish a continuous process in a sterile environment with greater throughput flexibility (DeMarco and Renzi, 2015). The specific surface area of the dried spheres was measured using BET and was found to be 7.03 m^2/g, compared to freeze-dried cakes (0.47 m^2/g), allowing greater interaction with solvent during rehydration (IMA Life, 2019b). Moreover, the dried spherical product can be distributed into syringes, vials, inhalation systems etc. which is not possible with freeze-dried cakes (IMA Life, 2019c). Continuous bulk processing can allow the use of more PAT tools for real-time process and product monitoring.

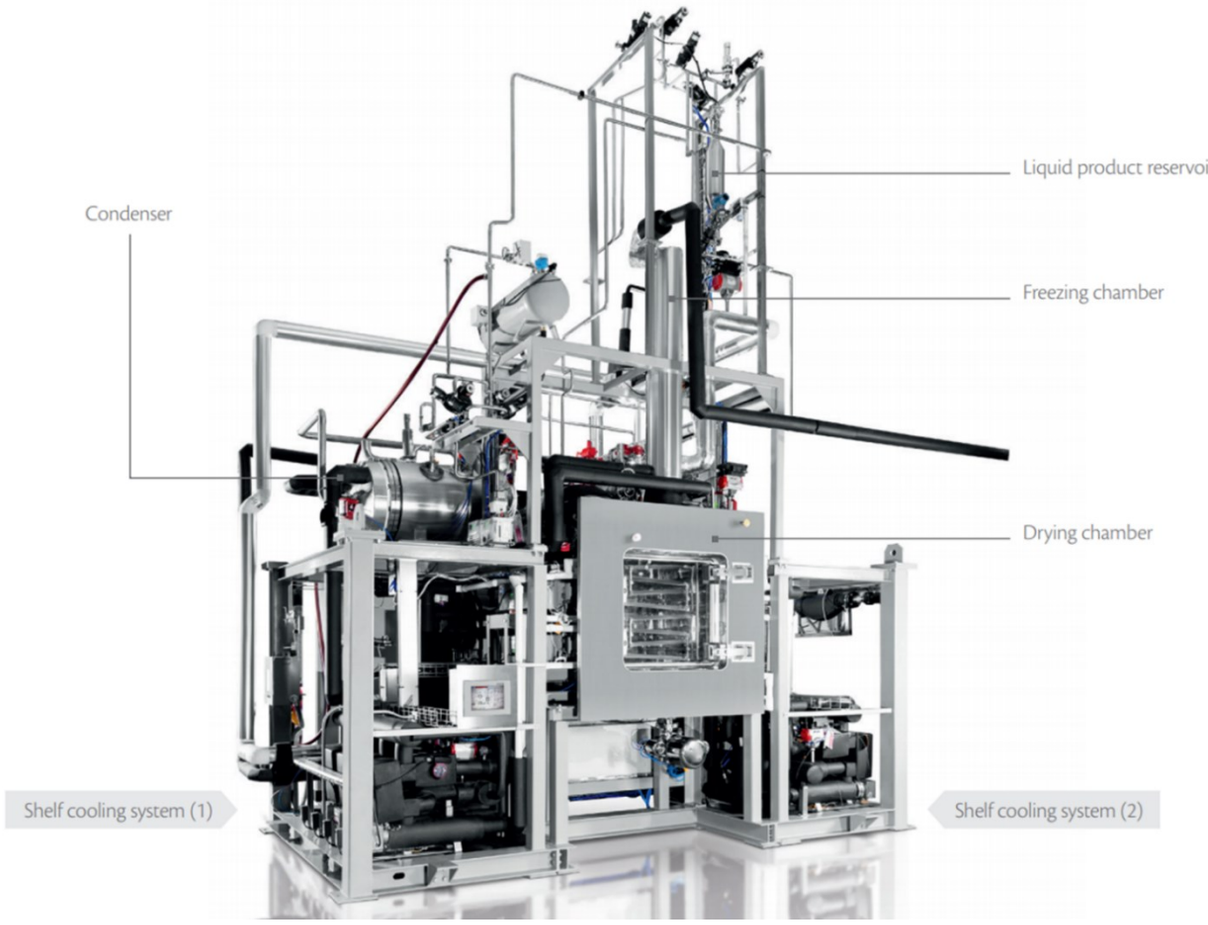

Figure 1.25: LYnfinity® Spray-freeze-dryer. Reprinted from (IMA Life, 2019c).

1.3.2.3.4 Effects of Spray-freeze-drying on the stability of pharmaceuticals

When talking about the stability of biologics, protein denaturation and aggregation are hurdles that have been dealt with and are still a concern. Pharmaceutical aggregation occurs due to high surface energy. This makes the product unstable and unfit for therapeutic purposes and prevents it from delivering the intended properties at the target site (Ishwarya *et al.*, 2015). To combat such stability concerns, it has been asserted that the use of freezing adjuvants and excipients that provide an encapsulation effect prior to the atomization process can be a beneficial approach (Ishwarya *et al.*, 2015). One of the factors responsible for influencing protein stability was observed to be specific surface area (SSA) as denaturation is facilitated at the air-particle interface and so reduced surface area promoted protein stability (Costantino *et al.*, 2000; Yu *et al.*, 2004). It has been mentioned that high SSA is required to maintain proper drug release and encapsulation, hence, a balance between the levels of protein and SSA needs to be achieved (Costantino *et al.*, 2000).

Furthermore, IMA Life reported some product quality attributes post spray-freeze-drying using Lynfinity® technology. Comparable reconstitution time was observed between spray-freeze-dried and conventionally lyophilised products. Increased turbidity was observed in the rehydrated spray-freeze-dried product due to particle aggregation (Figure 1.26) (IMA Life, 2019b). On the other hand, increased wettability and faster reconstitution was reported in polyvinyl alcohol and polyvinylpyrrolidone based drug formulations that exhibit poor water solubility. Additionally, a potential benefit of using surfactants in protein formulations could reduce protein aggregation, thereby, reducing turbidity in rehydrated spray-freeze-dried samples (IMA Life, 2019b).

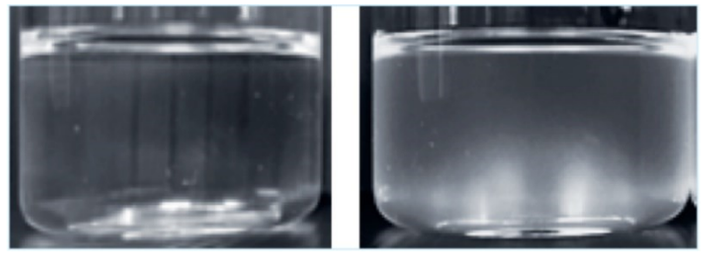

Figure 1.26: Rehydration characteristics of control drug product (left) and spray-freeze-dried product (right) (IMA Life, 2019b).

1.3.2.4 PRINT® Technology

Particle Replication in Non-Wetting Templates, also known as PRINT® technology, originated from lithographic techniques applied in the microelectronics and semiconductor industry. PRINT® is a micro-moulding based particle design / engineering technology employed to generate monodisperse, uniquely shaped (i.e. filaments, rods, spheres, discs, toroids) micro and nano-particles of hydrogels, polymers, APIs etc. with tunable size and morphology (Kelly and DeSimone, 2008; Garcia *et al.*, 2012; Galloway *et al.*, 2013). The fabrication of PRINT® particles was first demonstrated by Rolland *et al.* (Rolland *et al.*, 2005) and the pharmacokinetic characteristics of these particles as delivery vectors were first studied by Euliss *et al.* and Gratton *et al.* (Euliss *et al.*, 2006; Gratton *et al.*, 2007). Kelly and DeSimone demonstrated the generation of protein particles, namely, insulin and albumin using PRINT® technology (Kelly and DeSimone, 2008). With the incorporation of cGMP practices, this technique has been scaled-up with continuous roll-to-roll system which allows continuous

particle production for pre-clinical and clinical study of pharmaceutical inhalation powders by Liquidia Corporation (DeSimone, 2016; Liquidia Corporation, 2021).

The process flow for generating PRINT® particles reported by authors is discussed here (Gratton *et al.*, 2007; Kelly and DeSimone, 2008; Garcia *et al.*, 2012). Perfluoropolyether (PFPE) was poured onto a prepared silicon master template containing the desired etching patterns of 2 µm, 5 µm and 200 nm sized shapes to produce a mould containing the same sized cavities (Figure 1.27 (a)). Following the preparation of the PFPE mould, aqueous protein samples containing insulin, albumin and albumin mixtures with siRNA or paclitaxel were sandwiched between the cavities present in the mould and a high surface energy polyethylene film (Figure 1.27 (b)). A pressure of 50 psi was applied through a roller to prevent the formation of layers between the filled cavities and to laminate the samples present between the mould and the film (Figure 1.27 (c)). Subsequently, the polyethylene film was removed and the mould containing the samples was freeze-dried (Figure 1.27 (d)). The dehydration process can also occur through either photocuring, vitrification or evaporation (Xu et al., 2013). A liquid harvesting layer, made of either polycyano acrylate (PCA) or polyvinyl pyrrolidinone (PVP), was casted onto a glass slide (Figure 1.27 (e)). Post freeze-drying, the PFPE mould was placed over the adhesive harvesting film (Figure 1.27 (f)). Once the harvesting layer was dried, the PFPE mould was removed yielding dried protein particles on the adhesive film (Figure 1.27 (g)). Finally, free-flowing protein powder was recovered by dissolving the adhesive film (Figure 1.27 (h and i)). SEM images of the uniquely shaped powders are shown in Figure 1.28.

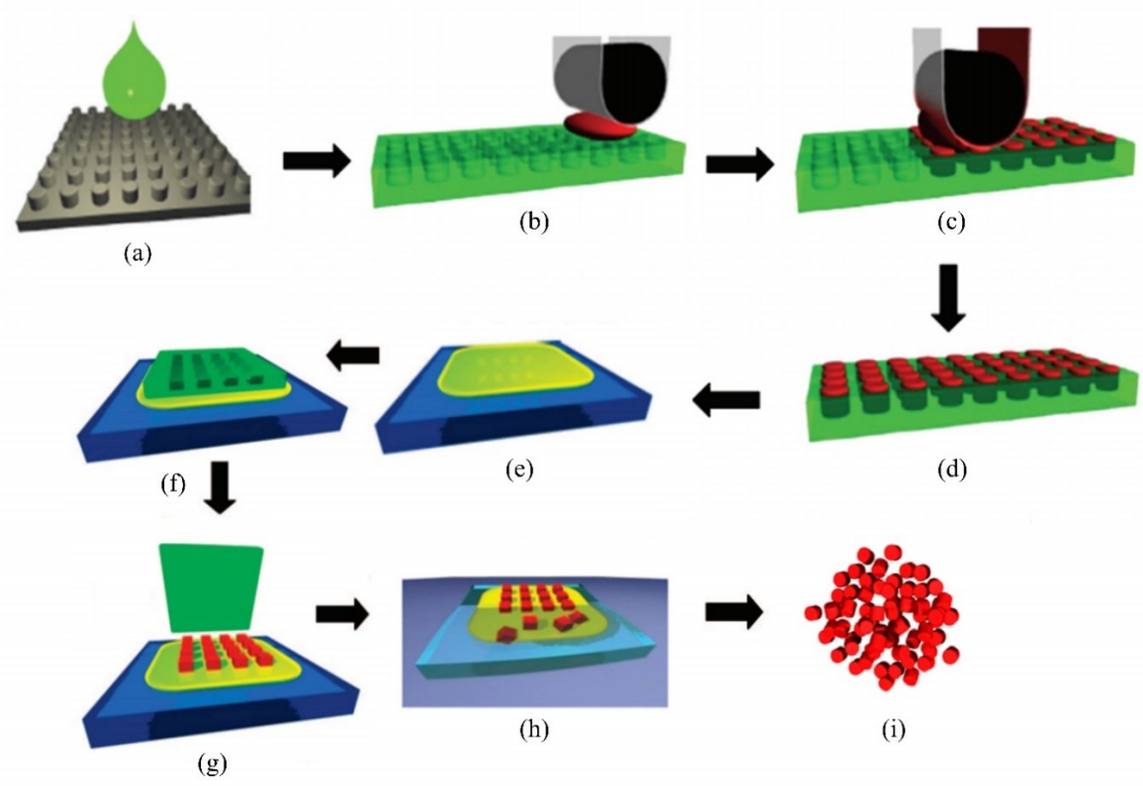

Figure 1.27: The process flow diagram of PRINT® Technology. Reprinted (adapted) from (Kelly and DeSimone, 2008; Garcia *et al.*, 2012; Hofmann *et al.*, 2019) with permission from ACS and Hindawi Publishing Corporation.

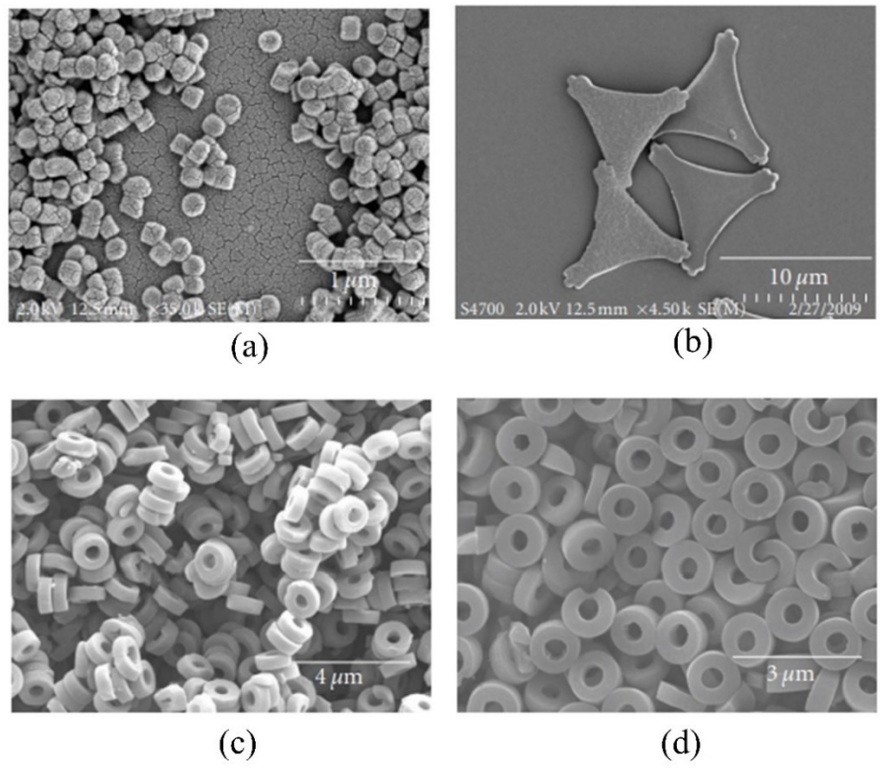

Figure 1.28: SEM images of (a) 200 × 200 nm cylindrical BSA-Lactose, (b) 10 µm pollen IgG-Lactose, (c) 1.5 µm torus DNase and (d) 1.5 µm torus siRNA PRINT® fabricated particles. Reprinted (adapted) from (Garcia *et al.*, 2012) with permission from Hindawi Publishing Corporation.

It was shown that no aggregation was observed in albumin and insulin particles generated via PRINT® technology. Additionally, Pulmozyme (DNase) and siRNA therapeutic molecules were processed using PRINT® technology (Garcia *et al.*, 2012). Minimal aggregation was observed in the size exclusion chromatography (SEC) profile of DNase PRINT® microparticles with comparable enzyme activity to native DNase and the chemical structure of PRINT® generated siRNA particles was preserved without any denaturation.

Furthermore, PRINT® technology was combined with a scalable Spray-Assisted layer-by-layer (LbL) technique to enhance the characteristics of the fabricated nanoparticles (Morton *et al.*, 2013). The combination of these techniques offer improved stability, sustained drug release and improved physicochemical properties of nanoparticles (Poon, Chang, *et al.*, 2011; Poon, Lee, *et al.*, 2011; Morton *et al.*, 2013). In this case, the polyvinyl alcohol (PVA) harvesting layer was crosslinked using 50 % glutaraldehyde and 10 % hydrochloric acid to reduce its solubility in water. This was carried

out to prevent any loss of particles during the spraying process. An aqueous solution of cationic polyelectrolyte was sprayed at a concentration of 1 mg/mL onto the nanoparticles for 3 s. To remove excess cationic polyelectrolyte, a wash step with water was included for another 3 s. This was followed by another spray of anionic polyelectrolyte at a concentration of 1 mg/mL for 3 s and a final wash with water. The sprayed-LbL particles were finally recovered by sonification, 0.45 μm filtration and ultracentrifugation. DLS analysis showed consistent monodisperse particles with the polydispersity ranging between 0.01 and 0.1 and hydrodynamic diameter between 190 nm – 246 nm for uncoated and coated nanoparticles (Morton *et al.*, 2013). A decrease in the hydrodynamic diameter of coated particles was observed due to contraction forces on the PVA layer. The shape and integrity of the recovered particles was confirmed by electron microscopy images wherein particles were entirely coated by polyelectrolytes. Moreover, the biological functionality of these particles was retained and could be fine-tuned by altering the film thickness as per its application.

Furthermore, researchers developed cylindrical nanoparticles of commercially available vaccines, such as Fluzone® (Sanofi-Pasteur), Fluvirin® and AgriFlu® (Novartis) and Afluria® (Merck), using this technology (Galloway *et al.*, 2013). PRINT® fabricated vaccine particles showed 200-fold improved antigen binding along with enhanced immune response. It was elucidated that the shape, size along with other surface properties play an important role in the interaction of these nanoparticles with other biomolecules in their surroundings (Galloway *et al.*, 2013). Xu et al. demonstrated the fabrication of transiently insoluble BSA particles after being cross-linked by a disulphide-based cross-linker using PRINT® with new opportunities for drug and gene delivery (Xu *et al.*, 2012). More recently, results of a phase 1 clinical trial study reported for a PRINT® fabricated dry-powder ribavirin formulation by GSK showed improved physicochemical properties, efficient and convenient delivery of API to the lungs (Dumont *et al.*, 2020).

Overall, this technology has shown promising results for some inhaled proteins, gene therapy products and vaccines with the ability for continuous production in a large-scale cGMP facility, though the stability of large parenteral mAbs and enzymes via PRINT® will be an interesting area of study.

1.3.2.5 Microglassification™

In therapeutic protein formulations water substitution by excipients, generally saccharides and polyalcohols, stabilize therapeutic proteins in their dehydrated state (Allison *et al.*, 1999) (Liao *et al.*, 2002) (Mensink *et al.*, 2017a). Aniket *et al.* developed a new technique called Microglassification™ for the preservation of proteins by dehydrating protein microdroplets in an immiscible drying solvent (Aniket *et al.*, 2014). The technique was performed at room temperature and produced stable, excipient-free protein microglassified beads. The technique was performed using two chambers; one containing BSA solution and the other filled with an organic solvent (Su *et al.*, 2010) (Aniket *et al.*, 2014). A small plug of organic solvent, either pentanol or decanol, was withdrawn into a micropipette. The micropipette was then positioned into the chamber containing BSA solution and the desired amount of protein was pulled into it. The micropipette was then positioned back into the organic chamber, releasing a single droplet of the protein solution which was held firmly at the tip of the micropipette in the organic chamber. By doing so, water from the single droplet was extracted into the organic chamber, thereby, leading to the formation of a microglassified™ bead (Figure 1.29).

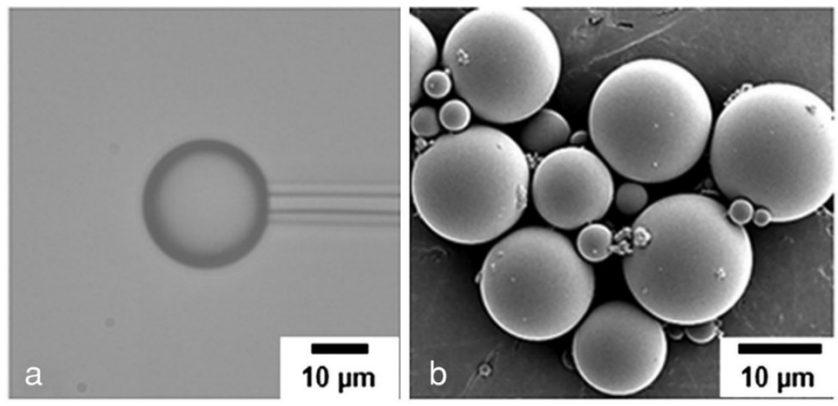

Figure 1.29: (a) Optical image of Microglassified™ BSA in decanol. (b) SEM image of Microglassified™ beads (Aniket *et al.*, 2014).

Through one of their studies, they demonstrated this technique on model protein BSA and studied the reconstituted protein characteristics using FTIR, fluorescence, XRD and gel electrophoresis (Aniket *et al.*, 2014). BSA concentration, measured using UV-Vis spectroscopy, Bradford assay and BCA

assay, exhibited full protein recovery with no sign of insolubility. FTIR analyses showed that the secondary structure of microglassified™ BSA was restored upon rehydration. Minor changes observed in the α-helix and β-sheet content of BSA were reversible and did not result in protein unfolding. The fluorescence spectra of native and rehydrated microglassified™ BSA were comparable, showing that the tertiary structure of BSA was preserved. The microglassified™ beads were purely amorphous which was shown through X-ray diffraction spectroscopy. This was due to rapid dehydration of the microdroplet which did not give enough time for crystallization. Furthermore, protein aggregation was studied through gel electrophoresis. The reconstituted microglassified™ BSA resulted in 3.3 % of aggregates, whereas the rehydrated lyophilized sample exhibited a higher content of aggregates (10 %) showing that microglassification™ induced lower stress on the protein compared to lyophilization (Aniket *et al.*, 2014). They also used a digital DR-A1 Abbe refractometer as an independent method to determine protein concentration in the microglassified™ bead. As water is withdrawn from the protein droplet into the drying medium, the density of the protein microdroplet increases, which increases the refractive index of the droplet. This change in the refractive index of the microdroplet with respect to the drying solvent is correlated to the change in the protein concentration. Accelerated storage results for microglassified™ BSA showed that by increasing the saturation factor of water to 0.4 – 0.5, there was a drastic decrease in the soluble monomeric content of BSA after just the first 10 min of storage at 65 °C. This meant that by increasing the availability of water to the microglassified™ bead, an increase in the formation of protein aggregates was observed for a total of 60 min of storage at 65 °C. Native gel electrophoresis along with $A_{278\ nm}$ measurements were used to quantify the percentage of BSA monomer.

Through another study, microglassification™ was performed on lysozyme, α-chymotrypsin, catalase and horseradish peroxide (Aniket, Gaul, *et al.*, 2015). Five different organic solvents, namely, *n*-pentanol, *n*-octanol, *n*-decanol, triacetin and butyl lactate were used as immiscible drying solvents. In this study, the refractive index method was used to measure the water solubility in the drying solvent. It was reported that butyl lactate showed higher water solubility compared to other solvents (Aniket, Gaul, *et al.*, 2015). FTIR analyses showed that even though distortions in the secondary

structural conformation of microglassified enzymes, mainly transformation from the α-helix to β-sheet structure were observed, these changes reverted to their native-like conformation upon reconstitution. Moreover, the microglassified^{TM} enzymes exhibited significantly higher activity in *n*-pentanol compared to triacetin and butyl lactate. Accelerated storage results for lysozyme showed significant reduction in enzyme activity of the microglassified^{TM} and lyophilised samples after 1 month of storage at 40 ºC. Bioactivities of both microglassified^{TM} and lyophilized enzyme were comparable. Through FTIR analyses, the reduction in enzyme activity was explained by the significant decrease in the β-sheet content and increase in the random structures. Post 1 month and up to 3 months of storage, minimal changes in the enzyme activity and secondary structure content was observed (Aniket, Gaul, *et al.*, 2015).

Furthermore, the potential to MicroglassifyTM a recombinant biopolymer – elastin-like polypeptide (ELP) with controlled size and morphology for chemotherapy has been shown (Aniket, Tang, *et al.*, 2015). More recently, this technique has seen application in the fabrication of biolasers for biosensing and optical device implantation purposes (Nguyen *et al.*, 2019; Nguyen and Ta, 2020). In summary, this technique has demonstrated the potential as a novel drying technique on a wide range of enzymes without the incorporation of any excipients at room temperature. Further study is required to elucidate its application to large-scale biopharmaceutical manufacturing along with the time associated with the formation of MicroglassifiedTM beads and their reconstitution. Moreover, the evaluation of MicroglassificationTM on commercial enzymes, mAbs, vaccines and the development of high concentration biopharmaceutical parenteral formulations are areas that can increase the scope of this technique.

In summary, this technique has demonstrated the potential as a novel drying technology on a wide range of enzymes without the incorporation of any excipients at room temperature. Efforts have been made to implement this technique at bulk scale, though further study is required to elucidate its application to large-scale biopharmaceutical manufacturing along with the time associated for the formation of microglassified^{TM} beads and reconstitution. Evaluation of microglassification^{TM} on commercial lyophilised biologics, development of high concentration biopharmaceutical parenteral

formulations and controlled release of drugs by encapsulation are areas that can increase the scope of this technique.

1.3.3 Other Drying Technologies

In addition to some of the potential alternative drying technologies described in this review, other drying techniques such as Microwave drying, Foam drying, Vacuum drying, Supercritical Fluid drying, Electrospinning, Fluidized bed drying, Hybrid drying etc. are gradually gaining popularity as alternatives to freeze-drying of biopharmaceuticals as well but are beyond the scope of this review. Recently, authors have demonstrated Microwave vacuum drying via REV^{TM} technology to produce efficacious and stable biopharmaceuticals, including a live virus vaccine, with an 80 % reduction in the time associated with batch freeze-drying (Bhambhani *et al.*, 2021). Similar studies exploiting microwaves for the drying of mAbs, have been found in literature as Microwave-assisted freeze-drying (Gitter *et al.*, 2018, 2019). Moreover, Electrostatic Spray-drying (ESD) is a promising technology as exposes products to reduced thermal stress than traditional spray-drying (Tejasvi Mutukuri *et al.*, 2021). Furthermore, various other microsphere generation technologies under evaluation have been listed in Table 1.6. For further reading on other drying technologies, readers are referred to the cited reviews herein (Walters H. *et al.*, 2014; Emami *et al.*, 2018, 2022; Vass *et al.*, 2019a; Durance *et al.*, 2020; Lovalenti and Truong-Le, 2020; Thorat *et al.*, 2020; Pardeshi *et al.*, 2021; Farinha *et al.*, 2022; Munir *et al.*, 2022).

Table 1.6: Microsphere Technologies under evaluation for pharmaceuticals.

Microsphere Technology	Manufacturer	Reference
Q-Sphera™ Technology	MidaTech Pharma	(Seaman *et al.*, 2019; Midatech Pharma, 2021)
iSPHERE™ Technology	Pulmatrix	(Pulmatrix, 2021)
Kureha Microsphere Technology	Kureha	(Kureha, 2019; Vhora *et al.*, 2019)
Plexis® Technology	Auritec Pharmaceuticals	(Auritec Pharmaceuticals, 2016; NCT03626714, 2019)
Stratum™ Technology	Orbis Biosciences	(Dormer *et al.*, 2016; Vhora *et al.*, 2019)
FormEZE™ Microparticle Technology	Evonik Industries	(Evonik, 2015; Vhora *et al.*, 2019)

1.4 Biopharmaceutical Characterization

As described in the ICH Q5E guidelines, product comparability subject to any changes in the manufacturer's manufacturing process requires the evaluation of the impact of an alternative process on the safety, quality and efficacy of biopharmaceutical products (ICH, 2004). Any aberrations in the CQAs of biopharmaceutical products post drying can be assessed using various analytical and characterization techniques. Figure 1.30 shows a comprehensive list of techniques currently employed to study some of the product CQAs in the solid and liquid-state. Some of these techniques are not employed for routine analyses but can provide additional information in understanding the impact of CPPs on product CQAs. These techniques are broadly categorised as spectroscopic, chromatographic and thermoanalytical techniques.

While some chromatographic and spectroscopic techniques are employed as QC release tests, they fail to provide intricate and high-resolution information in understanding protein stability and their interactions with excipients in the solid-state. Solid-state Hydrogen Deuterium Exchange – Mass Spectrometry (ssHDX-MS) (Moorthy *et al.*, 2014; Wilson *et al.*, 2019; Kammari and Topp, 2020) and solid-state Photolytic Labelling – Mass Spectrometry (ssPL-MS) (Iyer *et al.*, 2013, 2016) are

novel, high resolution mass spectrometric techniques that have provided further insights in understanding and elucidating protein stability. HDX-MS has been previously demonstrated to study the conformational stability of proteins in liquid solutions (Wales and Engen, 2006; Tsutsui and Wintrode, 2007; Houde *et al.*, 2011), in frozen solutions (Zhang *et al.*, 2011, 2012) and protein adsorption onto solid surfaces (Zhang and Smith, 1993; Buijs *et al.*, 1999, 2000, 2003). One of the potential applications of this technique is predictive stability. Moreover, this technique offers an insight into protein degradation in the solid-state which is a poorly understood area. In addition to the application of NMR in studying protein-excipient interactions (Tian *et al.*, 2007; Yoshioka *et al.*, 2011; Mensink *et al.*, 2016; Chen, Ling, *et al.*, 2021), time-domain Nuclear Magnetic Resonance Spectroscopy (TD-NMR) has been demonstrated to determine the residual moisture content (RMC) in freeze-dried biopharmaceuticals (A. Abraham *et al.*, 2019). Also, NMR coupled with Magnetic Resonance Imaging (MRI) has been studied to determine complete reconstitution of freeze-dried products (Partridge *et al.*, 2019). More recently, the determination of reconstitution time of freeze-dried BSA has been demonstrated using fluorescence spectroscopy (ElKassas *et al.*, 2021). Furthermore, advancements in CD spectroscopy have allowed researchers to study intricate information in the lower vacuum ultraviolet (VUV) region (< 190 nm) using Synchrotron Radiation Circular Dichroism Spectroscopy (SRCD) spectroscopy (Wallace *et al.*, 2004; Miles and Wallace, 2006, 2020; Miles *et al.*, 2008; Wallace, 2009, 2019). SRCD has also seen application in protein photostability, photoisomerization, protein-ligand interactions and RNA characterization (Hussain *et al.*, 2018; Nasser *et al.*, 2018; Auvray *et al.*, 2019; Wien *et al.*, 2021).

Overall, the characterization techniques listed in Figure 1.30 may have certain merits and demerits on their own but if employed as complimentary techniques, they can provide further insights on biopharmaceutical stability. These characterization techniques combined with different drying technologies can help the biopharmaceutical industry in choosing appropriate methods for manufacturing and testing their products. Some of these techniques are described in the following sections.

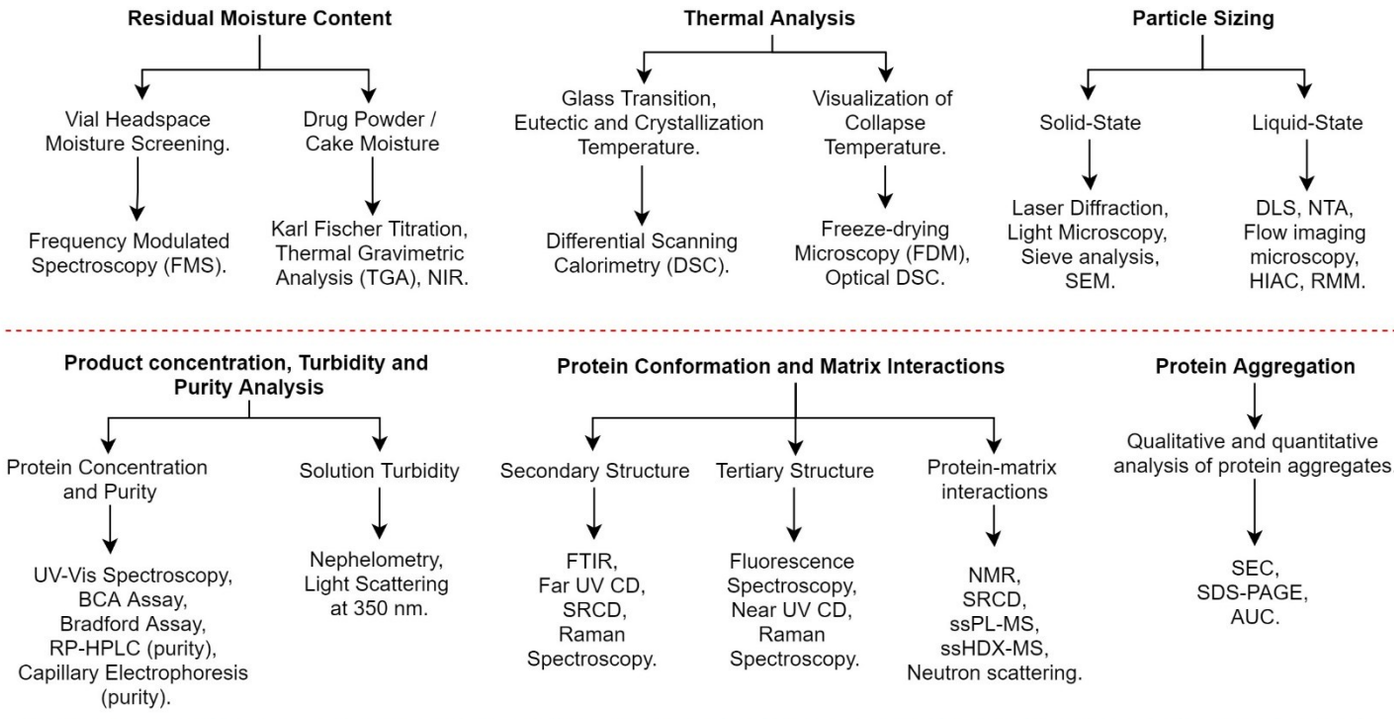

Figure 1.30: Offline analytical and characterization techniques for biopharmaceutical products. AUC, Analytical Ultracentrifugation; BCA, Bicinchoninic acid Assay; CD, Circular Dichroism Spectroscopy; DLS, Dynamic Light Scattering; FTIR, Fourier Transform Infrared Spectroscopy; HIAC, High Accuracy Fluid Particle Counting; NIR, Near Infrared Spectroscopy; NMR, Nuclear Magnetic Resonance Spectroscopy; NTA, Nanoparticle Tracking Analysis; RMM, Residual Mass Measurement; RP-HPLC, Reverse Phase – High Performance Liquid Chromatography; SDS-PAGE, Sodium Dodecyl Sulfate – Polyacrylamide Gel Electrophoresis; SEC, Size Exclusion Chromatography; SEM, Scanning Electron Microscopy; ssHDX-MS, solid-state Hydrogen Deuterium Exchange – Mass Spectrometry; ssPL, solid-state Photolytic Labelling; SRCD, Synchrotron Radiation Circular Dichroism Spectroscopy; UV–Vis, Ultraviolet–Visible Spectroscopy.

1.5 Formulation aspects for Drying Technologies

The majority of freeze-dried biopharmaceutical formulations contain buffers, salts, amino acids, sugars, bulking agents, surfactants, tonicifiers, preservatives etc. (Gervasi *et al.*, 2018; Bjelošević *et al.*, 2020). Minimizing pH shifts, protein mobility in the solid-state and denaturation at air-liquid interfaces, increasing colloidal stability and providing increased solubility etc. are some of the key roles played by formulation components. Buffer salts such as sodium phosphate show a tendency to crystallize, thereby, causing pH shifts during freezing and depress critical temperatures of formulations crucial for freeze-drying (Kolhe *et al.*, 2009; C. Wu *et al.*, 2015). These challenges may be eliminated for spray-drying of formulations containing such buffers.

Some of amorphous saccharides provide improved stability for freeze-dried and spray-dried proteins (Green and Angell, 1989; Carpenter *et al.*, 1994; Kreilgaard *et al.*, 1999; Chang, Shepherd, Sun, Ouellette, *et al.*, 2005). Trehalose, compared to sucrose, is less frequently used in freeze-dried formulations but is the most preferred disaccharide for spray-drying (Pinto *et al.*, 2021). Trehalose can significantly protect biopharmaceuticals at higher temperatures during spray-drying due to its high T_g (>100 °C) (Liao *et al.*, 2004; Simperler *et al.*, 2006; Massant *et al.*, 2020). Authors have demonstrated that while sucrose preserves the protein's secondary structure during dehydration, trehalose provides protection during long-term storage of freeze-dried and spray-dried lysozyme (Starciuc *et al.*, 2020). Apart from disaccharides, cyclodextrin is widely used in spray-dried protein formulations (Pinto *et al.*, 2021). A good stabilizing effect was observed at a 2:1 (protein : sugar) ratio, respectively and an optimized inclusion of both trehalose and sucrose could improve the overall stability of lysozyme (Liao *et al.*, 2003; Sun *et al.*, 2022). A 9:1:10 blend of mannitol, trehalose and lysozyme, respectively, exhibited higher bioactivity and stability post spray-drying (Hulse *et al.*, 2008). Moreover, the inclusion of ethanol as a co-solvent improved the aerosol performance of spray-dried lysozyme by exhibiting a higher percentage of fine particle fraction (FPF) compared to the water-based lysozyme formulation (Ji *et al.*, 2016). In spite of their benefits, it is important to note that trehalose and sucrose may crystalize in their frozen state as well as in their dried state during storage at accelerated temperature and moisture and cause damage to protein structure and stability

(Singh *et al.*, 2011; Singh, 2018). Therefore, biopharmaceutical products are processed and stored below their T_g or eutectic temperature.

On the other hand, crystalline bulking agents such as mannitol and glycine may not necessarily confer protein stability but provide robust and elegant freeze-dried cakes structures (Johnson *et al.*, 2002; Varshney *et al.*, 2007; Peters *et al.*, 2016; Thakral *et al.*, 2023). Mannitol has also been reported to reduce the reconstitution times in high concentration freeze-dried cakes (Kulkarni *et al.*, 2018) and improve the aerosol performance of spray-dried anti-IgE formulations and salbutamol (Costantino *et al.*, 1998; Kaialy *et al.*, 2010; Molina *et al.*, 2019). Mannitol is the most popular monosaccharide in dried biopharmaceuticals (Gervasi *et al.*, 2018; Pinto *et al.*, 2021), although, crystallization of mannitol in the absence of amorphous stabilizers can negatively impact protein structure and stability. Crystallization of mannitol leads to phase separation that reduces the possible number of interactions between the protein and excipient, thereby, rendering the protein unstable (Wilson *et al.*, 2019). Approximately, 20 – 40 % of sugar content is sufficient to safe guard the antibody in terms of its stability (Maury *et al.*, 2005; Dani *et al.*, 2007). In spite of studies carried out on the stability of antibodies, the effect of elevated temperature stress (>180 °C) on mAbs due to high inlet temperatures of large-scale spray-dryers was still a concern. Bowen et al. conducted studies by testing different commercial mAb : trehalose formulations (2:1 and 1:2 ratio by weight, respectively) and stated that the percentage of monomers was lower in the freeze-dried product even though the residual water content was quite low compared to the spray-dried product (Bowen *et al.*, 2013). A yield of > 95 % and improved storage stability was reported for commercial mAbs post spray-drying (Gikanga *et al.*, 2015). More recently, authors have shown comparable stability of sucrose-containing myoglobin and lysozyme post freeze-drying and spray-freeze-drying (Mutukuri *et al.*, 2021). Along with trehalose, sucrose and mannitol, excipients such as polyethylenimine, hyaluronic acid, leucine, phenylalanine, arginine, cysteine and glycine have been used for spray-freeze-drying of some biopharmaceuticals (Adali *et al.*, 2020; Chaurasiya and Zhao, 2020).

Amongst amino acids, L-arginine and L-arginine hydrochloride have been reported to increase protein stability and solubility and reduce the viscosity of protein solutions (Shah *et al.*, 2012; Inoue

et al., 2014; Stärtzel *et al.*, 2015; Stärtzel, 2018). Interestingly, it has been reported that arginine along with other excipients and by itself in protein formulations is capable of acting as the main stabilizer (Tsumoto *et al.*, 2004; Baynes *et al.*, 2005; Shukla and Trout, 2011b; Reslan *et al.*, 2017). Moreover, the stabilizing effect of a large number of amino acids and their combinations were studied on spray-dried catalase, lysozyme and Pandemrix influenza vaccine containing haemagglutinin (Ajmera and Scherließ, 2014). A combination of arginine, glycine, and protein in the ratio of [(1+1) +1] resulted in a very good stabilizing effect post spray-drying. Amongst the commonly used excipients for proteins, a combination of trehalose, arginine and protein in a ratio of 1:1 (excipient : protein) by weight improved the properties of spray-dried mAbs in terms of reconstitution time and stability (Massant *et al.*, 2020). Furthermore, leucine, isoleucine and trileucine have been reported to effectively protect the protein from sheer stress caused during atomization and improve powder flowability, dispersibility and aerosolization (Ganderton *et al.*, 1999; Staniforth *et al.*, 2001; Lechuga-Ballesteros *et al.*, 2008; Schüle *et al.*, 2008; Zillen *et al.*, 2021). While histidine is the most popular amino acid used in liquid and freeze-dried protein formulations (Gervasi *et al.*, 2018), leucine is the most preferred in spray-dried protein formulations (Pinto *et al.*, 2021).

In addition, surfactants play a major role in reducing aggregation due to protein exposure at air-liquid, solid-liquid and liquid-liquid interfaces (Y. F. Maa *et al.*, 1998; Chernysheva *et al.*, 2018; Chen, Mutukuri, *et al.*, 2021). These interfaces may be generated during freezing, atomization, reconstitution etc. Therefore, consideration in selecting appropriate excipients specific to the product and process right at the formulation development stage is crucial to ensure product stability. A summary of some of the commonly used excipients for freeze-drying and spray-drying has been described in Table 1.7, though further investigations are required to elucidate the mechanism of stabilization by excipients for other drying technologies.

Table 1.7: Key roles of some commonly used excipients for Freeze-drying and Spray-drying of biopharmaceuticals.

Excipients	Examples	Freeze-drying	Spray-drying
Amorphous saccharides	Sucrose	Preservation of protein secondary structure by glassy-state stabilization, H-bonding (Liao *et al.*, 2002, 2003; Starciuc *et al.*, 2020).	
	Trehalose	Protection during long-term storage by glassy-state stabilization, H-bonding and high T_g (>100 °C) (Liao *et al.*, 2004; Simperler *et al.*, 2006; Massant *et al.*, 2020; Starciuc *et al.*, 2020).	
	Raffinose	n/a.	Glassy-state stabilization, high T_g (114 °C), increased fine particle fraction and aerosolization (Amaro *et al.*, 2011; Zhao *et al.*, 2018; Alhajj *et al.*, 2021).
	Glucose	Reducing sugars not preferred due to pH shifts and Maillard reaction (Mensink et al., 2017).	Glassy-state stabilization (Ying *et al.*, 2012).
	Lactose		Improved particle dispersibility (Seville *et al.*, 2007; Pilcer *et al.*, 2012; Horn *et al.*, 2020) but high hygroscopicity (Hebbink and Dickhoff, 2019).
Polyols	Mannitol	Bulking agent and reduced reconstitution time (Kulkarni et al., 2018; Mehta et al., 2013).	Improved aerosol performance (Costantino *et al.*, 1998; Kaialy *et al.*, 2010; Molina *et al.*, 2019).
	Sorbitol	Plasticize α-motions but antiplasticize β-motions in combination with non-reducing amorphous sugars (Cicerone and Soles, 2004; Chang, Shepherd, Sun, Tang, *et al.*, 2005).	
	Glycerol		
Amino Acids	Leucine, isoleucine, trileucine	n/a.	Protection from atomization stress, improved powder flowability, dispersibility and aerosolization (Seville *et al.*, 2007; Lechuga-Ballesteros *et al.*, 2008; Alhajj *et al.*, 2021).
	Arginine	Increased protein stability, solubility and reduced viscosity (Inoue et al., 2014; Shah et al., 2012; Stärtzel, 2018; Stärtzel et al., 2015).	Improved protein stability, reduced turbidity and reconstitution time (Ajmera and Scherließ, 2014; Massant *et al.*, 2020).
	Glycine	Bulking agent (Varshney et al., 2007).	Improved protein activity and stability (Ajmera and Scherließ, 2014).
	Histidine	Amino-acid buffer (Al-hussein and Gieseler, 2013; Liao et al., 2013).	Improved protein activity and stability (Ajmera and Scherließ, 2014).
Surfactants	Non-ionic (Tween 80, 20)	Reduced air-liquid interfacial protein adsorption, reduced aggregation, improved protein refolding (Y. F. Maa *et al.*, 1998; Arsiccio and Pisano, 2018; Chernysheva *et al.*, 2018).	
	Anionic (Sodium stearate, magnesium stearate)	n/a.	Moisture protectant, improved pore formation and aerosolization (Parlati *et al.*, 2009; Tewes *et al.*, 2014; Yu *et al.*, 2018).
	Pulmonary (DPPC, DSPC)	n/a.	Improved aerosolization and surface enrichment properties (Weers and Tarara, 2014; Cuvelier *et al.*, 2015; Miller *et al.*, 2015).
Other polysaccharides	Cyclodextrin	Improved protein stability, elegant cake appearance (Haeuser et al., 2020).	Glassy-state stabilization, improved powder flowability, anti-hygroscopicity (Branchu *et al.*, 1999; Serno *et al.*, 2010; Zhao *et al.*, 2018).
	Inulin	Improved protein stability (Hinrichs *et al.*, 2001; Ke *et al.*, 2020).	

DPPC, Dipalmitoyl phosphatidylcholine; n/a, not application or not available.

1.6 Feasibility of PAT for Drying Technologies

As per the 'Pharmaceutical Development' ICH Q8(R2) guidelines, PAT is a QbD approach to design, analyse and control manufacturing (ICH, 2009). Several PATs have been explored in literature, however, some drawbacks associated with their feasibility during batch freeze-drying have been identified. Most of the PATs provide an average result of the batch and cannot be implemented in-line, invasively or non-invasively for all individual product vials during processing. The risk of damage due to sterilization in the drying chamber makes these tools unfit for commercial cGMP cycles. On the contrary, most of these PATs can be potentially employable, in-line or at-line for unit doses or bulk product for some of the alternative drying technologies.

Typically, pressure and temperature sensors are used to monitor freeze-drying cycles (Nail and Johnson, 1992; Nail *et al.*, 2017; Fissore *et al.*, 2018). This is essential for the development and optimization of freeze-drying cycles and to account for the RMC in freeze-dried cakes. Optical fiber sensors (OFS) (Kasper *et al.*, 2013) and wireless data loggers such as temperature remote interrogation system (TEMPRIS) (Schneid and Gieseler, 2008) and TrackSense® (Ellab, 2020) are other available options for product temperature monitoring during freeze-drying. Comparative measurements between the pirani gauge and the capacitance manometer, and between the temperature probes and the shelf temperature are used to determine the primary drying end-point (Nail *et al.*, 2017; Fissore *et al.*, 2018). In comparison, Tunable Diode Laser Absorption Spectroscopy (TDLAS) and Mass Spectrometry (MS) have been used as better alternatives (Gieseler *et al.*, 2007; Patel, Chaudhuri, *et al.*, 2010; Patel, Doen, *et al.*, 2010; Ganguly *et al.*, 2018). Along with estimating the primary drying end-point, vapour flow rate, average product temperature, heat transfer coefficient and mass transfer resistance, these tools can also be used to monitor the secondary drying end-point and RMC with high sensitivity and accuracy (Gieseler *et al.*, 2007; Schneid *et al.*, 2009; Patel, Chaudhuri, *et al.*, 2010; Ganguly *et al.*, 2018). Ganguly et al. showed that MS was highly sensitive to an average cake moisture of < 3 % in the late secondary drying phase (Ganguly *et al.*, 2018). Additionally, MS can be used to detect silicon oil and helium gas leaks in a freeze-dryer. In contrast

to some of the drawbacks associated with these tools during batch freeze-drying, TDLAS and MS can be potentially configured with most of the continuous drying technologies to estimate the RMC for all individual vials or bulk product.

More interestingly, authors explored potential applications of Near Infrared – Chemical Imaging (NIR-CI) and 4D Micro-Computed X-ray tomography and imaging for Spin-freeze-drying (Brouckaert *et al.*, 2018; Goethals *et al.*, 2020; Vanbillemont, Lammens, *et al.*, 2020). NIR-CI was able to capture different polymorphs of mannitol and the distribution of residual moisture in mannitol and mannitol-sucrose containing Spin-freeze-dried vials whereas 4D Micro-Computed X-ray tomography and imaging were able to detect intra-vial differences in the mass transfer resistance and primary drying end-point. Also, a NIR probe coupled to a FT-NIR analyser was connected to the vial holder to demonstrate the primary and secondary drying end-point (De Meyer *et al.*, 2015). However, concerns relating to heat generation from NIR radiating halogen bulbs, mechanical challenges, and the feasibility of implementing this PAT in a cGMP environment need to be addressed. Moreover, Near Infrared – Frequency Modulated Spectroscopy (NIR-FMS) is a non-invasive, easy and a quick method for determining headspace oxygen and moisture levels in freeze-dried vials (Lin and Hsu, 2002; Cook and Ward, 2011b, 2011a; Victor *et al.*, 2017). Correlation observed between Karl Fisher analysis and NIR spectroscopy can make it easier to predict the RMC post drying (Brouckaert *et al.*, 2018; Carfagna *et al.*, 2020). This technique can be employed in-line or at-line to analyze all dried vials or bulk product generated via some of the alternative drying technologies. Furthermore, NIR, MIR and Raman spectroscopy have been used as potential PATs for process control and quality assurance of infant formula and dairy ingredients powders (Wang *et al.*, 2018). NIR and Raman spectroscopy have also been employed in-line to study the protein conformational stability and aggregation (Pieters *et al.*, 2012, 2013; Nitika *et al.*, 2021). A NIR or a Raman probe can be positioned to analyze vials as they move across different drying chambers during continuous freeze-drying of suspended vials. Similarly, a probe can be placed in-line at the different stages of Active-freeze-

drying, spray-drying, and spray-freeze-drying or at-line during powder filling into unit doses. These PATs can also reduce batch release test time from fill finish to the market.

Particle size is one of the major CQAs for free-flowing powder-based products. Laser diffraction has been used both in-line and at-line to measure the particle size distributions during spray-drying (Chan *et al.*, 2008). Moreover, a variety of different PATs such as Spatial Filtering Velocimetry (SFV), Focused Beam Reflectance Measurements (FBRM), Photometric Stereo Imaging (PSI) and Eyecon® technology have been explored for analysing dry powder particle size (Silva *et al.*, 2013). These PATs can be configured in-line or at-line for Active-freeze-drying, spray-freeze-drying and PRINT® Technology to measure the particle size of dry powder. However, discrepancies observed in the particle size measurements of the PATs have been discussed by the authors (Silva *et al.*, 2013) and so, users must consider pre-requisite knowledge on the theory, mechanism and equipment for appropriate results.

In summary, RMC, protein structural conformation and aggregation, particle size and polymorphism of excipients are some of the major CQAs for biopharmaceutical products that can be monitored using PATs. Monitoring CPPs such as product temperature, drying rate etc. are as important as product CQAs and so, some of the continuous drying technologies offer a greater advantage from PAT perspective. Table 1.8 summarizes the application of some PATs based on authors' assessments for only some of the drying technologies. The potential compatibility of these PATs with other drying technologies listed in Table 1.8 has not been found in literature and is based on opinion.

Table 1.8: Potential / compatible PAT for Drying Technologies.

PAT	Application	Batch Freeze-drying	Active-freeze-drying	Spin-freeze drying	Spray-freeze-drying	Continuous Freeze-drying of suspended vials	Spray-drying	PRINT®
Temperature Probes: • **Thermocouples and RTDs** (Nail *et al.*, 2017; Fissore *et al.*, 2018)**.** • **Wireless Probes: TrackSense®, TEMPRIS** (Schneid and Gieseler, 2008; Ellab, 2020). • **Optical Fibers** (Kasper *et al.*, 2013).	Average product temperature mapping.	Yes	Yes (RTDs can be installed At-line)	No	Yes (RTDs can be installed At-line)	Yes (Wireless probes can be installed in-line)	Yes (RTDs can be installed At-line)	n/a
	Product temperature mapping for all individual vials or bulk product.	No	Yes (At-line)	No	Yes (At-line)	No	Yes (At-line)	n/a
• **IR Thermography** (Harguindeguy and Fissore, 2021).	Product temperature mapping for all individual vials or bulk product only within the camera's field of view.	Yes, but the center vials are calculated based on average.	Yes	Yes	Yes	Yes	Yes (At-line)	Yes (At-line)
• **NIR Spectroscopy** (De Beer *et al.*, 2009; Pieters *et al.*, 2012; Mensink *et al.*, 2015; Wang *et al.*, 2018). • **Raman Spectroscopy** (De Beer *et al.*, 2009; Pieters *et al.*, 2013; Wang *et al.*, 2018; Nitika *et al.*, 2021).	In-line protein structure analysis, protein aggregation and distribution of excipient polymorphs for all individual vials or bulk product.	No, but can provide an average measurement.	Yes	Yes	Yes (At-line)	Yes	Yes (At-line)	Yes (At-line)
• **NIR-FMS** (Lin and Hsu, 2002; Cook and Ward, 2011b, 2011a; Victor *et al.*, 2017; Carfagna *et al.*, 2020).	In-situ vial headspace oxygen and moisture measurements for all individual vials or bulk product.	No, but can provide an average measurement.	Yes	No	Yes (At-line)	Yes	Yes (At-line)	n/a
• **NIR-CI** (Brouckaert *et al.*, 2018).	In-situ RMC estimation and distribution of excipient polymorphs in all individual vials or bulk product.	Yes	Yes	Yes	Yes	Yes	Yes (At-line)	Yes
• **TDLAS** (Kessler *et al.*, 2006; Gieseler *et al.*, 2007; Kuu *et al.*, 2009, 2011; Schneid *et al.*, 2009, 2011; Sharma *et al.*, 2019). • **MS** (Nail *et al.*, 2017; Fissore *et al.*, 2018; Ganguly *et al.*, 2018).	In-situ RMC, drying end point, vapor flow rate estimation for all individual vials or bulk product.	No, but can provide an average measurement.	Yes	Yes	Yes	Yes	Yes	Yes
• **MS** (Connelly and Welch, 1993; Barfuss, 2014; Ganguly *et al.*, 2018).	In-line silicon oil or gas leak detection.	Yes	Yes	Yes	Yes	Yes	Yes	Yes
• **Laser Diffraction** • **Light Microscopy** • **SFV** • **PSI** • **FBRM** • **Eyecon®**	(Chan *et al.*, 2008; Silva *et al.*, 2013; Petrak *et al.*, 2018; Dos Reis *et al.*, 2021).	In-line / at-line dry powder particle sizing.	n/a	Yes	n/a	Yes	n/a	Yes	Yes

RTDs, Resistance Temperature Detectors; n/a, not application or not available.

1.7 Scale-up Packaging, and Validation aspects for Drying Technologies

Scale-up and technology transfer involve moving a pharmaceutical manufacturing process from one facility to another i.e. from a development / pilot-scale to a commercial-scale or an intra-site / inter-site fill finish line to line transfer. As per ICH Q12 guidelines, technology transfer may also be required for lifecycle changes across different commercial facilities (ICH, 2019).

Freeze-drying in vials requires the qualification of not only the drying process, but several other critical fill finish operations such as compounding, filtration and vial filling. This brings in further technical and compliance requirements such as mixing studies, filter bacterial retention, fill volume cycle development, media fill qualification and environmental monitoring (FDA, 2014c). Moreover, large loading times (4 – 12 h) for vial filling impacts process efficiency, may lead to issues such as product splashing and/or foaming and may also impact product stability upon increased validated time out of refrigeration (Rathore and Rajan, 2008; Patel *et al.*, 2017). Along with large loading times, large unloading times and vial inspection also impact the efficiency of commercial operations and slows the inventory turnover time in the most expensive footprint area of a commercial site i.e., controlled areas for aseptic fill finish. Such additional steps are eliminated for Active-freeze-drying, spray-drying and spray-freeze-drying technologies. These drying technologies can also provide the option for drug substance (DS) – drug product (DP) validation as continuous processes and eliminate the requirement for additional validation steps, thereby, minimizing the complexities associated with the regulatory filing and qualification of an end-to-end fill finish process (Pisano, 2020). Also, with the bulk product stored in the dried state as opposed to the liquid or frozen state, cold chain shipping validation of the bulk can be reduced. On the negative side, a more comprehensive cleaning validation for alternative drying technologies may be a requirement as per cGMP.

Furthermore, many of the freeze-dried biopharmaceuticals such as Eloctate® (FDA, 2014b), Alprolix® (FDA, 2014a), Fabrazyme® (FDA, 2010a) etc. are manufactured in multiple dose strengths. Batch freeze-drying for multiple dose strengths require completely different fill finish processes with

additional qualification and validation for primary packaging components supply chain, fill finish line equipment, sterilization methods, fill volume, freeze-drying cycles, capping, inspection, container closure integrity etc. In contrast, alternative drying technologies such as Active-freeze-drying, spray-drying, spray-freeze-drying etc. make it easier to fill and pack free-flowing product into different container types such as vials, ampules, syringes, sachets etc. at multiple dose strengths. This also helps in simplifying infusion requirements at clinics.

To enable successful scale-up and technology transfer, drying processes require a QbD approach where the process boundaries are well defined and provide adequate robustness for commercial operations (Nail and Searles, 2008; Cullen *et al.*, 2022). Small scale process modelling for freeze-drying is complex as each individual vial behaves as its own drying system, is subject to variability, and is a function of vial heat transfer coefficient, freezing temperature and location on the shelf. Active-freeze-drying, spray-drying and spray-freeze-drying, for example, are not as hindered by the challenges of drying in individual containers as they provide a more predictive and consistent manufacturing performance.

In terms of scalability, moving an existing commercial product from a batch freeze-drying process to an alternative drying process is regarded as a major regulatory change and comprehensive comparability data would be required as part of implementation and approval (Pisano, 2020). The significant cost of biopharmaceutical DS, commercial line time for engineering, validation batches, long term stability data and the requirement for filing a change mean any efficiency gain obtained by alternative drying processes may be offset by such costs. Overall, the most viable route to introduce alternative drying processes may very well be on the back of the development and industrialization of new products.

1.8 Aims and objectives of this thesis

The scope of this thesis focuses on the manufacturability and the effect of novel drying technologies on the safety, quality and efficacy of biopharmaceuticals. Specific aims of this thesis include:

1. To identify novel drying techniques and to compare alternative drying techniques, such as Spray-drying, Active-freeze-drying, Spray-freeze-drying, etc. in order to assess the potential benefit of alternative technologies for the processing of biopharmaceutical products.

2. To assess a novel alternative process, including the incorporation of excipients, which will be cost effective and efficient for processing of biologics.

3. To explore analytical methodologies in tandem to assess the novel formulation produced with a view to developing a rapid, screening method for biologics.

4. To develop molecular models using molecular dynamics simulations to understand the impact and the mechanism of interaction of excipients with biologics.

Chapter 2:

Freeze-Drying of Lysozyme

2.1 Introduction

Freeze-drying or lyophilisation is the primary commercial means of producing solid biopharmaceuticals. Even though aqueous biopharmaceutical formulations are preferred as injectables, in some cases protein-water interactions raise concerns for biochemical degradation pathways such as hydrolysis, deamination, oxidation, etc. resulting in aggregation and/or denaturation of the protein (Carpenter *et al.*, 2002). The removal of water confers several benefits such as improved stability, prolonged shelf-life, ease of storage and reduced cost in transportation at ambient temperatures (Moeller and Jorgensen, 2008; Langford *et al.*, 2017).

Lysozyme, also known as muramidase, lysozyme c or Mucopeptide N-acetylmuramoylhydrolase (EC 3.2.1.17) is an antimicrobial enzyme belonging to the Glycoside hydrolase family (Sigma; Mörsky, 1983). Lysozyme acts by catalysing the hydrolysis of b-(1 → 4) glycosidic linkages between N-acetylmuramic acid and N-acetyl-d-glucosamine residues present in the mucopolysaccharide cell wall of typically gram positive microbes (Helal and Melzig, 2008). The primary and secondary structure of lysozyme are shown in Figure 2.1 (Protein Data Bank 1DPX). The primary structure of lysozyme consists of 129 amino acids and the molecule has a molecular weight of 14.3 kDa. The secondary structure consists of 7 helices; 53 residues (40 - 45 % a α-helical content) and 9 strands; 14 residues (10 - 19 % β-sheets), 23 – 27 % β-turn and 13 – 14 % random structures (Protein Data Bank 1DPX; Levitt and Greer, 1977; Dong *et al.*, 1992; Luo *et al.*, 1994; Kong and Yu, 2007). The tertiary conformation of lysozyme is shown in Figure 2.2 (Protein Data Bank 1DPX).

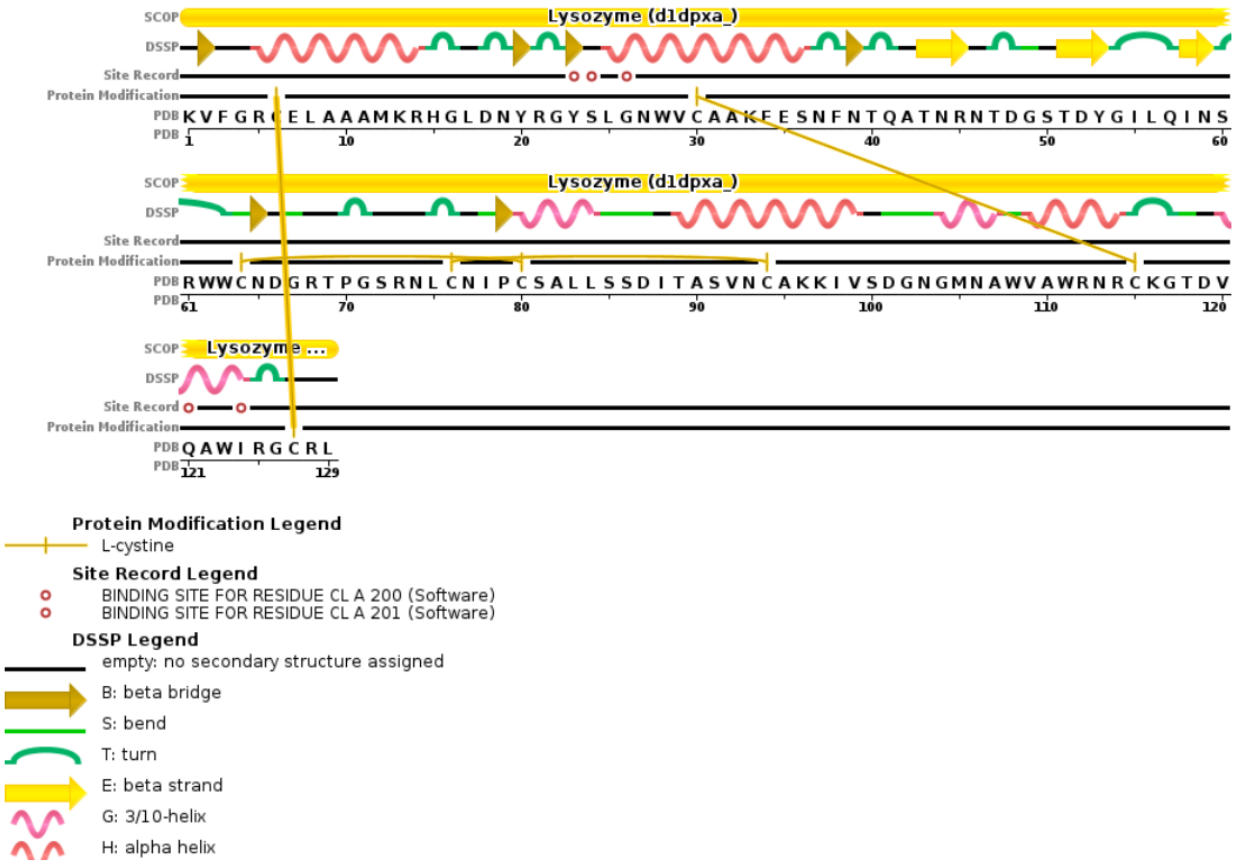

Figure 2.1: Amino Acid sequence of lysozyme (retrieved from: Protein Data Bank 1DPX).

Various mechanisms have been reported that partly explain the stabilizing effect of different excipients during protein dehydration (Elversson and Millqvist-Fureby, 2005; Ajmera and Scherließ, 2014):

a) The "water replacement hypothesis" states that stabilizers form hydrogen bonds at specific sites on the surface of the protein during dehydration. As water is removed from the protein solution, the hydrogen bonds between the protein and water molecules are disrupted. The hydrogen bonds formed between the stabilizer and protein create a water-like environment that stabilizes the native structure of the protein (Carpenter *et al.*, 1994; Allison *et al.*, 1999; Kreilgaard *et al.*, 1999).

b) The "glass dynamics mechanism" explains that amorphous stabilizers form a rigid, inert matrix around protein molecules wherein the motion of the protein is coupled to the motion

of the matrix, thereby, limiting its structural relaxation and thus stabilizing the tertiary structure (Green and Angell, 1989; Chang, Shepherd, Sun, Ouellette, *et al.*, 2005).

c) The theory of "preferential exclusion" states that excipients in solution preferentially exclude themselves from the surface of proteins, thereby, stabilizing the native structure of the protein as a result of increased chemical potential and interaction with water molecules (Arakawa and Timasheff, 1982; Carpenter *et al.*, 1994; Lerbret *et al.*, 2008; Sudrik *et al.*, 2019).

d) The "reducing surface adsorption hypothesis" states that protein adsorption at the surface of the drying layer is reduced in the presence of surfactants, thereby, preventing protein denaturation at the air-liquid interface (Y.-F. Maa *et al.*, 1998). Moreover, the mechanism of dilution of protein, upon addition of sugars, reduces molecular interactions amongst protein molecules, thereby, reducing protein aggregation in the solid state (Costantino *et al.*, 1994).

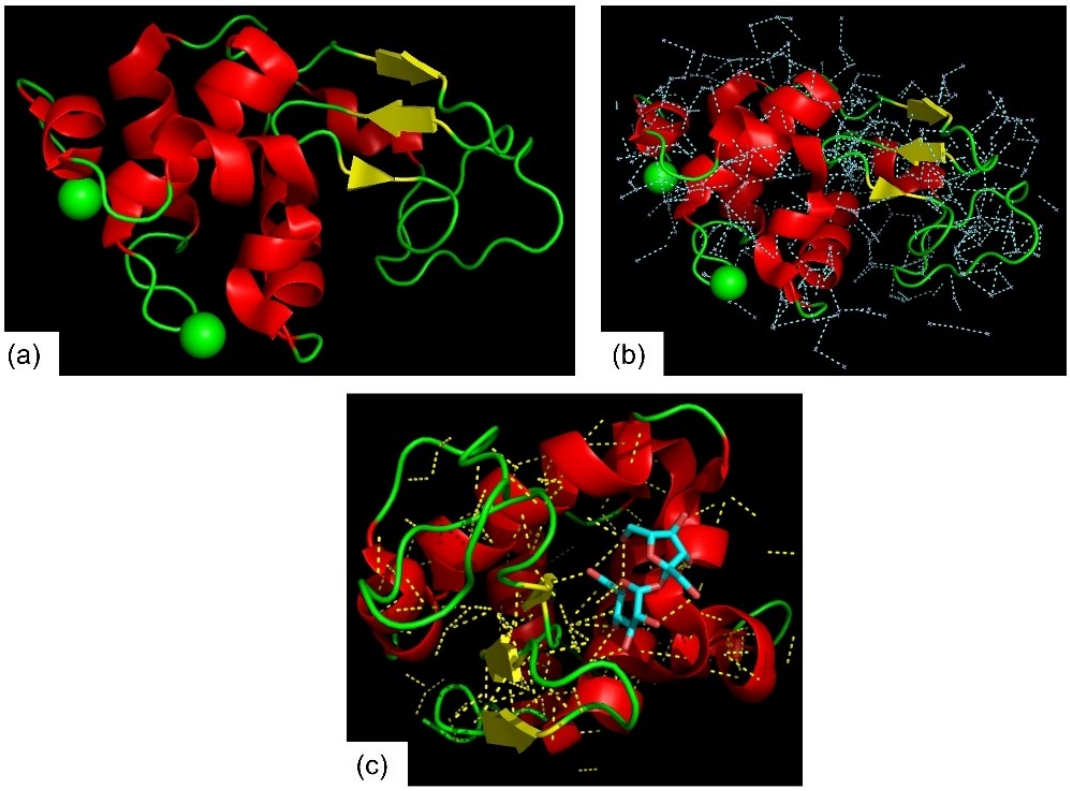

Figure 2.2: 3-D simulated structure of (a) lysozyme, (b) intramolecular H-bonds and H-bonds between lysozyme and water molecules, (c) H-bonds between lysozyme and 40 % sucrose. α-helix (red), β-sheets (yellow), loops (green), H-bonds (Blue and yellow dotted lines), water molecules

(white cross), sucrose molecule (blue and red sticks), chlorine molecule (green ball). Pictures generated using PDB (Protein Data Bank 1DPX; Protein Data Bank 3T6U) and Pymol 2.3.4 software.

The thermal stability of the freeze-dried lysozyme formulations was found to be a function of excipient-enzyme mass ratio with the trehalose-based formulation exhibiting a higher T_g to the equivalent sucrose-based formulation (Liao *et al.*, 2003). While the trehalose-based lysozyme formulation was thermally more stable, the sucrose-based formulation containing glycerol preserved the secondary structure of the enzyme more effectively (Liao *et al.*, 2002, 2004). Lewis *et al.* studied the freeze-drying behaviour of sucrose-based lysozyme, BSA and IgG formulations at different concentrations and freeze-drying conditions (Lewis *et al.*, 2010). Using several biophysical techniques, it was shown that the behaviour of the three proteins was more evident at higher concentrations (25 mg/mL) and elucidated that at higher concentrations the proteins significantly influenced the behaviour of the formulation, whereas stabilizers influenced the formulations at lower protein concentrations (5 mg/mL). The stability and protein structure of the three proteins was preserved even at aggressive primary drying conditions resulting in shorter drying time (Lewis *et al.*, 2010). The enzyme activity and stability of marine lysozyme was best protected by trehalose and tween 80 together, rather than trehalose, sucrose and maltose individually post freeze-drying (Ji *et al.*, 2009). Through in situ micro-Raman Spectroscopy investigations on lysozyme and chymotrypsinogen, it was elucidated that trehalose stabilizes proteins during the ice sublimation and desorption phases of freeze-drying (Hedoux *et al.*, 2013). Moreover, Blumlein and McManus studied the liquid state reversibility of unfolding via thermal denaturation of lysozyme at different protein concentrations (20 mg/mL – 100 mg/mL) and solution conditions (Blumlein and McManus, 2013). They concluded that the reversibility index (RI) was a function of pH and ionic strength. Refolding of lysozyme decreased with an increase in ionic strength of the buffer and no refolding was observed at pH ≥ 7.0. The denaturation temperature for lysozyme ranged from 69.9 °C – 85.1 °C at different pH values. Additionally, the inclusion of trehalose and maltose increased the denaturation

temperature, but did not necessarily help in protein refolding (Blumlein and McManus, 2013). Structural refolding, reduced adsorption of lysozyme at interfaces and preservation of its secondary structure and bioactivity was observed when the enzyme was formulated at a pH furthest from its isoelectric point (pH 11) at lower ionic strength (Malzert *et al.*, 2002; Blumlein and McManus, 2013).

Furthermore, the effect of freeze-drying and spray-drying on mannitol-based lysozyme formulations at different protein concentrations were studied using X-ray powder diffraction. It was observed that polymorphic forms of mannitol shifted from β-mannitol to δ-mannitol post freeze-drying, whereas a shift from β-mannitol to α-mannitol was observed post spray-drying (Grohganz *et al.*, 2013). They concluded that the change in mannitol polymorphs was process dependent rather than dependent on temperature itself. Interestingly, studies on aggressively freeze-dried cycles, resulting in cake collapse, have shown no detrimental effect on the stability of a variety of enzymes, monoclonal antibodies and other proteins (Wang *et al.*, 2004; Chatterjee *et al.*, 2005b; Schersch *et al.*, 2010, 2012; Horn *et al.*, 2018). Horn *et al.* reported significant reduction in the primary drying cycle from 47 h to 7 h with comparable protein stability in both cycles (Horn *et al.*, 2018). While crystalline mannitol as a bulking agent may not necessarily confer protein stability, it provides robust and elegant cake structures upon freeze-drying (Johnson *et al.*, 2002; Varshney *et al.*, 2007; Peters *et al.*, 2016). In terms of the reconstitution time of lyophilised cakes, it was reported that mannitol can potentially reduce the reconstitution time in high concentration lyophilized protein formulations (Kulkarni *et al.*, 2018). Crystalline mannitol cakes were observed to reduce the reconstitution time compared to partially crystalline cakes. Fully crystalline cakes promoted phase separation which improved cake wettability and penetration of the reconstitution liquid into the interior of the cake (Kulkarni *et al.*, 2018). The reconstitution times of certain high concentration lyophilized protein products, namely, Raptiva® 100 mg/mL (FDA, e), Nucala® 100 mg/mL (FDA, d) are < 5 min whereas products such as Ilaris® 150 mg/mL (FDA, c), Xolair® 144.64 mg/mL (FDA, f), Cosentyx® 150 mg/mL (FDA, b) and Cimizia® 200 mg/mL (FDA, a) can take up to 15 – 40 min to reconstitute.

In addition, the effect of glycerol in trehalose-based lysozyme formulation was analysed. Glycerol was found to have a plasticizing effect during the primary drying phase and an antiplasticizing effect during the secondary drying phase of freeze drying (Starciuc *et al.*, 2017). Using Raman imaging, it was found that the molecular mobility of lysozyme was increased in the presence of glycerol and trehalose during the removal of frozen water, whereas the conformational distortion of the protein was reduced in the presence of glycerol and trehalose during the secondary drying phase. Glycerol formed stronger hydrogen bonds with the hydroxyl groups of trehalose than those between water and trehalose, thereby, creating a stronger network in the amorphous matrix. This antiplasticizing property of glycerol was enhanced after the water desorption phase keeping the protein embedded within the matrix (Starciuc *et al.*, 2017). More recently, a novel study was conducted on lysozyme, recombinant human albumin (rHA), mAb and an insect antifreeze protein (iAFP) to investigate protein-ice interaction using High-Resolution Synchrotron X-Ray Diffraction (Bhatnagar *et al.*, 2019). Their results showed that lysozyme exhibited minor microstrain and so it interfered the least with hexagonal ice crystal formation compared to other proteins. rHA and mAb interacted strongly with ice crystal formation which could interfere with the growth of ice crystals from liquid to ice phase during freezing. They asserted that proteins interacted in an indirect manner, as the proteins were partitioned into the quasi-liquid layer and did not show direct sorption onto ice crystals (Bhatnagar *et al.*, 2019).

This chapter focuses on the characterization of the model protein lysozyme and the impact of lyophilization on the protein. The enzyme was studied in 3 different formulations to investigate the effect of individual excipients on the protein prior to and post lyophilization. The protein was characterized in terms of its thermal properties using Freeze-drying Microscopy (FDM) and Differential Scanning Calorimetry (DSC) and its structural properties using Fourier Transform Infrared Spectroscopy (FTIR) and Circular Dichroism (CD). Additional techniques such as Size-Exclusion Chromatography (SEC) was employed to study the protein's aggregation profile, X-Ray Diffractometry (XRD) to identify crystalline and amorphous components, Dynamic Light Scattering

(DLS) for particle size analysis, Karl Fisher titration and Light House to measure the residual moisture content and headspace moisture and pressure post lyophilization. While lysozyme is well-studied, this study was carried out to generate benchmark data for a model protein to compare and evaluate the feasibility of alternate drying technologies on lysozyme and large biopharmaceuticals.

2.2 Materials and Methods

2.2.1 Preparation of lysozyme formulations

The model protein lysozyme from Chicken Egg White, Trehalose, and Histidine were procured from Merck / Sigma Aldrich, Ireland. Mannitol and Polysorbate 80 (Tween 80) were obtained from Fisher and Sucrose was obtained from Merck / Sigma Aldrich and Pfanstiehl and all were used without modification. 4 different formulations of lysozyme were prepared in 5 mM Histidine Buffer containing 10 mg/mL protein and 40 mg/mL excipient. 0.01% v/v Tween 80 was added into 3 of these formulations. The fourth was retained as a standard. All bulk formulations were buffered to pH 6.30 – 6.35 as shown in Table 2.1.

Table 2.1: Lysozyme formulations.

Formulation	**Standard (Lysozyme)**	**Lysozyme Trehalose (Formulation 1)**	**Lysozyme Mannitol (Formulation 2)**	**Lysozyme Sucrose (Formulation 3)**
Buffer (concentration)	Histidine (5 mM)	Histidine (5 mM)	Histidine (5 mM)	Histidine (5 mM)
Excipient (concentration)	None	Trehalose (40 mg/mL)	Mannitol (40 mg/mL)	Sucrose (40 mg/mL)
Protein (concentration)	Lysozyme (10 mg/mL)	Lysozyme (10 mg/mL)	Lysozyme (10 mg/mL)	Lysozyme (10 mg/mL)
Surfactant (concentration)	None	Tween 80 0.01% (v/v)	Tween 80 0.01% (v/v)	Tween 80 0.01% (v/v)
Measured pH	6.3	6.3	6.3	6.3

2.2.2 Glass Transition and Eutectic/Melt Temperature analyses

The eutectic temperature (T_{eu}) in the frozen state and melt temperature (T_m) in the dried state and the glass transition temperatures of the frozen (T_g') and dried (T_g) samples were measured using the TA DSC Q2000. 20 µL of each liquid sample was sealed in an aluminum pan. For liquid samples, modulated DSC was ramped from – 60 °C to 60 °C at 2 °C/min with modulation amplitude of ±1 °C and modulation period 100 s. Approximately, 10 – 15 mg of each solid sample was sealed in an aluminum pan at relative humidity ≤ 5 %. Modulated DSC was ramped from 0 °C to 200 °C at 2 °C/min with modulation amplitude of ± 1 °C and modulation period of 100 s for solid samples. Samples were analyzed in triplicate (n = 3).

2.2.3 Freeze-drying Microscopy (FDM)

The collapse temperature of amorphous material and the melt temperature of crystalline substances were measured using FDM. Approximately, 1.5 µL of sample was pipetted on to the sample block. The sample was frozen at – 40 °C at 20 °C/min and a vacuum of 0.1 mBar was applied after 10 min of freezing. The frozen sample was ramped at 0.5 °C/min until the material started collapsing in the drying front. The onset collapse of the material was recorded every 5 s. Samples were analyzed in triplicate (n = 3).

2.2.4 Lyophilization

All bulk materials were freeze-dried in a LyoStar II from SP Scientific. 5 mL of sample was pipetted into 20 mL Schott vials with a total of 35 sample vials of product surrounded by placebo. A few vials were probed using thermocouples to monitor the product temperature. Different recipes were employed as mentioned in Table 2.2, Table 2.3 and Table 2.4 to lyophilize each formulation. Post-lyophilization, the vials were rubber stoppered, crimped and stored at 5 ± 2 °C.

Table 2.2: Lyophilization recipe for lysozyme standard.

Lysozyme Standard – A301118			
Freezing	**1**	**2**	**3**
Shelf Set-Point (°C)	5	- 35	- 35
Ramp Rate (°C/min)	0	0.5	0
Time (min)	60	0	180
Primary/ Secondary	**4**	**5**	**6**
Shelf Set-Point (°C)	0	25	-
Ramp Rate (°C/min)	0.5	0.5	-
Time (min)	2100	600	-
Vacuum SP (µBar)	135	135	-

Table 2.3: Lyophilization recipe for lysozyme formulated with trehalose and sucrose independently.

Lysozyme with Trehalose and Sucrose - A051018 and A191118			
Steps	**1**	**2**	**3**
Shelf Set-Point (°C)	5	- 45	- 45
Ramp Rate (°C/min)	0	0.5	0
Time (min)	60	0	180
Primary/ Secondary	**4**	**5**	**6**
Shelf Set-Point (°C)	- 10	25	-
Ramp Rate (°C/min)	0.5	0.5	-
Time (min)	2100	600	-
Vacuum SP (µBar)	135	135	-

Table 2.4: Lyophilization recipe for lysozyme formulated with mannitol.

Lysozyme with Mannitol – B301118				
Steps	**1**	**2**	**3**	**4**
Shelf Set-Point (°C)	5	- 45	- 20	- 45
Ramp Rate(°C/min)	0	0.5	0.5	0.5
Time (min)	60	120	120	120
Primary/Secondary	**5**	**6**	**7**	**8**
Shelf Set-Point	0	25	-	-
Ramp Rate	0.5	0.5	-	-
Time	2100	600	-	-
Vacuum SP (mBar)	0.135	0.135	-	-

2.2.5 Vial headspace moisture analyses

The vials headspace moisture (mBar) was measured using the FMS Light House® instrument post lyophilization. The device was calibrated using calibration standards. All samples were analyzed in triplicate (n=3).

2.2.6 Residual Moisture Content (RMC) analyses

The lyophilized cake residual moisture was measured using Karl Fisher, KF Titrando by Metrohm. The vials were prepared at relative humidity ≤ 5 % and capped with Karl Fisher caps. The samples were subjected to a temperature of 100 °C, the blank vials were at 120 °C and the water standard was subjected to a temperature of 170 °C (as per the manufacturer's recommendation).

2.2.7 Concentration, Turbidity and Reconstitution Time Analyses

All freeze-dried formulations were reconstituted with 5 mL Milli-Q® ultrapure water and the concentration and turbidity were measured in a 1x1 cm transparent glass cuvette using a UV spectrometer (Spectro Star nano by BMG Labtech) at 280 nm and 350 nm, respectively. The concentration was calculated using Beer lambert's law (Equation 2.1) and the molar extinction coefficient for the lysozyme used was 2.64 mL mg^{-1} cm^{-1} (Blumlein and McManus, 2013). The reconstitution time was measured using a stopwatch.

$$A = \varepsilon . C . L \qquad \textbf{Equation 2.1}$$

Where A is the absorbance (unit less quantity),

ε is the molar extinction coefficient in mL mg^{-1} cm^{-1},

C is the concentration in mg/mL,

L is path length in cm.

2.2.8 Secondary Structure analyses using FTIR Spectroscopy

All freeze-dried lysozyme formulations were analyzed using the Thermo Fisher Nicolet ATR-FTIR spectrophotometer. Approximately, a few milligrams of solid samples were placed onto the ATR crystal and analyzed using the FTIR spectrophotometer. 164 scans were collected at a resolution of 4 cm^{-1} from 4000 cm^{-1} to 400 cm^{-1} and the Norris second derivative was analyzed from 1700 cm^{-1} to 1600 cm^{-1} across the amide I region. All samples were analyzed in triplicate (n=3).

2.2.9 Secondary and Tertiary Structure analyses using CD Spectroscopy

The secondary structure of lysozyme was studied using the Far UV CD across 180 nm – 260 nm, at every 1 nm for 2 s per point with a 1 nm bandwidth. A 0.1 mm cuvette was used with 1 mg/mL protein concentration. The Near UV CD region was used to study Tryptophan, Tyrosine and Phenyl alanine residues in the protein's tertiary structure across 260 nm – 320 nm, at every 1 nm for 5 s per point with a 1 nm bandwidth. 0.3 mg/mL of protein was analyzed in a 1 cm cuvette using the ChiraScan CD spectrophotometer by Applied Photophysics. A temperature study was performed at every 10 steps from 20 °C to 80 °C at the rate of 1°C per minute. All samples were analyzed in triplicate (n=3). Secondary structure predictions were performed using the CDSSTR algorithm on the DICHROWEB online server (Whitmore and Wallace, 2004, 2007; Wallace, 2020).

2.2.10 Dynamic Light Scattering (DLS)

Lysozyme formulations were analyzed for particle size distribution (PSD) using single-angle Dynamic Light Scattering (Zetasizer μV by Malvern Panalytical). 1 mL of sample was filtered through a 0.45 μm filter into a transparent disposable cuvette. The equilibration time was 120 s. Additionally, lysozyme samples prepared in reaction buffer and histidine buffer were centrifuged at 20,000 g at 4 °C for 20 min to study soluble and insoluble aggregates. The supernatant and the pellet were separated and analyzed separately using DLS. All samples were analyzed in triplicate (n=3).

2.2.11 Size Exclusion Chromatography (SEC)

The aggregation profiles of lysozyme in different formulations were analyzed on the Agilent 1200 HPLC with TSK gel 3000 SWXL column. The mobile phase was 100 mM sodium phosphate at pH 6.7. The flow rate was 0.5 mL/min with an injection volume of 20 μL. Multiwavelength signals were recorded at 210 nm, 214 nm, 254 nm, 260 nm, 280 nm.

2.2.12 Powder X-Ray Diffraction (pXRD)

Qualitative XRD analyses was performed using Rigaku Miniflex to identify amorphous and crystalline states of the lyophilised cakes of lysozyme. The lyophilized cake was crushed and homogenised and a few milligrams of powder was smeared onto a standard glass holder inside a glovebox at relative humidity ≤ 5 %. The sample was scanned from 3° to 60° at the rate of 3° per minute every 0.02° steps. The applied voltage was 40 kV, and the current was 15 mA.

2.2.13 Enzyme Activity

The antimicrobial activity of lysozyme was measured against *Micrococcus lysodeikticus*. The turbidimetric assay for lysozyme was performed in a 1 x 1 cm transparent glass cuvette. All sample solutions and suspensions were prepared and diluted in reaction buffer. 100 µL of approximately 7.5 µg/mL (300 U/mL) of lysozyme was added to 2.5 mL of 0.1 mg/mL *Micrococcus lysodeikticus* suspension. The reaction mixture in the glass cuvette was immediately mixed by inversion and placed into a UV spectrometer (Spectro Star nano by BMG Labtech). The decrease in the absorbance at 450 nm was recorded every minute for 8 min at 25 °C. The units of enzyme/mg were calculated using Equation 2.2 and Equation 2.3. As per Sigma's definition, "one unit will produce a ΔA_{450} of 0.001 per minute at pH 6.24 at 25 °C, using *Micrococcus lysodeikticus* as a substrate in a 2.6 mL reaction mixture." (Sigma Aldrich, 2017).

$$U_e = \left[\left(\Delta A_{450}^{S}\right) - \left(\Delta A_{450}^{B}\right)\right] * \frac{[d_f]}{[0.001 V_e]} \qquad \textbf{Equation 2.2}$$

$$U_s = \left[\frac{U_e}{\mathrm{W_e}}\right] \qquad \textbf{Equation 2.3}$$

Where, ΔA_{450}^{S} is the slope of the test sample, ΔA_{450}^{B} is the slope of the blank, d_f is the dilution factor, V_e is the volume of sample in m, U_e is the units of enzyme/mL, W_e is the weight of enzyme in mg.

2.2.14 Statistical Analyses

Where necessary, the data was represented as the means ± standard deviation. Where appropriate, the data was analyzed statistically by one-way ANOVA using Tukey's post-hoc test and a p-value < 0.05 was considered statistically significant.

2.3 Results and Discussion

2.3.1 Freeze-drying Microscopy

Since primary drying accounts for the largest fraction of the freeze-drying cycle, the product must be maintained below its T_g' (glass transition temperature of amorphous material in the frozen state), T_{eu} (eutectic temperature of crystalline material in the frozen state) and T_c (collapse temperature) to prevent its collapse during sublimation (Tang and Michael J Pikal, 2004). FDM was carried out to determine the collapse temperature of the formulations. The collapse temperature values are shown in Table 2.5.

Table 2.5: Critical/Collapse Temperatures of lysozyme formulations.

Sample	Average T_c (Onset) Temperature (°C)	Literature T_c (°C)
Lysozyme Trehalose	-27.95 ± 0.07	-28°C (T_c Trehalose) (Cook, 2003)
Lysozyme Mannitol	-26.10 ± 12.56 (micro-collapse)	-1.4°C (T_{eu} Mannitol) (Cook, 2003), -28.1°C (T_c Mannitol) (Horn and Friess, 2018)
Lysozyme Sucrose	-31.05 ± 0.01	-31°C (T_c Sucrose) (Cook, 2003)

Formulations containing amorphous excipients, namely trehalose and sucrose, showed white spots (glass transition) in the drying front followed by a total collapse (Figure 2.3). The formulation containing trehalose exhibited a higher collapse temperature compared to sucrose. The crystalline component, mannitol, exhibited a micro-collapse, but did not show a complete collapse unlike the amorphous materials as shown in Figure 2.3. The critical temperature values for lysozyme trehalose (-27.95 °C) and sucrose-based formulation (-31.05 °C) were very comparable to literature values (Table 2.5) showing that trehalose and sucrose were present in their amorphous state upon freezing. The lysozyme mannitol-based formulation did not show a complete melt at -1.4 °C, instead micro-collapse was observed at - 26.10 °C. This value was similar to its T_g' (- 26.87 °C) in Table 2.6. The high standard deviation observed in the collapse temperature of the lysozyme mannitol formulation could be due to partial crystallization of mannitol. Moreover, this technique is based on visual identification and so, the onset of micro-collapse can be subjective (Figure 2.3). Horn *et al.* reported a collapse temperature of - 28.1 °C for pure non-crystalline mannitol using an optical fiber system (Horn and Friess, 2018). These values demonstrated that mannitol in the presence of lysozyme did not crystallize completely upon freezing. Dixon *et al*. showed that two fusion proteins inhibited mannitol crystallization when the amount of mannitol was below 45 % of the dry weight of the lyophilized cake and protein concentration was greater than 10 mg/mL. It was elucidated that proteins during freezing and annealing can impact the nucleation of mannitol and growth of crystals through viscosity effects or through interactions at the molecular level (Dixon *et al.*, 2009). As suggested by

Bhatnagar *et al*., the interference of protein molecules in the crystallization process during freezing could also be a possible reason for partial crystallization of mannitol (Bhatnagar *et al.*, 2019).

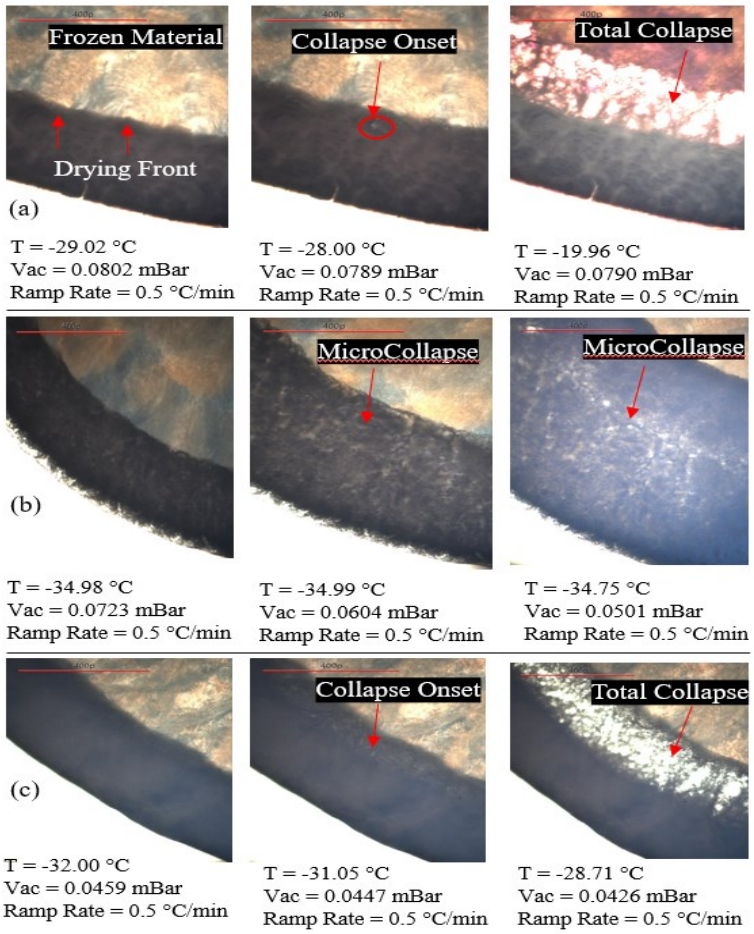

Figure 2.3: Figure showing the drying front (left), collapse onset (middle) and total collapse (right) for trehalose, mannitol and sucrose based formulations on the FDM.

2.3.2 Glass Transition and Melt Temperature Analyses

T_g' values for each formulation are shown in Table 2.6. Frozen-state DSC was performed prior to freeze-drying to determine the T_g' of the amorphous material and the T_{eu} for the crystalline material. This technique complements FDM as it determines the T_g' which is a few degrees lower than the collapse of a material (Tang and Michael J. Pikal, 2004). Therefore, the primary drying step must be carried out at temperatures lower than the T_g' or T_{eu} to prevent collapse of the material (Tang and

Michael J. Pikal, 2004). The T_g' values of all formulations were close to the T_g' values of pure trehalose, mannitol and sucrose reported in literature (Table 2.6). The T_g' values for histidine (- 6.24 °C) and lysozyme in histidine buffer (- 5.46 °C) were the highest. The T_g' values of trehalose (- 29.47 °C), mannitol (- 31.6 °C) and sucrose (- 32.62 °C) were very comparable to literature values (Table 2.6), whereas the T_g' values of lysozyme formulations containing trehalose, mannitol and sucrose were relatively higher than that of individual excipients due to the presence of lysozyme and histidine exhibiting very high T_g' by themselves. Factors affecting the glass transition temperature of materials include molecular weight, molecular structure and mobility, free volume, moisture content etc. (Montserrat and Colomer, 1984; Zeng *et al.*, 2001; Roudaut *et al.*, 2004; Jadhav *et al.*, 2014). The Fox-Flory equation elucidates the correlation between T_g and molecular weight (Equation 2.4). A low molecular weight results in low T_g, whereas an increase in molecular weight results in an asymptotic increase in the T_g (Larrain *et al.*, 1981; Brady *et al.*, 2017). Due to the complex structure and high molecular weight, proteins and amino acids exhibit high glass transition temperatures.

$$T_g = T_g^{\infty} - K * M^{-1} \qquad \textbf{Equation 2.4}$$

Where T_g is the glass transition temperature of the material,

T_g^{∞} is the glass transition temperature at infinite molecular weight,

M is the molecular weight of the material and K is a constant.

Table 2.6: T_g' of frozen-state lysozyme formulations.

Sample	Measured $T_{g'}$ (°C)	Literature $T_{g'}$ (°C)
Histidine buffer	-6.24 ± 0.13	-
Lysozyme in Histidine buffer	-5.46 ± 0.35	-
Lysozyme Trehalose	-25.05 ± 0.85	-
Lysozyme Mannitol	-26.87 ± 0.07	-
Lysozyme Sucrose	-29.86 ± 0.53	-
Trehalose	-29.47 ± 0.02	-30°C (TaPrime Consulting)
Mannitol	-31.60 ± 0.02	-31°C (TaPrime Consulting)
Sucrose	-32.62 ± 0.10	-32°C (Lewis *et al.*, 2010)

The thermal properties of the freeze-dried cakes were determined by solid-state DSC. The T_g and T_m of freeze-dried materials are shown in Table 2.7. The lysozyme trehalose and sucrose-based formulations exhibited T_g, unlike the mannitol-based formulation which exhibited a melt temperature (T_m). This was because the mannitol-based formulation was annealed during the freezing phase of the freeze-drying process to allow complete crystallization of mannitol. This method has been used previously to study the impact of mannitol crystallization on proteins (Lu and Pikal, 2004; Hawe and Frieß, 2006; Liao *et al.*, 2007; Al-Hussein and Gieseler, 2012). The lysozyme formulation containing trehalose showed a significantly higher T_g compared to the sucrose-based formulation. These results were consistent and comparable to the T_g values of the two sugars reported in literature (Table 2.7). Lyophilized lysozyme alone exhibited a very high T_g (142.15 °C). The T_g values of various proteins, namely, Ovalbumin (170 °C), α-Casein (165 °C), lysozyme (179 °C), Bovine Serum Albumin (156 °C) and Human Growth Hormone (136 °C) have been reported (Jirgensons, 1962; Whitaker and Tannenbaum, 1977; Matveev *et al.*, 1997; Pikal *et al.*, 2007). The T_g of pure lysozyme observed (142 °C) was lower than the reported value (179 °C) in literature due to high RMC in the original lysozyme powder procured from Sigma Aldrich. The strong glass-like behavior of proteins, evident from their

T_g values, was attributed to a large strength parameter with a very large T_g range (Fan *et al.*, 1994; Green *et al.*, 1994; Pikal *et al.*, 2007).

The measured T_g or T_m of all formulations results were verified using the Fox equation (Equation 2.5) as reported in Table 2.7. The experimental T_g or T_m values obtained for each formulation were consistent, except for the formulation containing lysozyme and histidine buffer only.

$$\frac{W_T}{T_{g/melt}} = \left(\frac{W_1}{T_{g1}}\right) + \left(\frac{W_2}{T_{g2}}\right) + \left(\frac{W_3}{T_{g3}}\right) + \cdots \qquad \textbf{Equation 2.5}$$

Where W_T is the total weight of the formulation,

$T_{g/melt}$ is the glass transition or the melt temperature of the formulation,

W_1, W_2, W_3 are the weight fractions of individual components in the formulation,

T_{g1}, T_{g2}, T_{g3} are the glass transition or melt temperature of the components.

Table 2.7: T_g and T_m of lyophilised lysozyme formulations.

Sample	Measured T_g / T_m (°C)	Predicted T_g / T_m (°C) By Fox-Equation	Literature T_g / T_m (°C)
Lysozyme Powder (as received)	142.15 ± 0.05 (T_m)	-	T_g = 179 (Whitaker and Tannenbaum, 1977; Matveev *et al.*, 1997)
Histidine Powder (as received)	134.77 ± 5.74 (T_m)	-	-
Lysozyme and Histidine (Lyo Cake)	174.39 ± 5.05 (T_m)	141.6	-
Lysozyme Trehalose (Lyo Cake)	108.48 ± 3.62 (T_g)	110.6	T_g = 103.0 ± 1.6 (Liao *et al.*, 2004), 106.85 (Simperler *et al.*, 2006)
Lysozyme Mannitol (Lyo Cake)	155.67 ± 1.94 (T_m)	160.25	T_m = 166.0 (Ye and Byron, 2008)
Lysozyme Sucrose (Lyo Cake)	67.23 ± 1.21 (T_g)	68.49	T_g = 60.8 ± 1.5 (Liao *et al.*, 2004), 59.85 (Simperler *et al.*, 2006)

The T_g of the freeze-dried formulations were calculated by substituting the weight fraction and glass transition temperatures of individual components in Equation 2.5. While the experimental values for the freeze-dried trehalose and sucrose-based formulations were consistent with the Fox equation, higher deviations were observed in the lysozyme mannitol and histidine-based formulation. The Fox equation does not incorporate factors such as density, heat capacities, variations in the conformational entropy and the interactions between components in a formulation, so, it does not provide a good prediction for the thermal properties of materials (Shamblin *et al.*, 1998; Seo *et al.*, 2006; Pinal, 2008; Weng *et al.*, 2014).

2.3.3 Freeze-drying

3 different conventional lyophilization cycles were employed to study the impact of freeze-drying on lysozyme and its formulations. Formulations containing trehalose and sucrose were freeze-dried using the same recipe, batch number A051018 and A191118 respectively, whereas mannitol followed a different cycle with an additional annealing step, batch number B301118. The additional step was introduced to study the impact of annealing on the protein. Lysozyme was freeze-dried without any excipients or stabilizers in a separate cycle with an increased freezing temperature and reduced primary drying duration (batch number A301118). These parameters were altered as pure lysozyme and lysozyme in histidine buffer exhibited a very high T_g' (- 5.46 °C) compared to other formulations and so it could be sublimed at higher temperature, thereby, preventing its collapse (Tang and Michael J Pikal, 2004). From Figure 2.4, it is evident that the product temperature remained below the T_g' of the formulation until most of the water was sublimed. Thermocouples were used to monitor the product temperature during the lyophilization process. Figure 2.4 depicts the lyophilization cycle for lysozyme in histidine buffer. The product was frozen at -35 °C for 3 h. The temperature was ramped up to 0 °C to increase the rate of sublimation. The temperature probes indicated that the product temperature was still below its T_g' until the product temperature reached the shelf temperature approximately after 21 h. The product was maintained at 0 °C for approximately 20 h. During the

secondary drying step, the shelf temperature was ramped up to 25 °C for 10 h which allowed the desorption of residual water from the lyophilized cake. In this case, no further loss of water was observed during secondary drying in the Pirani pressure gauge, as shown in Figure 2.4. The product temperature was maintained at 5 °C. This marked the end of the lyophilization cycle.

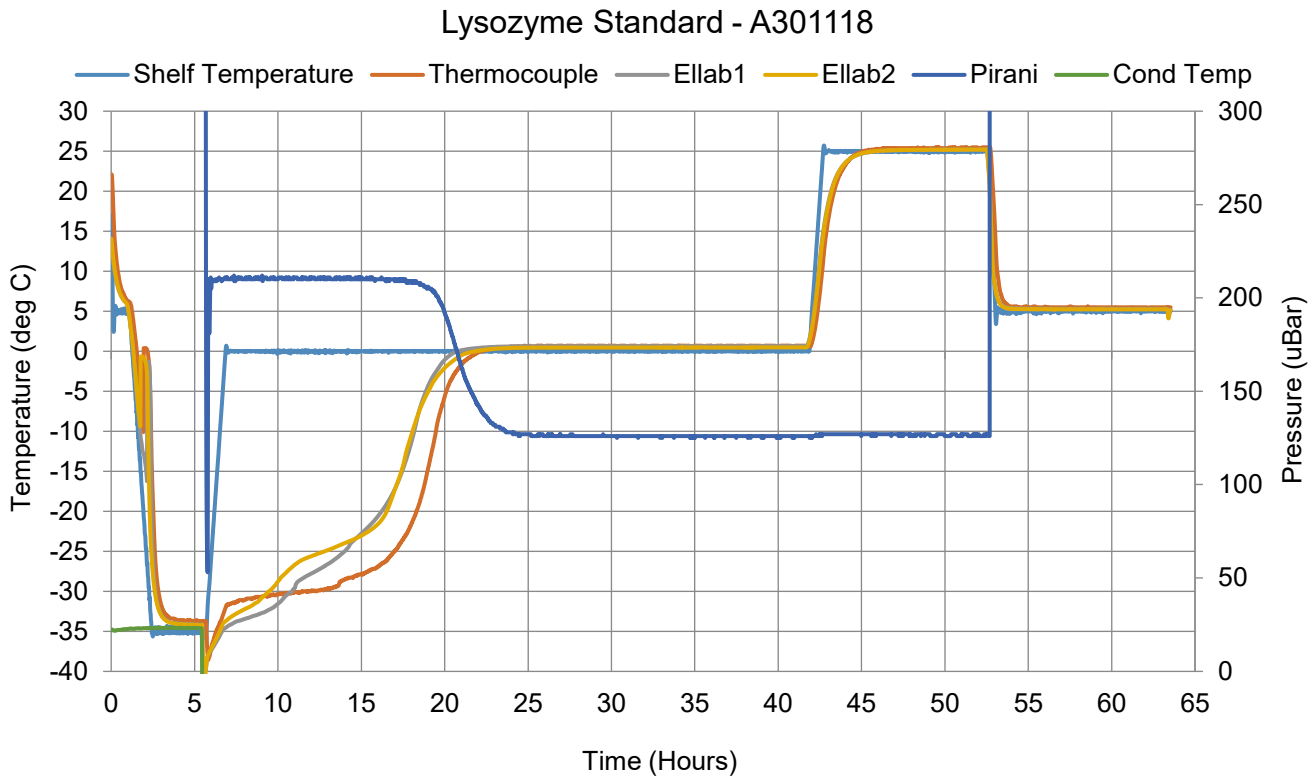

Figure 2.4: Lyophilization cycle for lysozyme in histidine buffer.

Lyophilized products are assessed in terms of visual cake appearance, container closer defects, RMC, reconstitution time and other release and stability tests for regulatory requirements. This is carried out to ensure that the product's safety, quality and efficacy requirements are met. According to "Lyophilization of Parenteral (7/93)" by the FDA, one of the major concerns in terms of cake appearance is meltback (FDA, 2014c). Meltback is referred to as partial or total collapse of the freeze-dried cake due to a change of state from solid to liquid. Other related problems include poor solubility, increased rehydration time, partial loss of potency, presence of less stable crystalline or amorphous

state etc. (FDA, 2014c). Moreover, several other defects with respect to visual cake appearance have been reported. These include product ejection (Wittaya-Areekul *et al.*, 2002), slanted cake (Patel *et al.*, 2017), puffing (Patel *et al.*, 2017), lifted cake (Patel *et al.*, 2017), cake shrinkage and cracked cake (Rambhatla *et al.*, 2005; Ullrich *et al.*, 2015b, 2015a, 2015c), broken cake (Patel *et al.*, 2017), vial fogging (Abdul-Fattah *et al.*, 2013), lyo ring, splashing, skin and foam formation (Kochs *et al.*, 1991; Esfandiary *et al.*, 2016), volcano (Searles *et al.*, 2001), cake texture and colour, dried product between vial and stopper, and the presence of droplets on the interior walls of the vial (Patel *et al.*, 2017). The acceptance criteria for lyophilised cake appearance varies across the industry and certain markets can be very particular. The acceptability of cake appearances as per Patel *et al.*, 2017 is summarized in Table 2.8.

Table 2.8: Acceptability of Lyophilized Cake Appearance (adapted from Patel *et al.*, 2017).

Cake Appearance	Does it impact CQAs?	Is it acceptable?
Total Collapse	Yes	No
Meltback	Yes	No
Product Ejection	Yes	No
Product between vial and stopper	Yes	No
Puffing, lifted cake, splashing	Yes	No
Cake shrinkage and cracking	No	Yes
Dusting, chipping, fogging	No	Yes
Broken cake	No	Yes
Lyo ring	Yes	No
Bubble and foam	No	Yes
Volcano	No	Yes
Glassy droplet	No	Yes
Partial Collapse	No	Yes
Texture	No	Yes
Colour	No	Maybe

The lyophilized lysozyme cake is shown in Figure 2.5. The cake was shrunken, very brittle and light. It contained cracks and grooves. This was because of the absence of any stabilizing or bulking agent. Cake shrinkage has been linked to cake collapse but may not necessarily be a consequence of cake collapse (Patel *et al.*, 2017). A direct and inverse correlation between cake shrinkage, cracking and the amount of unfrozen water has been reported. The removal of unfrozen water during freeze-drying builds up mechanical stress in the cake which is manifested as volume contraction (cake shrinkage) or cake cracking (Rambhatla *et al.*, 2005; Ullrich *et al.*, 2015b, 2015a, 2015c).

Figure 2.5: Lyophilized cakes of lysozyme in histidine buffer.

No direct correlation was observed between cake shrinkage, cracking and unfrozen water during the drying of trehalose, sucrose and maltose-based solutes. With the increase in the concentration of trehalose, cake shrinkage decreased and cracking increased and vice-versa (Patel *et al.*, 2017). Lyophilized lysozyme cake containing trehalose as an excipient is shown in Figure 2.6. The cake appeared intact and strong, but not rigid. No major cracks or spaces could be seen, and the cake appeared dry. The cake was slightly shrunken and flipped when the vial was inverted. Possible reasons could include the presence of amorphous components and reduced adsorption and adhesion to the inner walls of the vials due to the presence of SiO_2 coating in Schott vials which is used to minimize interaction between the drug product and the container (Schott; Ullrich *et al.*, 2015a). The lyophilization cycle for formulation containing trehalose was similar to that of sucrose.

Figure 2.6: Lyophilized cakes of Lysozyme formulated with trehalose.

Furthermore, the impact of freezing rate was studied by Ullrich *et al.* on cake shrinkage and cracking. A decrease in the freezing rate from 0.4 °C/min to 0.2 °C/min led to an increase in cake shrinking rather than cracking (Ullrich *et al.*, 2015c). The freeze-drying cycle of the lysozyme formulation containing mannitol included an annealing step to study the impact of crystallization. Annealing is preferred to crystallize crystalline components during freeze-drying to avoid any compromise with storage stability (Lueckel *et al.*, 1998). Moreover, crystallization during the primary drying phase may result in vial breakage (Williams *et al.*, 1986). A slow freezing step is preferred during the annealing step (Williams *et al.*, 1986; Tang and Michael J. Pikal, 2004).

The lyophilization cycle of lysozyme mannitol is shown in Figure 2.7. The product was frozen at – 40 °C for 2 h. During the annealing step, the shelf temperature was ramped up to – 20 °C for 2 h and then lowered back to – 40 °C for 2 h. This step was implemented to crystallize mannitol in the frozen state (Tang and Michael J. Pikal, 2004). The heating and cooling rate were 0.5 °C/min at every step. The shelf temperature was raised to 0 °C to increase the rate of sublimation. As shown in Figure 2.7, the product temperature was maintained below its eutectic temperature to prevent collapse of the frozen material. The primary drying step continued until 46 h, after which the shelf temperature was ramped up to 25 °C for 10 h to initiate secondary drying. In this case also, no further loss of water was observed during secondary drying through the Pirani pressure gauge. The product was later brought to 5 °C which marked the end of the process.

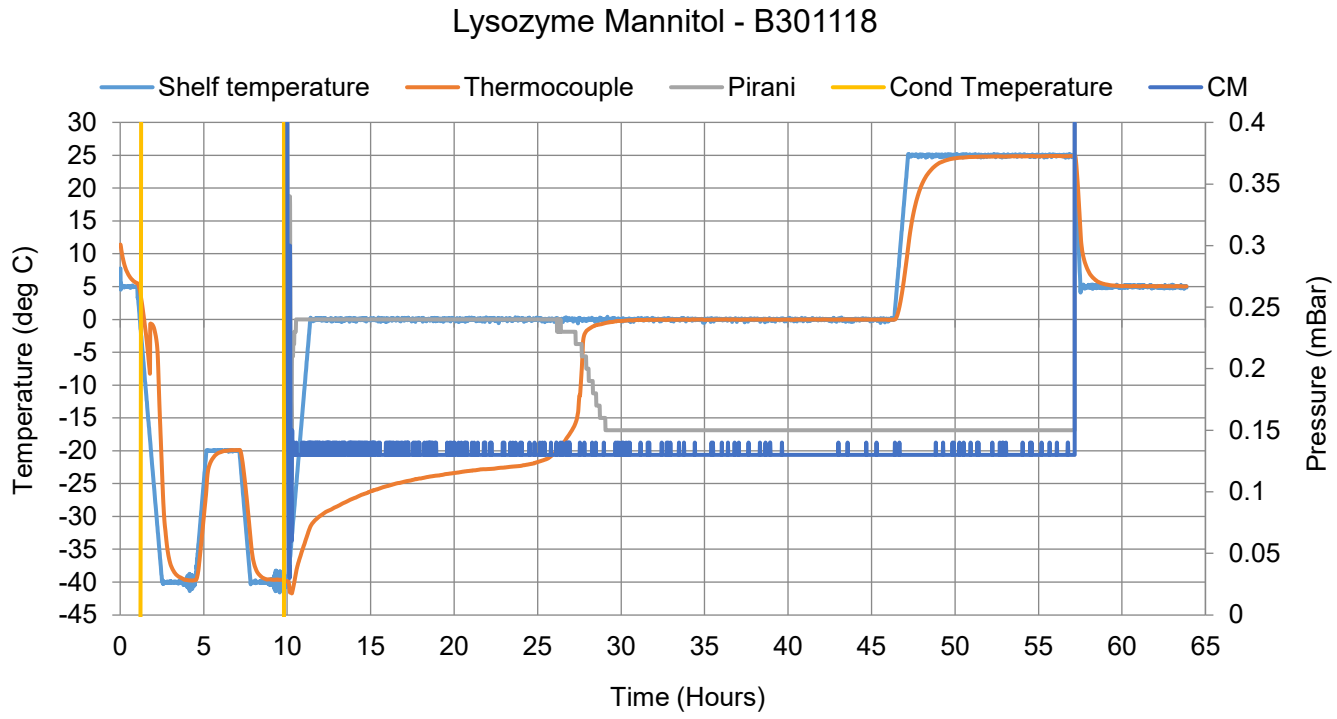

Figure 2.7: Lyophilization cycle for lysozyme formulated with mannitol.

Figure 2.8 shows the lyophilized cake of the lysozyme formulation containing mannitol. The cake appeared very strong, intact and rigid showing crystallization of mannitol. It has been reported that annealing resulted in moderate shrinkage (Ullrich *et al.*, 2015c; Patel *et al.*, 2017). Crystallization of the bulking component, mannitol explains the rigid and intact cake structure with minimal cake shrinkage and cracking. Additionally, volcano formation (spike in the cake) was observed in this case (Figure 2.8). Volcano formation is observed in the frozen matrix as a result of inward radial freezing due to limited or no space for expansion between the cake and the inside wall of the glass vial (Patel *et al.*, 2017). This aberration has no impact on the product's CQAs and is acceptable.

Figure 2.8: Lyophilized cakes of lysozyme formulated with mannitol.

Figure 2.9 depicts the lyophilization cycle for the lysozyme formulation containing sucrose. The product was frozen at - 45 °C for 2 h and then the shelf temperature was ramped up to -10 °C to increase the rate of sublimation. At this point, even though the product temperature was slightly above its T_g', no collapse was observed in the lyophilized cake. Freeze-drying above the T_g' in certain high concentration amorphous protein formulations, with no compromise on the product's physical and chemical stability has been reported (Depaz *et al.*, 2016). It is important to note that the Pirani gauge took more than 15 h to drop from ~ 207 µbar to ~ 128 µbar. This could have been due to different cake resistances amongst product and placebo vials at the end of primary drying. High cake resistance increases the resistance to mass transfer of water vapor, thereby, increasing the time required to complete the primary drying phase (Paptoff and Overcashier, 2002; Awotwe-Otoo *et al.*, 2013). The primary drying step continued until 42 h after which the shelf temperature was increased to 25 °C to initiate secondary drying. This step continued for 10 h in this case. As a result of different cake resistances, further loss of water was observed during secondary drying through the Pirani gauge as shown in Figure 2.9. This confirmed that the residual moisture after the primary drying phase was relatively higher than other formulations. The product temperature was held at 5 °C which marked the end of the cycle.

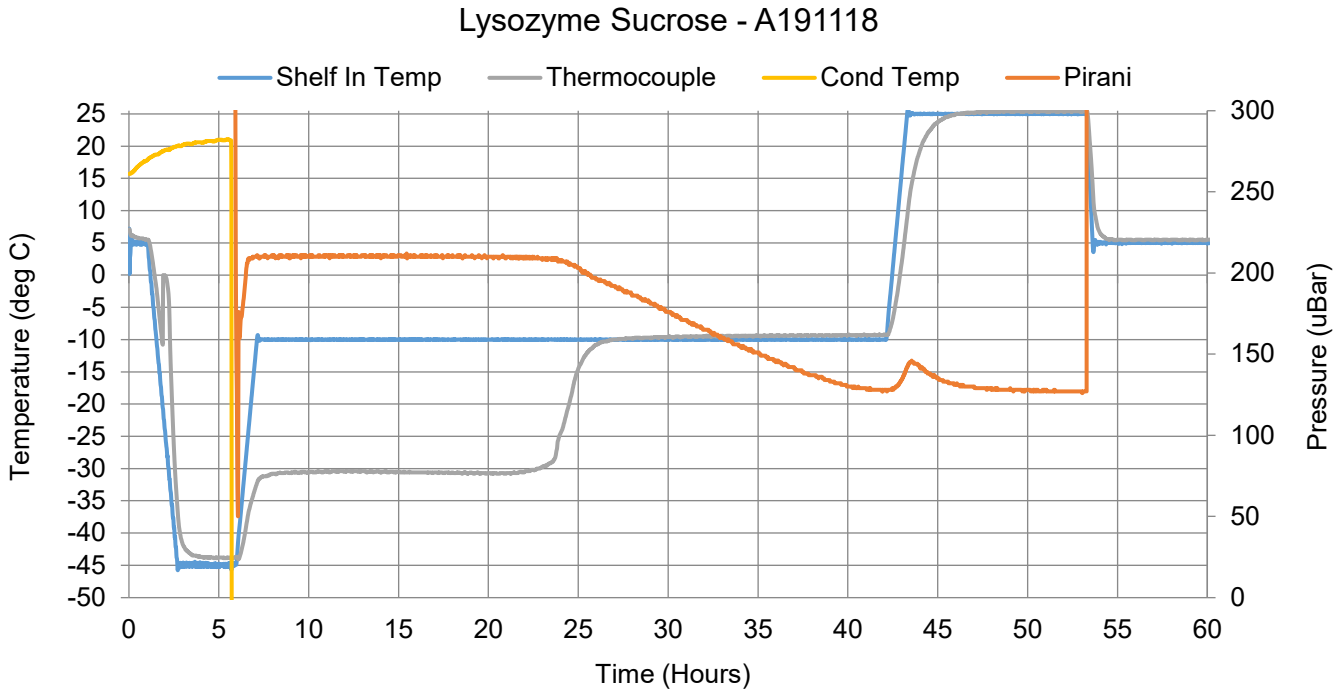

Figure 2.9: Lyophilization cycle for lysozyme formulated with sucrose.

The lyophilized lysozyme formulation containing sucrose can be seen in Figure 2.10. The cake appeared to be similar to the cake containing trehalose. The cake was strong, intact and devoid of any major cracks, but was not rigid. In this case, the cake flipped when the vial was inverted, thereby, showing cake shrinkage due to the presence of purely amorphous components and minimum product interaction with the container.

Figure 2.10: Lyophilized cakes of lysozyme formulated with sucrose.

Lam and Patapoff introduced two methods of encapsulation for freeze-dried cakes in Dow Corning Sylgard 184 polydimethylsiloxane (PDMS) for visualizing intricate cake structures normally not visible to naked eyes (Lam and Patapoff, 2011). They studied the physical impact of different freezing methods, namely, normal freezing, directional ice growth and ice growth via rapid freezing on freeze-dried cake structure and appearance. Through a fluorescence imaging system, they were able to obtain cross-sectional cake images with better resolution, magnification and contrast (Lam and Patapoff, 2011). More recently, Haeuser *et al.* used a variety of techniques such as three-dimensional laser scanning, polydimethylsiloxane embedding, scanning electron microscopy (SEM) and microcomputed tomography (μ-CT) to study and characterize freeze-dried cakes (Haeuser *et al.*, 2018). They concluded that even though all imaging techniques gave complementary information on cake structures at different levels, μ-CT was the most powerful non-invasive tool to qualitatively and quantitatively measure changes in cake structure and appearance and could be used during process development and at-line monitoring of lyophilized pharmaceutical products (Haeuser *et al.*, 2018). These techniques can be employed to study and characterize lyophilized cakes in the future.

2.3.4 Vial headspace moisture analyses

The vial's headspace moisture was measured using the Light House® instrument (LightHouse Instruments, 2018). This is based on Frequency Modulated Spectroscopy (FMS). This non-invasive technique employs laser light of wavelength 1400 nm which is passed through the vial's headspace and is collected onto a photo detector (Cook and Ward, 2011b, 2011a). This frequency resonates with the internal vibrational frequency of the water molecule, thereby, measuring the moisture concentration as vapor pressure. The moisture vapor pressure varied between 0.21 – 0.36 mbar for all lysozyme formulations (Figure 2.11).

It is interesting to note that a coefficient of determination ($R^2 = 0.97$) was achieved showing a good correlation between the vials' headspace moisture and the RMC for all freeze-dried lysozyme formulations (Figure 2.12). The residual moisture content is reported in section 2.3.5 (Figure 2.13).

This correlation can be used to estimate the average RMC in freeze-dried cakes in a batch of lysozyme formulations containing either trehalose, mannitol or sucrose using the non-invasive FMS Light House® instrument without the need for Karl Fischer titration. On average, it takes 3 – 4 s per vial to measure the headspace moisture using FMS Light House®, whereas it can take ≥ 30 min per vial to measure the RMC using Karl Fischer titration. This technique can significantly reduce time and the need for sample preparation for a number of drug product vials for batch release testing. Moisture mapping of freeze-dried vials can further help in lyophilization cycle development. Moreover, this technique can be configured as a PAT tool for real-time in-process measurements. Recently, authors have developed non-invasive models to determine the RMC in freeze-dried cakes using FMS (Affleck *et al.*, 2021; Pu *et al.*, 2022).

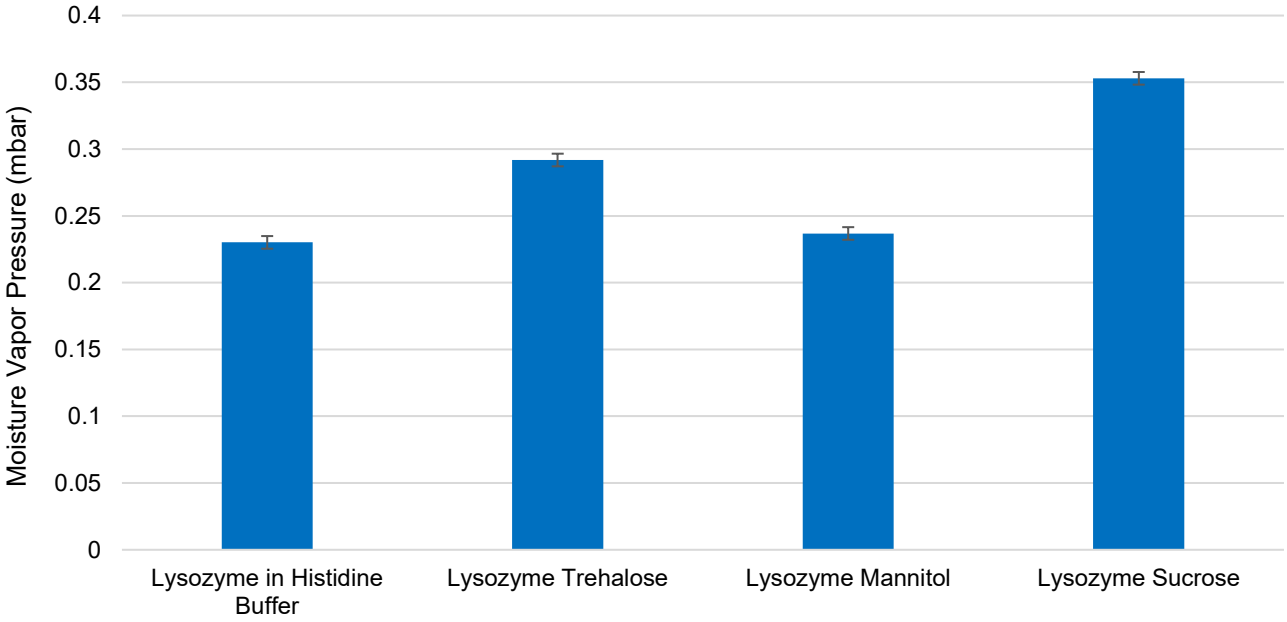

Figure 2.11: Vial headspace moisture content in lyophilized lysozyme formulations (n = 3).

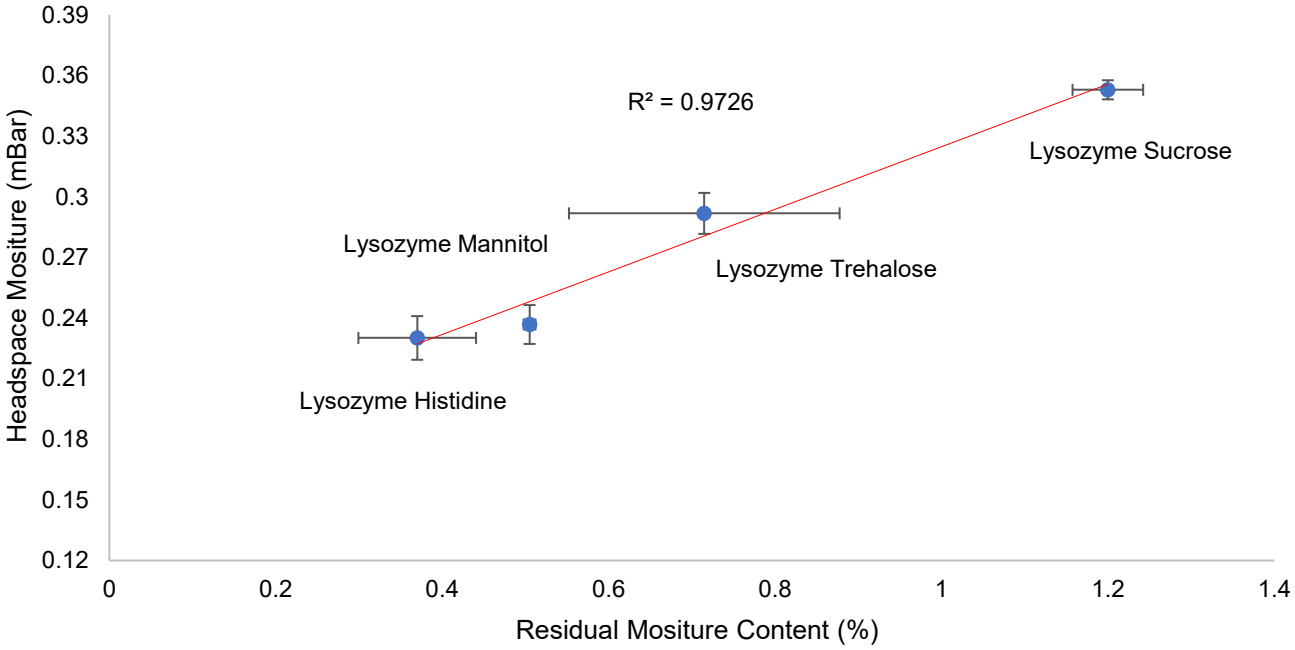

Figure 2.12: Correlation between Vial headspace moisture and RMC for all lysozyme formulations (n = 3).

2.3.5 Residual Moisture Content analyses

The RMC in the lyophilized lysozyme cakes was measured using Karl Fischer titration and was found to be in the range 0.32 % – 1.23 % as shown in Figure 2.13. The RMC values were within the specifications for lyophilized biologics (≤ 2.0 %) as per Table 2.9. The relatively high RMC in lysozyme sucrose cakes observed can be explained as per Figure 2.9. High cake resistance hinders the rate of vapor flow resulting in higher moisture levels. This is evident with the further loss of water observed during the secondary drying phase through a spike in the Pirani gauge between 40 – 45 h (Figure 2.9).

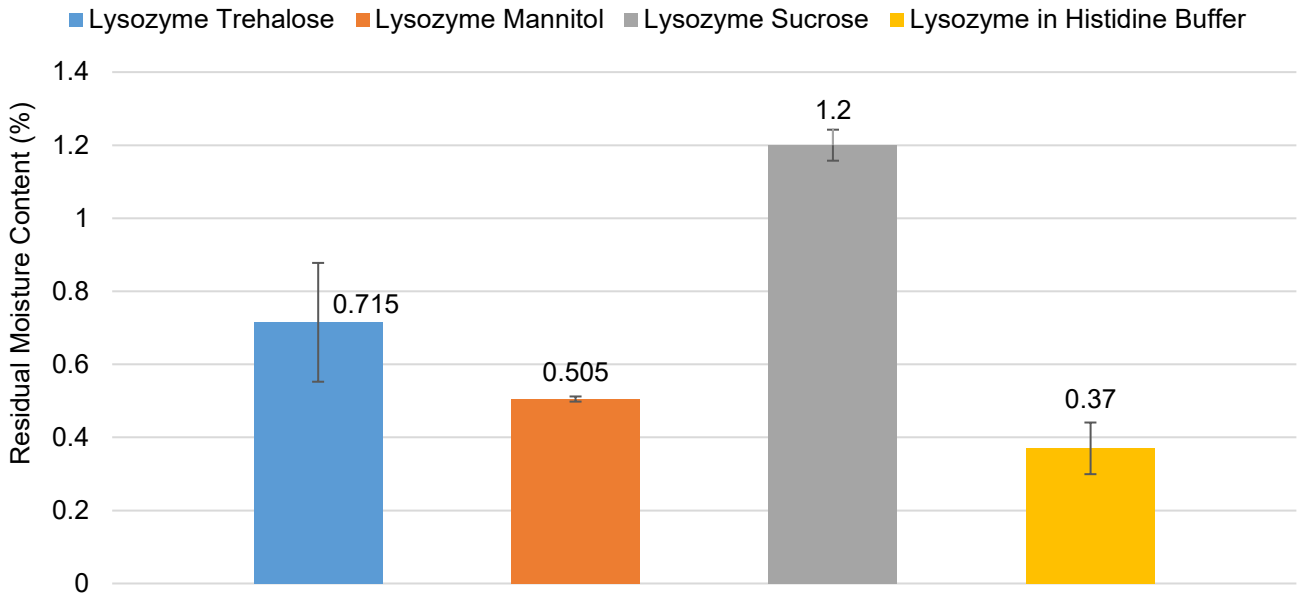

Figure 2.13: RMC in lyophilised lysozyme formulations (n = 3).

Table 2.9: General specifications for lyophilized biologics.

Method	Specification
Residual Moisture	≤ 2.0 %
Reconstitution Time	≤ 10 minutes
Dimer	≤ 8 %
Aggregation	≤ 3 %

2.3.6 Concentration, Turbidity and Reconstitution Time analyses

The reconstituted freeze-dried vials are shown in Figure 2.14. While several methods such as Bradford Protein Assay (Bradford, 1976), Bicinchoninic Acid (BCA) Assay (Smith *et al.*, 1985), Lowry (Alkaline Copper Reduction) Assay (Lowry *et al.*, 1951) and other dye based assays have been used historically to measure the concentration of proteins (Noble and Bailey, 2009), the UV absorbance-based technique at 280 nm is a simple method to quantify proteins with minimum sample preparation. This method works in the range of 20 – 3000 µg/mL (Noble and Bailey, 2009).

Moreover, UV absorbance in the light scattering region (320 nm – 350 nm) can be performed to identify and quantify turbid protein samples or suspended particles (Leach and Scheraga, 1960). In some cases, UV absorbance at 205 nm can result in more sensitivity and less variability amongst different protein molecules as a large number of peptide bonds absorb more photons at 205 nm (Noble and Bailey, 2009). Measurements at 205 nm are typically carried out at short path lengths and where the number of peptide bonds are more compared to aromatic amino acids.

The UV absorbance-based method at 280 nm along with Beer Lambert's Law (Equation 2.1) was used to calculate the concentration of the reconstituted freeze-dried lysozyme samples. The freeze-dried cakes were reconstituted within 1.5 min as the vials were gently rotated at an angle of 45°. The concentration of rehydrated freeze-dried lysozyme formulations was comparable to the original formulated bulk (10 mg/mL), as shown in Table 2.10. A simple way of visually estimating protein aggregation in terms of the level of turbidity was performed by categorizing the rehydrated protein solution as clear, slightly opalescent, opalescent, very opalescent, slightly cloudy, cloudy and very cloudy (Eckhardt *et al.*, 1994). Visually no distinction could be made between clear and opalescence in the reconstituted vials (Figure 2.14), so, the optical density of these samples was recorded at 350 nm (Table 2.10).

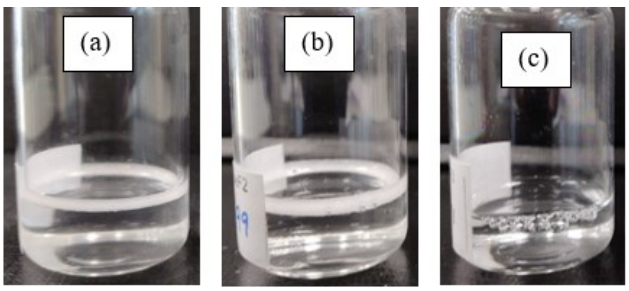

Figure 2.14: Reconstituted freeze-dried (a) lysozyme trehalose, (b) lysozyme mannitol and (c) lysozyme sucrose.

Table 2.10: Reconstitution time, concentration and turbidity of rehydrated freeze-dried lysozyme formulations.

Sample	Reconstitution Time (min)	Concentration (mg/mL)	Optical Density A_{350}
Freeze-dried excipient-free Lysozyme	1.0	9.99 ± 0.007	0.030 ± 0.0010
Freeze-dried Lysozyme Trehalose	1.5	9.09 ± 0.09	0.026 ± 0.0057
Freeze-dried Lysozyme Mannitol	2.0	10.31 ± 0.05	0.037 ± 0.0106
Freeze-dried Lysozyme Sucrose	1.0	9.70 ± 0.04	0.046 ± 0.0127

Figure 2.15 depicts the optical density of rehydrated freeze-dried lysozyme formulations in the light scattering region (350 nm). Mahler *et al.* studied the impact of shaking and shearing stress on chimeric mouse/human mAb (IGg1) formulation in terms of turbidity and protein aggregation (Mahler *et al.*, 2005). They reported some absorbance values at 350 nm as clear solution (0.008 – 0.019), slightly opalescent solution (0.0029 – 0.0035), opalescent solution (0.049 – 0.086) and very opalescent solution (0.139 – 2.196) (Mahler *et al.*, 2005). Moreover, the optical density of some reconstituted freeze-dried lactate dehydrogenase (LDH) was reported to be in the range of 0.005 – 0.024 (Al-hussein and Gieseler, 2013). They elucidated that the turbidity values of protein formulations containing citrate and histidine buffer was lower than formulations containing phosphate buffers. Protein denaturation in terms of the presence of insoluble aggregates was minimum in formulations containing histidine, whereas protein denaturation in terms of the presence of soluble aggregates could not be quantified using this technique (Al-hussein and Gieseler, 2013). They also reported that turbidity values of LDH samples was the lowest at pH 6 and enzyme activity decreased with increase in turbidity (Al-hussein and Gieseler, 2013). Based on the turbidity values (Table 2.10 and Figure 2.15), the rehydrated freeze-dried lysozyme samples can be categorized as clear/slightly opalescent solutions indicating minimal presence of insoluble aggregates.

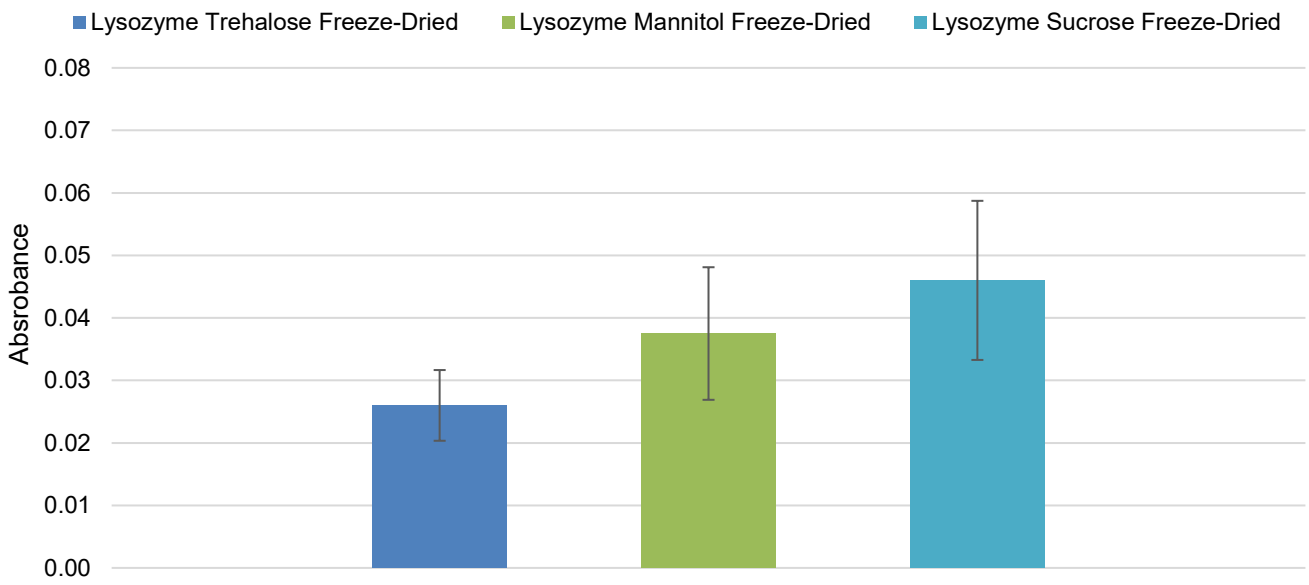

Figure 2.15: Optical Density of reconstituted freeze-dried lysozyme formulations measured at 350 nm.

2.3.7 Secondary Structure analyses using FTIR Spectroscopy

Infrared spectra of lysozyme formulations were collected using Attenuated Total Reflectance (ATR) Fourier Transform Infrared (FTIR) spectroscopy to study the secondary structure of the protein in the dried state, particularly across the amide I region. Figure 2.16 represents the FTIR spectra of lysozyme formulations in the dried state post lyophilization. The basic FTIR spectrum shape of lysozyme is similar to the spectrum shown in literature (Lewis *et al.*, 2010). An α-helical structure is assigned between 1654 cm^{-1} – 1658 cm^{-1}, β-sheets structure is assigned at 1624 cm^{-1} and 1641 cm^{-1} and bands between 1655 cm^{-1} and 1710 cm^{-1} were assigned to β-sheets and turns in the protein structure (Susi and Byler, 1986; Dong *et al.*, 1990; Liao *et al.*, 2002; Yang *et al.*, 2015). Moreover, the bands around 1638 cm^{-1} and 1683 cm^{-1} are assigned to intramolecular β-sheets and the bands at 1616 cm^{-1} and 1695 cm^{-1} are ascribed to intermolecular β-sheets (Dong *et al.*, 1994) (Allison *et al.*, 1999) (Al-Hussein and Gieseler, 2012).

Freeze-dried lysozyme in the absence of any excipient (saccharide) showed a shift in the α-helix band at 1643 cm^{-1}, whereas the α-helix bands for formulations containing trehalose, mannitol and sucrose were present between 1650 cm^{-1} – 1660 cm^{-1}. This shift in the frequency of α-helix band of lysozyme

without any excipient was due to the presence of weak hydrogen bonds, whereas formulations containing excipients exhibited α-helix bands at higher wavenumbers due to the presence of strong hydrogen bonds between lysozyme and the excipient. This shift can further be elucidated by the mechanism for the stabilization of proteins proposed by various authors (Carpenter *et al.*, 1994; Allison *et al.*, 1999; Kreilgaard *et al.*, 1999; Ajmera and Scherließ, 2014). The water replacement hypothesis states that proteins form hydrogen bonds with stabilizers during dehydration. These hydrogen bonds protect and stabilize proteins from external stress. In the absence of stabilizers, weak hydrogen bonding can be observed in the lyophilized spectra of lysozyme (blue) in Figure 2.16.

Broader and smaller bands seen at 1616 cm^{-1} and 1690 cm^{-1} indicated the presence of intermolecular β-sheets and Turn structures and bands around 1680 cm^{-1} were ascribed to the intramolecular β-sheet structure. Lysozyme formulations containing trehalose and sucrose showed an intact α-helical peak at 1655.1 cm^{-1} and 1654.6 cm^{-1} respectively, post lyophilization. A small shoulder was observed in the spectra of trehalose and sucrose-based formulations which can be seen between 1640 cm^{-1} and 1650 cm^{-1}. Unordered structure or random coils have been reported to be present between 1640 cm^{-1} and 1650 cm^{-1} (Krimm and Bandekar, 1986; Kong and Yu, 2007). More recently, random coils were reported to be present at ~ 1646 cm^{-1} (Wilson *et al.*, 2019). Therefore, in-line with the water replacement hypothesis, these results showed that the secondary structure of lysozyme, in the presence of saccharides, was preserved post freeze-drying.

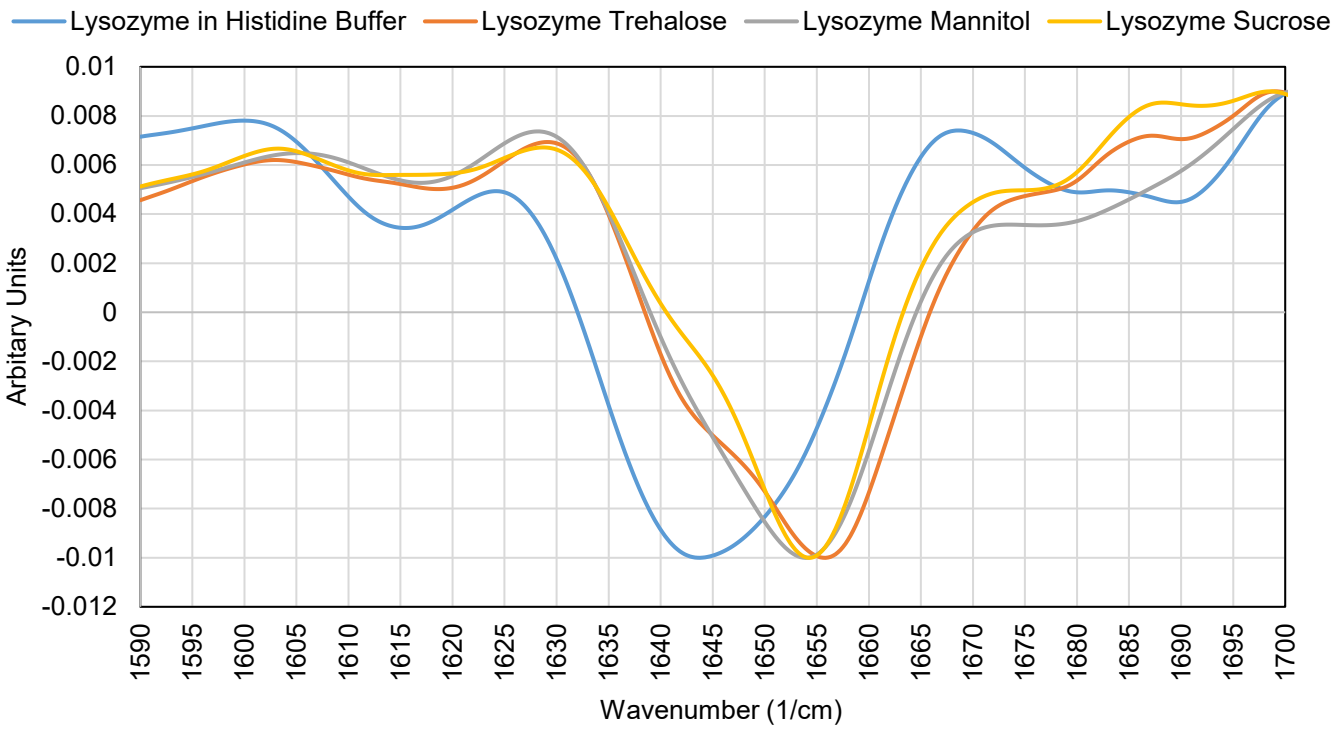

Figure 2.16: Solid-State second derivative FTIR Spectrum of lysozyme formulations. 164 scans were collected at a resolution of 4 cm^{-1} from 4000 cm^{-1} to 400 cm^{-1} and the Norris second derivative was analyzed from 1700 cm^{-1} to 1600 cm^{-1} across the amide I region.

2.3.8 Secondary and Tertiary Structure analyses using CD Spectroscopy

Information about the secondary structure composition of lysozyme was obtained through the far ultraviolet region (180 nm – 260 nm) of the CD spectrum. In this region, peptide bonds are the chromophores that absorb electromagnetic radiation below 240 nm (Kelly *et al.*, 2005). Figure 2.17 shows a comparison between the lysozyme formulations in the liquid state prior to and post lyophilization. The α-helical content of the protein was seen at 208 nm (strong band) and 222 nm (weak band) (Figure 2.17) (Kelly *et al.*, 2005; Nemzer *et al.*, 2013) showing that the protein is rich in helical content. A weak band at 218 nm corresponded to β-sheet structures (Lewis *et al.*, 2010). Absorption peaks due to β-sheet structures are weaker in helical rich proteins. Typically, proteins rich in β-sheet structures show a negative peak ~ 215 nm and a positive peak ~ 195 nm (Sreerama, 2003; Wallace, 2009). Moreover, natively disordered or unfolded proteins show a small peak around 180

nm – 185 nm and a broad negative peak around 195 nm – 198 nm (Matsuo *et al.*, 2007; Wallace, 2009). Some disordered proteins exhibited a single negative peak at 200 nm (Miles and Wallace, 2020). These peaks were absent in all lysozyme formulations showing that the protein's secondary structure was intact post lyophilization.

Absorption occurs as electrons in the chromophore are excited from ground state to a higher energy state. Peptide bonds in the far UV region exhibit two electronic transitions, i.e., an $n \rightarrow \pi^*$ and a $\pi \rightarrow \pi^*$ transition. A broad negative peak at 222 nm is due to $n \rightarrow \pi^*$ transition and a negative peak at 208 nm and a positive peak at 192 nm correspond to $\pi \rightarrow \pi^*$ transition (Figure 2.17) (Kelly *et al.*, 2005; Bulheller *et al.*, 2007; Miles and Wallace, 2020). The positive peak (192 nm) and the negative peak (208 nm) arise due to the splitting of the higher energy level during the $\pi \rightarrow \pi^*$ transition. This occurs due to the coupling of adjacent chromophores absorbing in this region (Gilbert and Hirst, 2004). Proteins rich in β-sheet structures exhibit $\pi \rightarrow \pi^*$ transitions with a much lower intensity than α-helical content (Miles and Wallace, 2020). The comparable far UV CD spectra of lysozyme prior to and post lyophilization showed that the secondary structure of lysozyme was preserved (Figure 2.17).

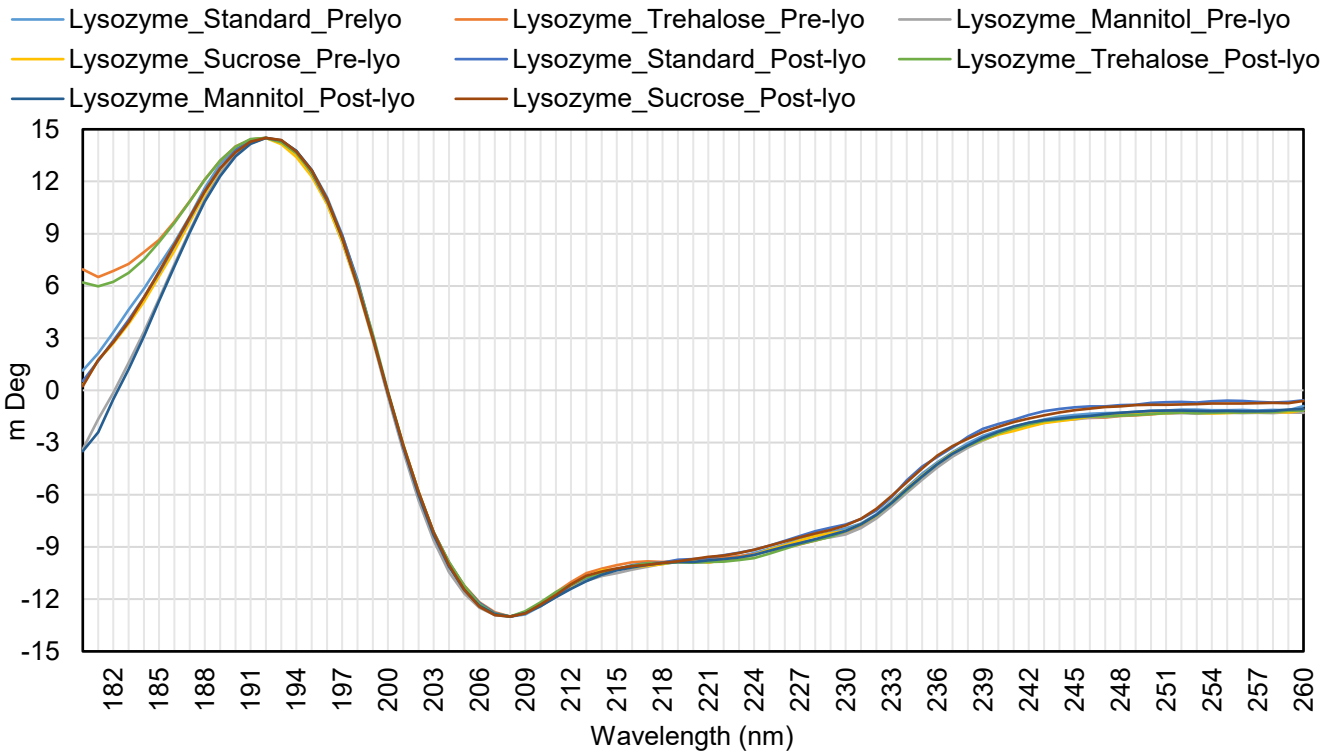

Figure 2.17: Far UV CD spectrum of lysozyme formulations across 180 nm – 260 nm, at every 1 nm for 2 s per point with a 1 nm bandwidth.

Quantitative analysis of the far UV CD spectrum obtained in Figure 2.17 was performed using CDSSTR analysis program on the DICHROWEB server (Whitmore and Wallace, 2004, 2007; Wallace, 2020). The secondary structure predictions are shown in Table 2.11. A NRMSD value of < 0.05 represents a good fit of the sample data with the reference set. The lysozyme trehalose-based formulation exhibited higher helical content and lower sheet content prior to and post lyophilization. Unlike other formulations, the helical (47 %) and sheet (6 %) content of the trehalose-based formulation was not consistent with the data reported for native lysozyme (Protein Data Bank 1DPX; Kong and Yu, 2007; Siddhanta *et al.*, 2015). Interestingly, Ji *et al.* reported 49 % helical and 6 % sheet content in a lysozyme formulation containing trehalose, ethanol and water which was correlated to the higher intensity of the α-helix peak observed using FTIR spectroscopy (Ji *et al.*, 2017).

Table 2.11: CDSSTR analysis of lysozyme formulations prior to and post lyophilization. Secondary structure predictions were performed using DICHROWEB (Whitmore and Wallace, 2004, 2007; Wallace, 2020). The reference set was adapted from Abdul-Gader *et al.*, 2011.

Sample	Helix	Sheet	Turn	Unordered	NRMSD
Lysozyme Histidine Pre-Lyo	42 %	8 %	17 %	32 %	0.024
Lysozyme Histidine Post-Lyo	41 %	10 %	16 %	33 %	0.022
Lysozyme Trehalose Pre-Lyo	47 %	6 %	16 %	31 %	0.022
Lysozyme Trehalose Post-Lyo	48 %	7 %	16 %	31 %	0.024
Lysozyme Mannitol Pre-Lyo	41 %	9 %	16 %	32 %	0.026
Lysozyme Mannitol Post-Lyo	41 %	11 %	15 %	33 %	0.023
Lysozyme Sucrose Pre-Lyo	42 %	10 %	16 %	32 %	0.023
Lysozyme Sucrose Post-Lyo	42 %	10 %	16 %	33 %	0.022

The tertiary structure of lysozyme was studied in the far ultraviolet region (260 nm – 320 nm) of the CD spectrum. Aromatic amino acids and disulphide bonds are the chromophores that absorb in this region. Tryptophan, Tyrosine and Phenylalanine residues exhibit a characteristic band between 290 nm and 305 nm, 275 nm and 282 nm, 255 nm and 270 nm, respectively (Kelly *et al.*, 2005). Absorption by aromatic amino acid side chains correspond to $\pi \rightarrow \pi^*$ vibronic transitions (Miles and Wallace, 2020). In certain proteins, aromatic side chains can produce higher intensity signals in the far UV CD region also, but are generally small compared to absorption by peptide bonds (Krittanai and Johnson, 1997; Kelly *et al.*, 2005; Miles and Wallace, 2020). In Figure 2.18, a band at ~ 289 nm shows the presence of Tryptophan, a broader band at ~ 283 nm indicates the presence of Tyrosine and Phenylalanine exhibits a weaker band at ~ 265 nm. In this case, the shape and magnitude of the spectra depends on the number and type of aromatic amino acids, their mobility and local environment, i.e., polar groups, H-bonding, spatial orientation with the molecule and neighboring protein molecules (Kelly *et al.*, 2005; Miles and Wallace, 2020). Moreover, disulphide bonds also produce weak absorption bands around 260 nm due to $n \rightarrow \sigma^*$ transitions (Woody, 1995). The

comparable near UV CD spectra of lysozyme prior to and post lyophilization demonstrates that its tertiary structure was preserved (Figure 2.18).

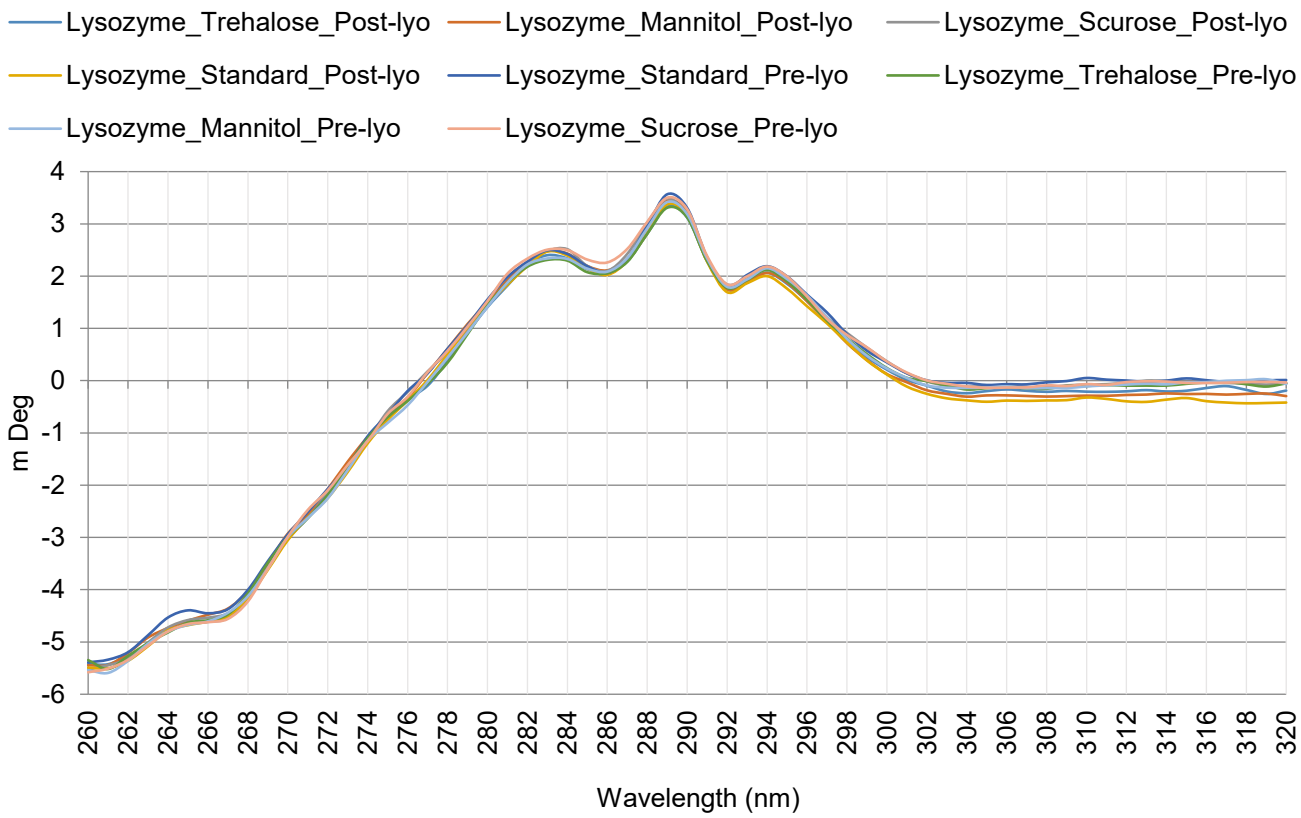

Figure 2.18: Near UV CD spectrum of lysozyme formulations across 260 nm – 320 nm, at every 1 nm for 5 s per point with a 1 nm bandwidth.

A temperature ramp study was performed to observe the shift in the spectra of lysozyme in the far as well as in the near UV CD regions as shown in Figure 2.19 and Figure 2.20 respectively. Figure 2.19 depicts the far UV CD spectra recorded every 10 °C from 20 °C to 80 °C. The protein was observed to be intact until 40 °C. Reduced alpha helical content with the increase in temperature was observed due to the decrease in absorbance showing the unfolding of the protein's secondary structure. Moreover, an isosbestic point was observed at 201 nm where the absorbance of the protein remained constant at different temperatures. A similar shift in the CD spectra of lysozyme was seen in the near UV region, shown in Figure 2.20. Complete flattening of the spectrum showed that the protein lost its tertiary structure at 80 °C.

The structural stability of a protein is studied in terms of its denaturation temperature along with other conditions such as pH, ionic strength etc. (Cooper, 1999; Chi *et al.*, 2003; Zhang and Cremer, 2009). The denaturation temperature of lysozyme and BSA solutions have been reported to be 73 °C and 58 °C, respectively (Giancola *et al.*, 1997; Almeida *et al.*, 2004; Iwashita *et al.*, 2017; Perez and Oliveira, 2017). Perez and Oliveira elucidated this using DSC, CD, SAXS (Small Angle X-ray scattering) and Fluorescence spectroscopy (Perez and Oliveira, 2017). They showed significant differences in the CD spectra of lysozyme at 20 °C and 90 °C indicating loss of secondary structure. Moreover, using SAXS and IFT analysis, they showed that at 70 °C radius of gyration of lysozyme increased but the molecular mass remained unchanged, whereas at ≥ 75 °C there was an increase in the size as well as the molecular weight of the protein indicating protein denaturation and aggregation. Lysozyme is a relatively stable molecule with higher denaturation temperature (73 °C) due to strong disulphide bridges and a lower molecular mass compared to BSA which contains a large number of amino acids and is more prone to structural flexibility and instabilities (Giancola *et al.*, 1997; Hirai *et al.*, 1998; Voets *et al.*, 2010; Sun *et al.*, 2015; Perez and Oliveira, 2017). Furthermore, Blumlein and McManus reported the melt transition temperature of lysozyme to be 74.6 °C (Blumlein and McManus, 2013). This data is consistent with the results obtained in Figure 2.19 and Figure 2.20.

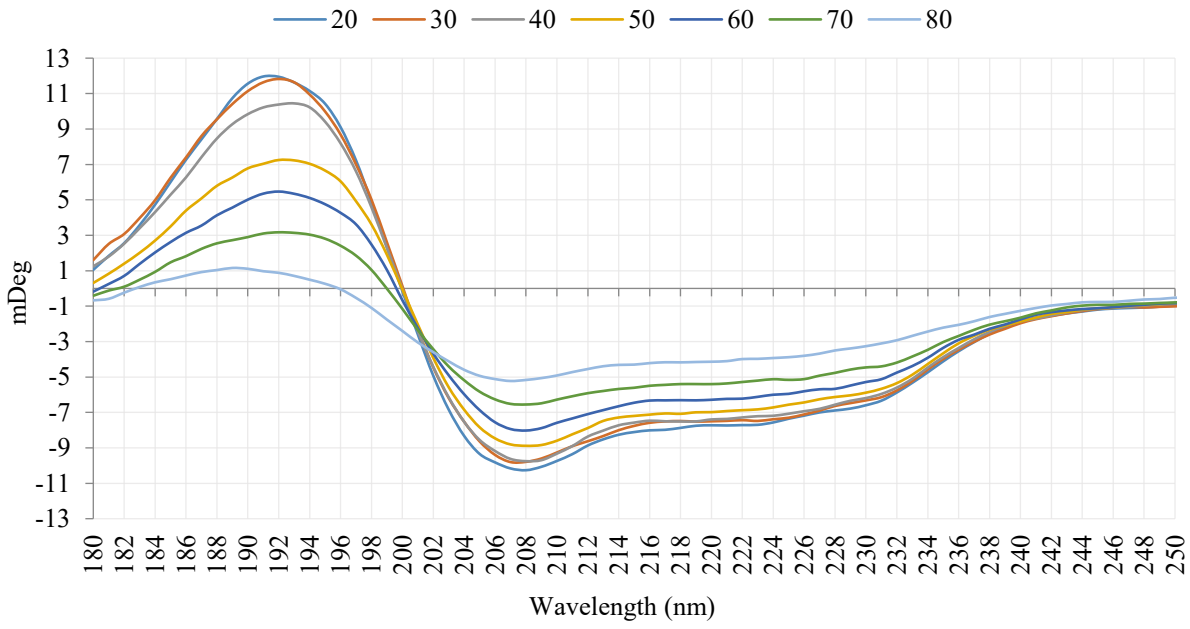

Figure 2.19: Temperature denaturation of lysozyme in the Far UV CD region.

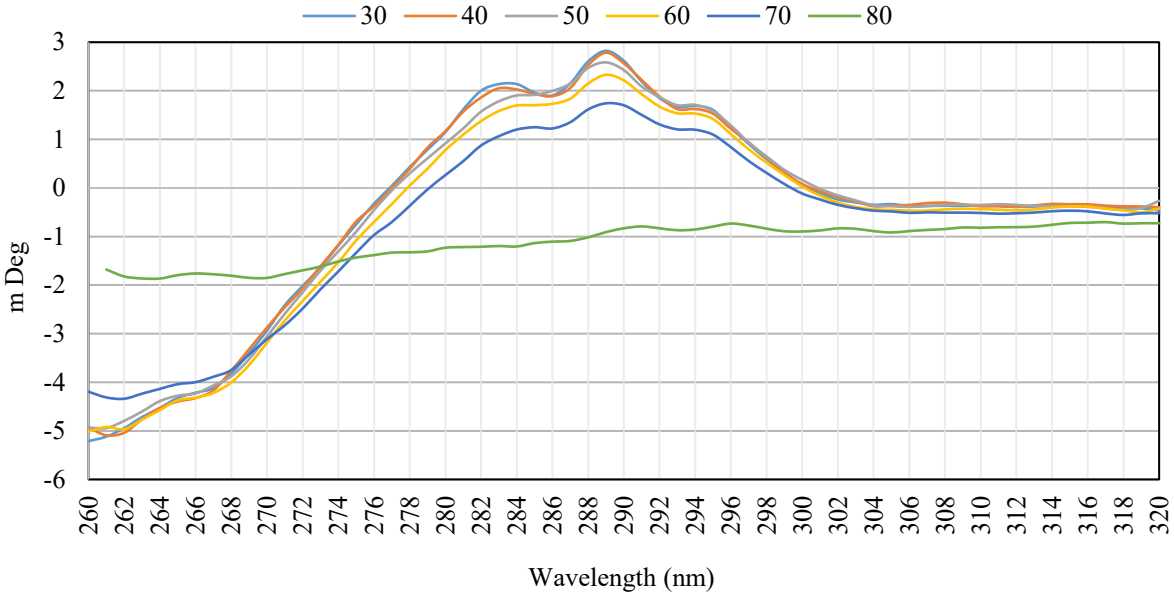

Figure 2.20: Temperature denaturation of lysozyme in the Near UV CD region.

To further quantify the differences between the secondary structure of lysozyme at room temperature (native) and at 80 °C, the CDSSTR analysis was run on the DICHROWEB online server (Table 2.12). A reduction in the helical and turn structures and an increase in the sheet and unordered structures indicated the loss of the protein's secondary structure at 80 °C, eventually leading to denaturation of the protein compared to its native state.

Table 2.12: CDSSTR analysis of lysozyme formulation at room temperature and 80 °C. Secondary structure predictions were performed using DICHROWEB (Whitmore and Wallace, 2004, 2007; Wallace, 2020). The reference set was adapted from Abdul-Gader *et al.*, 2011.

Sample	Helix	Sheet	Turn	Unordered	NRMSD
Lysozyme (native)	42 %	8 %	17 %	32 %	0.024
Lysozyme at 80 °C	7 %	35 %	13 %	42 %	0.073

2.3.9 Dynamic Light Scattering

Liquid-state particle size analyses was studied using DLS. Figure 2.21 shows the PSD by percentage intensity and percentage mass in a rehydrated freeze-dried lysozyme trehalose formulation. A multimodal PSD with three peaks were observed at ~1.5 nm, ~15 nm and ~100 nm in the size distribution by intensity, whereas only one peak was observed at ~1.5 nm in the size distribution by mass. The peak at ~1.5 nm may correspond to monomeric lysozyme (Figure 2.21). Due to the poor resolution of the single-angle DLS instrument (Den Engelsman *et al.*, 2011; Weinbuch *et al.*, 2015), the peaks for lysozyme, histidine and sucrose are unresolved between 0.5 nm – 4 nm (Figure 2.21). A similar size distribution profile was observed in all formulations prior to and post lyophilization. The polydispersity index (PDI) values (Table 2.13) for all samples was > 0.7 indicating that all samples contained particles of different sizes in the solution (Malvern Panalytical, 2011).

The hydrodynamic diameter of lysozyme was reported to be in the range 3.6 nm – 4.6 nm across a pH range of 4 – 10 (Bezemer *et al.*, 1999; Wei *et al.*, 2019; Zhang *et al.*, 2020). Upon increasing the ionic strength, the hydrodynamic diameter of lysozyme decreased due to the presence of a compact diffuse layer surrounding the protein, thereby, reducing the diameter of the shear plane of the charged protein (Zhang *et al.*, 2020). The hydrodynamic diameter of lysozyme was reported to be 4.1 nm at pH 7.4 (Bezemer *et al.*, 1999) whereas it was 3.64 nm at pH 3.3 (Valstar *et al.*, 1999). This data was only consistent with results shown below in Figure 2.22 (a). The additional peaks shown in Figure 2.21 could not be identified.

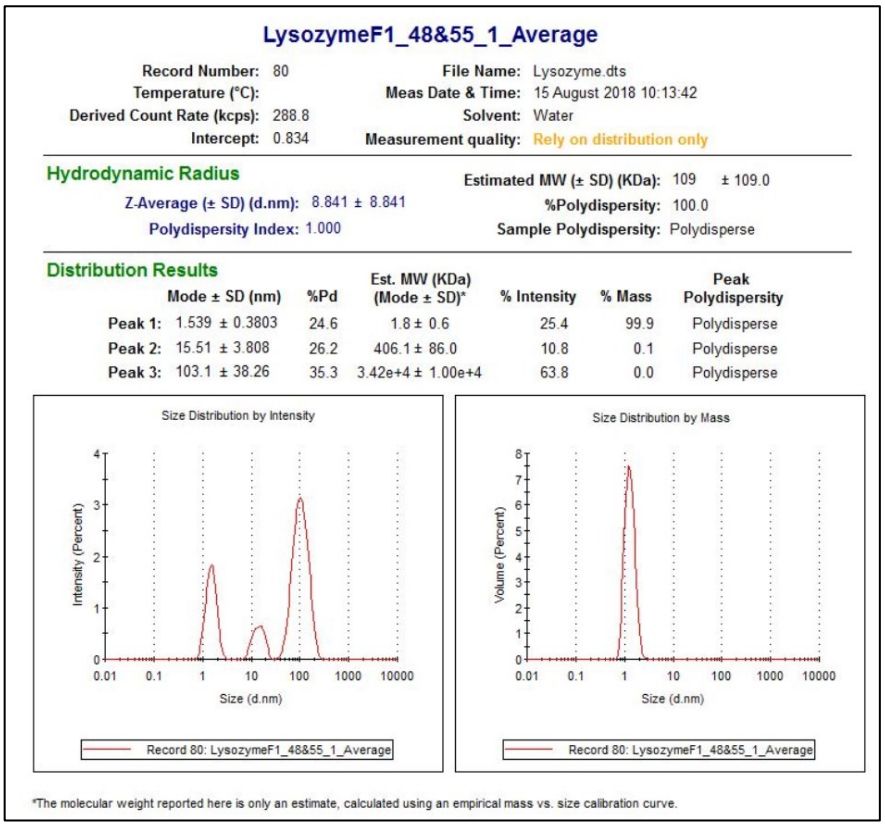

Figure 2.21: Representative PSD for all freeze-dried lysozyme formulations.

Since all 3 formulations were highly polydisperse, the Z-average values (Table 2.13) do not represent a true average of the monomeric protein and can be ignored. It is a reliable parameter for unimodal distributions (Malvern Panalytical, 2011). The presence of additional peaks may either correspond to agglomerates of impurities or aggregates of lysozyme. According to the manufacturer, Merck / Sigma Aldrich, the product's purity is ≥ 90 % (lysozyme) and the remaining ~10 % includes buffer salts such as sodium acetate and sodium chloride. The presence of additional peaks at ~100 nm – 200 nm in sucrose and sucrose containing protein solutions, which can interfere with the size analysis of proteins, have been reported (Kaszuba *et al.*, 2008; Hawe *et al.*, 2011; Weinbuch *et al.*, 2015). Weinbuch *et al.* reported the presence of interfering signals at ~100 nm – 200 nm in sugar containing lysozyme and IgG1 solutions using DLS and nanoparticle tracking analysis (NTA) (Weinbuch *et al.*, 2015). They investigated the presence of these peaks in various sugars (sucrose, trehalose, fructose, maltose and galactose) from various suppliers and different grades. They concluded that peaks appearing at ~100 nm – 200 nm were agglomerates of various impurities such as dextrans, ash and

aromatic colorants that may be present even after the refinement process. They demonstrated the removal of these impurities using a filter with a pore size of 0.02 μm (Weinbuch *et al.*, 2015). Moreover, Hawe *et al.* elucidated that surfactants, if present above the critical micelle concentration, could interfere with DLS measurements as they reported the presence of polysorbate 80 micelles at ~12 nm in the adalimumab formulation (Hawe *et al.*, 2011). The presence of peaks at ~100 nm in all lysozyme formulations (Figure 2.21 and Table 2.13) may correspond to impurities.

On the contrary, the presence of additional peaks in the range of 60 nm – 1000 nm were attributed to protein aggregates relative to the size of the monomeric protein (Panchal *et al.*, 2014; Wang *et al.*, 2016). Panchal *et al.*, using a Zetasizer ZS90 (Malvern Instruments), demonstrated that DLS was unable to resolve particles of size 20 nm from ≤ 200 nm, but were able to resolve 20 nm particles from ≥ 200 nm (Panchal *et al.*, 2014). They observed peaks shifts when the concentration of different sized particles in a mixture was varied. Furthermore, it was shown that for polydisperse solutions, DLS was unable to accurately measure the particle size (Filipe *et al.*, 2010).

Since the PDI for all lysozyme formulations was > 0.7, DLS was not a suitable technique for quantitative analysis of PSD. Furthermore, all samples were centrifuged to separate the monomeric protein to obtain a monodisperse solution.

Table 2.13: Z-average, Polydispersity Index and PSD for reconstituted freeze-dried lysozyme formulations.

Sample	Z-Average (nm)	PDI	Peak 1 (nm); Intensity (%)	Peak 2 (nm); Intensity (%)	Peak 3 (nm); Intensity (%)
Lysozyme Trehalose	8.84	1	1.54; 25.4	15.51; 10.8	103.1; 63.8
Lysozyme Mannitol	8.86	1	1.54; 20.0	11.22; 26.8	94.03; 53.2
Lysozyme Sucrose	26.33	1	1.4; 14.3	14.81; 8.1	136.1; 77.6

To separate out the additional peaks corresponding to either soluble or insoluble particulates, all lysozyme formulations were centrifuged at 20,000 g at 4 °C for 20 min. Post centrifugation, the supernatant and pellet (left over) were separated and analyzed separately using DLS. Visibly, no precipitates were observed in the pellet. Figure 2.22 (a) illustrates the PSD of centrifuged lysozyme formulated in reaction buffer. A single peak present at ~ 4.4 nm confirmed the presence of monomeric lysozyme. This value was consistent with literature values (Bezemer *et al.*, 1999; Wei *et al.*, 2019; Zhang *et al.*, 2020). A low polydispersity index (0.14) and Z-average (3.96 nm) were observed showing that centrifugation was able to separate the monomer and the large-sized species in the solution. On the other hand, greater sized particulates were separated out as observed in the pellet post centrifugation (Figure 2.22 (b)) as heavier particles settle down under the influence of centrifugal force and lighter particles are pulled towards the central axis of rotation.

Unlike Figure 2.22 (a), all other lysozyme formulations analyzed exhibited a multimodal distribution present in the supernatant as well as the left-over pellet post centrifugation (Figure 2.22 (b)). The PDI for all formulations except lysozyme in reaction buffer was ~ 0.7 (Table 2.14). This indicated that those solutions were polydisperse and were not suitable for DLS analysis. To further identify and quantify the particles present with greater size than that of lysozyme, size exclusion chromatography (SEC) was employed.

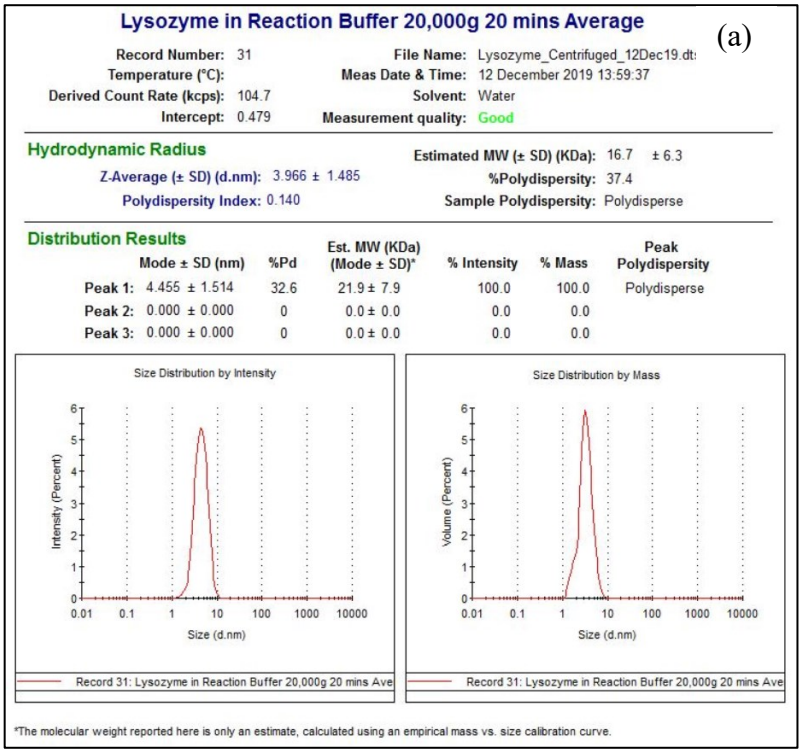

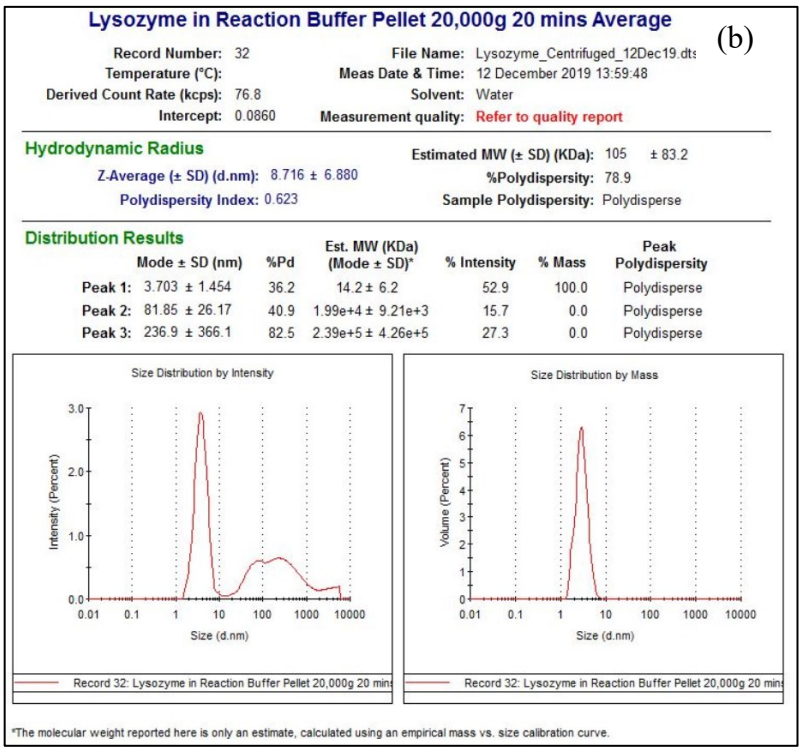

Figure 2.22: PSD of centrifuged supernatant (a) and pellet (b) for lysozyme in Reaction Buffer.

Table 2.14: Z-average and Polydispersity Index for centrifuged lysozyme formulations.

Sample	Z-Average (nm)	PDI	Peak 1 (nm); Intensity (%)	Peak 2 (nm); Intensity (%)	Peak 3 (nm); Intensity (%)
Lysozyme in Reaction Buffer (supernatant)	3.96	0.14	4.45; 100.0	0; 0	0; 0
Lysozyme in Reaction Buffer (pellet)	8.71	0.62	3.70; 52.9	81.85; 15.7	236.9; 27.3
Lysozyme in Histidine Buffer (supernatant)	4.35	0.72	1.54; 45.7	94.03; 54.3	0; 0
Lysozyme in Histidine Buffer (pellet)	24.49	0.73	1.4; 31.4	98.47; 68.6	0; 0
Lysozyme Trehalose (supernatant)	13.79	1	1.53; 21.0	11.76; 6.6	108.0; 72.0
Lysozyme Trehalose (pellet)	56.58	0.94	1.34; 22.7	0.84; 1.2	129.9; 86.8
Lysozyme Mannitol (supernatant)	25.17	1	1.61; 17.3	21.43; 2.10	136.1; 79.9
Lysozyme Mannitol (pellet)	81.61	0.66	1.34; 9.2	129.9; 88.8	1250; 2.0
Lysozyme Sucrose (supernatant)	9.59	1	1.54; 25.5	14.14; 8.80	103.1; 65.7
Lysozyme Sucrose (pellet)	-	-	-	-	-

2.3.10 Size Exclusion Chromatography

Quantitative analysis was carried out to further study the aggregation profile and the PSD in lysozyme formulations using SEC. This technique is a release test method for biologics and has been employed widely to quantify protein aggregates (L. Wu *et al.*, 2015; Farrell *et al.*, 2016; Iwashita *et al.*, 2017; Moorthy *et al.*, 2018; Wilson *et al.*, 2019). The BioRad protein calibration standard was run through TSK gel 3000 SWXL with an exclusion limit range from 10,000 Da to 500,000 Da. The molecular weight of the components in the standard are shown in Table 2.15. The calibration standard was used to then identify the elution of lysozyme in rehydrated freeze-dried formulations. All components eluted in the decreasing order of their molecular masses and were detected using a multiwavelength detector at 214 nm exhibiting greatest absorbance (Figure 2.23 and Table 2.16).

Table 2.15: BioRad Gel Filtration Standard Components.

Component	Molecular Weight (Da)
Thyroglobulin (bovine)	670,000
γ- Globulin (bovine)	158,000
Ovalbumin (chicken)	44,000
Myoglobin (horse)	17,000
Vitamin B12	1,350

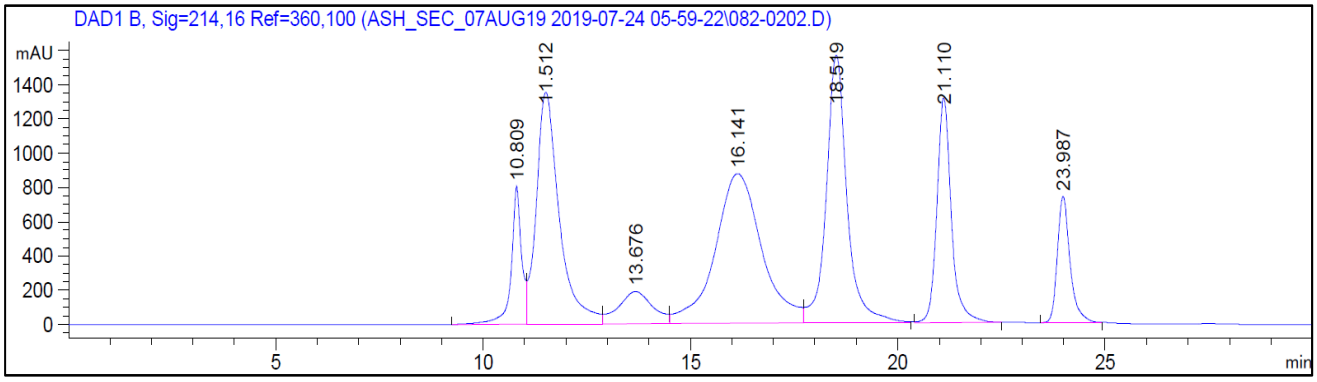

Figure 2.23: Chromatogram showing the elution of different proteins based on their molecular mass.

Table 2.16: Retention Time and Peak Area for the elution of BioRad Gel Filtration Standards.

Analyte	RT	Area	Area %
1	10.809	14132.7	5.70
Thyroglobulin	11.512	52195.9	21.05
3	13.676	10821.1	4.36
γ- Globulin	16.141	68518.8	27.63
Ovalbumin	18.519	54767.1	22.09
Myoglobin	21.110	31767.8	12.81
Vitamin B12	23.987	15713.5	6.33

Lysozyme formulations at concentrations of 10 mg/mL and 1 mg/mL were injected on the HPLC. Figure 2.24 illustrates a chromatogram showing the elution of lysozyme formulated in histidine buffer at 23.57 min. This peak eluted between Myoglobin (molecular weight = 17,000 g/mol and RT = 21.11 min) and Vitamin B12 (molecular weight = 1350 g/mol and RT = 23.98 min) confirming it to be a monomer of lysozyme (molecular weight = 14,307 g/mol and RT = 23.57). The SEC method employed was not able to provide a high resolution of separation between lysozyme (RT = 23.57) and Vitamin B12 (RT = 23.98), as both components lied on the lower side of the exclusion limit. A slight shoulder with a peak area of 0.69 % was observed at 22.71 min just before the elution of the monomeric lysozyme peak. No peaks were observed between 0 – 22 min indicating the absence of high molecular weight species (HMWS). Similar chromatographic profiles were obtained for all other lysozyme formulations (Figure 2.25).

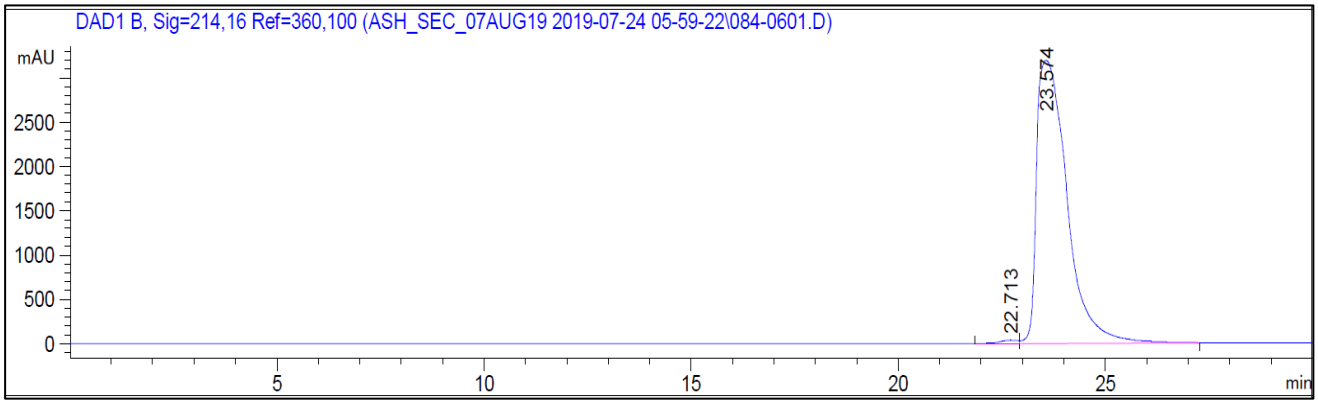

Figure 2.24: Chromatogram showing the elution of lysozyme (10 mg/mL) formulated in histidine buffer.

Table 2.17: Retention Time and Peak Area for lysozyme and its aggregates.

Analyte	RT	Area	Area %
HMWS	22.71	1133.6	0.69
Lysozyme	23.57	162907.5	99.30

The proportion of aggregates present were between 0.6 – 0.8 % of the total area and no additional peaks were observed indicating the absence of HMWS (Figure 2.25). These results indicated the presence of a very small fraction of lysozyme dimers but did not further elucidate the presence of additional peaks observed using DLS.

Lewis *et al.* employed two columns with different size exclusion limits (G3000SWXL and G2000SWXL) in series on their HPLC system to study the protein aggregation in gently and aggressively freeze-dried lysozyme, BSA and IgG (Lewis *et al.*, 2010). They found that the proportion of HMWS formed after 13 weeks of storage at 40 °C in lysozyme was ~ 0.35 % and in BSA was ~ 13 %. The proportion of aggregates reported were similar for both proteins at 5 mg/mL and 20 mg/mL. No differences in the formation of aggregates was observed when both proteins were freeze-dried gently and aggressively. A significant difference in the proportion of aggregates of IgG protein was reported at 5 mg/mL (~ 0.7 %) and 20 mg/mL (~ 2 %) at exaggerated storage conditions (Lewis *et al.*, 2010). The presence of lysozyme dimer with a molecular weight of 28.6 kDa has been reported (Thomas *et al.*, 1996; Onuma and Inaka, 2008; Cegielska-Radziejewska *et al.*, 2010; Utsumi *et al.*, 2017). Moreover, a chromatographic method was demonstrated to separate lysozyme dimers from a solution containing 66 mg/mL lysozyme in Tris-HCl buffer at pH 7.5 (Onuma and Inaka, 2008). They observed the appearance and disappearance of lysozyme dimers using SEC and SDS-PAGE. They elucidated that covalently bonded (strongly bonded) dimers appeared at the 28.6 kDa band in SDS-PAGE and weakly bonded dimers that showed non-specific hydrophobic interaction dissociated to form monomers at the 14.3 kDa band (Onuma and Inaka, 2008). Furthermore, out of the 78 identified hen egg white proteins, ovalbumin, ovotransferrin and lysozyme C are regarded as its major constituents (Mann, 2007). Iwashita *et al.* reported co-aggregation between ovalbumin and lysozyme in a mixture containing both the proteins using SEC and SDS-PAGE (Iwashita *et al.*, 2017). Lysozyme alone did not show aggregation and remained as a soluble monomer even after heat treatment for 30 min. The peak area of heat-treated lysozyme decreased with respect to the peak area of native lysozyme, but no additional peaks were observed indicating the absence of soluble

aggregates. However, aggregation in lysozyme was observed only by increasing the relative amounts of ovalbumin in the mixture (Iwashita *et al.*, 2017).

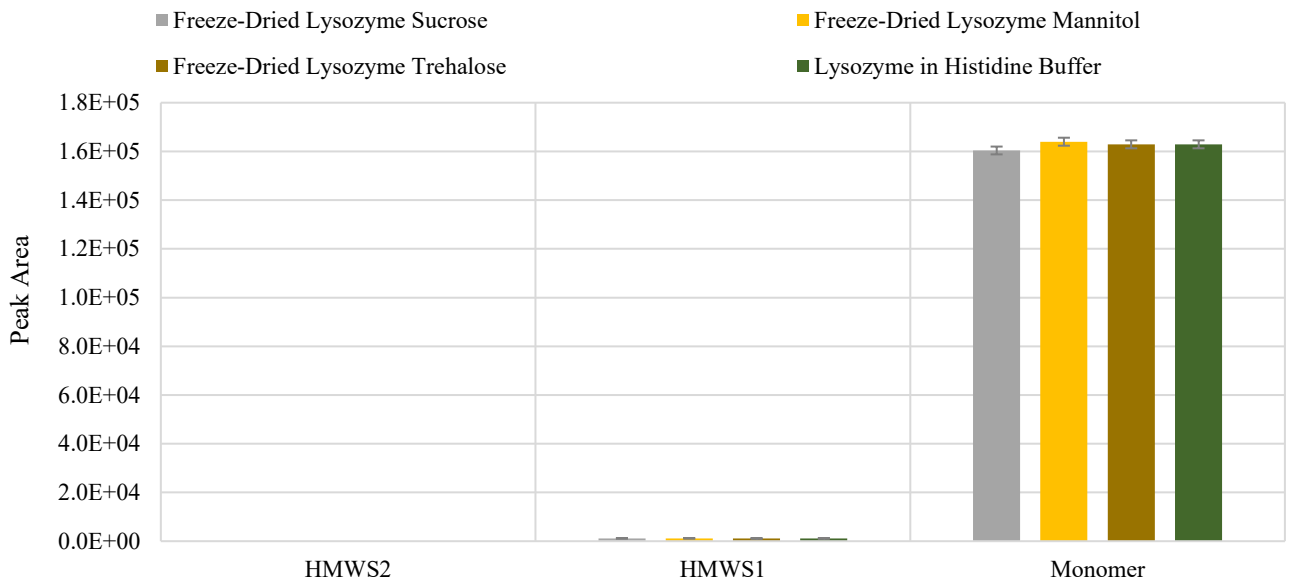

Figure 2.25: Aggregation profile of freeze-dried lysozyme formulations.

Some of the results from literature studies suggest that the additional peaks observed in DLS could either correspond to agglomerates of residual amounts of impurities or HMWS of lysozyme present below the limit of detection of the SEC method which are highly sensitive to light scattering. To explain the aggregation profile of lysozyme, alternative HPLC detectors and analytics would be required.

2.3.11 Powder X-Ray Diffraction (pXRD)

A qualitative powder XRD method was employed to identify formulations as amorphous and crystalline post lyophilization. Figure 2.26, Figure 2.27 and Figure 2.28 depict the X-ray diffraction patterns for lysozyme formulations containing trehalose, mannitol and sucrose, respectively. The XRD pattern for trehalose and sucrose-based formulations showed a broad peak from 3° to 60° suggesting the scattering of x-rays in many directions as a result of a random arrangement of atoms in the 3-D space indicating the presence of amorphous phase in the samples (Figure 2.26 and Figure 2.28, respectively). On the other hand, the XRD pattern for the mannitol-based formulation showed sharp distinct peaks of high intensity at periodic intervals from 3° to 60° suggesting x-ray scattering only in certain directions as a result of the presence of crystalline phase in the sample (Figure 2.27). Moreover, the XRD pattern of the mannitol-based formulation was compared to the different polymorphic forms of mannitol reported in literature. The XRD pattern in Figure 2.27 closely resembles the δ polymorphic form of mannitol (R. Smith *et al.*, 2017). Post freeze-drying, δ mannitol has been reported in the presence of lysozyme (Grohganz *et al.*, 2013). Therefore, lysozyme formulations containing trehalose and sucrose were amorphous and the formulation containing mannitol was crystalline post lyophilization. These results were consistent with the solid-state DSC results (section 2.3.2). A T_g was observed for amorphous lysozyme formulations (trehalose and sucrose) and a T_m was obtained for the crystalline lysozyme formulation containing mannitol. A crystalline lysozyme formulation containing mannitol was obtained as a result of the annealing step during the freeze-drying cycle. Crystallization of mannitol in protein formulations has been reported in literature (Johnson *et al.*, 2002; Tang and Michael J. Pikal, 2004; Chatterjee *et al.*, 2005a, 2005b).

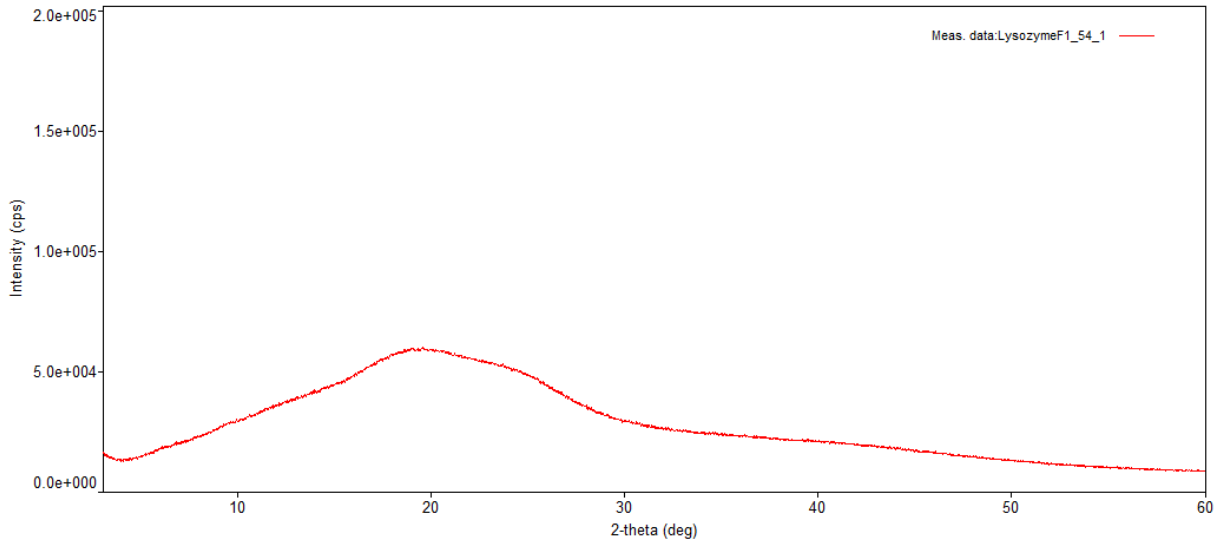

Figure 2.26: XRD pattern of Lysozyme formulation containing Trehalose.

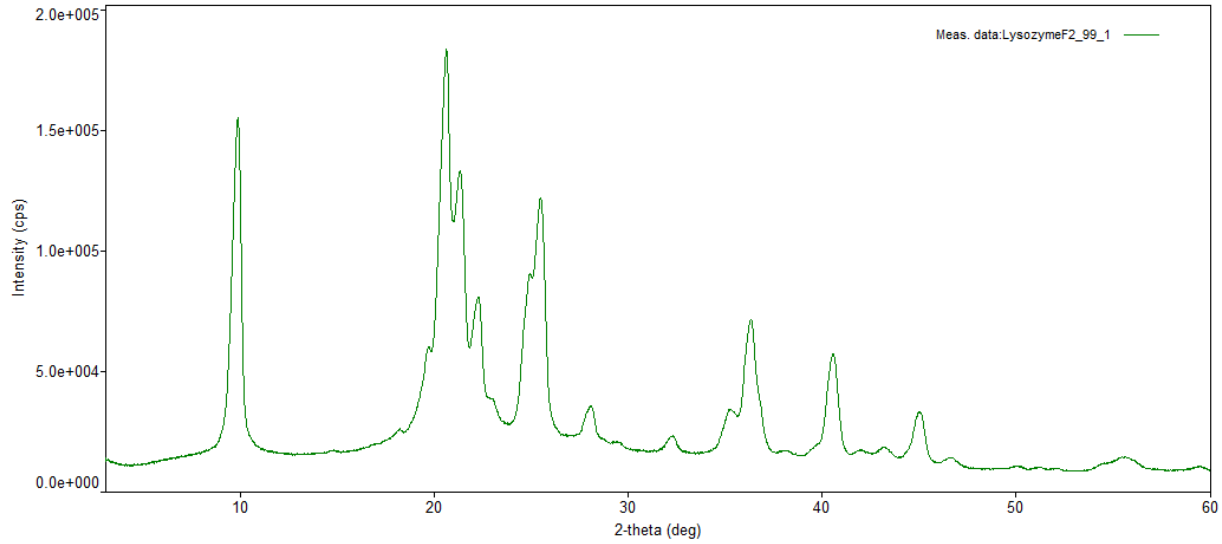

Figure 2.27: XRD pattern of Lysozyme formulation containing Mannitol.

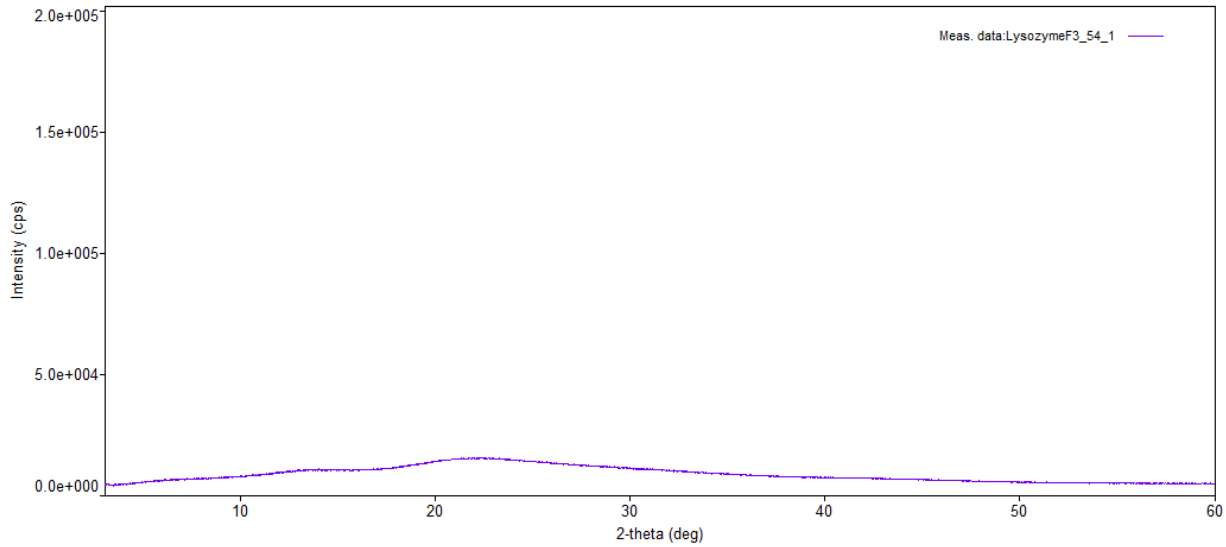

Figure 2.28: XRD pattern of Lysozyme formulation containing Sucrose.

2.3.12 Enzyme Activity

The enzyme activity of freeze-dried lysozyme formulations measured against *Micrococcus lysodeikticus* is shown in Figure 2.29. The specific enzyme activity was calculated using Equation 2.2 and Equation 2.3. The lysozyme standard in reaction buffer (control) was considered to exhibit 100 % activity as per the manufacturer's recommendation (Sigma Aldrich, 2017). Statistical differences amongst the enzyme activities of all lysozyme formulations were performed using one-way ANOVA – Tukey's post-hoc test (Appendix, Figure A2.1). On average, the enzyme activities of all freeze-dried lysozyme formulations were significantly higher than their pre-dried counterparts and the control (p-value < 0.05) except the sucrose-based formulation. Increased efficacy of biologics may not always be advantageous and desired based on the product's target efficacy range. The enzyme activities of pre-dried and freeze-dried lysozyme sucrose were comparable with no statistical differences (p-value > 0.05). Moreover, no significant differences were observed amongst for the enzyme activities of freeze-dried lysozyme formulations with a p-value of > 0.05. Therefore, the enzyme activity of all freeze-dried formulations was preserved.

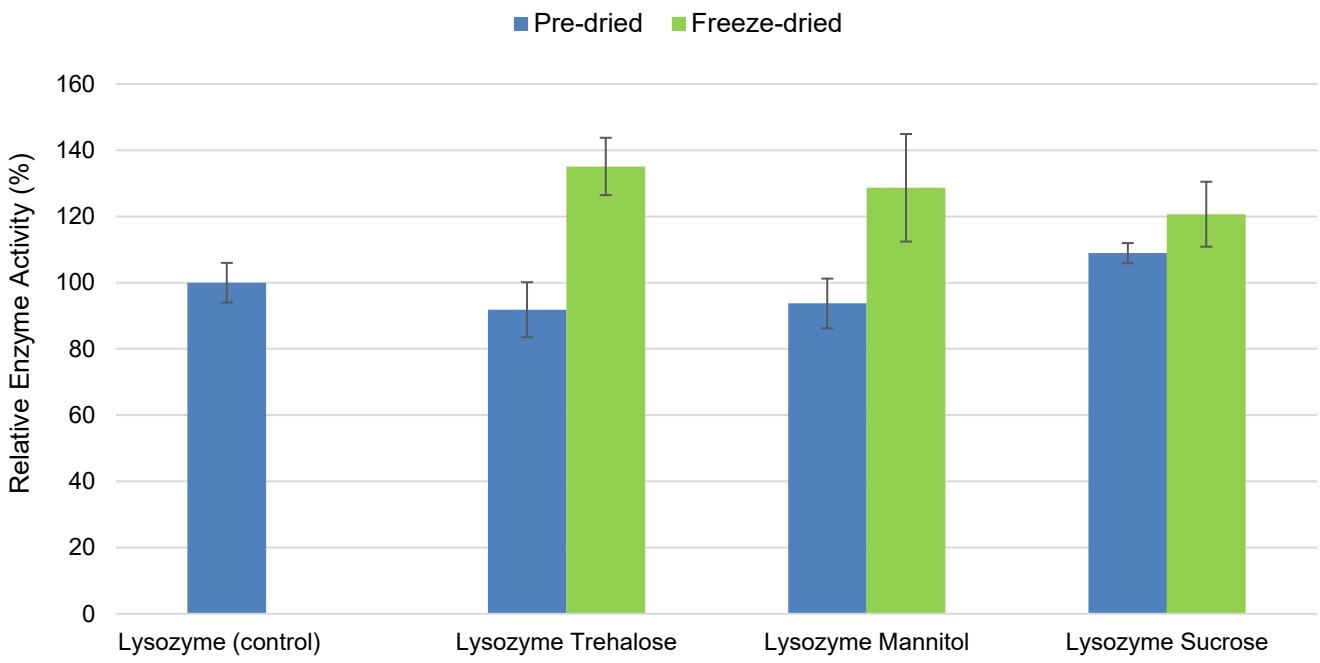

Figure 2.29: Enzyme activity for freeze-dried lysozyme formulations.

2.4 Conclusion

In conclusion, this study has provided information on the protein in terms of its thermal and structural properties in its solid as well as in its liquid state. Lysozyme was observed to be a robust protein prior to and post lyophilization with no major loss in its structure, though alternative techniques are required to study its aggregation profile along with long-term stability studies.

The most informative analytics implemented to study the protein's structural conformational stability included DSC, FTIR, CD and enzyme activity. Studying the thermal properties of the protein allowed the assessment of the critical temperatures required to carry out freeze-drying. Even though lysozyme alone exhibited a very high T_g, the lysozyme formulation containing trehalose showed a relatively higher T_g in both the liquid and solid states amongst other excipients. This implied that the protein could be protected at higher temperatures during a potential spray-drying process.

The second derivative FTIR spectrum provided information on the secondary structure of lysozyme. It was observed that the secondary structure of lysozyme with saccharides was preserved compared

to excipient-free lysozyme. Moreover, the FTIR spectrum of formulated lysozyme post lyophilization provided information on the intricate features including α-helix, β-sheets and turn structures. The lyophilized formulations containing excipients showed the presence of strong hydrogen bonds between lysozyme and the excipient compared to lysozyme in the absence of any excipients. Formulations with trehalose, mannitol and sucrose showed comparable α-helix bands, which were also comparable to literature values.

Moreover, CD spectroscopy results demonstrated that the protein was robust even in the absence of a stabilizer. Lysozyme retained its secondary and tertiary structure upon rehydration by showing a reproducible spectrum prior to and post lyophilization. Reconstitution did not have any effect on the secondary and tertiary structure of lysozyme. Furthermore, the temperature study provided information on the denaturation temperature of lysozyme and was observed to be intact up to 40 °C. Additionally, the preservation of enzyme activity of lysozyme was also demonstrated while the freeze-dried formulations exhibited higher enzyme activity than their pre-dried counterparts.

Furthermore, a good correlation ($R^2 = 0.97$) was obtained between Karl Fisher and the FMS for the lysozyme formulations. This result can be used as a preliminary model for further developing moisture maps for different lyophilized drug products. On average, it takes 3 – 4 s per vial to measure the headspace moisture using FMS Light House®, whereas it can take ≥ 30 min per vial to measure the RMC using Karl Fischer titration. This technique can significantly reduce time and the need for sample preparation for a number of drug product vials for batch release testing. Moisture mapping of freeze-dried vials can further help in the development and optimization of lyophilization cycles. Also, this technique can be configured as a PAT tool for real-time in-process measurements. Additionally, increased enzyme activity was observed in the freeze-dried samples which demonstrated the preservation of efficacy.

Overall, this chapter has demonstrated a wide range of analytics that can be employed for the analysis of both liquid and lyophilized biologic drug products while also generating benchmark data for the

chosen model protein lysozyme. The data generated is useful for comparability studies for investigating alternative drying technologies such as spray-drying. The feasiblity of spray-drying lysozyme and a commerical therapeutic biopharmaceutical has been demonstrated in chapters 3 and 4, respectively.

Chapter 3:

Spray-Drying of Lysozyme

3.1 Introduction

Spray-drying is an alternative drying technology that has potential application in the biopharmaceutical industry. The working principle and advantages of this technology has been previously discussed in section 1.3.2.2 of chapter 1.

Studies focusing on the stability of spray-dried lysozyme have been carried out. Liao *et al.* spray-dried lysozyme in the presence of trehalose and sucrose at different protein to sugar ratios with an inlet/outlet temperature range of 85/59 °C to 180/134 °C (Liao *et al.*, 2002, 2003). They concluded that while trehalose-based formulations provided better stability in terms of higher T_g, sucrose was found to provide better protection to the native structure of lysozyme. A good stabilizing effect was observed at a 2:1 (protein : sugar) ratio and an optimized inclusion of both trehalose and sucrose could improve the overall stability of lysozyme (Liao *et al.*, 2002, 2003). A 9:1:10 blend of mannitol, trehalose and lysozyme, respectively, exhibited higher bioactivity and stability post spray-drying which was studied using FT-Raman spectroscopy and biological activity assay of lysozyme (Hulse *et al.*, 2008). Additionally, studies were performed to improve the aerosol performance and particle characteristics of spray-dried lysozyme. Ethanol as a co-solvent improved the aerosol performance of spray-dried lysozyme by exhibiting a higher percentage of fine particle fraction (FPF) compared to the water-based lysozyme formulation (Ji *et al.*, 2016). Minor aberrations in the secondary structure of spray-dried lysozyme were observed at intermediate ethanol fractions using FTIR and CD spectroscopy. The changes in the secondary structure of lysozyme were reversible upon reconstitution. The bioactivity of spray-dried ethanol and water-based lysozyme solutions was significantly reduced by ~ 25 % which was reported to be due to the spray-drying process rather than ethanol itself (Ji *et al.*, 2016). The addition of trehalose, Tween 20 and phosphate buffer saline (PBS) individually in ethanol-water based lysozyme formulations resulted in 5 % – 10 % increase in the bioactivity of lysozyme post spray-drying (Ji *et al.*, 2017).

More recently, Ajmera and Scherließ screened a large number of amino acids and their combinations to study their stabilizing effect on spray-dried Catalase, Lysozyme and Pandemrix influenza vaccine containing Haemagglutinin in the ratios 1:1 and 2:1 (amino acid : protein) (Ajmera and Scherließ, 2014). Standard catalase and lysozyme and their formulations were spray-dried at an air inlet temperature of 180 °C and the outlet air temperature between 90 – 95 °C. The feed flow rate was kept between 5 – 7.5 mL/min, nozzle size was 1.5 mm, air speed was 470 L/h and the aspirator flow rate was kept at 35 m^3/min. The vaccine containing haemagglutinin and its formulations were spray-dried at an air inlet temperature of 120 °C and the air outlet temperature was between 50 – 55 °C. Through experimental results, they showed that arginine, glycine and protein in the ratio [(1+1) +1] resulted in a very good stabilizing effect post spray-drying compared to the non-formulated protein itself. They elucidated their results through bioactivity, FTIR, XRD, particle size and accelerated storage stability analysis on relatively large proteins, catalase and haemagglutinin, as well as a small protein lysozyme (Ajmera and Scherließ, 2014). Furthermore, the identification of critical process parameters (CPP) during spray-drying of proteins is equally important. Temperature, shear and protein adsorption at the air-liquid interface have been associated with protein aggregation and denaturation (Broadhead *et al.*, 1993; Y. F. Maa *et al.*, 1998; Koshari *et al.*, 2017; Wilson *et al.*, 2019; Ziaee *et al.*, 2020). Through a DoE, Ziaee *et al.* demonstrated that the outlet temperature was the most critical factor that affected the enzymatic activity of lysozyme (Ziaee *et al.*, 2020). Along with high outlet temperatures, ultrasonic vibrations and mechanical stress produced from ultrasonic nozzles had a negative impact on the activity of lysozyme. Further understanding of the impact of process parameters on the protein and its formulation components is required to improve the stability of proteins post spray-drying.

This chapter focuses on the impact of different spray-drying methods on a model protein lysozyme and the effect of individual excipients (trehalose, mannitol and sucrose) on the protein which were subsequently compared to the freeze-dried counterparts studied in chapter 2. While lysozyme is an extensively studied protein in literature, it's protein-excipient interactions are not completely

understood. Along with some of the analytics employed in chapter 2 such as DSC and Karl Fisher titration, UV-Vis spectroscopy, DLS, SEC and enzyme activity, molecular dynamics (MD) simulations were performed to substantiate experimental results and to also understand the behaviour of lysozyme at the molecular level post spray-drying. MD simulations assessed the stability of the lysozyme in terms of root mean-square deviation (RMSD), native contacts, secondary structure prediction and root mean square fluctuations (RMSF), thereby, providing information on the overall conformation as well as the secondary and tertiary structure of the protein.

3.2 Materials and Methods

3.2.1 Preparation of Formulations

All samples were procured and prepared as per section 2.2.1.

3.2.2 Spray-Drying

Formulated lysozyme was spray-dried in a 4M8-Trix Spray-dryer from Procept installed with a cyclone-based separator. Table 3.1 shows the process parameters employed during the spray-drying of lysozyme formulations. Process parameters that were altered during the process include air inlet temperature, outlet temperature, air flow rate, pump speed (feed flow rate) and the nozzle size. About 50 mL of each formulation was spray-dried with different process parameters and the spray-dried samples were transferred into 20 mL Schott glass vials inside a glove bag purged with nitrogen gas. The vials were overlaid with nitrogen gas, rubber stoppered, crimped, and stored at ~ 5 °C. Before analyses, 253.89 ± 0.50 mg of spray-dried powder for each formulation was weighed into a new 20 mL Schott glass vial at relative humidity ≤ 5 %. All spray-dried lysozyme formulations were compared to their freeze-dried counterparts. It is important to note that excipient-free lysozyme was spray-dried, but the obtained yield was below 30 % due to the absence of excipient resulting in a very low total solid content at the target concentration leading to insufficient material for characterization.

Table 3.1: Process parameters for spray-drying lysozyme formulations.

No.	Factors	1	2	3	4	5	6	7	8	9	10
1	Air Inlet Temp (°C)	90	100	120	180	150	120	150	180	180	200
2	Outlet Temp (°C)	38.9	43.1	48.7	91.5	70.9	70.9	82.8	95.8	103.5	107.2
3	Air Flow Rate (L/min)	100-110	100-110	100-110	80-90	100-110	80-90	80-90	80-90	80-90	80-90
4	Pump Speed (%)	50	50	50	50	50	25	25	25	25	20
5	Spray Rate (m^3/min)	0.3	0.3	0.3	0.3	0.3	0.3	0.3	0.3	0.3	0.3
7	Nozzle Pressure (Bar)	2	2	2	2	2	2	2	2	2	2
8	Nozzle Size (mm)	0.4	0.4	0.4	0.4	0.4	0.4	0.4	0.4	0.2	0.4

3.2.3 Glass Transition Temperature and RMC analyses

The T_g / T_m of spray-dried samples were measured using a DSC (TA Q2000). Approximately, 5 – 10 mg of each solid sample was sealed in an aluminum pan at relative humidity ≤ 5 %. Modulated DSC was ramped from 0 °C to 200 °C at 2 °C/min with modulation amplitude of ± 1 °C and modulation period of 100 s for solid samples. Samples were analyzed in triplicate (n = 3). The RMC of the spray-dried lysozyme formulations was measured using Karl Fischer titration (Karl Fischer Titrator by Metrohm). The vials were prepared at relative humidity ≤ 5 % and capped with Karl Fisher caps. The samples were subjected to a temperature of 100 °C, the blank vials were at 120 °C and the water standard was subjected to a temperature of 150 °C (as per the manufacturer's recommendation).

3.2.4 Concentration, Turbidity and Reconstitution Time

Method was performed as per section 2.2.7.

3.2.5 Dynamic Light Scattering

All spray-dried formulations were analyzed for PSD using the Malvern Zetasizer μV. 1 mL of sample was filtered through a 0.45 μm filter into a transparent disposable cuvette. The equilibration time was 300 s. All samples were analyzed in triplicate (n=3).

3.2.6 Size Exclusion Chromatography

Method was performed as per section 2.2.11.

3.2.7 Enzyme Activity

Method was performed as per section 2.2.13.

3.2.8 Molecular Dynamics Simulations

Molecular dynamics (MD) simulations were carried out using the Gromacs 2018.4 package (Van Der Spoel *et al.*, 2005) with a time step of 2 fs using the Leap frog integrator (Verlet, 1967; Hockney *et al.*, 1974). Bond lengths to hydrogen were constrained using the LINCS algorithm (Hess, 2007). Long-range electrostatics were treated by the Particle mesh Ewald (PME) method (Darden *et al.*, 1998). Protein and solvent molecules were coupled separately to an external heat bath (300 K) with the coupling time constant of 1 ps using the velocity rescaling method (Bussi *et al.*, 2007). CHARMM glycan parameters (Guvench *et al.*, 2011) were used for excipient molecules, while peptide molecules were represented by the CHARMM 36m (Huang *et al.*, 2016) force field. All systems were minimized for 100 ps and equilibrated for 500 ps in constant volume NVT ensemble. Production phases of 200 ns in the NPT ensemble were then carried out. MD simulations were performed on lysozyme to understand protein-excipient interactions during spray-drying. To simulate the high-temperature

environment of spray-drying, lysozyme was modelled at three different temperatures, 300K (27 °C), 340K (67 °C) and 380K (107 °C) in water solution in the presence of trehalose, sucrose and mannitol, and in the absence of excipient. The simulations were performed for two different excipient concentrations, the starting concentrations of experimental solution prior to spray-drying (labelled as 1x), to study the protein in its original solution, and at ten times the starting concentrations (labelled 10x), to study its behavior in its partially dried state as the excipients form more large-area, specific interactions with the surface of the protein. The data were analyzed in terms of excipient-induced changes in the protein structure as monitored through root mean square deviation (RMSD) of residues away from their starting positions (from X-ray crystal structure PDB ID 4WLD), distance between active site residues, fraction of native contacts, root mean square fluctuation (RMSF) with respect to the time-averaged structure as a measure of the flexibility of the protein and the preservation of secondary structure.

3.2.9 Statistical Analyses

Method performed was as per section 2.2.14.

3.3 Results and Discussion

3.3.1 Glass Transition Temperature and RMC

The results for thermal and RMC analyses for spray-dried lysozyme formulations are shown in Table 3.2 and Figure 3.1. The RMC of the lysozyme trehalose-based formulation was significantly reduced from 4.87 % to 1.11 % w/w by employing different process parameters during spray-drying (Table 3.2). This was possible by increasing the air inlet temperature, thereby, attaining high outlet temperatures as shown in literature (Büchi Labortechnik AG, 2002). Consistent with reported results (Masters, 1991; Maa *et al.*, 1997; Büchi Labortechnik AG, 2002; Vass *et al.*, 2019b; Ziaee *et al.*, 2019), reducing the feed flow rate, the aspirator air flow rate and the nozzle size also resulted in high outlet temperatures. These methods were used to achieve a lower moisture content (≤ 2 % w/w) in lysozyme mannitol and sucrose-based formulations at inlet temperatures ≥ 180 °C. It was found that the spray-dried lysozyme mannitol-based formulation exhibited a T_m of 152 °C, showing the crystallization of mannitol post spray-drying at a concentration of 40 mg/mL (Table 3.2).

Several authors have demonstrated spray-drying of water-based lysozyme formulations and other proteins at gentle and extreme inlet/outlet temperatures varying from 70/50 °C to 180/134 °C and the reported RMC in the dried formulations were in the range of 2.5 % - 9.5 % w/w (Maa *et al.*, 1997; Elkordy *et al.*, 2002; Liao *et al.*, 2002, 2003; Hulse *et al.*, 2008; Ajmera and Scherließ, 2014; Saß and Lee, 2014; Ziaee *et al.*, 2020). Saß and Lee achieved lower RMC (1.38 % - 3.26 % w/w) in spray-dried organic solvent and water-based lysozyme solutions (Saß and Lee, 2014). Moreover, it was reported that increasing the concentration of mannitol to ≥ 30 % of the total solid content in the formulation resulted in crystallization during spray-drying (Chew and Chan, 1999; Lee, 2002) and was confirmed using Wide-Angle X-Ray scattering (WAXS) (Costantino *et al.*, 1998; Schaefer and Lee, 2015a).

Table 3.2: T_g / T_m and RMC of spray-dried lysozyme formulations using different process parameters.

Spray-dried formulation	Air inlet/outlet Temperature (°C), Air flow rate (L/min), pump speed (%), nozzle size (mm)	T_g / T_m (°C)	RMC % (± 0.1 %)	Yield (%)
Lysozyme Trehalose (Formulation 1)	90/38.9, 110, 50, 0.4	61.14 ± 0.49	4.87	60 – 70
	100/43.1, 110, 50, 0.4	65.14 ± 0.24	4.33	
	110/45, 110, 50, 0.4	68.74 ± 0.3	3.96	
	120/48.7, 110, 50, 0.4	69.51 ± 1.36	4.06	
	120/70.9, 80, 25, 0.4	90.82 ± 0.52	2.09	
	150/70.9, 100, 50, 0.4	89.79 ± 0.32	2.17	
	150/82.8, 80, 25, 0.4	89.08 ± 1.14	2.24	
	180/91.5, 80, 50, 0.4	102.96 ± 3.59	1.33	
	180/95.8, 80, 25, 0.4	99.86 ± 2.13	1.29	
	180/103.5, 80, 25, 0.2	102.42 ± 0.65	1.11	
Lysozyme Mannitol (Formulation 2)	180/89.3, 80, 25, 0.4	150.46 ± 4.68 (T_m)	0.61	75 – 80
	200/107.2, 80, 20, 0.4	152.53 ± 3.47 (T_m)	0.51	
Lysozyme Sucrose (Formulation 3)	150/82.8, 80, 25, 0.4	61.76 ± 0.08	1.42	60 – 65
	180/95.8, 80, 25, 0.4	66.05 ± 0.28	0.90	
	200/102.1, 80, 20, 0.4	67.88 ± 1.11	0.78	

The yield obtained for the mannitol-based formulation was relatively higher due to the low hygroscopic nature of mannitol. The yield increased with decreasing residual moisture content. Yield was not the primary target of these experiments and so this parameter was not optimized.

The T_g or T_m of each formulation was consistent with their freeze-dried counterparts, except for the spray-dried trehalose-based formulation which exhibited a relatively lower T_g of 102.42 °C at an RMC of 1.11 % w/w. The T_g of the freeze-dried lysozyme trehalose cake was 108.48 °C. This is because of the relatively higher RMC obtained post spray-drying. T_g decreases steadily with an

increase in water content to a point after which no further decrease is observed (Reimschuessel, 1978). Water acts as a plasticizer and forms reversible hydrogen bonds with hydrophilic polymers, thereby, increasing molecular mobility in materials, resulting in a decrease in the T_g or T_m of materials (Reimschuessel, 1978; Drake *et al.*, 2018).

Figure 3.1 shows an inverse correlation ($R^2 > 0.98$), between the T_g and the RMC in the spray-dried lysozyme trehalose and sucrose-based formulations at different outlet temperatures, well-known in theory (Drake *et al.*, 2018). The correlation can be exploited to develop improved empirical models to predict the RMC and T_g of different biologic formulations at different spray-drying conditions as also shown by authors for the optimization of freeze-drying cycles (Gervasi *et al.*, 2019).

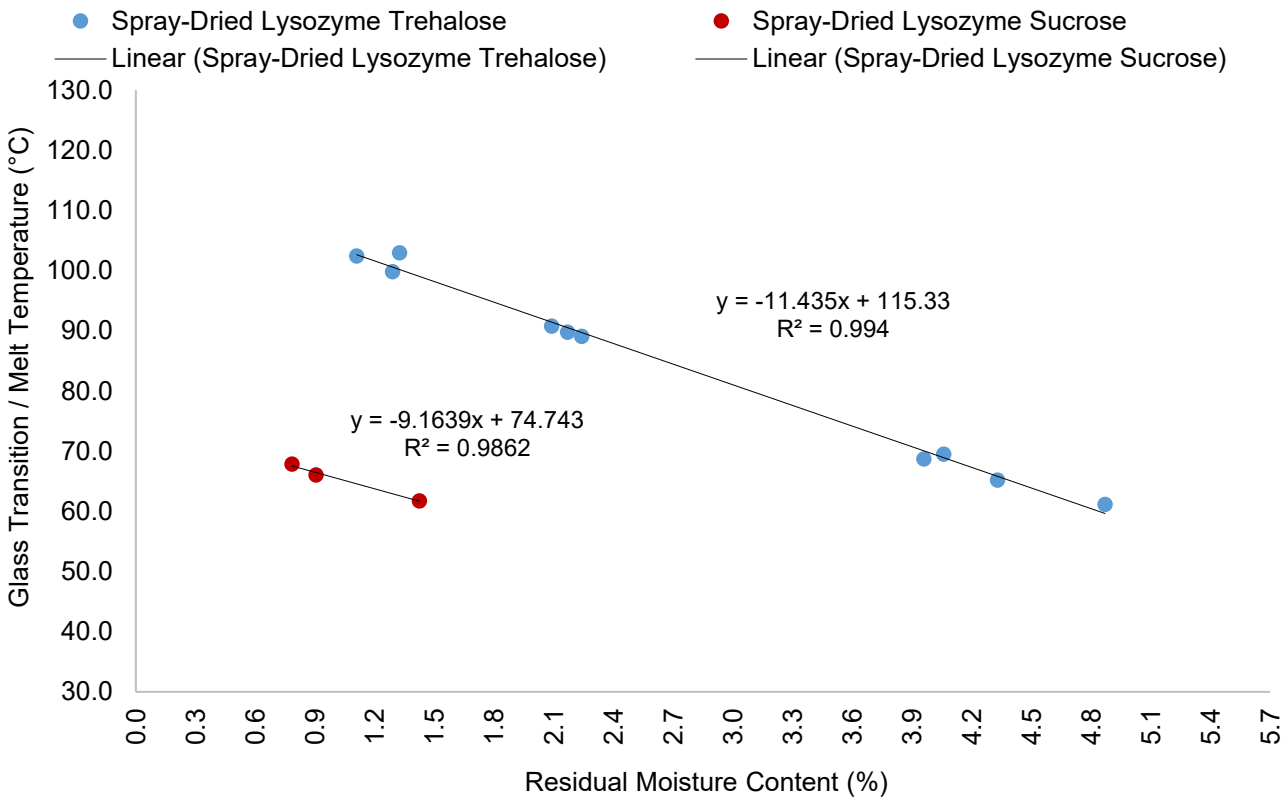

Figure 3.1: Co-relation between T_g and RMC for lysozyme formulations at different air inlet/outlet temperatures.

3.3.2 Concentration, Turbidity and Reconstitution Time Analyses

Upon rehydration, the behaviour of spray-dried lysozyme formulations was different compared to their freeze-dried counterparts. A visual representation of the reconstituted freeze-dried and spray-dried lysozyme formulations is shown in Figure 3.2. The spray-dried powder took slightly longer (1.5 min – 3.5 min) to reconstitute, as it formed small clumps and sedimented at the bottom of the vial as shown in Figure 3.3. As shown in Figure 3.2, the spray-dried vials appeared opalescent compared to the rehydrated freeze-dried vials.

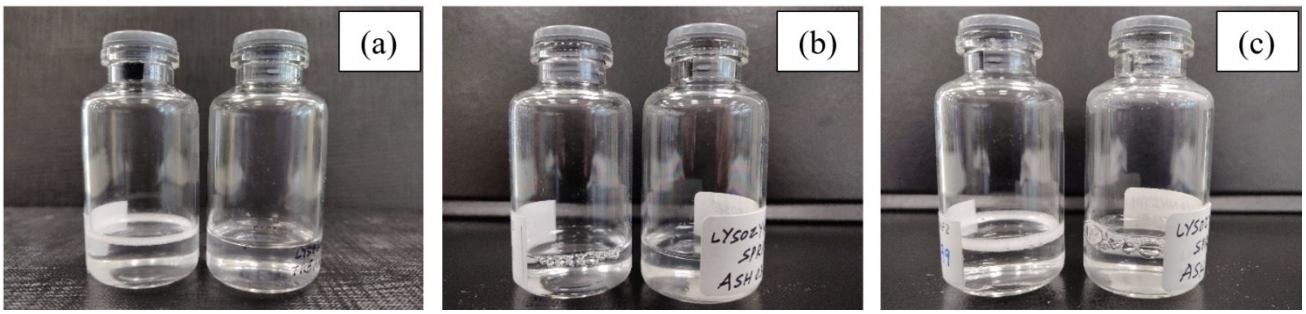

Figure 3.2: (a) Reconstituted lysozyme trehalose freeze-dried (left) and spray-dried (right), (b) reconstituted lysozyme mannitol freeze-dried (left) and spray-dried (right), (c) reconstituted lysozyme sucrose freeze-dried (left) and spray-dried (right). The spray-dried samples correspond to inlet/outlet temperatures of 180/103.5 °C (trehalose), 180/89.3 °C (mannitol), 180/95.8 °C (sucrose).

Figure 3.3: Rehydration behaviour of spray-dried lysozyme powder.

Particle agglomeration in spray-dried powders of rhuMAb25/trehalose and native phosphocaseinate and have been reported (Andya, Y. F. Maa, *et al.*, 1999a; Gaiani *et al.*, 2007). The agglomerated

protein particles took longer to rehydrate than the non-agglomerated particles. Particle agglomeration has been associated with high moisture content as a result of large droplet size and reduced rate of heat and mass transfer (Vehring, 2008; Schaefer and Lee, 2015a, 2015b; Ziaee *et al.*, 2020). Moreover, drying at a lower inlet temperature would result in increased RMC, thereby, increasing the stickiness amongst particles (Gaiani *et al.*, 2007). Since comparable moisture levels (≤ 2 % w/w) were obtained between the freeze-dried and spray-dried samples, moisture is less likely the cause for aggregation than high temperature and shear in the spray-dried samples. Moreover, the concentration of lysozyme in the reconstituted spray-dried vials measured using UV-vis spectroscopy was comparable to the concentration of lysozyme post freeze-drying (Table 3.3). The reconstitution times of freeze-dried and spray-dried mannitol-based formulations were higher due to the presence of crystalline mannitol with a greater solid content of 40 %. Cakes with higher density and a higher total solid content resulted in longer reconstitution time (Kulkarni *et al.*, 2018).

Table 3.3: Reconstitution time, concentration and turbidity of reconstituted freeze-dried and spray-dried lysozyme formulations.

Sample	Reconstitution Time (min)	Concentration (mg/mL)	Optical Density A_{350}
Freeze-dried excipient-free Lysozyme	1.0	9.99 ± 0.007	0.030 ± 0.0010
Spray-dried excipient-free Lysozyme	1.5	9.49 ± 0.015	0.086 ± 0.0010
Freeze-dried Lysozyme Trehalose	1.5	9.09 ± 0.09	0.026 ± 0.0057
Spray-dried Lysozyme Trehalose	1.5	9.77 ± 0.10	0.070 ± 0.0095
Freeze-dried Lysozyme Mannitol	2.0	10.31 ± 0.05	0.037 ± 0.0106
Spray-dried Lysozyme Mannitol	3.5	9.27 ± 0.79	0.069 ± 0.0153
Freeze-dried Lysozyme Sucrose	1.0	9.70 ± 0.04	0.046 ± 0.0127
Spray-dried Lysozyme Sucrose	1.5	10.03 ± 0.96	0.132 ± 0.0113

Visual turbidity observed in the rehydrated spray-dried vials was studied in the light scattering region. Results showed higher light scattering in the reconstituted spray-dried vials (0.06 – 0.13) compared to their freeze-dried (0.02 – 0.05) counterparts (Figure 3.4). Various authors have reported turbid protein solutions post spray-drying (Broadhead *et al.*, 1993; Mehta *et al.*, 1996; Y.-F. Maa and Hsu, 1997; Y. F. Maa *et al.*, 1998; Andya, Y. F. Maa, *et al.*, 1999b; Tzannis and Prestrelski, 1999). This has been associated with protein denaturation and aggregation due to process related stress such as sheer, temperature and denaturation at the liquid-air interface. To detect and quantify the presence of aggregates or impurities, the spray-dried samples were further analysed using DLS and SEC in section 3.3.3 and 3.3.4, respectively.

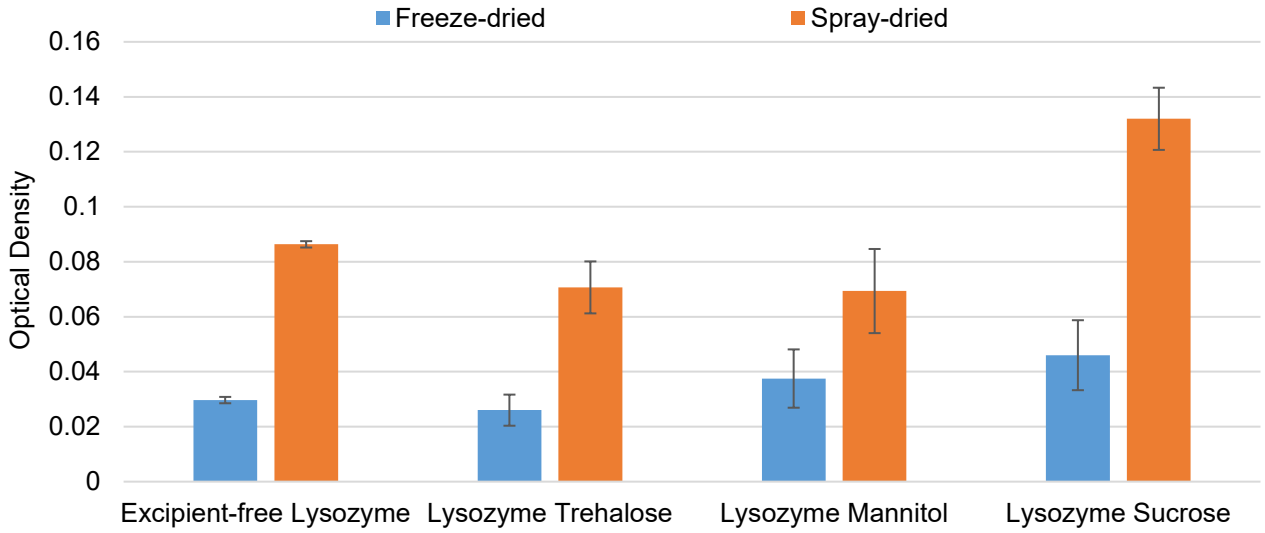

Figure 3.4: Optical Density of reconstituted freeze-dried and spray-dried lysozyme formulations measured at 350 nm.

3.3.3 Dynamic Light Scattering

Figure 3.5 (a), (b) and (c) shows the PSD by percentage intensity and percentage mass in rehydrated spray-dried lysozyme formulations at extreme temperatures. Monomeric lysozyme was present at ~ 1.5 nm in trehalose and mannitol-based formulations but was absent in the sucrose-based formulation. Since all 3 formulations were highly polydisperse, the Z-average values (Table 3.4) do not represent a true average of the monomeric protein and can be ignored. In this case, these results are qualitative

rather than being quantitative. Consistent with the results obtained in chapter 2, section 2.3.9, multimodal distributions were obtained both prior to and post drying and reconstitution of lysozyme formulations. While the absence or reduced intensity of the monomer peak at ~ 1.5 nm and the presence of additional peaks from 9 nm – 300 nm could indicate protein aggregation, peaks in that range were also ascribed to the presence of impurities which require alternative techniques for the identification and quantification of the multimodal distribution as also discussed in chapter 2, section 2.3.9.

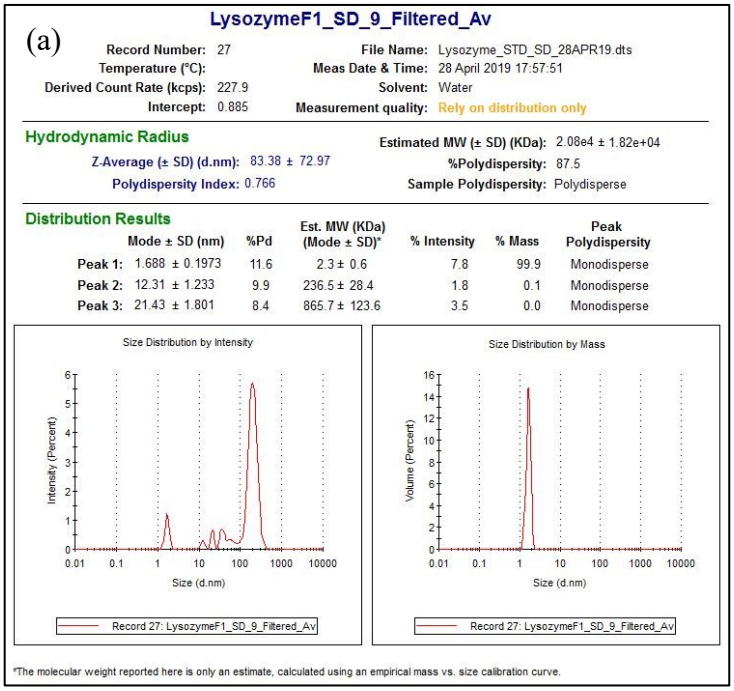

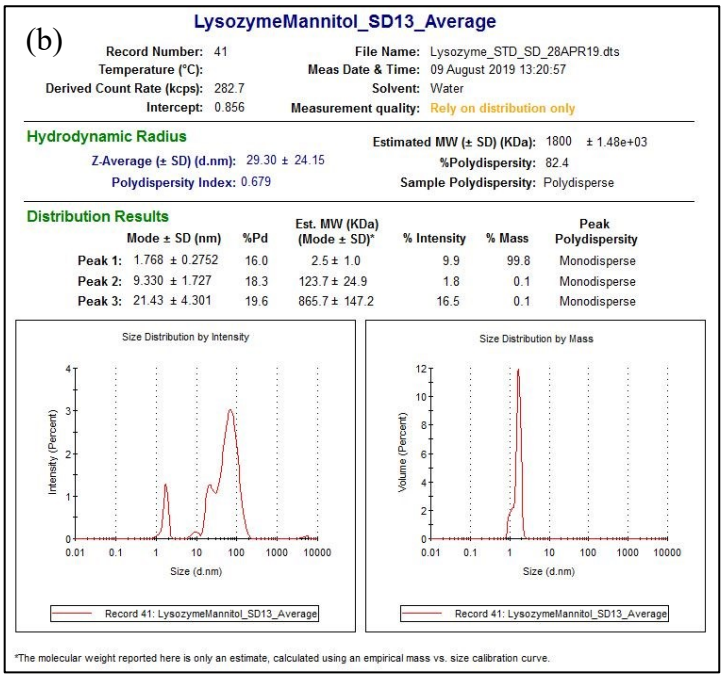

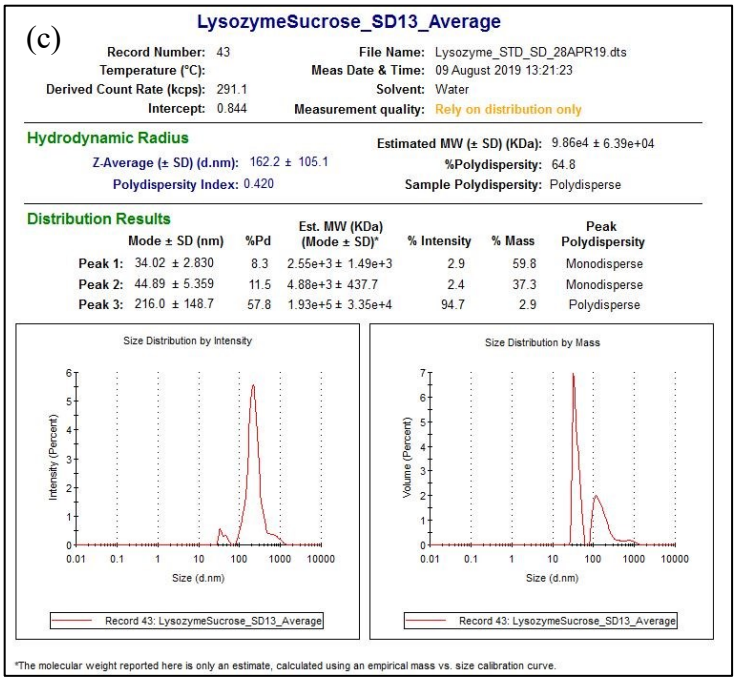

Figure 3.5: PSD of spray-dried (a) lysozyme trehalose, (b) lysozyme mannitol and (c) lysozyme sucrose.

Table 3.4: Z-Average, Polydispersity Index and PSD for freeze-dried and spray-dried lysozyme formulations.

Sample	Z-Average (nm)	PDI	Peak 1 (nm); Intensity (%)	Peak 2 (nm); Intensity (%)	Peak 3 (nm); Intensity (%)
Freeze-dried Lysozyme Trehalose	8.84	1	1.54; 25.4	15.51; 10.8	103.1; 63.8
Freeze-dried Lysozyme Mannitol	8.86	1	1.54; 20.0	11.22; 26.8	94.03; 53.2
Freeze-dried Lysozyme Sucrose	26.33	1	1.4; 14.3	14.81; 8.10	136.1; 77.6
Spray-dried Lysozyme Trehalose	83.38	0.76	1.68; 7.80	21.31; 1.80	21.43; 3.50
Spray-dried Lysozyme Mannitol	29.30	0.67	1.76; 9.90	9.33; 1.80	21.43; 16.5
Spray-dried Lysozyme Sucrose	162.2	0.42	34.02; 2.9	44.89; 2.4	216.0; 94.7

Lysozyme formulations were subjected to extreme outlet temperatures (≤ 107 °C) during spray-drying which could be a possible reason for turbidity and the presence of additional peaks in the rehydrated solutions. Factors affecting the process stability of proteins such as shear, temperature and denaturation at liquid-air interface have been reported (Maa *et al.*, 1997; Y. F. Maa *et al.*, 1998; Lee, 2002; Ziaee *et al.*, 2020). Ziaee *et al.* demonstrated a design of experiments to identify parameters that affect lysozyme post spray-drying (Ziaee *et al.*, 2020). The outlet temperature was determined to be the most significant parameter affecting the stability and enzyme activity of lysozyme. The maximum wet bulb temperature (45 °C) during atomization at a very high air inlet temperature of 132 °C and the shear force experienced through the nozzle, without the application of heat, had a negligible effect on lysozyme. To further verify and quantify the presence of lysozyme aggregates in rehydrated spray-dried formulations, all samples were analyzed using SEC (section 3.3.4).

3.3.4 Size Exclusion Chromatography

While UV-Vis spectroscopy and DLS indicated the presence of aggregates in the spray-dried lysozyme formulations, the proportion of aggregates present were only between 0.6 – 0.8 % of the total area by SEC and no additional peaks were observed, indicating the absence of higher aggregates (HMWS2) as shown in Figure 3.6. The aggregation profile of spray-dried lysozyme was similar to freeze-dried lysozyme and the same method was employed as described in chapter 2, section 2.2.11. These results could not further elucidate the presence of additional peaks observed using DLS.

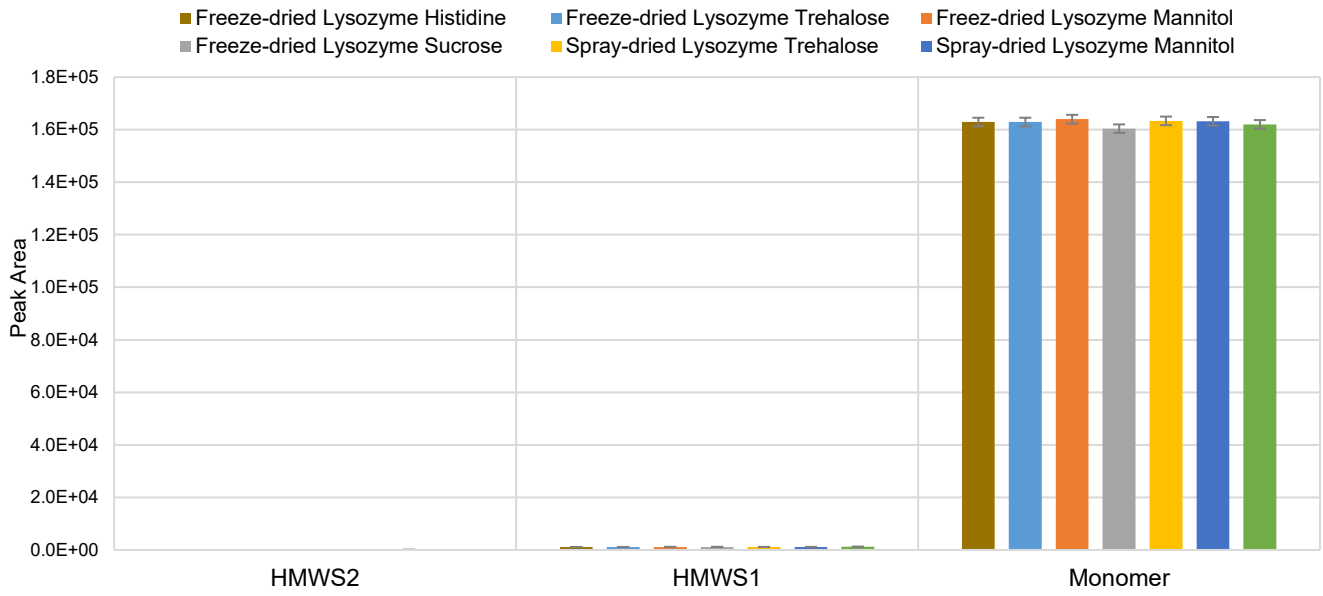

Figure 3.6: Aggregation profile of lysozyme formulations represented as monomers and high molecular weight species (HMWS).

Several studies have shown protein denaturation and aggregation via spray-drying. Increasing the air inlet temperature from 60 °C to 140 °C led to inactivation of β-galactosidase (Broadhead *et al.*, 1993). The inclusion of 1 % w/w hydroxypropyl-β-cyclodextrin in a β-galactosidase formulation reduced its inactivation at a high inlet/outlet temperature of 190 °C/61 °C (Branchu *et al.*, 1999). The incorporation of a sucrose/protein ratio of 1:1 protected trypsinogen at a high inlet/outlet temperature of 120 °C /85 °C (Tzannis and Prestrelski, 1999). Interestingly, the major reason for aggregation of

spray-dried recombinant growth hormone (rhGH) and tissue-type plasminogen activator (tPA) was the adsorption of protein at liquid-air interfaces rather than shear or temperature (Mumenthaler *et al.*, 1994; Y.-F. Maa and Hsu, 1997). The addition of surfactants and Zinc ions suppressed the generation of soluble aggregates of rhGH (Mumenthaler *et al.*, 1994; Y.-F. Maa and Hsu, 1997; Y. F. Maa *et al.*, 1998). Moreover, the extent of aggregation of rhGH increased at higher protein concentrations at air-liquid interfaces but were not observed when subjected to high shear stress.

More recently, ssHDX-MS analyses has shown that spray-dried lysozyme trehalose, sucrose and mannitol-based formulations exhibited greater aggregation compared to their freeze-dried counterparts (Wilson *et al.*, 2019). Decreased storage stability of proteins in terms of loss of monomer has been correlated with higher uptake of deuterium (Moorthy *et al.*, 2014, 2018; Wilson *et al.*, 2019). This correlation has been studied on myoglobin, BSA, β-lactoglobulin and lysozyme. The maximum extent of deuterium exchange was observed to be the highest in mannitol-based formulations in all proteins. The incorporation of deuterium depends on the intermolecular interactions between the protein and excipients. Moreover, crystallization of mannitol resulted in phase separation, thereby, decreasing the protein-excipient interaction (Wilson *et al.*, 2019). It was also shown than mannitol samples exhibited higher protein aggregation compared to sucrose and trehalose-based samples. Moreover, the presence of a higher fraction of heterogeneous population in spray-dried samples was attributed to exposure of protein sites at liquid-air interface and high shear forces during the atomization process of spray-drying (Koshari *et al.*, 2017; Wilson *et al.*, 2019).

It is important to note that some of the limitations of DLS and SEC have been explored with different protein modalities in chapter 5. Nonetheless, other analytics such as AUC would be required to quantify and elucidate the presence of aggregates and/or impurities in spray-dried and freeze-dried lysozyme formulations along with the optimization of the SEC method with other detectors.

3.3.5 Enzyme Activity

The enzyme activities of pre-dried, freeze-dried and spray-dried lysozyme formulations are shown in Figure 3.7 and were calculated using Equation 2.2 and Equation 2.3 (chapter 2). The lysozyme standard in reaction buffer (control) was considered to exhibit 100 % bioactivity as per the manufacturer's recommendation (Sigma Aldrich, 2017). Statistically significant differences in the enzyme activity of the reconstituted freeze-dried and spray-dried lysozyme formulations were determined using one-way *ANOVA* (*ANalysis Of VAriance*) with *post-hoc Tukey* HSD (Honestly Significant Difference) test shown in Figure A3.1 of Appendix. Statistically, no significant differences were observed amongst the enzyme activities of formulated lysozyme prior to drying and were comparable to the control ($p > 0.05$). The enzyme activities of freeze-dried and spray-dried lysozyme trehalose were not statistically different, but they were significantly higher than their pre-dried counterpart ($p < 0.05$). In the presence of mannitol, the enzyme activity of freeze-dried lysozyme was significantly higher than its spray-dried and pre-dried counterpart. While the activity of spray-dried lysozyme mannitol was preserved and comparable to its pre-dried counterpart and the control, the presence of crystalline mannitol has been associated with phase separation which results in decreased protein-excipient interactions (Moorthy *et al.*, 2014; Wilson *et al.*, 2019). Therefore, the effect of high temperature along with rapid crystallization of mannitol during spray-drying could possibly explain the relatively lower enzyme activity. Moreover, this may also be attributed to the different polymorphs of mannitol formed during the two drying processes. In the presence of lysozyme, a shift from β-mannitol to α-mannitol was reported post spray-drying while the α-polymorph was reported to be less stable (Hulse *et al.*, 2009; Grohganz *et al.*, 2013), which may contribute to the relatively lower enzyme activity of lysozyme compared to its freeze-dried counterpart. The shift in the polymorphic forms of mannitol has been attributed to the drying process rather than the effect of temperature (Grohganz *et al.*, 2013). Additionally, the presence of both amorphous and crystalline mannitol have also been reported post spray-drying of BSA which resulted in its partial stabilizing effect on BSA (Chen, Ling, *et al.*, 2021). On the contrary, authors showed

that mannitol stabilizes lysozyme against aggregation while also exhibiting greater enzyme activity compared to sucrose in the liquid state (Singh and Singh, 2003). More recently, authors showed that the crystallization of mannitol to its hemihydrate form did not impact protein stability (Sonje *et al.*, 2022, 2023).

Furthermore, the enzyme activities of pre-dried, freeze-dried and spray-dried lysozyme sucrose were comparable, and no significant differences were observed between the formulations containing trehalose and sucrose. Even though the lysozyme formulations were spray-dried at extreme temperatures, the freeze-dried and spray-dried lysozyme trehalose and sucrose formulations showed consistently higher activity compared to the control.

Ziaee *et al.* reported a 10 % – 20 % decrease in the activity of spray-dried excipient-free lysozyme at a high inlet/outlet temperatures of 97 °C /70 °C and 130 °C /70 °C (Ziaee *et al.*, 2020). Ajmera *et al.* reported ~ 15 % decrease in spray-dried excipient-free lysozyme at an inlet/outlet temperature of 180 °C /95 °C and ~ 20 % decrease when stored at 40 °C /75 % RH for a month (Ajmera and Scherließ, 2014). Increased activity was observed when a lysozyme formulation containing glycine and arginine were spray-dried. Moreover, improved enzyme activity results were obtained for spray-dried catalase and Pandemrix influenza vaccine in the presence of glycine and arginine (Ajmera and Scherließ, 2014).

Overall, in agreement with the theories of stabilization of proteins by amorphous saccharides and excipients described earlier in chapter 2, section 2.1, the enzyme activity of lysozyme in the presence of trehalose and sucrose was enhanced post drying while mannitol preserved its activity post rehydration. To further gain insights into the stability of the lysozyme formulations, molecular dynamics simulations were performed in section 3.3.6.

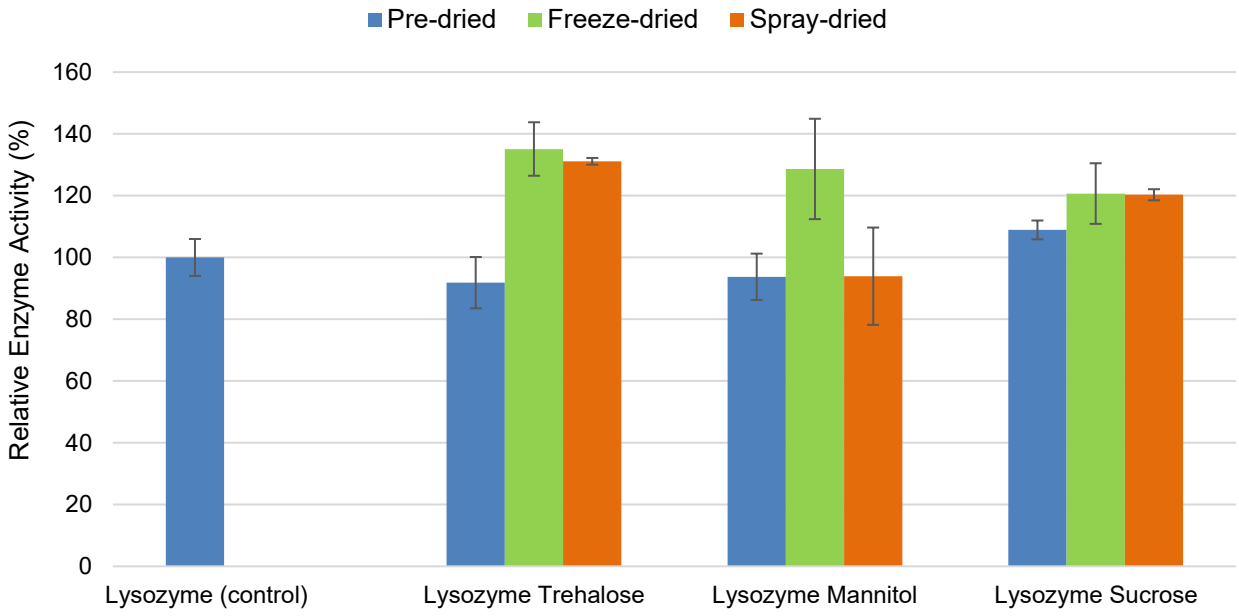

Figure 3.7: Relative enzyme activities of pre-dried and post-dried lysozyme formulations.

3.3.6 Molecular Dynamics Simulations

The root mean-square deviations (RMSD) for 1x and 10x concentrations of lysozyme formulations at 300 K, 340 K and 380 K are shown in Figure 3.8. The RMSD illustrates the overall conformational changes occurring in the protein's structure over time. The RMSD of lysozyme exhibited lower values at 10x compared to 1x, in particular for 340 K and 380 K, suggesting that the protein's native structure was better preserved at higher excipient concentration with an increase in temperature. However, it is important to note that the protein without excipient showed greater stability similar to that of high excipient concentration (Figure 3.8 (a)). The stability of lysozyme was attributed to strong disulphide bridges and low molecular mass (Sun *et al.*, 2015; Perez and Oliveira, 2017). These results so far not only demonstrate the inherent stability of lysozyme, but they also show that there is an interplay between the protein and the excipients. At low concentration (Figure 3.8 (b - d)), all the excipients induced conformation changes in the protein at 380 K, beyond the changes observed for the base solution. Sugars bind to specific residues driving changes in the protein conformation enabled by the increase in kinetic energy. At high concentration, lysozyme's conformation was better stabilized.

Figure 3.8 (f) and (h) briefly explore a different conformation before falling back to the native one. This showed that the binding of sugars to more residues contributed to the protein stability together with a crowding effect. Moreover, mannitol (Figure 3.8 (g)) showed the smallest deviation from the native structure, even compared to the base solution. The larger, yet stable, RMSD was observed at high concentration for the three excipients suggesting that the protein underwent a conformation change without unfolding. At experimental timescales, this conformation change could take place in the solutions at 300 K prior to spray-drying, which could explain the enhanced activity measured for some protein-excipients powders (Figure 3.7).

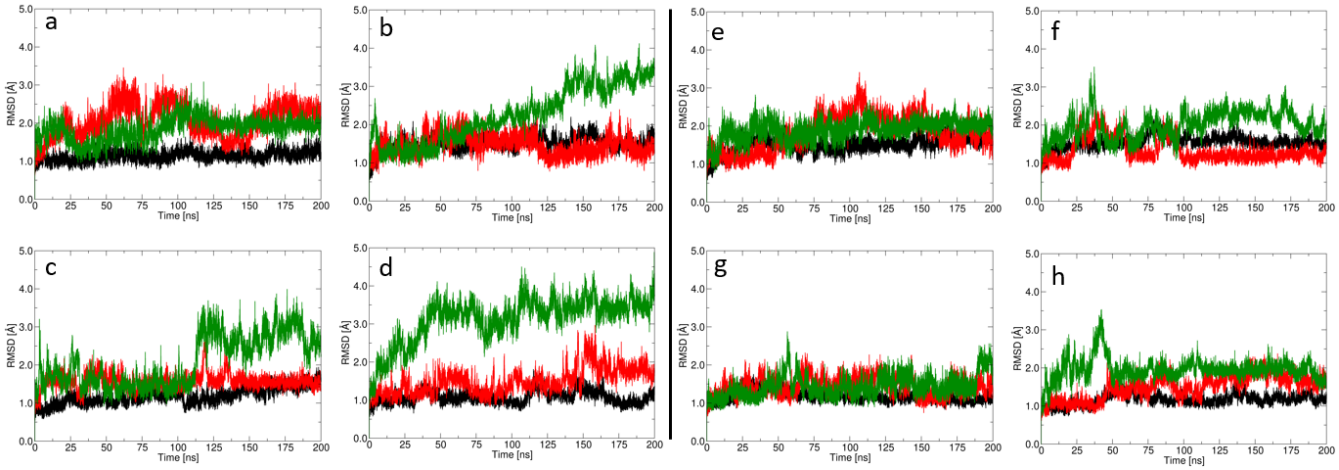

Figure 3.8: Plot of RMSD for 1x concentration of (a) excipient-free lysozyme, (b) lysozyme trehalose, (c) lysozyme mannitol and (d) lysozyme sucrose. The corresponding 10x concentration solutions are shown in panels (e) to (h). Temperatures are 300K (black), 340K (red) and 380K (green).

Figure 3.9 shows the native contacts timelines for lysozyme at 10x. While the RMSD represents the overall conformational changes (or the absence of any) in proteins, the native contacts are more specifically sensitive to the tertiary structure. In all cases, even at 380K, the protein retained 85 % of its native contacts. There is still a striking difference between excipients. At 300 K and 340 K, all excipients preserved the native contacts better than the excipient-free solution. This is in good agreement with the RMSD. However, at 380 K, trehalose and sucrose showed a greater loss in the

native contacts compared to the excipient-free solution. Only mannitol consistently conserved the native contacts, which is consistent with the RMSD.

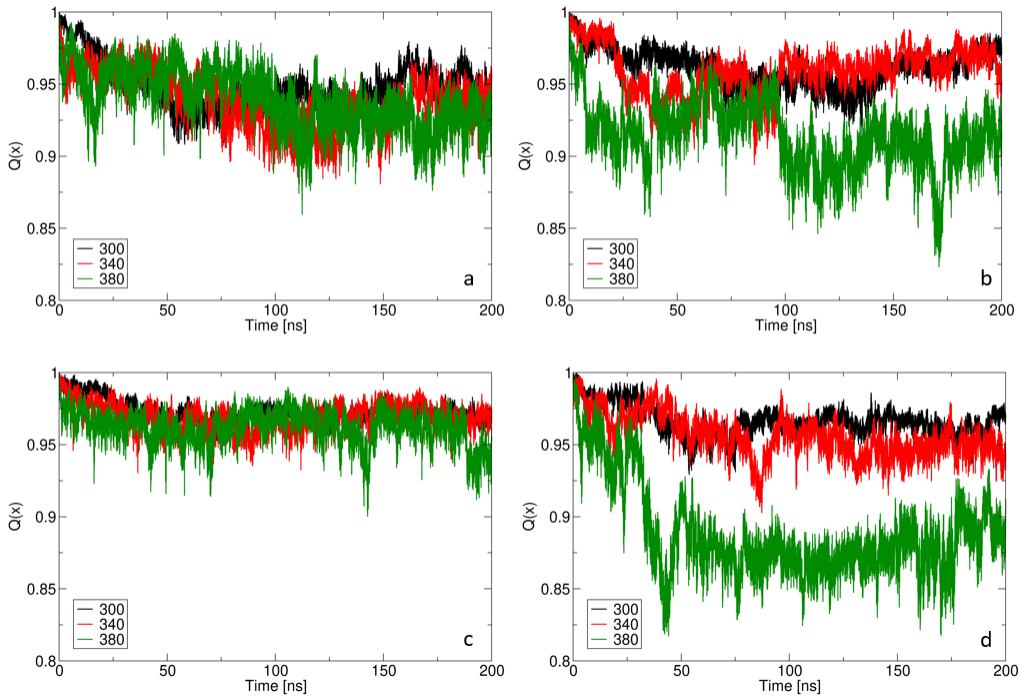

Figure 3.9: Native contacts of (a) lysozyme, (b) lysozyme trehalose, (c) lysozyme mannitol and (d) lysozyme sucrose at 300K (black), 340K (red) and 380K (green).

Figure 3.10 shows the secondary structure for all systems high concentration. No significant changes in the secondary structure were observed, except for the system containing sucrose at high temperature wherein the fraction of secondary structure including α-helices, β-sheets, etc. were observed to increase. This confirmed that the conformational changes captured by the RMSD corresponded mostly to the native contacts, and thus, the tertiary structure. This is in agreement with literature reports that sucrose provides better preservation of the secondary structure of lysozyme, as it provides a greater number of intramolecular H-bonds (Liao *et al.*, 2002; Singh, 2018; Starciuc *et al.*, 2020). By contrast, trehalose makes a greater number of intermolecular H-bonds with water, thereby, reducing the molecular mobility of the overall glassy matrix, which may provide protection against high temperature and long-term storage. Authors showed that trehalose played a role by clustering at different regions on the surface of lysozyme which resulted in better stabilization of

tertiary structure compared to the secondary structure (Fedorov *et al.*, 2011). The lysozyme trehalose and sucrose containing systems enabled conformational changes at high temperature that lead to an equally or more folded protein. This change is more likely responsible for the enhanced activity reported in our experiments. Moreover, it has been reported that trehalose increases the backbone mobility providing more flexibility and access to the active site residues glutamic acid (GLU35) and aspartic acid (ASP52) (Fedorov *et al.*, 2011) which substantiates our results shown in section 3.3.5 and Figure 3.9. However, mannitol preserves the native state of the protein which is confirmed experimentally by an enzymatic activity similar to that of the protein in excipient-free solution prior to drying. A similar result for mannitol was reported in the presence of lysozyme showing greater enzyme activity and protection against protein aggregation (Singh and Singh, 2003).

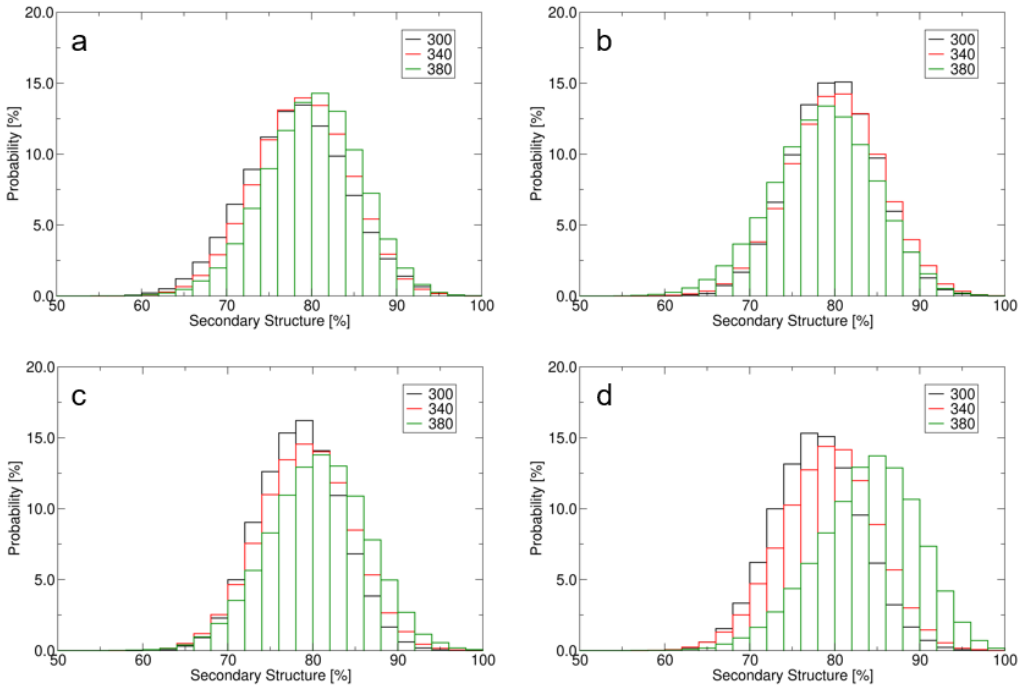

Figure 3.10: Secondary structure prediction for 10 x concentration of (a) lysozyme, (b) lysozyme trehalose, (c) lysozyme mannitol and (d) lysozyme sucrose at 300 K (black), 340 K (red) and 380 K (green).

Finally, the root mean-square fluctuations (RMSF) (Figure 3.11) averaged over time and projected per residue help identify which regions of the protein were the most prone to the observed changes. Higher fluctuations of lysozyme residues were again observed for trehalose and sucrose at 380K, mainly around residues 15 – 20, 35, and 100 – 125 that included β-bridges and turn structures. Trehalose showed increased fluctuations in the 40 – 50 region. It is important to note that in all cases residue 70 fluctuated the most which corresponds to disordered regions. Mannitol, however, dampened residue fluctuations compared to the excipient-free solution, which showed its ability to stabilize the native structure of lysozyme in solution even at high temperature.

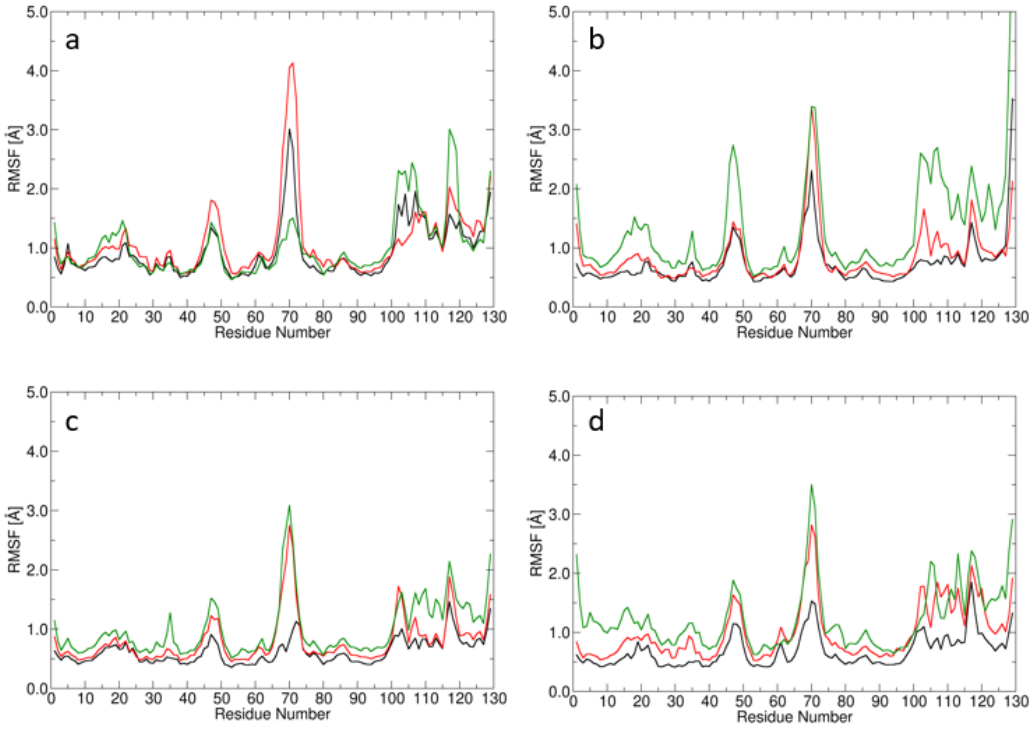

Figure 3.11: RMSF at 10 x concentration for residues of (a) lysozyme, (b) lysozyme trehalose, (c) lysozyme mannitol and (d) lysozyme sucrose at 300 K (black), 340 K (red) and 380 K (green).

3.4 Conclusion

A wide range of analytics have provided information on the quality and efficacy of the spray-dried model protein lysozyme. RMC of ≤ 2 % was achieved for all spray-dried lysozyme formulations, as per the specifications for freeze-dried biologic products. This was possible by employing different process parameters during spray-drying. High air inlet and outlet temperatures, low feed flow rates and aspirator flow rates, and smaller nozzle sizes resulted in lower RMC and greater T_g / T_m. Moreover, the correlation between the RMC and the T_g at different outlet temperatures, consistent with the Fox equation, can be exploited to develop sophisticated models to predict the residual moisture content and T_g / T_m for different formulations post spray-drying. Furthermore, the rehydrated spray-dried solutions appeared opalescent, even though the measured protein concentration was comparable to their freeze-dried counterparts. Slight opalescence indicated the presence of insoluble aggregates which was further analysed using DLS and SEC. While DLS showed polydisperse lysozyme solutions, no aggregates were observed by SEC in both freeze-dried and spray-dried samples. Some of the advantages and limitations of DLS and SEC have been explored in chapter 5, though further optimization of the SEC method for lysozyme along with the implementation of other analytics would be required for the quantitative analysis of protein aggregation.

The enzyme activity results substantiated with molecular dynamics simulations demonstrated the robustness of lysozyme by itself and in the presence of different excipients. The enhanced enzyme activities of both freeze-dried and spray-dried lysozyme trehalose and sucrose were attributed to the conformational changes (without unfolding) observed in its tertiary structure, thereby, providing more flexibility and access to its active sites. While the simulations showed that mannitol preserved the native structure of lysozyme in its partially dried state, the relatively lower activity of spray-dried lysozyme mannitol could be attributed to the formation of a less stable polymorph post spray-drying. Overall, spray-drying has shown to be a potentially favourable method in obtaining dried lysozyme

formulations with significantly lower drying time and comparable efficacy, though further optimization of the spray-drying process and the formulations can help achieve better results.

Chapter 4:

Drying of a Therapeutic Enzyme

4.1 Introduction

With the rising demand for more complex Active Pharmaceutical Ingredients (APIs) to treat various diseases, parenteral biopharmaceuticals are formulated as either liquid or solid products. In order to overcome the disadvantages associated with conventional shelf-based freeze-drying, alternative drying methods must be evaluated in the development of efficient, safe and cost-effective drying technologies for the manufacturing of biologics (Sharma *et al.*, 2021). More recently, spray-drying technology has been successfully employed for a wide range of antibodies (Massant *et al.*, 2020; Duran *et al.*, 2021; Fiedler *et al.*, 2021; Shepard *et al.*, 2021, 2022; Tejasvi Mutukuri *et al.*, 2021; Pan *et al.*, 2022). As assessed in chapter 3, spray-drying is a promising candidate for the biopharmaceutical industry, however, factors such as uncontrolled dehydration, large increases in temperature, shear and protein adsorption at interfaces have been reported to affect the stability of proteins (Rajan *et al.*, 2021).

Protein aggregation/denaturation is one of the major challenges faced in the biopharmaceutical industry (Wang, 1999; Wang *et al.*, 2010; Moussa *et al.*, 2016; Wang and Roberts, 2018). This can occur throughout the lifecycle of biologics, i.e. upstream, downstream and fill finish manufacturing, storage, shipping and manual handling (Mahler *et al.*, 2009; Moussa *et al.*, 2016). The factors responsible for protein aggregation have been broadly classified as intrinsic (structural conformation of the protein) and extrinsic (environment conditions such as temperature, pH, shear etc.) (Wang and Roberts, 2010). 3 pathways or mechanisms for protein aggregation have been proposed in literature (Wang *et al.*, 2010; Moussa *et al.*, 2016). These include:

1. Protein self-association through chemical linkages and colloidal interactions.
2. Aggregation through non-native conformations such as partially unfolded intermediates and unfolded states.
3. Aggregation through covalent interactions caused by chemical degradation reactions.

Evidence from literature has shown spray-drying induced stresses such as temperature, shear and adsorption at air-liquid interfaces on large and small proteins; namely, β-galactosidase, trypsinogen, recombinant growth hormone, tissue-type plasminogen activator, myoglobin, bovine serum albumin, catalase, Pandemrix influenza vaccine, lysozyme etc. (Broadhead *et al.*, 1993; Mumenthaler *et al.*, 1994; Y.-F. Maa and Hsu, 1997; Y. F. Maa *et al.*, 1998; Tzannis and Prestrelski, 1999; Ajmera and Scherließ, 2014; Moorthy *et al.*, 2014, 2018; Koshari *et al.*, 2017; Wilson *et al.*, 2019; Ziaee *et al.*, 2020). However, mechanisms of stabilization of proteins with a wide range of excipients have been postulated and have shown to provide protection against process induced instability. (Green and Angell, 1989; Carpenter *et al.*, 1994; Costantino *et al.*, 1994; Allison *et al.*, 1999; Chang, Shepherd, Sun, Ouellette, *et al.*, 2005; Elversson and Millqvist-Fureby, 2005; Mensink *et al.*, 2017b).

In this chapter, we characterised the stability of Active-freeze-dried and spray-dried Enzyme 'A', a therapeutic, low concentration sucrose-based product of Sanofi, and compared our measurements with molecular dynamics models, allowing us to identify the protein-surface interaction networks created with excipients including sucrose, trehalose, arginine and arginine hydrochloride post spray-drying. These excipients are among the most commonly used stabilizers in freeze-dried and spray-dried protein formulations (Sharma *et al.*, 2021) yet little is known about their mechanisms of interaction with proteins during freeze-drying and spray-drying (Bjelošević *et al.*, 2020; Pinto *et al.*, 2021). Here, the critical quality attributes (CQAs) of Enzyme 'A' were evaluated in terms of its dry powder characteristics and reconstitution properties measured by DSC, UV-Vis spectroscopy, DLS, SEC, enzyme activity and supported by atomically-detailed MD simulations of the protein-excipient co-assembly in aqueous solution. To the best of our knowledge, the stability of spray-dried Enzyme 'A' has not been studied before. Here we resolve its protein–excipient interaction networks and mechanism of stabilization by alternative drying methods.

4.2 Materials and Methods

4.2.1 Preparation of Enzyme 'A' formulations

Trehalose, L-arginine (Arg) and L-arginine hydrochloride (Arg-HCl) were purchased from Sigma Aldrich, Ireland. Formulated liquid and lyophilized Enzyme 'A' with 5 % (w/v) sucrose and 100 mM methionine in sodium phosphate buffer at pH 6.5 was received from Sanofi, Waterford, Ireland. 5 % (w/v) each of trehalose, Arg and Arg-HCl were separately added to the as-received liquid formulation to make the alternative formulations. The original Enzyme 'A' formulation with sucrose was Active-freeze-dried and spray-dried, whereas the alternative formulations of Enzyme 'A' were only spray-dried. Unless specified, Enzyme 'A' by itself refers to the original sucrose-based formulation. It is important to note that excipient-free Enzyme 'A' was not processed as the received drug from Sanofi Waterford was a pre-formulated drug substance including excipients. The removal of excipients would require additional buffer exchange using TFF filtration which was out of scope of this chapter.

4.2.2 Active-freeze-drying.

The Active-freeze-drying process was performed in the Active-freeze-drier (AFD-5) by Hosokawa Micron B.V., Netherlands. Enzyme 'A' was frozen and transformed into snowflake like ice particles with the help of constant stirring at a temperature of – 40 °C and pressure 4 mBar. The transformation of frozen granules took approximately 1.5 h. Primary drying was performed at 320 µBar while the temperature of the wall of the vessel was – 35 °C. This phase lasted for 46 h. The temperature of the wall of the vessel was set to – 20 °C during the secondary drying phase. After the process was completed, the dried powder was transferred and sealed into aluminium packets.

4.2.3 Spray-drying

Spray-drying of Enzyme 'A' was performed using Procept's 4M8-Trix Spray-dryer installed with a cyclone-based separator. Table 4.1 depicts the process parameters employed during the spray-drying of Enzyme 'A'. Process parameters that were altered during the process included air inlet temperature, outlet temperature, pump speed (feed flow rate), nozzle pressure and nozzle size. All other alternative formulations of Enzyme 'A' were spray-dried at air inlet temperatures of 120 °C and 60 °C as per Table 4.1. For each spray-drying method, about 25 mL of the formulated drug substance was spray-dried and the bulk dried powder were transferred into 20 mL Schott glass vials inside a glove bag purged with nitrogen gas. The vials were overlaid with nitrogen gas, rubber stoppered, crimped and stored at ~ 5 °C. Before analysis, the spray-dried powder was weighed into a new 20 mL Schott glass vial at relative humidity of ≤ 5 %. Moreover, to assess the impact of shear on the enzyme, the received formulated drug substance was sprayed through the spray nozzle with nozzle diameters of 0.4 mm and 1.2 mm, at a nozzle pressure of 0 bar and 4 bar and feed flow rates of 1 mL/min and 4 mL/min without drying. The sprayed liquid was collected in a glass beaker.

Table 4.1: Spray-drying Process Parameters for Enzyme 'A'.

No.	Factors	1	2	3	4	5	6
1	**Air Inlet Temp (°C)**	90	120	150	200	60	45
2	**Outlet Temp (°C)**	51.3	66.4	76.9	97.3	35.6	25
3	**Air Flow Rate (L/min)**	80 - 90	80 - 90	80 - 90	80 - 90	80 - 90	80 - 90
4	**Pump Speed (%)**	20	20	20	20	25	25
5	**Air Speed (m^3/min)**	0.3	0.3	0.3	0.3	0.3	0.3
6	**Nozzle Pressure (Bar)**	1.63	1.63	1.63	1.63	1	1
7	**Nozzle Size (mm)**	0.4	0.4	0.4	0.4	0.8	0.8

4.2.4 Glass Transition Temperature and RMC

The T_g / T_m of the Active-freeze-dried and spray-dried Enzyme 'A' were measured using Differential Scanning Calorimetry (DSC) – TA Q2000. Approximately, 5 – 10 mg of each dried sample sealed in an aluminum pan at relative humidity ≤ 5 %. Modulated DSC was ramped from 0 °C to 120 °C at 2 °C/min with modulation amplitude of ± 1 °C and modulation period of 100 s for solid samples. Samples were analyzed in triplicate (n = 3). The RMC of Active-freeze-dried and spray-dried Enzyme 'A' was measured using Karl Fischer titration (Karl Fischer Titrator by Metrohm). The vials were prepared at relative humidity ≤ 5 % and capped with Karl Fisher caps. The samples were subjected to a temperature of 100 °C, the blank vials were at 120 °C and the water standard was subjected to a temperature of 150 °C (as per the manufacturer's recommendation).

4.2.5 Homogeneity, Turbidity and Reconstitution Time analyses

The freeze-dried, Active-freeze-dried and spray-dried Enzyme 'A' samples, including the alternative formulations, were reconstituted with 5 mL of deionized water and the concentration and turbidity were measured in a 1x1 cm transparent glass cuvette using a UV-Vis spectrometer (Spectro Star nano by BMG Labtech) at 280 nm and 350 nm, respectively. The concentration was calculated using Beer lambert's law with the molar extinction coefficient of 2.41 mL mg^{-1} cm^{-1}. The reconstitution time was measured using a stopwatch.

4.2.6 Multi-Angle Dynamic Light Scattering (MADLS)

All samples were analysed by the Zetasizer Ultra (Malvern Panalytical Ltd.) equipped with a nominally 10 mW He-Ne laser at a wavelength of 633 nm. 1 mL of sample was measured in a 1 cm x 1 cm transparent disposable cuvette. The cell position was set to 4.64 mm to allow for measurement of the sample across all detector angles. All MADLS measurements were collected at 3 different

angles of detection, namely, back scatter (174.7°), side scatter (90°) and forward scatter (12.78°) with an equilibration time of 120 s. The refractive index of the protein and water used were 1.45 and 1.33, respectively. The viscosity of the low concentration dispersant for the enzyme at 25 °C was 0.8872 mPa.s. The equilibration time was 120 s. All samples were analyzed in triplicate ($n \geq 3$).

4.2.7 Size Exclusion Chromatography

The aggregation profiles of all Enzyme 'A' samples (including the alternative formulations) were analyzed using SEC on the Agilent 1200 HPLC with a Diode Array Detector. The mobile phase contained 20 mM Sodium Phosphate dibasic and 200 mM Sodium Chloride at pH 6.5. All samples were analyzed on a TSK gel 3000 SWXL column with a flow rate of 0.5 mL/min at 25 °C and an injection volume of 75 µL.

4.2.8 Enzyme Activity

The enzyme activity of all freeze-dried and spray-dried Enzyme 'A' samples were tested by the Analytical Science Department at Sanofi, Waterford. The enzyme activity of Enzyme 'A' was measured based on the hydrolysis of a substrate. The assay protocol contains proprietary information which cannot be disclosed. The results obtained for enzyme activity are shown in section 4.3.5.

4.2.9 Molecular dynamics simulations

MD simulations were performed on Enzyme 'A' and its alternative formulations to understand the influence of excipient-specific protein–excipient interactions on protein stability during spray-drying. To simulate the high-temperature environment of spray-drying, the enzyme was modelled at three different temperatures, 300K (27 °C), 340K (67 °C) and 380K (107 °C) in water solution in the

presence of sucrose, sucrose + Arg-HCl, and sucrose + trehalose. The simulations were performed for two different excipient concentrations; the starting concentrations of experimental solution prior to spray-drying (labelled 1x) to study the protein in its original solution, and at ten times the starting concentrations (labelled 10x), to study its behavior in its partially dried state as the excipients form more large-area, specific interactions with the surface of the protein. The data was analyzed in terms of excipient-induced changes in the protein structure as monitored through root mean square deviation (RMSD) of residues away from their starting positions (from X-ray crystal structure PDB ID 4WLD), fraction of native contacts, root mean square fluctuation (RMSF) with respect to the time-averaged structure as a measure of the flexibility of the protein, and preservation of secondary structure. MD simulations are carried out using the Gromacs 2018.4 package (Van Der Spoel *et al.*, 2005) with a time step of 2 fs using the Leap frog integrator (Verlet, 1967; Hockney *et al.*, 1974). Bond lengths to hydrogen were constrained using the LINCS algorithm (Hess, 2007). Long-range electrostatics were treated by the Particle mesh Ewald (PME) method (Darden *et al.*, 1998). Protein and solvent molecules were coupled separately to an external heat bath (300 K) with a coupling time constant of 1 ps using the velocity rescaling method (Bussi *et al.*, 2007). CHARMM glycan parameters (Guvench *et al.*, 2011) were used for excipient molecules, while peptide molecules were represented by the CHARMM 36m (Huang *et al.*, 2016) force field. All systems were minimized for 100 ps and equilibrated for 500 ps in constant volume NVT ensemble. Production phases of 1 μs in the NPT ensemble were then carried out for each formulation.

4.2.10 Statistical Analyses

Method performed was as per section 2.2.14.

4.3 Results and Discussion

4.3.1 Glass Transition Temperature and RMC

The results for thermal and RMC analyses for freeze-dried and Active-freeze-dried Enzyme 'A' are shown in Table 4.2. The RMC and the T_g of Active-freeze-dried Enzyme 'A' were very comparable to its freeze-dried counterpart. The reported T_g of sucrose is ~ 60 °C (Liao *et al.*, 2004; Simperler *et al.*, 2006) while the T_g of the formulation (~ 79 °C) was elevated as proteins and amino acids exhibit a higher T_g compared to sugars (Matveev *et al.*, 1997; Pikal *et al.*, 2007). The low RMC (0.17 %) achieved during Active-freeze-drying was as a result of a very long drying cycle that can be optimized further. The length of the primary drying phase can be reduced by installing a condenser, by using a tube of large diameter connecting the drying vessel and the vacuum pump, and/or by increasing the surface area of the filter to improve the removal of water vapour (Hosokawa Micron B.V., 2019).

Table 4.2: T_g and RMC of freeze-dried and Active-freeze-dried Enzyme 'A'.

Sample	T_g (◦C)	RMC (%)
Freeze-dried Enzyme 'A' + sucrose	79.78 ± 0.69	0.11 ± 0.02
Active-freeze-dried Enzyme 'A' + sucrose	78.60 ± 0.37	0.17 ± 0.02

The results for thermal and RMC for spray-dried Enzyme 'A' are shown in Table 4.3. The inlet and outlet temperatures are represented as inlet/outlet (Table 4.3). The RMC was significantly reduced from 4.95 % to 1.91 %. This was achieved by employing similar process parameters as reported in chapter 3, section 3.3.1 (Büchi Labortechnik AG, 2002; Vass *et al.*, 2019a; Ziaee *et al.*, 2019). For example, in the fourth row of Table 4.3 it can be seen that Enzyme 'A' was aggressively spray-dried at an inlet/outlet temperature of 200/97.3 °C, significantly above its T_g, with an air flow rate of 80

L/min, a pump speed (feed flow rate) of 20 %, a nozzle pressure of 1.63 bar and a nozzle size of 0.4 mm. A T_g of 45.52 °C and an RMC of 2.63 % was obtained. Similarly, the enzyme was gently spray-dried at an inlet/outlet temperature of 45/25 °C, where the enzyme remained significantly below its T_g. The air flow rate and the pump speed were kept constant at 80 L/min and 20 %, respectively. In this case, the nozzle pressure was kept at 1 Bar and a nozzle size of 0.8 mm was employed. The T_g (28.99 °C) obtained was lower and the RMC (4.95 %) was increased. Through gentle spray-drying process conditions, the enzyme was kept below its freeze-drying secondary drying temperature (35 °C). These conditions were employed to study the effect of both temperature and shear on the enzyme and to achieve comparable CQAs with respect to its freeze-dried counterpart.

Table 4.3: T_g and RMC of Enzyme 'A' spray-dried at different process parameters.

Sample	**Air inlet/outlet Temperature (°C), Air flow rate (L/min), pump speed (%), nozzle pressure (Bar), nozzle size (mm)**	**T_g (°C)**	***RMC % (± 0.1 %)**
Spray-dried Enzyme 'A' + sucrose.	90/51.3, 80, 20, 1.63, 0.4	41.31 ± 2.04	3.47
	120/66.4, 80, 20, 1.63, 0.4	49.21 ± 0.77	2.13
	150/76.9, 80, 20, 1.63, 0.4	52.43 ± 1.85	1.91
	200/97.3, 80, 20, 1.63, 0.4	45.52 ± 0.19	*2.63
	60/35.6, 80, 20, 1, 0.8	33.73 ± 4.78	4.84
	45/25, 80, 20, 1, 0.8	28.99 ± 0.91	4.95

*The resultant yield of the spray-dried Enzyme 'A' formulations varied in the range of 60 – 65 %. The yield decreased as the RMC increased due to the hygroscopic nature of sucrose. The yield was not the primary target of these experiments and so this parameter was not optimized. The RMC obtained was higher for the 200/97.3 run than the 150/76.9 run due to a failure of the 200/97.3 run towards the end of the cycle resulting in insufficient drying of the powder obtained.

From Table 4.3, it can again be noted that along with lowering the inlet/outlet temperatures, the nozzle pressure (1 Bar) was decreased, and the nozzle size (0.8 mm) was doubled as part of the gentle spray-drying conditions. These parameters were altered to study the combined effect of shear and temperature on the protein. The effect of nozzle size on the particle size, morphology and the RMC have been studied in literature (Grasmeijer *et al.*, 2019; Ziaee *et al.*, 2019, 2020). As reported in chapter 3, section 3.3.1, an inverse correlation (R^2 = 0.974) between the T_g and the RMC in spray-dried Enzyme 'A' at different outlet temperatures (Figure 4.1) verified the consistency of results and can be employed to generate empirical models for the prediction of RMC and T_g during spray-drying of biologic drug products. Moreover, comparable CQAs can be achieved by further optimizing the spray-drying process.

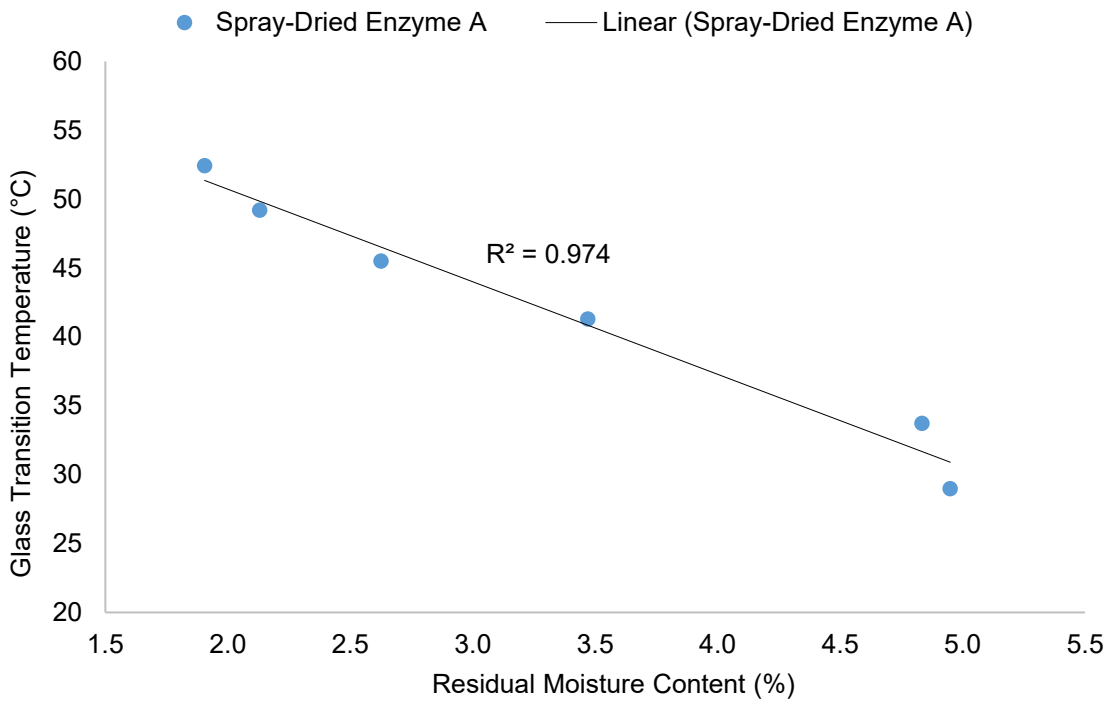

Figure 4.1: Correlation between T_g and RMC for Enzyme 'A' at different air outlet temperatures.

4.3.2 Homogeneity, Turbidity and Reconstitution Time analyses

The behaviour of rehydrated freeze-dried, Active-freeze-dried, and spray-dried Enzyme 'A' can be seen in Figure 4.2. A clear solution was obtained within 1 min of reconstitution of the freeze-dried cake (Figure 4.2 (a) and Table 4.4). The Active-freeze-dried and spray-dried samples took ≥ 15 min to reconstitute compared to the freeze-dried samples Table 4.4. Unlike the rehydrated freeze-dried vials that appeared clear, the reconstituted Active-freeze-dried and spray-dried vials appeared highly turbid due to the presence of high amounts of insoluble particles formed during the two drying processes. These insoluble particles are protein aggregates. Turbid protein solutions associated with aggregation have been reported by various authors (Mehta *et al.*, 1996; Y. F. Maa *et al.*, 1998; Andya, Y. F. Maa, *et al.*, 1999b; Tzannis and Prestrelski, 1999; Giurleo *et al.*, 2008; Yamaguchi *et al.*, 2013; Owczarz and Arosio, 2014).

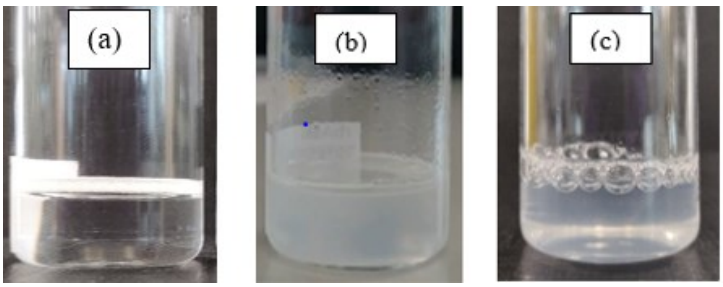

Figure 4.2: Reconstituted Enzyme 'A': (a) freeze-dried, (b) Active-freeze-dried and (c) spray-dried.

The behaviour of dried powder in these samples just before complete reconstitution can be seen in the Appendix, Figure A4.1. Upon the addition of ultrapure water, the majority of the particles in the Active-freeze-dried powder began to float on water, whereas the majority of the particles in the spray-dried powder formed small clumps and sedimented at the bottom of the vial. This showed that the particle size and the density of Active-freeze-dried powder was significantly lower than particles in the spray-dried powder. Possible reasons for the presence of insoluble agglomerates causing turbidity may be due to temperature, shear, adsorption at liquid-air interfaces and dehydration stresses induced via the two drying processes. Moreover, higher moisture content, as present in spray-dried samples,

increases the stickiness amongst particles that also results in particle agglomeration (Vehring, 2008; Schaefer and Lee, 2015a, 2015b; Ziaee *et al.*, 2020).

It has been reported that simply shaking protein solutions can induce aggregation (Mahler *et al.*, 2005; Wang *et al.*, 2010). Vigorous shaking or stirring increases the kinetic energy as well as creates liquid-air interfaces. This allows proteins to adsorb at the interface resulting in exposure of hydrophobic residues to air. These exposed hydrophobic residues tend to induce aggregation (Wang, 1999; Wang *et al.*, 2010). The creation of these interfaces further facilitate the impact of sheer stress on proteins (Yu *et al.*, 2006; Abdul-Fattah *et al.*, 2008; Bee, Chiu, *et al.*, 2009). The stirring motion involved in the Active-freeze-drying process could be one of the major reasons for protein aggregation of Enzyme 'A'. While the formulated drug substance as well as the rehydrated spray-dried Enzyme 'A' solutions were handled with care, the atomization of liquid feed during the spray-drying process could be responsible for the creation of liquid-air interfaces leading to aggregation of the enzyme. Although temperature and shear are responsible for some protein aggregation (Andrews *et al.*, 2008; Bee, Chiu, *et al.*, 2009), protein adsorption at the liquid-air interface has also been reported to be the major reason for aggregation in spray-dried recombinant growth hormone (rhGH), tissue-type plasminogen activator (tPA) and other proteins (Mumenthaler *et al.*, 1994; Y.-F. Maa and Hsu, 1997; Kumar *et al.*, 2009; Mukherjee *et al.*, 2009).

The measured protein concentrations in freeze-dried, Active-freeze-dried and spray-dried Enzyme 'A' vials were not consistent (Table 4.4). On average, the concentration of the protein in the Active-freeze-dried and spray-dried samples was 5.01 ± 0.55 mg/mL. The change in the protein concentrations in the Active-freeze-dried and spray-dried samples corresponded to the relative change in the concentrations of the monomers and higher aggregates in the solution. Moreover, the optical densities of all reconstituted samples were measured in the light scattering region (350 nm) as shown in Appendix, Figure A4.2. While measuring the scattering of light at 350 nm as a function of protein aggregation is not the best quantitative method, it does provide a quick estimate of the level of turbidity in protein solutions (Al-hussein and Gieseler, 2013). The spray-dried samples were

represented as per the inlet/outlet temperatures that they were subjected to. Significant differences in the optical densities of rehydrated Enzyme 'A' samples have been shown in Figure A4.3 of the Appendix. Light scattering due to particles in Active-freeze-dried samples was the highest amongst all samples ($p < 0.05$) suggesting that the sample was highly aggregated. The optical densities of gently spray-dried Enzyme 'A' samples at an air inlet/outlet temperature of 60/35.6 °C and 45/25 °C were significantly lower ($p < 0.05$) than the aggressively spray-dried samples at air inlet/outlet temperatures of 120/66.4 °C, 150/76.9 °C, 200/97.3 °C. These results indicate that lower temperatures and a larger nozzle size resulted in less turbid solutions. Furthermore, to assess the impact of shear alone, the sprayed enzyme solution through the spray nozzle (without drying) exhibited aggregate levels of < 2 % and O.D. of < 0.1 which were comparable to the reconstituted freeze-dried product. This confirmed that temperature significantly affected the stability of Enzyme 'A', rather than just shear alone.

Additionally, the impact of other excipients on the stability of spray-dried Enzyme 'A' was also evaluated (Figure 4.3). The reconstituted spray-dried Enzyme 'A' formulations containing sucrose/trehalose, sucrose/Arg and sucrose/Arg-HCl are shown in Figure 4.3 (c – e), respectively. The turbidity of reconstituted spray-dried Enzyme 'A' was significantly improved in the presence of sucrose/trehalose, sucrose/Arg and sucrose/Arg-HCl compared to the turbidity in sucrose by itself (Figure 4.3 (b)).

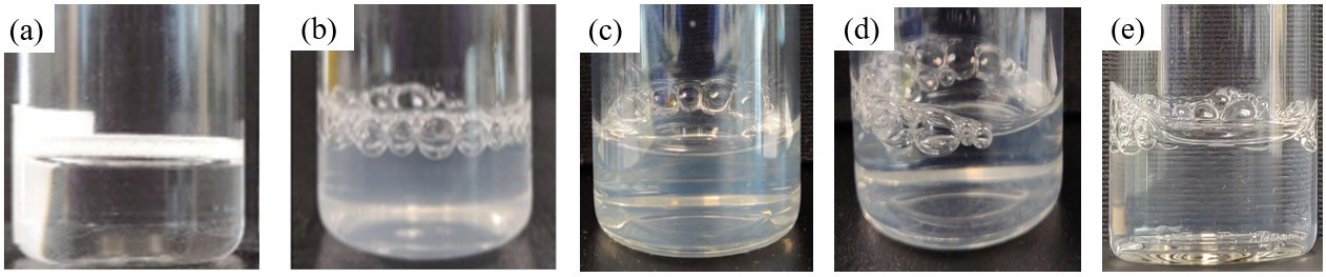

Figure 4.3: Reconstituted Enzyme 'A' (a) freeze-dried with sucrose (control), (b) spray-dried with sucrose, (c) spray-dried with sucrose/trehalose, (d) spray-dried with sucrose/Arg, (e) spray-dried with sucrose/Arg-HCl.

A significant improvement in the reconstitution behaviour of spray-dried Enzyme 'A' sucrose/Arg and sucrose/Arg-HCl was observed and was consistent with the results obtained for the O.D. in the light scattering region (Figure 4.4), reconstitution time and concentration as shown in Table 4.4. As shown in Figure 4.4, a reduction in the O.D. of the spray-dried enzyme formulation with sucrose/trehalose was also observed, while the O.D. of the reconstituted formulation containing sucrose/Arg and sucrose/Arg-HCl was significantly lower than that of sucrose and sucrose/trehalose. Moreover, a significant reduction in the reconstitution time was observed for sucrose/Arg (8 min) and sucrose/Arg-HCl (5.5 min) but the formulation containing sucrose/trehalose did not show any reduction in the reconstitution time (15 min) (Table 4.4). A reduction in the reconstitution time and improved stability in the presence of arginine was also reported for humanized IgG4 monoclonal antibodies (Massant *et al.*, 2020). Also, the enzyme concentrations obtained for the formulations containing sucrose/trehalose, sucrose/Arg and sucrose/Arg-HCl were consistently within the specification range of the product (4.0 ± 0.5 mg/mL).

Table 4.4: Reconstitution time, concentration and turbidity of reconstituted freeze-dried, Active-freeze-dried and spray-dried Enzyme 'A'.

Sample	Reconstitution Time (min)	Concentration (mg/mL)	Optical Density A_{350}
Freeze-dried Sucrose (Control)	1	4.15 ± 0.05	0.074 ± 0.05
Active-freeze-dried Sucrose	> 15	5.01 ± 1.16	3.50 ± 0.00
Spray-dried Sucrose (60 °C)	15	4.47 ± 0.17	0.450 ± 0.10
Spray-dried Sucrose (120 °C)	15	5.56 ± 2.44	0.890 ± 0.03
Pre-dried Sucrose/Trehalose	-	4.01 ± 0.02	0.030 ± 0.001
Spray-dried Sucrose/Trehalose (60 °C)	15	3.81 ± 0.01	0.271 ± 0.002
Spray-dried Sucrose/Trehalose (120 °C)	15	4.00 ± 0.01	0.228 ± 0.001
Pre-dried Sucrose/Arginine	-	3.88 ± 0.06	0.029 ± 0.001
Spray-dried Sucrose/Arginine (60 °C)	8	3.43 ± 0.01	0.106 ± 0.001
Spray-dried Sucrose/Arginine (120 °C)	8	3.93 ± 0.01	0.090 ± 0.003
Pre-dried Sucrose/Arg-HCl	-	4.38 ± 0.03	0.068 ± 0.001
Spray-dried Sucrose/Arg-HCl (60 °C)	5.5	3.97 ± 0.05	0.179 ± 0.01
Spray-dried Sucrose/Arg-HCl (120 °C)	5.5	4.01 ± 0.01	0.149 ± 0.001

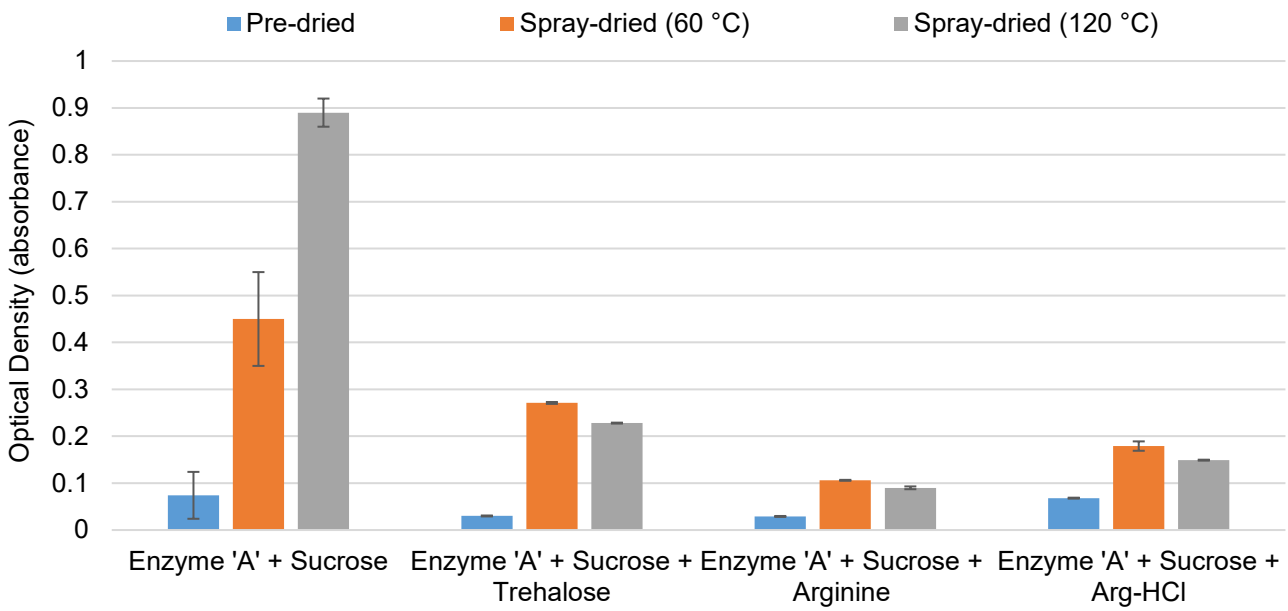

Figure 4.4: Optical density of reconstituted spray-dried Enzyme 'A' formulations.

4.3.3 Multi-Angle Dynamic Light Scattering

To further identify and elucidate the reason for high turbidity and reconstitution time in the above samples, the PSD was studied using multi-angle DLS (MADLS). MADLS is an improvement in the single-angle DLS technique and has been evaluated and discussed extensively in chapter 5. The PSD by intensity of the rehydrated freeze-dried, Active-freeze-dried and spray-dried Enzyme 'A' samples are shown in Figure 4.5. It was observed that the monomeric protein was present around 10 nm with a minor fraction of HMWS present around 95 nm in freeze-dried samples (Figure 4.5 (a)). Moreover, the Z-average (10.65 nm) and a PDI of 0.3 indicated a fairly monodisperse solution (Table 4.5). A clear solution was obtained with the absence of insoluble protein aggregates as shown in section 4.3.2, Figure 4.2 (a) and Figure 4.3 (a).

Table 4.5: Z-Average and PDI for freeze-dried, Active-freeze-dried and spray-dried Enzyme 'A'.

Sample	Z-Average (nm)	PDI
Freeze-dried Enzyme 'A'	10.65	0.30
Active-freeze-dried Enzyme 'A'	146.2	0.39
Spray-dried Enzyme 'A'	185.5	0.50

The PSD of spray-dried and Active-freeze-dried Enzyme 'A' are shown in Figure 4.5 (b) and (c). The reduced distribution by intensity of the monomer and the shift in the particle sizes from 10 nm to 15.05 and 22.36 nm along with an increased distribution by intensity of multiple peaks between 100 nm and 500 nm, clearly indicated protein aggregation compared to Figure 4.5 (a). This was later confirmed by SEC in section 4.3.4. The presence of additional peaks in the range of 60 nm – 1000 nm have been attributed to protein aggregates previously (Panchal *et al.*, 2014; Wang *et al.*, 2016). The results obtained so far were consistent with those presented in section 4.3.2. Higher reconstitution time, increased turbidity and the presence of higher molecular weight species elucidate protein aggregation. The continuous stirring motion during the freezing step in the Active-freeze-drying process may have accounted for shear and liquid-air interface-induced protein aggregation (Touzet *et al.*, 2018; Hosokawa Micron B.V., 2019). Enzyme 'A', being a large molecule, is susceptible to process-induced stresses. Similarly, the PSD of spray-dried samples indicated protein aggregation which confirmed the presence of a large fraction of insoluble protein aggregates leading to a turbid solution (Figure 4.2 (c) and Figure 4.3 (b)). In this case, high temperature significantly contributed to the increase in protein aggregates leading to a turbid solution with high reconstitution time.

The PSD of Enzyme 'A' in the presence of co-excipients trehalose, Arg and Arg-HCl are shown in Figure 4.5 (d – h). While a minor shift in the monomer peak (12.93 nm) was observed in the presence of sucrose/trehalose prior to drying (Figure 4.5 (d)), the enzyme showed a multimodal distribution

post spray-drying (Figure 4.5 (e)), thereby, indicating protein aggregation. In the presence of sucrose/Arg, a monodisperse PSD was observed with a peak at 14.9 nm (Figure 4.5 (f)). Post spray-drying, a multimodal distribution was obtained with the peak at 14.77 nm that exhibited the highest light scattering intensity (70 %) (Figure 4.5 (g)). While there was a shift in the monomodal monomer peak size from 10 nm to 14 nm (Figure 4.5 (f)), it is important to note that DLS results in this case can be deceiving as fundamentally DLS isn't a high resolution technique and could not resolve monomer-dimer species, so, other complementary techniques such as SEC were employed in section 4.3.4. The peak at ~ 14 nm was confirmed as the dimer of the enzyme by SEC in section 4.3.4, while the monomer peak was masked by the dimer peak. Factors impacting MADLS particle size accuracy, precision and resolution have been thoroughly evaluated and discussed in chapter 5. Furthermore, the PSD of pre-dried and spray-dried sucrose/Arg-HCl (Figure 4.5 (h)) was similar to the PSD obtained for sucrose/trehalose (Figure 4.5 (d)). Although, a multimodal PSD was obtained for spray-dried Enzyme 'A' with sucrose/Arg-HCl, Arg-HCl played a significant role in suppressing insoluble aggregates and decreasing the reconstitution time as also reported in section 4.3.2.

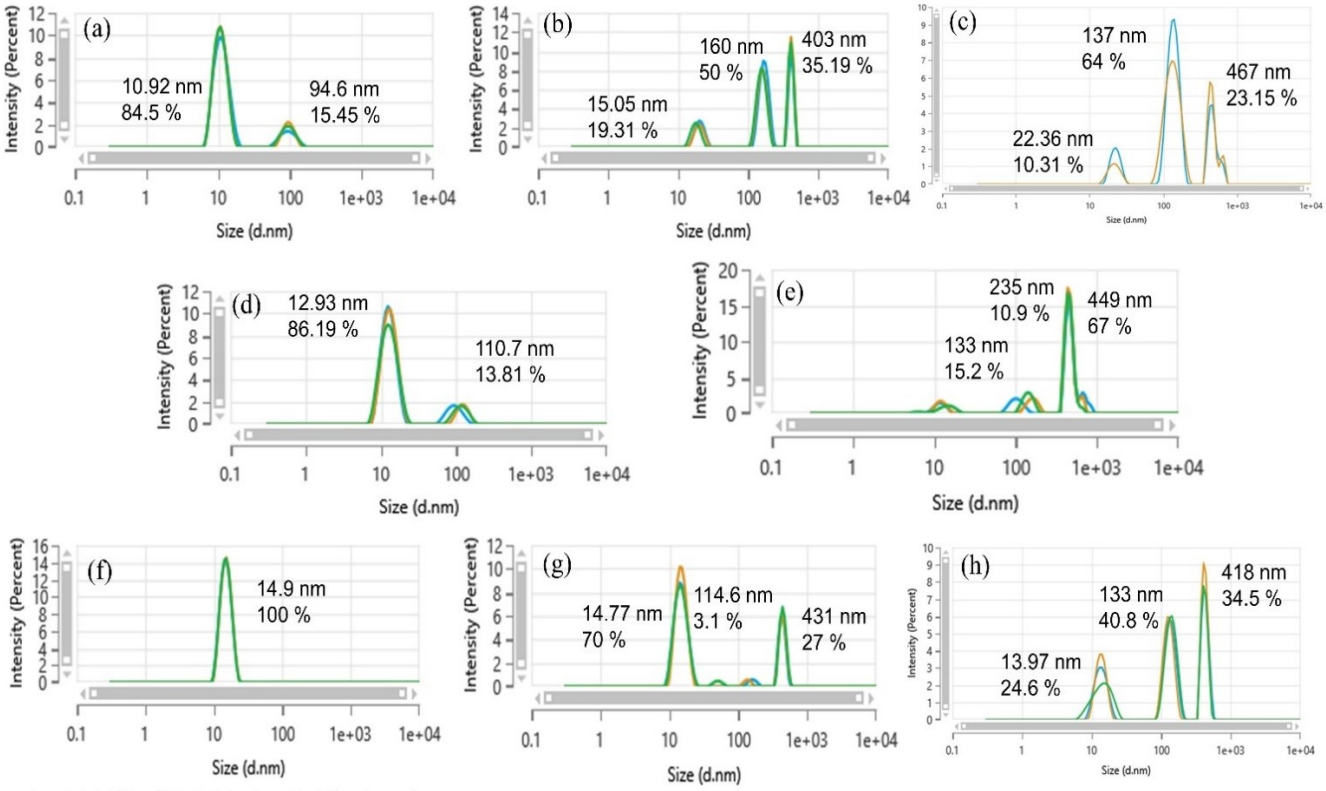

Figure 4.5: MADLS PSD of Enzyme 'A' (a) freeze-dried sucrose, (b) spray-dried sucrose, (c) Active-freeze-dried sucrose, (d) pre-dried sucrose/trehalose, (e) spray-dried + sucrose/trehalose, (f) pre-dried sucrose/Arg, (g) spray-dried sucrose/Arg and (h) spray-dried sucrose/Arg-HCl.

4.3.4 Size Exclusion Chromatography

SEC was performed to quantify protein aggregates present in all freeze-dried, Active-freeze-dried and spray-dried samples of Enzyme 'A'. The loss of monomer of the enzyme is shown in Figure 4.6 and the aggregation profiles in reconstituted freeze-dried, Active-freeze-dried and spray-dried Enzyme 'A' samples are shown in Figure A4.4 of the Appendix. With respect to freeze-dried Enzyme 'A', a 20 % and a 15 % loss of monomer was observed in the Active-freeze-dried and spray-dried samples, respectively (Figure 4.6). The decrease in the monomer content was associated with the increase in protein aggregates. While the freeze-dried samples showed only 3.69 % dimers and no HMWS, the Active-freeze-dried samples showed a higher dimer (4.12 %) and HMWS (10.76 %) content. The MADLS results obtained in section 4.3.3 were only qualitative while SEC provided a

quantitative aggregation profile. The two techniques complemented each other by confirming the presence of higher aggregates. These results confirmed process-induced protein aggregation, as discussed in section 4.3.2 and 4.3.3.

With respect to the alternative formulations of Enzyme 'A', the formulation containing sucrose/Arg exhibited maximum loss of monomer (70 – 80 %) which was ascribed to a significant pH shift from 6.5 to 9.8. The large shift in the pH resulted in significant dimerization (> 50 %) of the enzyme, thereby, leading to maximum loss of the monomer. The loss of monomer in the formulations containing sucrose, sucrose/trehalose and sucrose/Arg-HCl were comparable, though on average the loss of monomer was 5% higher in sucrose/Arg-HCl (Figure 4.6). This showed that even though Arg-HCl played a significant role in suppressing insoluble aggregation, it resulted in fragmentation of the monomer as observed by SEC. The loss of monomer has been associated with a decrease in protein stability and concentration in formulations of lysozyme and myoglobin (Mutukuri *et al.*, 2021). Loss of monomer due to increased protein aggregation can lead to increased immunogenicity and decreased product efficacy (Moussa *et al.*, 2016). However, in some cases dimerization and oligomerization can be integral to protein activity (Marianayagam *et al.*, 2004).

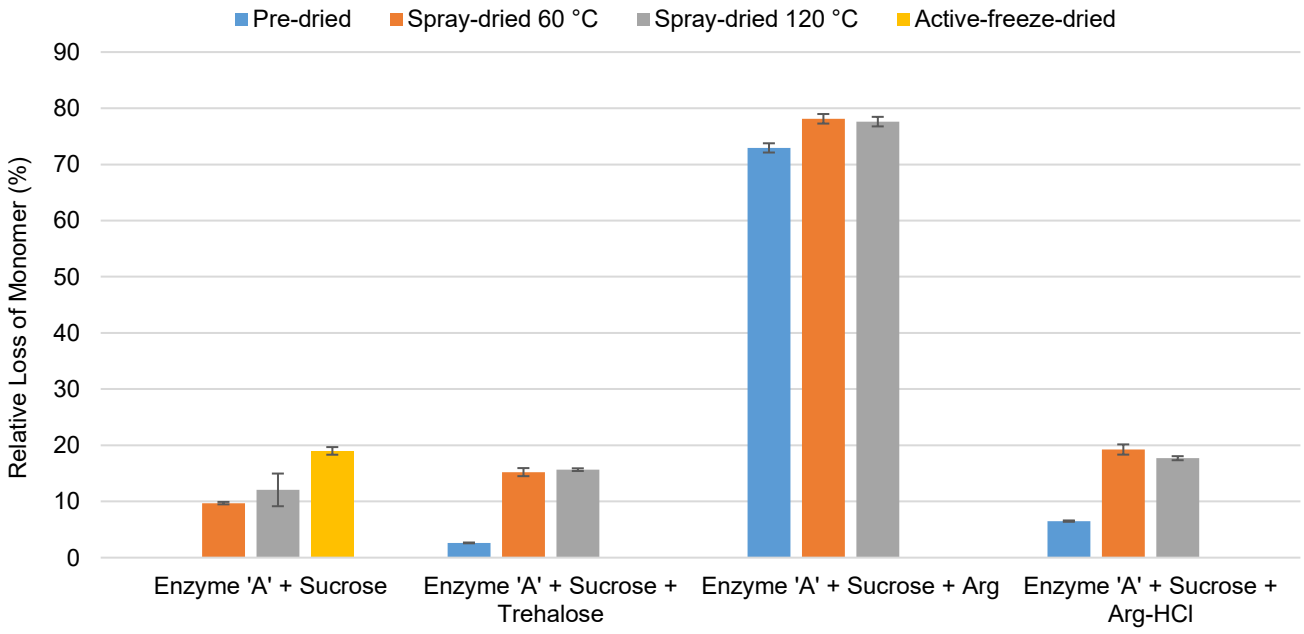

Figure 4.6: Percentage loss of monomer in Enzyme 'A' formulations by SEC.

Several theories have been reported to explain the mechanism of stabilization of proteins by arginine. According to preferential interaction, arginine preferentially excludes itself from the surface of lysozyme, BSA and α-chymotrypsinogen A, particularly at high concentrations, leading to an increase in the transfer free energy, thereby, stabilizing the protein against unfolding and aggregation (Kita *et al.*, 1994; Schneider and Trout, 2009; Shukla and Trout, 2011a). An alternative explanation based on surface tension posits that at high arginine concentrations, the rate of increase in the surface tension is low, which suggests that arginine forms molecular clusters that interact with the hydrophobic surface of proteins, thereby, suppressing protein aggregation (Das *et al.*; Tsumoto *et al.*, 2005; Arakawa *et al.*, 2007). A third theory, based on the solubility of amino acids, proposes that arginine increases the solubility of amino acids by weakening both hydrophobic and polar interactions, thus, suppressing protein aggregation (Das *et al.*; Arakawa *et al.*, 2007). Finally, the excluded-volume effect, also known as the gap effect, states that the presence of excipients such as arginine creates an energy barrier between protein molecules which decreases the rate of protein aggregation (Baynes and Trout, 2004; Baynes *et al.*, 2005; Shukla and Trout, 2010). In spite of the reported mechanisms for protein stabilization by arginine, protein destabilization by arginine has also been reported (Kim *et al.*, 2016). The guanidinium group present in arginine contributes to the destabilizing effect as guanidine hydrochloride (GdnHCl) is a well-known chaotrope, while the destabilizing effect of GdnHCl is lower than that of arginine itself (Ishibashi *et al.*, 2005). This is in agreement with the results obtained here with Enzyme 'A' for Arg *vs.* Arg-HCl.

4.3.5 Enzyme Activity

Figure 4.7 shows the relative retained enzyme activity of the different Enzyme 'A' formulations and Table 4.6 summarizes the CQAs of freeze-dried and spray-dried Enzyme 'A' formulations. The spray-dried formulations containing sucrose, sucrose/trehalose and sucrose/Arg-HCl exhibited increased enzymatic activity compared to the freeze-dried formulation containing sucrose (control),

while the formulation containing sucrose/Arg exhibited the lowest activity due to significant loss of monomer and an increase in dimerization of Enzyme 'A' as shown by SEC in section 4.3.4. A similar increase in the enzyme activity of spray-dried lysozyme was reported in chapter 3, section 3.3.5. To further elucidate and understand the obtained activity results and the stability of Enzyme 'A', MD simulations were performed in section 4.3.6.

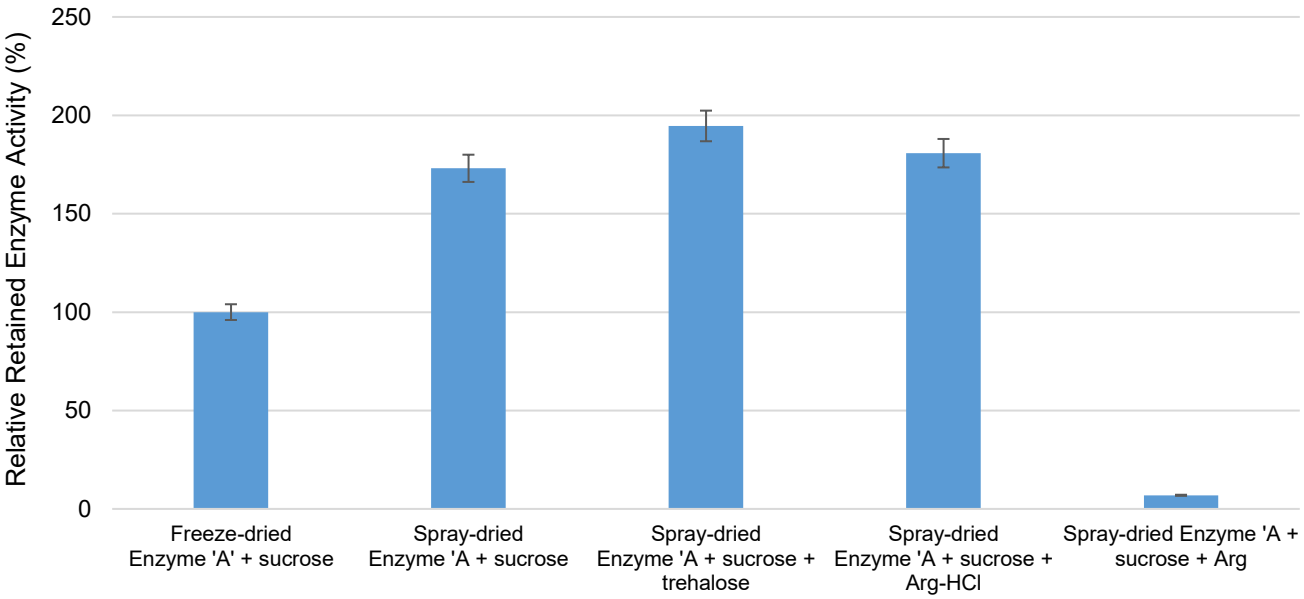

Figure 4.7: Relative retained enzyme activity of the different spray-dried Enzyme 'A' formulations.

Table 4.6: A summary of CQAs of freeze-dried and spray-dried Enzyme 'A' formulations.

Sample	pH	Recon Time	Turbidity	Monomer loss	Activity
Freeze-dried Enzyme 'A'	6.5	1	0.074 ± 0.05	control	100
Spray-dried Enzyme 'A'	6.5	15	0.890 ± 0.03	12.06	173
Spray-dried Enzyme 'A' + Trehalose	6.5	15	0.890 ± 0.03	15.6	194
Spray-dried Enzyme 'A' + Arg	9.8	8	0.090 ± 0.003	78.12	6.9
Spray-dried Enzyme 'A' + Arg-HCl	6.5	5.5	0.149 ± 0.001	17.7	180

4.3.6 Molecular Dynamics Simulations

The comparison of all properties at low and high concentrations of excipients (Appendix, Figure A4.5 – A4.8) showed that the macromolecular crowding of the excipients on the protein surface tends to reduce the change in the protein conformation induced by the increase in temperature. At high concentrations, similar to the local environment in a droplet as drying takes place, the differential effects of each excipient on the protein structure were clearly shown in the molecular models. Figure 4.8 shows the fraction of native contacts that were conserved during the simulation. This captured changes in the tertiary structure. At room temperature (300 K) and at the temperature reached during the spray-drying (340 K) process, both sucrose and the sucrose/Arg-HCl mixture conserved a large fraction of the native contacts, suggesting a minimal change in the tertiary structure. Furthermore, in both cases, the fraction converged towards an equilibrium value. The fraction of native contacts conserved was also larger for sucrose/Arg-HCl, in good agreement with experimental results showing the stabilization effect of Arg-HCl. This result was also substantiated with the increase in the secondary structure of the sucrose/Arg-HCl system at 340 K (Appendix, Figure A4.10). Sucrose/trehalose, however, only conserved the protein structure at room temperature, but failed to do so at a higher temperature of 340 K corresponding to operating temperature of the spray-dryer. Again, this was consistent with experimental results showing increased reconstitution time and a large fraction of insoluble aggregates. 380 K was used as a control temperature, as the spray-dryer could potentially reach such a high value. For all excipients, a loss of native contacts was observed but with sucrose and sucrose/Arg-HCl reaching a new equilibrium at 340 K and 380 K and, therefore, a new conformation. Similar enzyme activity results obtained for lysozyme in chapter 3, section 3.3.5 could possibility explain the increased efficacy observed in Enzyme ‘A’ as a result of increased flexibility and access to the active site residues although an assessment of the distance between active site residues with respect to the native conformation would be required using coarse-grained models.

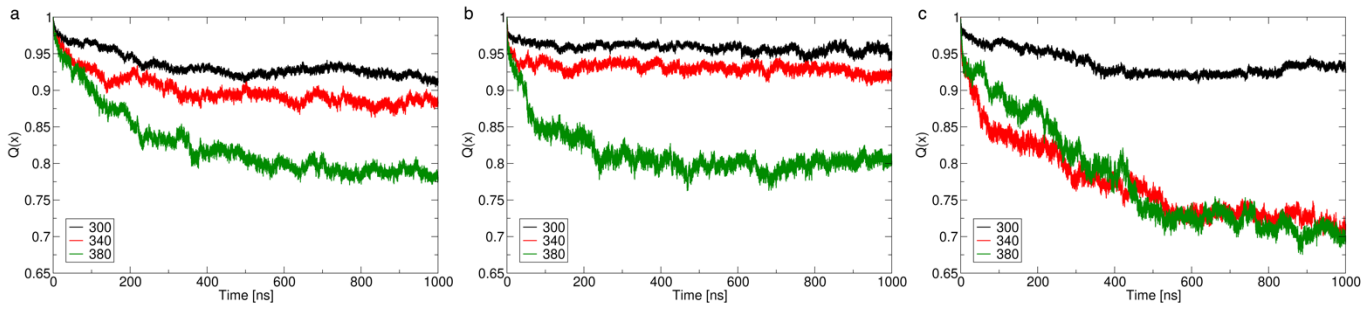

Figure 4.8: Plot of the fraction of native contacts of Enzyme 'A' with 10x concentration of (a) Sucrose, (b) Sucrose/Arg-HCl and (c) Sucrose/Trehalose.

The RMSF, depicted in Figure 4.9, shows the fluctuations of each residue of Enzyme 'A'. Sucrose maintained very low fluctuations at 300 K and 340 K, as does Arg-HCl, although the domains 100-110 and 145-155 showed slightly larger fluctuations. At 380 K however, Arg-HCl dampened protein dynamics compared to sucrose-alone, in particular around the termini. The presence of trehalose resulted in large fluctuations starting from 340 K. The regions 50-200 and 450-528 were particularly affected and explained the loss of native contacts. These results corroborate the experimental findings that the combination of sucrose and Arg-HCl was the most suitable for Enzyme 'A' during spray-drying.

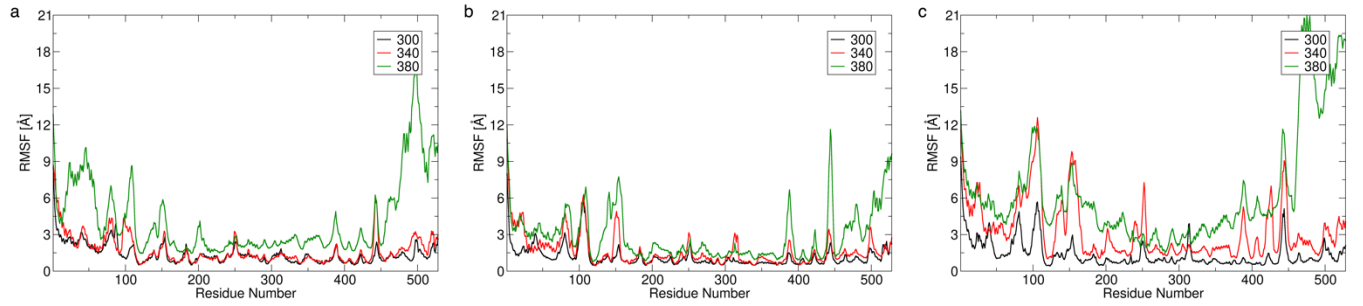

Figure 4.9: Plot of the RMSF of Enzyme 'A' with 10x concentration of (a) Sucrose, (b) Sucrose/Arg-HCl and (c) Sucrose/Trehalose.

Figure 4.10 shows the total number of excipient molecules bound to the protein and the number of protein amino acid residues coordinating these bound excipient molecules at 300 K and 380 K. While sucrose and trehalose interacted likewise via fewer hydrogen bonds (Figure 4.10 (a) and (b)), Arg-HCl interacted at a significantly greater level at both 300 K and 380 K with other excipients and the amino acid residues of the enzyme (Figure 4.10 (c) and (d)). A detailed representation of the number of sucrose, Arg-HCl and trehalose molecules in close vicinity of each amino acid residue of Enzyme 'A' at 300 K and 380 K is shown in Figure 4.10 (c) and (d), respectively. The simulations revealed that Arg-HCl interacted the most with the negatively and positively charged residues on the surface of Enzyme 'A'. The interaction of Arg-HCl was preferentially higher with glutamic acid (Glu) and aspartate (Asp) residues. Authors have shown that the inclusion of Arg and Glu increases protein solubility, stability and prevents aggregation (Golovanov *et al.*, 2004). Moreover, the polar group of Arg interacted with Asp and Glu residues via hydrogen bonds present on the surface of E3 ubiquitin-protein ligase, while the other charged groups interacted with other Arg and Glu molecules in the solution (Shukla and Trout, 2011b). Such increased interactions lead to a crowding effect on the surface of the protein, thereby, suppressing protein-protein associations. These results were consistent with the Excluded-Volume effect discussed in section 4.3.4. Furthermore, Arg-Arg and Arg-lysine interactions were fairly pronounced at both 300 K and 380 K though an increase in the number of Arg-HCl molecules in close vicinity of proline (Pro), tyrosine (Tyr) and glutamine (Gln) were observed at 380 K. This showed that Arg also interacted with polar uncharged, aromatic and aliphatic residues of the enzyme but to a lesser extent. Non-specific interactions of Arg with hydrophobic and aromatic residues has also been reported to improve solubility and reduce the development of aggregation-prone intermediate states (Li *et al.*, 2010; Shah *et al.*, 2012). Therefore, MD simulations have clearly demonstrated the unique protein-excipients interactions of Enzyme 'A' and elucidate the mechanism by which Arg-HCl improves the stability of spray-dried Enzyme 'A' in line with postulated mechanisms in literature.

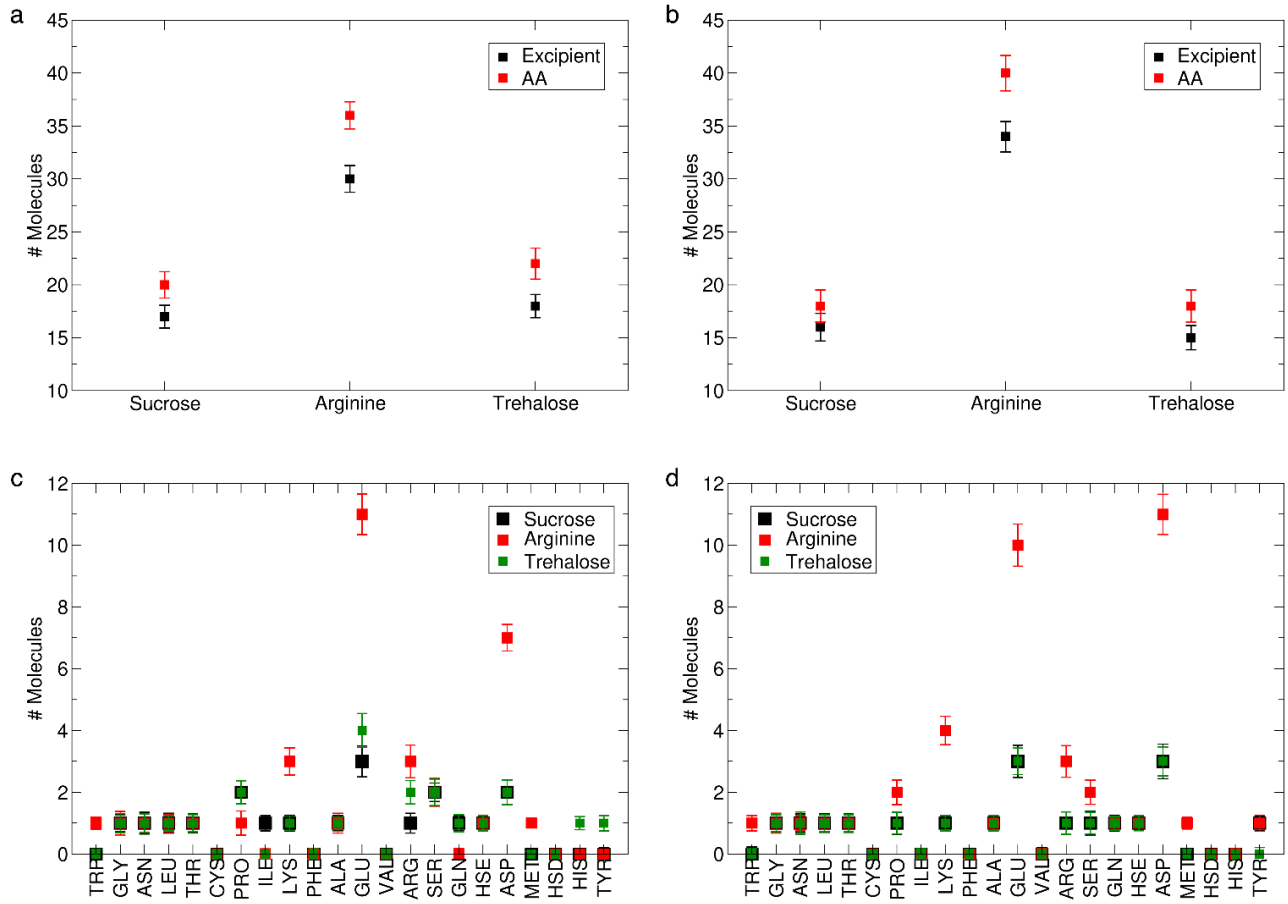

Figure 4.10: (a, b) Number of excipient molecules (sucrose, arginine, and trehalose) binding to the protein is shown in black, while the corresponding number of coordinating protein amino acids is depicted in red. (c, d) Number of sucrose (black), arginine (red) and trehalose (green) molecules bound to the protein as a function of the protein amino acid type. (a, c) Data obtained in simulations at 300 K and (b, d) for simulations at 380 K.

4.1 Conclusion

This chapter has reported some of the CQAs of Active-freeze-dried and spray-dried Enzyme 'A' in order to evaluate its processability. The Active-freeze-dried enzyme showed comparable RMC and T_g to the freeze-dried counterpart. Further optimization can be performed to reduce the total drying time as suggested by Hosokawa Micron, Netherlands. A significant reduction in the RMC and increase in the T_g of Enzyme 'A' was achieved at higher outlet temperatures via spray-drying. Consistent with the Fox equation, a good correlation was observed between the RMC and the T_g at different outlet temperatures. Moreover, the total drying time was significantly lower during spray-drying (1 L in 1.1 days at the rate of 0.9 L/day or 4 h for 150 mL) compared to a 55 h freeze-drying cycle (1 L in 2.3 days at the rate of 0.065 L/day). However, poor reconstitution properties were observed post both Active-freeze-drying and spray-drying. The product concentration, reconstitution time and turbidity of the spray-dried and Active-freeze-dried samples were significantly different compared to the freeze-dried sample. The presence of insoluble and soluble protein aggregates were observed in these samples using three different analytical techniques. While UV-Vis spectroscopy, DLS and SEC complemented each other, SEC was a reliable quantitative method for protein aggregation. The reasons for process-induced protein aggregation during Active-freeze-drying could be attributed to shear due to stirring and improper handling of the formulated bulk (other factors have also been discussed in section 1.3.2.1 of chapter 1), whereas process-induced protein aggregation during spray-drying was attributed to high temperature and dehydration rather than shear alone. Furthermore, the combined experimental and modelling dataset demonstrated the feasibility and mechanism of spray-drying as an alternative to freeze-drying for the manufacture of a parenteral biopharmaceutical.

Amongst the co-excipients studied in this chapter, it was found that the inclusion of Arg-HCl significantly reduced the reconstitution time of spray-dried Enzyme 'A' by 63 % and its turbidity by 83 % and was capable of acting as the main stabilizer, while the presence of both sucrose and trehalose did not improve the reconstitution time. In terms of protein aggregation, only the sucrose/Arg and

sucrose/Arg-HCl based formulations were able to suppress the formation of insoluble aggregates, but Arg by itself resulted in significant dimerization of Enzyme 'A' which further resulted in maximum loss of monomer and enzyme activity. However, Arg-HCl also promoted fragmentation which resulted in 5 % higher loss of monomer while its protein aggregation suppressing effect dominated its destabilizing effect. Despite the destabilizing effect, the enzyme activity of spray-dried Enzyme 'A' was enhanced by more than 50 %. A good agreement between the experimental results and molecular dynamics simulations provided further insights on protein–excipient interactions. The simulations revealed that while sucrose and trehalose interacted likewise and showed the least protection against the formation of insoluble aggregates, Arg-HCl interacted the most with the negatively and positively charged residues of Enzyme 'A'. More specifically, the preferential interaction of Arg-HCl was the greatest with Glu and Asp residues on the surface of the enzyme, though it also interacted with other polar uncharged, hydrophobic aromatic and aliphatic residues to a lesser extent. Along with the specific interactions of Arg-HCl with Enzyme 'A', these results were consistent with the Excluded-Volume effect hypothesis wherein Arg acted as a neutral crowder to suppress protein aggregation and was the probable mechanism of stabilization of Enzyme 'A' by Arg-HCl post spray-drying. Therefore, the inclusion of appropriate formulation components with respect to the spray-drying process is a key consideration for selecting an alternative drying process. Product-specific data coupled with molecular dynamics simulations can provide intricate insights required for product-process development and optimization in the biopharmaceutical industry.

Chapter 5:

Evaluation and Screening of Biopharmaceuticals using multi-angle Dynamic Light Scattering

5.1 Introduction

It is well known that proteins are sensitive molecules and susceptible to physical and chemical instability resulting in aggregation, denaturation, etc. (Arakawa *et al.*, 2001; Wang *et al.*, 2007; Declerck, 2012; Wang and Roberts, 2018). Protein aggregation is one of the critical quality attributes (CQAs) that can lead to increased immunogenicity and decreased product efficacy (Moussa *et al.*, 2016), though in some cases dimerization and oligomerization can be integral to protein activity (Marianayagam *et al.*, 2004). To ensure the safety, quality and efficacy of these products as per the International Council for Harmonisation (ICH) guidelines and current good manufacturing practices (cGMP), various analytical and characterization techniques are employed prior to batch release (Sharma *et al.*, 2021). Historically, several methods such as Bradford protein assay, Bicinchoninic acid (BCA), Lowry's assay and other dye-based methods have been used to assess protein concentration. However, the drawbacks associated with these methods include the requirement for additional reagents, sample preparation, compatibility with sample type, interference from multiple absorbing species and analysis time (Knight and Chambers, 2003; Olson and Markwell, 2007). Currently, UV-Vis spectroscopy and chromatographic methods including reversed-phase high performance liquid chromatography (RP-HPLC) and size exclusion chromatography (SEC) are the quality control (QC) release tests for concentration, purity, aggregation and degradation (FDA, 2010b). However, the chromatographic methods are destructive techniques which typically require long equilibration and analysis times, while there is a requirement for additional reagents and consumables, including buffers and columns. Although some ultra high pressure liquid chromatographic (UHPLC) methods can have shorter run times, method development and validation for each product and different formulations are time consuming. Even though SEC employs mild isocratic and elution conditions that confer minimal impact on the conformational stability, protein aggregates with weak intermolecular affinity can dissociate into monomers in the mobile phase (Fekete *et al.*, 2014; Al-Ghobashy *et al.*, 2017). Along with these techniques, several process analytical technologies (PATs) available for product and process characterization have been

summarized in literature (Sharma *et al.*, 2021). Of these, DLS (Patel *et al.*, 2018), UV-Vis spectroscopy (Ramakrishna *et al.*, 2022), Raman spectroscopy (Pieters *et al.*, 2013; Nitika *et al.*, 2021), infrared (IR) spectroscopy (Wang *et al.*, 2018) and flow imaging techniques (Zölls *et al.*, 2012) can be employed to characterize and analyse protein structure and aggregation. These techniques are non-destructive, can reduce analysis time and monitor all individual vials or bulk product with high specificity and reproducibility, thereby, speeding up the batch release process.

Multi-angle dynamic light scattering (MADLS) is an improvement in the single-angle DLS technique for the analysis of multimodal size distribution of particles with better resolution in the size range of 0.3 nm – 1 μm (Bryant and Thomas, 1995; Bryant *et al.*, 1996; Naiim *et al.*, 2015; Malvern Panalytical, 2022). This method is an indicator of protein aggregation or impurities that may be present (Weinbuch *et al.*, 2015). Moreover, parameters such as the interaction parameter (k_D) and the second virial coefficient (B_{22}) are widely used to quantify protein-protein interactions using DLS and static light scattering (SLS) (Corbett *et al.*, 2019). While there are other methods available such as DLS plate reader, CTech™ SoloVPE® and analytical ultra-centrifugation (AUC) for the determination of particle size, product concentration, and aggregation, respectively, multi-angle DLS removes angular dependence and is capable of analysing at low sample volumes (20 μL) without the need for extensive method development, additional reagents, information about the molar extinction coefficient and calibration (Markova *et al.*, 2021).

DLS is based on the principle of Brownian motion and Rayleigh scattering. Brownian motion is characterised by the collisions of different sizes of particles and their subsequent changes in directions and velocities. As a laser is passed through the solution, the incident ray is reflected and scattered in all directions. The energy of the scattered and incident light is the same with no loss of energy; this phenomenon is known as Rayleigh scattering. The autocorrelation function measures the scattered light fluctuations over time. The autocorrelation coefficient is given by Equation 5.1 and the hydrodynamic diameter is deduced from the Stokes-Einstein's equation (Equation 5.2). Readers are

referred to the cited references herein on the detailed theory of DLS (Bhattacharjee, 2016; Malvern Panalytical, 2018; Austin *et al.*, 2020).

$$G\ (\tau) = 1 + \ \beta . e^{-2D.q^2.\tau} \qquad \textbf{Equation 5.1}$$

$$D = \frac{k_B . T}{3\ \pi . \eta . d} \qquad \textbf{Equation 5.2}$$

where $G\ (\tau)$ is the autocorrelation function at lag time τ, q is the scattering vector, β is the coherence factor, D is the diffusion coefficient, d is hydrodynamic diameter, k_B is the Boltzmann constant, T is the temperature, η is the viscosity of the fluid.

In addition, this technique has been demonstrated to measure the particle concentration of nanoparticles (Austin *et al.*, 2020). The number of particles is deduced by Equation 5.3.

$$N_d = \ \rho_d . A . L \qquad \textbf{Equation 5.3}$$

Where N_d is the number of particles per mL, ρ_d is the particle concentration distribution, A is the cross-sectional area of the scattering volume and L is the length of the scattering volume.

Previously, correlations between DLS and SEC have been shown by authors (Al-Ghobashy *et al.*, 2017; Bhirde *et al.*, 2020), though quantification of protein aggregation is hard to achieve by DLS alone. While MADLS along with orthogonal techniques have been employed for the characterization of a wide range of CQAs of adeno-associated viruses (AAVs) and lipid-based nanoparticles (LNPs) (Cole *et al.*, 2021; Markova *et al.*, 2021), polystyrene nanoparticles and extracellular vesicles (Vogel *et al.*, 2021), the 3-in-1 capability of MADLS for the screening of particle size, concentration and aggregation of different protein-based biopharmaceuticals has not been explored. In this study, we

evaluated the application of MADLS in tandem with UV-Vis spectroscopy and SEC and provide a 3-in-1 approach for the screening of particle size, particle concentration and protein aggregation for three different proteins. To increase the scope of this study, a generic protein standard - Bovine Serum Albumin (BSA), a high concentration and high molecular weight monoclonal Antibody (mAb) and a therapeutic enzyme were selected.

5.2 Materials and Methods

5.2.1 Preparation of solutions

BSA (A9647, heat shock fraction, ≥ 98 %), sodium phosphate monobasic and dibasic were purchased from Merck / Sigma Aldrich, Ireland. 10 mg/mL BSA was prepared in 10 mM sodium phosphate buffer at pH 7.2 . Sucrose-based formulated drug substances, a low concentration enzyme (4 mg/mL) and a high concentration mAb (150 mg/mL), were received from Sanofi, Waterford, Ireland. All protein solutions were filtered using a 0.22 µm cellulose acetate filter.

5.2.2 Treatment of BSA

Five dilutions of BSA were prepared as per Table 5.1. 10 mg/mL of native BSA was heated at temperatures of 65 °C for 30 min and 24 h, and at 90 °C for 3 h. A mixture of the native (25 °C) and the heat-treated (65 °C for 24 h) BSA solution in the ratio of 9:1 (900:100 µL) was prepared by pipetting 100 µL of the heat-treated solution to 900 µL of the native solution to make up a final volume of 1 mL. Similarly, mixtures of the native and heat-treated solutions were prepared in the different ratios by volume shown in Table 5.1.

5.2.3 Treatment of the mAb

Ten dilutions of the mAb were prepared as per Table 5.1. Two different concentrations of the mAb at 150 mg/mL and 9.37 mg/mL were heat-treated at a temperature of 65 °C for 10 min and 30 min. A mixture of the native (25 °C) and heat-treated (65 °C) mAb solution in the ratio of 1:1 (500:500 µL) was prepared by pipetting 500 µL of the heat-treated solution to 500 µL of the native solution to make up a final volume of 1 mL. Similarly, different mixture ratios by volume were prepared as shown in Table 5.1.

5.2.4 Treatment of the Enzyme

Nine dilutions of the enzyme were prepared as per Table 5.1. 4 mg/mL of the native enzyme was heat-treated at a temperature of 65 °C for 10 min. A mixture of the native (25 °C) and heat-treated (65 °C) enzyme solution in the ratio of 99:1 (990:10 µL) was prepared by pipetting 10 µL of the heat-treated solution to 990 µL of the native solution to make up a final volume of 1 mL. Similarly, different mixture ratios by volume were prepared as shown in Table 5.1.

Table 5.1: Sample preparation and treatment methods for the analysis of the selected proteins.

Protein	Dilutions (mg/mL)	Heat Treatment	Mixture ratios by volume of the native and heat-treated solutions (µL)
BSA	10 5 1 0.5 0.1	10 mg/mL at 65 °C for 30 min, 65 °C for 24 h, 90 °C for 2 – 3 h.	900:100 (9:1) 500:500 (1:1) 990:10 (99:1)
mAb	150 75 37.5 18.75 9.37 7 4.68 2.34 1.17 0.58	150 mg/mL and 9.37 mg/mL at 65 °C for 10 – 30 min.	500:500 (1:1) 850:150 (17:1) 900:100 (9:1)
Enzyme	4 3 2.5 2 1.5 1.25 1 0.5 0.25	4 mg/mL at 65 °C for 7 – 10 min.	990:10 (99:1) 975:25 (39:1) 950:50 (19:1) 850:150 (17:3) 700:300 (7:3) 500:500 (1:1) 300:700 (3:7) 150:850 (3:17)

The different heat-treatment conditions and mixture ratios chosen for the 3 proteins were based on their propensity to aggregate and form polydispersed solutions. The native and heat-treated samples were mixed together to obtain different known ratios by volume of the monomer to aggregate in a defined range for analysis by MADLS.

5.2.5 Multi-angle Dynamic light scattering

All samples were analysed by the Zetasizer Ultra (Malvern Panalytical Ltd.) equipped with a nominally 10 mW He-Ne laser at a wavelength of 633 nm. 1 mL of sample was measured in a 1 cm x 1 cm transparent disposable cuvette. The cell position was set to 4.64 mm to allow for measurement of the sample across all detector angles. All MADLS measurements were collected at 3 different angles of detection, namely, back scatter (174.7°), side scatter (90°) and forward scatter (12.78°) with an equilibration time of 120 s. The refractive index of the protein and water used were 1.45 and 1.33, respectively. The viscosity of the low concentration dispersant for BSA and the enzyme at 25 °C was 0.8872 mPa.s. The viscosity of the high concentration mAb was corrected using the measured values by rheometry (HAAKE^{TM} MARS^{TM} Rheometer by Thermo Scientific). MADLS data was acquired and processed by the ZS XPLORER software version 1.3.2.27 (Malvern Panalytical Ltd.). The dispersant's scattering mean count rate (kcps) was measured prior to particle concentration measurements.

5.2.6 UV-Vis Spectroscopy

All protein concentrations were measured in a 1x1 cm transparent quartz cuvette by a UV-Vis spectrometer (Spectro Star nano from BMG Labtech) at 280 nm with molar extinction coefficients of 0.67 mL mg^{-1} cm^{-1} (BSA), 1.41 mL mg^{-1} cm^{-1} (mAb) and 2.41 mL mg^{-1} cm^{-1} (enzyme) using Beer Lambert's Law (Equation 2.1).

5.2.7 Size Exclusion Chromatography

The aggregation profile of enzyme samples was determined using High Performance Liquid Chromatography (HPLC 1260 by Agilent Technologies) with a UV-Vis detector at 280 nm, at a flow rate of 0.5 mL/min through a TSK gel 3000 SWXL column with an injection volume of 20 µL. The

mobile phase contained 20 mM sodium phosphate dibasic and 200 mM sodium chloride at pH 6.5. All data were analysed on the Empower Chromatography Data System (Waters^{TM}).

5.3 Results

5.3.1 Protein Size and Particle Concentration Analyses

In this section, MADLS assessment for particle size and concentration measurements was performed to define the operational range, linearity, and reproducibility for the three proteins.

5.3.1.1 BSA

The hydrodynamic diameter of monomeric BSA was measured to be 7.5 nm across a concentration range of 0.1 – 10 mg/mL with an RSD of 4.5 %. While all samples were monomodal with a polydispersity index (PDI) of < 0.2, small artifacts were observed at low concentration in the size range of 20 – 200 nm but with poor reproducibility. The PSD by intensity along with the corresponding correlograms are reported in Figure 5.1 (a, b). All particle number concentration measurements were performed as per section 5.2.5. A coefficient of determination (R^2) of 0.9999 with an average RSD of 22 % was obtained between the particle number concentration by MADLS and the concentration by UV-Vis spectroscopy (Figure 5.2 (a)). This result is well-known and consistent with literature results (Austin *et al.*, 2020). The RSD of the particle concentration increased to 30 % at low concentrations in the range of 0.1 – 0.5 mg/mL. Furthermore, it was observed that the RSD of the particle concentration at a concentration of 10 mg/mL was 23.3 %. Additionally, an R^2 of 0.9963 with an average RSD of 2.5 % obtained for the derived mean count rate (DCR) verified that linearity was maintained within a particle concentration range of 0.1 – 10 mg/mL (Figure 5.2 (b)). Therefore, the calibration curve obtained by MADLS can be used as a quick screening tool to

assess the concentration and size of native BSA in tandem with conventional techniques such as UV-Vis spectroscopy.

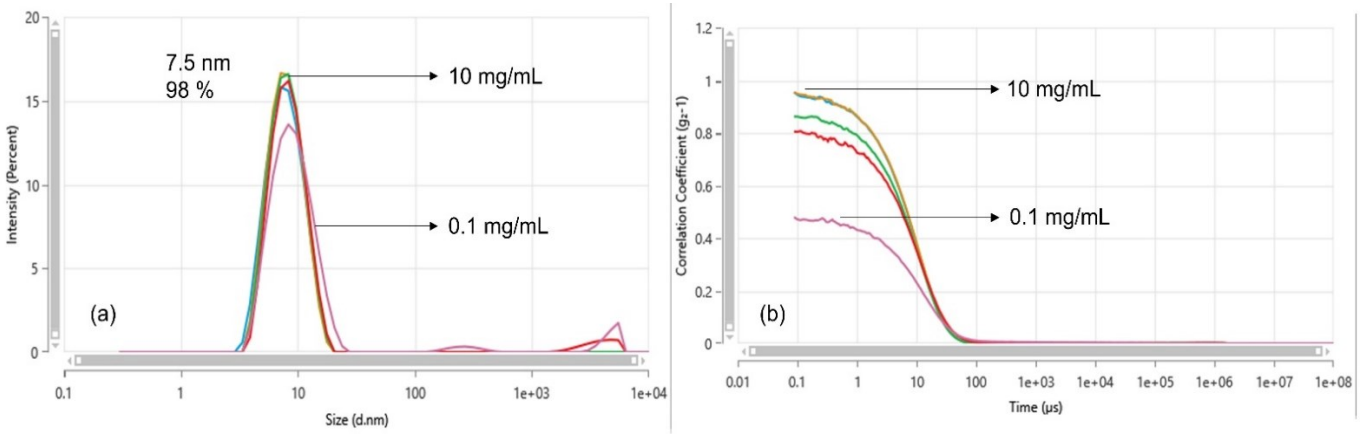

Figure 5.1: BSA (a) peak size and (b) their corresponding correlograms in the concentration range of 0.1 – 10 mg/mL.

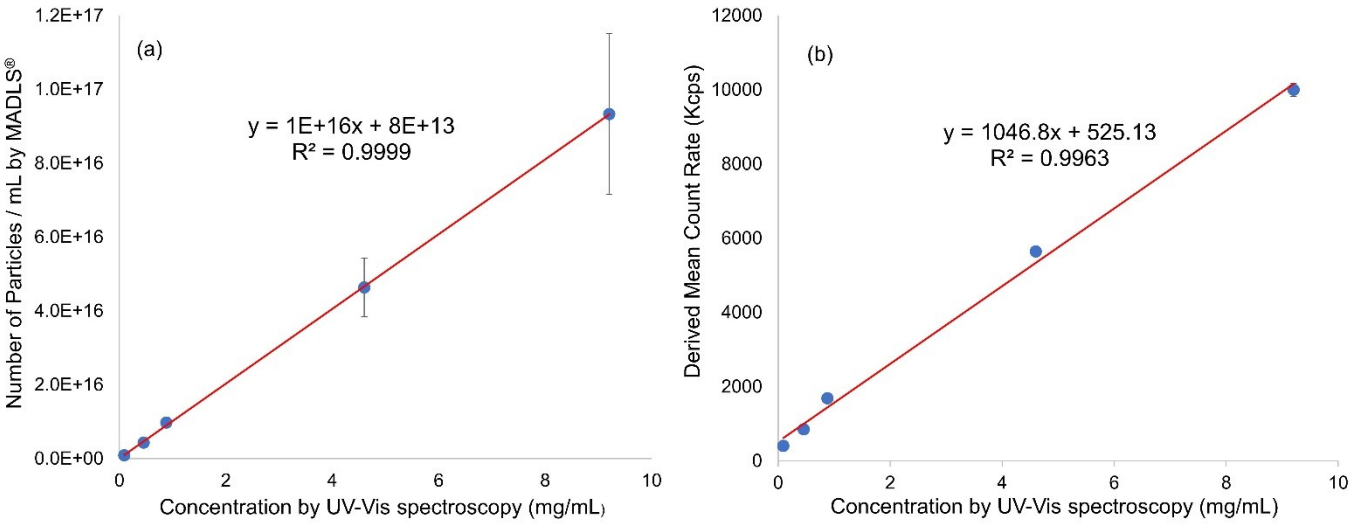

Figure 5.2: Correlation curve for (a) the particle concentration, (b) the derived mean count rate of BSA.

5.3.1.2 mAb

The particle size and concentration of the mAb was measured over a wide concentration range of 0.5 – 150 mg/mL as per Table 5.1. The hydrodynamic diameter of the mAb (9.65 nm) was observed to be consistent within a concentration range of 1.17 – 37.5 mg/mL with an RSD of 3.6 % and PDI < 0.15. The viscosity-corrected hydrodynamic diameter at high concentrations of 150 mg/mL (8.23 mPa.s) and 75 mg/mL (2.33 mPa.s) resulted in a lower particle size. The PSD by intensity along with their corresponding correlograms are shown in Figure 5.3. The operational particle concentration range between MADLS and UV-Vis spectroscopy was observed in the range of 1.17 – 9.37 mg/mL with an R^2 of 0.9963 and an average RSD of 24 % (Figure 5.4 (a)). At high mAb concentrations of ≥ 18 mg/mL, the coefficient of determination significantly dropped to an R^2 of 0.15 represented by the inset reported in Figure 5.4 (a). An RSD of up to 60 % observed in the concentration range of 1.17 – 2.34 mg/mL. Additionally, the DCR showed linearity (R^2 = 0.9887) and reproducibility (average RSD of 4.8 %) in the concentration range of 1.17 – 9.37 mg/mL which verified the linearity of particle concentration (Figure 5.4 (b)). Therefore, the calibration curve obtained in the operational concentration range can be employed in tandem with orthogonal techniques to assess any aberrations in the size and concentration of the native mAb by MADLS.

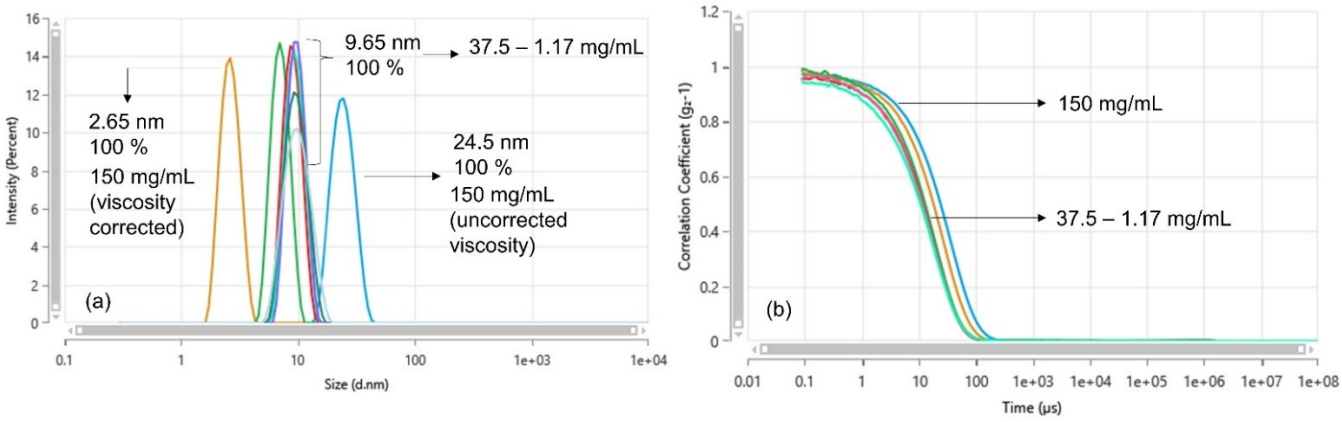

Figure 5.3: mAb (a) peak size, and (b) their corresponding correlograms in the concentration range of 1.17 – 150 mg/mL.

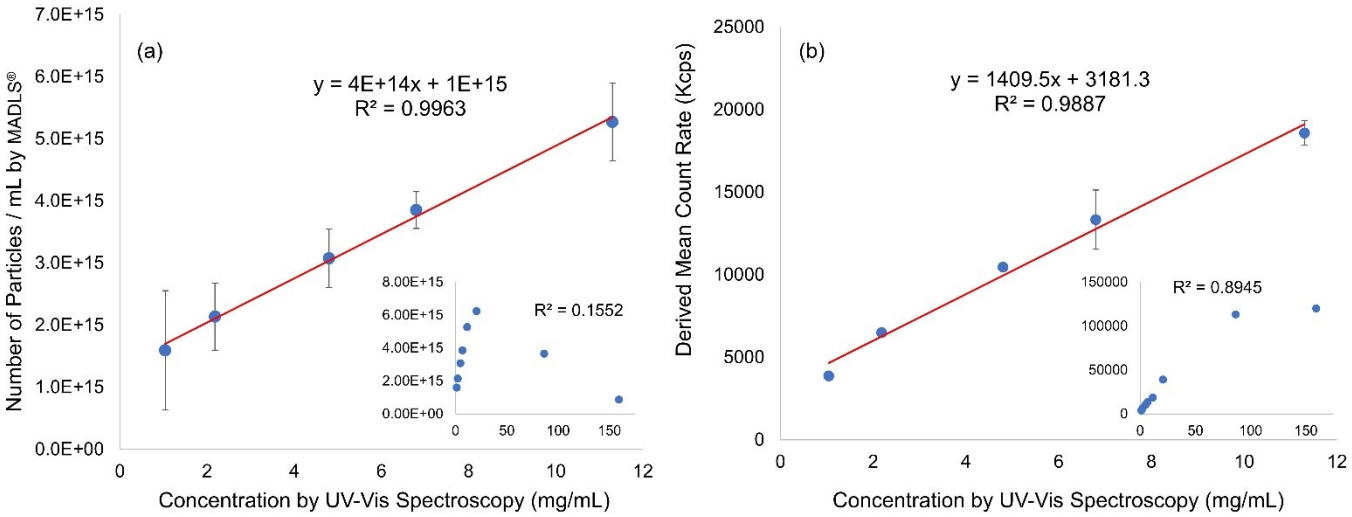

Figure 5.4: Correlation curve for (a) the particle concentration and (b) the derived mean count of the mAb.

5.3.1.3 Enzyme

The hydrodynamic diameter of the monomeric enzyme (9.4 nm) was consistent over a concentration range of 0.5 – 4 mg/mL with an RSD of 8 %. A PDI of 0.3 was obtained with a multimodal distribution by intensity. The additional peaks between 20 – 500 nm indicated the presence of high molecular weight species (HMWS) of the enzyme. The RSD of the peaks appearing at 88.9 nm and 400 nm was 10 % and 4.3 %, respectively, though the peak at 400 nm was only observed at low concentrations as evident from the delay in the gradient of the correlation coefficient at 0.5 mg/mL. The PSD by intensity along with their corresponding correlograms are shown in Figure 5.5. The operational particle concentration range between MADLS and UV-Vis spectroscopy was observed to be 0.5 – 2 mg/mL with an R^2 of 0.9514 and an average RSD of 19 % (Figure 5.6 (a)). An RSD of ≤ 20 % was observed both at lower concentrations in the range of 0.5 – 1 mg/mL and at higher concentrations of > 2.5 mg/mL above which the correlation curve began to drop with an $R^2 < 0.90$ as represented by the inset in Figure 5.6 (a). In this case, the R^2 of the particle concentration obtained was comparatively lower to that of BSA (0.9999) and the mAb (0.9963). Additionally, the DCR was linear ($R^2 = 0.9745$) and reproducible over a concentration range of 0.5 – 2 mg/mL (Figure 5.6 (b)). Therefore, the

calibration curve obtained in the operational concentration range for the polydispersed enzyme solution by MADLS can be employed as a screening method to assess any deviations in the size and concentration of the enzyme.

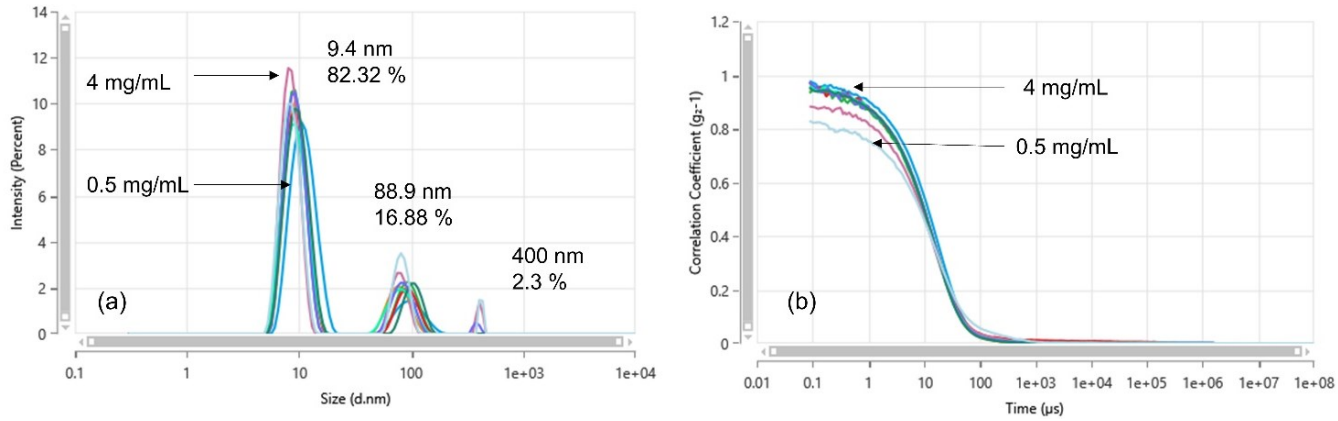

Figure 5.5: Enzyme (a) peak size and (b) their corresponding correlograms in the concentration range of 0.5 – 4 mg/mL.

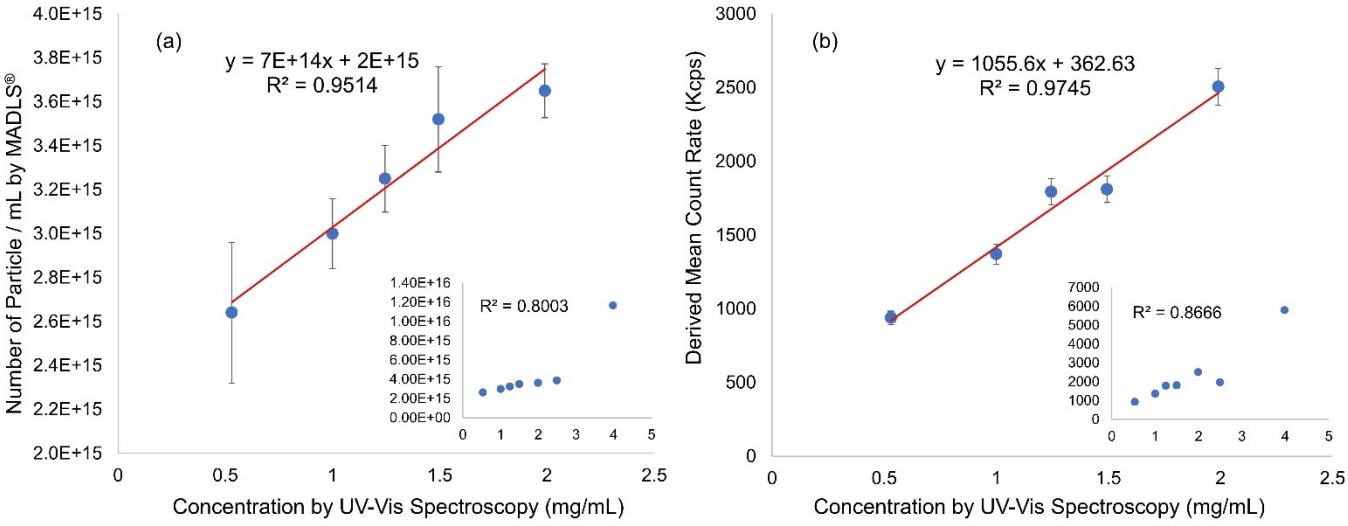

Figure 5.6: Correlation curve for (a) the particle concentration and (b) the derived mean count rate of the enzyme.

5.3.2 Protein Aggregation Analyses

In this section, MADLS was employed to measure protein aggregation of the three proteins.

5.3.2.1 BSA

As per section 5.3.1.1, the hydrodynamic diameter of monomeric BSA was measured to be 7.5 nm (Figure 5.7 (a)). Upon heat-treating the protein at 65 °C and 90 °C, a shift in the particle size was observed at 17 nm and 20 nm, respectively, though the sample remained monomodal (PDI < 0.2) (Figure 5.7 (b) and (c)). The prepared mixtures of the native and the heat-treated (65 °C for 24 h) protein in the ratio of 1:1 (500:500 µL) and 9:1 (900:100 µL) showed the presence of two peaks at 5 – 8 nm and 16 – 13 nm (Figure 5.7 (d) and (e)), respectively. The presence of one additional peak in the sample mixtures (Figure 5.7 (d) and (e)) indicated the presence of high molecular weight species (HMWS) of BSA as shown by SEC in literature [30,31], but these aggregation peaks were not observed in all sample mixtures. On increasing the fraction of the native protein in the mixture to 99:1 (990:10 µL), a monodisperse sample (PDI ≤ 0.2) was obtained with a single peak at 7 nm (Figure 5.7 (f)). This showed that MADLS analyses were unable to detect and resolve dimers and/or HMWS from the native protein at a low concentration. Therefore, in this case MADLS would not be the most appropriate technique for the analyses of aggregation of BSA but can be employed as a rapid screening method to detect any deviation in the PSD of the native protein.

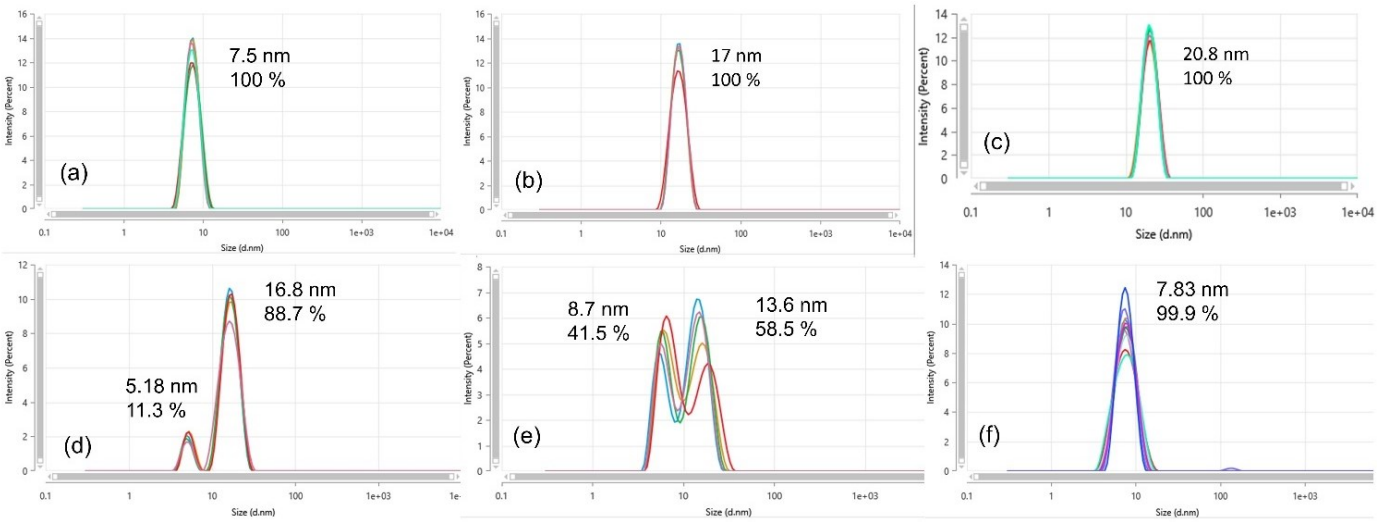

Figure 5.7: PSD by intensity of BSA: (a) native at 25 °C, (b) at 65 °C for 24 h, (c) at 90 °C for 3 h, (d) a mixture of the native and heat-treated (65 °C for 24 h) sample in the ratio of 500:500 µL, (e) a mixture of the native and heat-treated (65 °C for 24 h) sample in the ratio of 900:100 µL, (f) a mixture of the native and heat-treated (65 °C for 24 h) sample in the ratio of 990:10 µL.

5.3.2.2 mAb

In the operational range, as described in section 5.3.1.2, the hydrodynamic diameter of the mAb was measured to be 9.65 (Figure 5.8 (a)). Upon heat-treating the mAb at 65 °C for 10 – 30 min, a monomodal distribution was obtained at 9.37 mg/mL (Figure 5.8 (b) and (c)), whereas a multimodal distribution by intensity was observed at 150 mg/mL but with poor reproducibility (Figure 5.8 (d) and (e)) (PDI > 0.2). Moreover, a monomodal distribution was obtained on analysing mixtures of the native and heat-treated samples at different ratios of 1:1 (500:500 µL) and 17:1 (850:150 µL) (Figure 5.8 (f) and (g)). This suggests that MADLS was unable to resolve the dimers and/or HMWS and would not be suitable for the analyses of aggregation of the mAb but can be employed as a rapid screening tool to detect any change in the native mAb PSD.

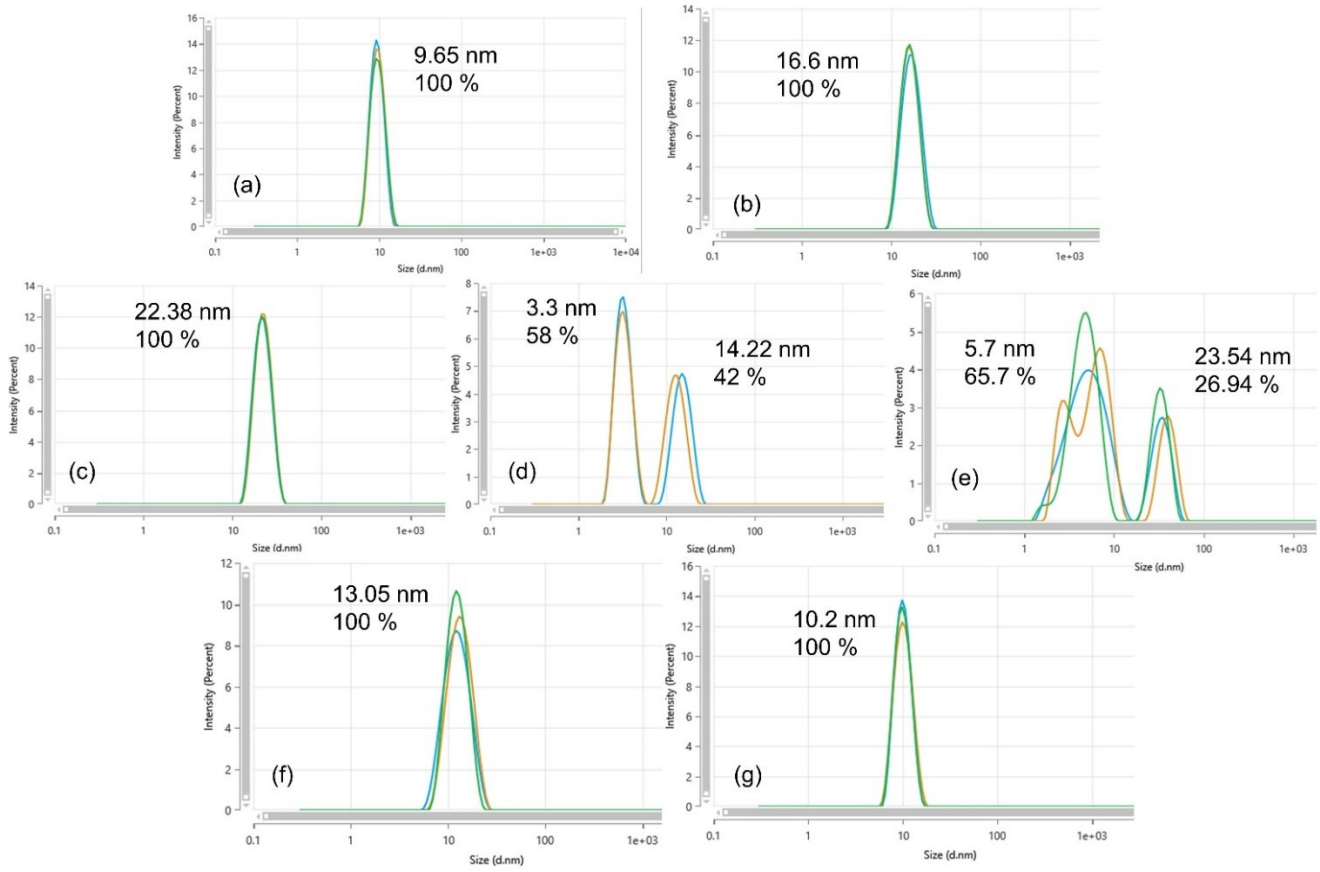

Figure 5.8: PSD by intensity of the (a) native mAb at 9.37 mg/mL, (b) 65 °C for 10 min at 9.37 mg/mL, (c) 65 °C for 30 min at 9.37 mg/mL, (d) 65 °C for 10 min at 150 mg/mL, (e) 65 °C for 30 min at 150 mg/mL. Mixtures of the native and heat-treated mAb in the ratios of (f) 500:500 µL and (g) 850:150 µL at 9.37 mg/mL.

5.3.2.3 Enzyme

The hydrodynamic diameter of the monomeric enzyme at 4 mg/mL was observed to be 10.9 nm (RSD = 2.5 %) along with a HMWS at 90 nm (RSD = 8%), as shown in Figure 5.9 (a). The HMWS peak at 90 nm, confirmed by SEC analyses, was attributed to 'HMWS1' of the enzyme. Upon heat-treating the enzyme at 65 °C for 10 min (Figure 5.9 (b)), the monomer showed a shift in the particle size (7.9 nm) with a lower intensity distribution of 11.47 %, while the particle size of the HMWS1 was significantly lowered to 26.7 nm with an increase in the intensity distribution (88.15 %) and an

additional minor peak at ~ 400 nm corresponded to ‘HMWS2’ of the enzyme. An average RSD of < 20 % was achieved for the distribution by intensity of the heat-treated sample.

While the monomer, ‘HMWS1’ and ‘HMWS2’ of the enzyme were well resolved by MADLS, as the size ratio of each species was greater than a factor of 3, resolution of the dimer was not observed. Nonetheless, to further evaluate the resolution and reproducibility of MADLS measurements of the aggregated samples, a mixture of the native and the heat-treated (65 °C for 10 min) solution in the ratio of 99:1 (990:10 µL) (Figure 5.9 (c)), showed the presence of 3 distinct peaks at 11 nm, 91.62 nm and 407 nm which were identified as the monomer, ‘HMWS1’ and ‘HMWS2’, respectively, by SEC. In this case, an average RSD of < 10 % was achieved for the PSD by intensity. Similarly, upon decreasing the fraction of the monomer in the mixtures (Figure 5.9 (d - h)), a relative decrease and increase in the intensity distribution of the monomer and ‘HMWS1’, respectively, was observed. The relative changes in the intensity distribution for the different ratios of the monomer and ‘HMWS1’ were confirmed by the corresponding changes in the peak areas by SEC as shown in Figure 5.10.

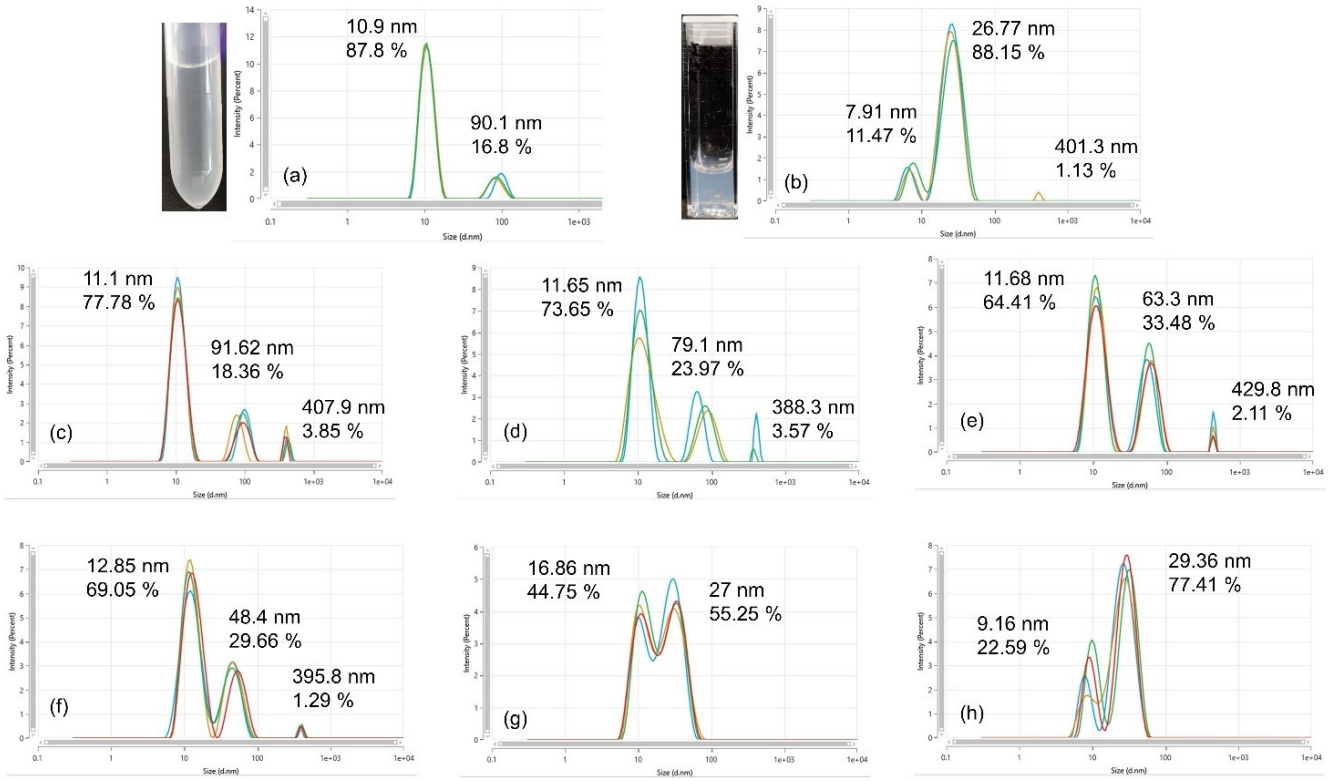

Figure 5.9: PSD by intensity of the (a) native enzyme, (b) 65 °C for 10 min. Mixtures of the native and heat-treated enzyme (65 °C for 10 min) in the ratios of (c) 990:10 µL, (d) 975:25 µL, (e) 950:50 µL, (f) 700:300 µL, (g) 500:500 µL, (h) 300:700 µL.

It is important to note that while the resolution of dimers was not observed by MADLS, the concentration of dimers remained < 6 % in all samples and did not change significantly as evident from the SEC profile in Figure 5.10. Moreover, the presence of 'HMWS2' of the enzyme could not be detected in the different mixtures by SEC as the concentration of 'HMWS2' was below the limit of detection while MADLS was able to detect trace amounts of 'HMWS2' with greater sensitivity due to light scattering.

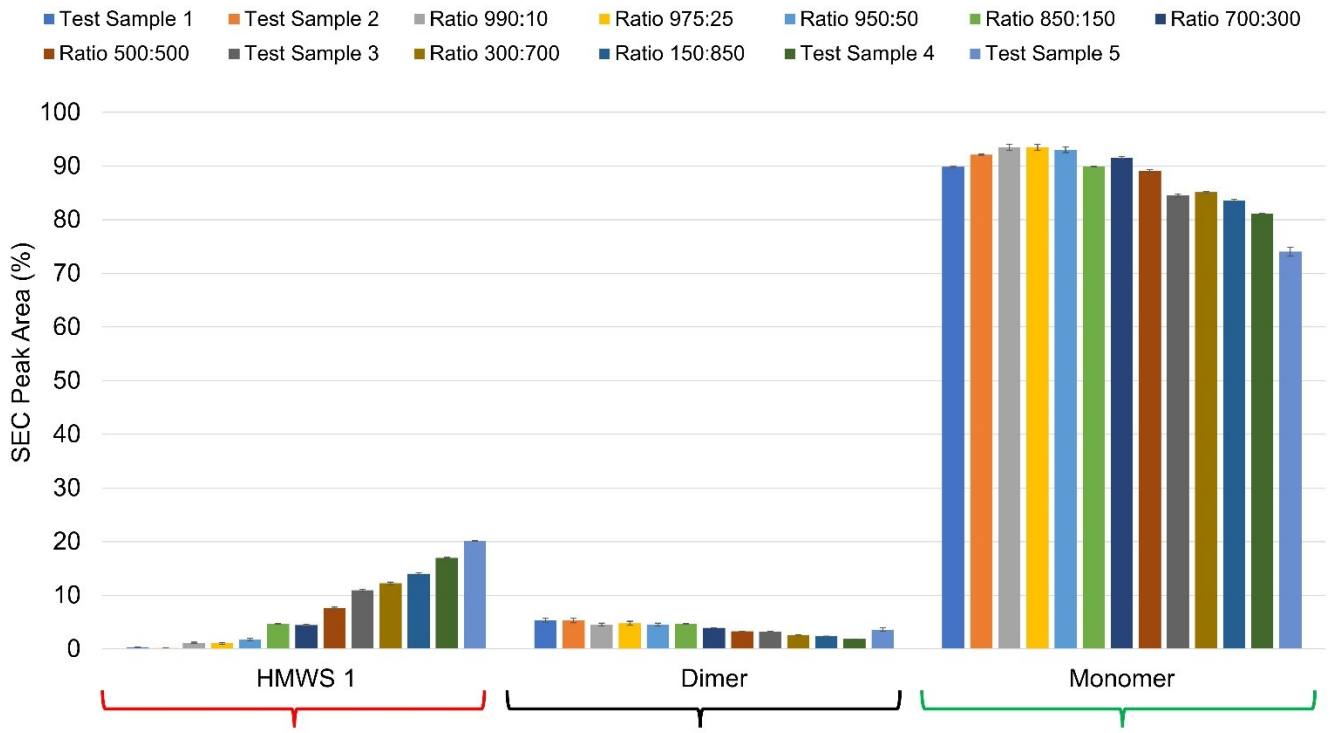

Figure 5.10: Aggregation profiles of the different mixture ratios by volume of the monomer and HMWS1 of the enzyme.

Interestingly, a plot between the ratios of the peak areas of the 'HMWS1' and the monomer by SEC versus the ratios of the light scattering intensities of the 'HMWS1' and the monomer by MADLS of the prepared mixtures, including 5 unknown test samples, exhibited an excellent quadratic correlation with an R^2 of 0.9938 (Figure 5.11). The levels of 'HMWS1' in the enzyme samples are shown in Table 5.2. The level of aggregation increased in the order from Zone A – D (Figure 5.11). The percentage of 'HMWS1' in test samples 1 and 2 was in the range of 0.1 – 2 %, whereas that in test sample 3 was between 10 – 14 % and in test sample 4 and 5 was in the range of 15 – 20 %.

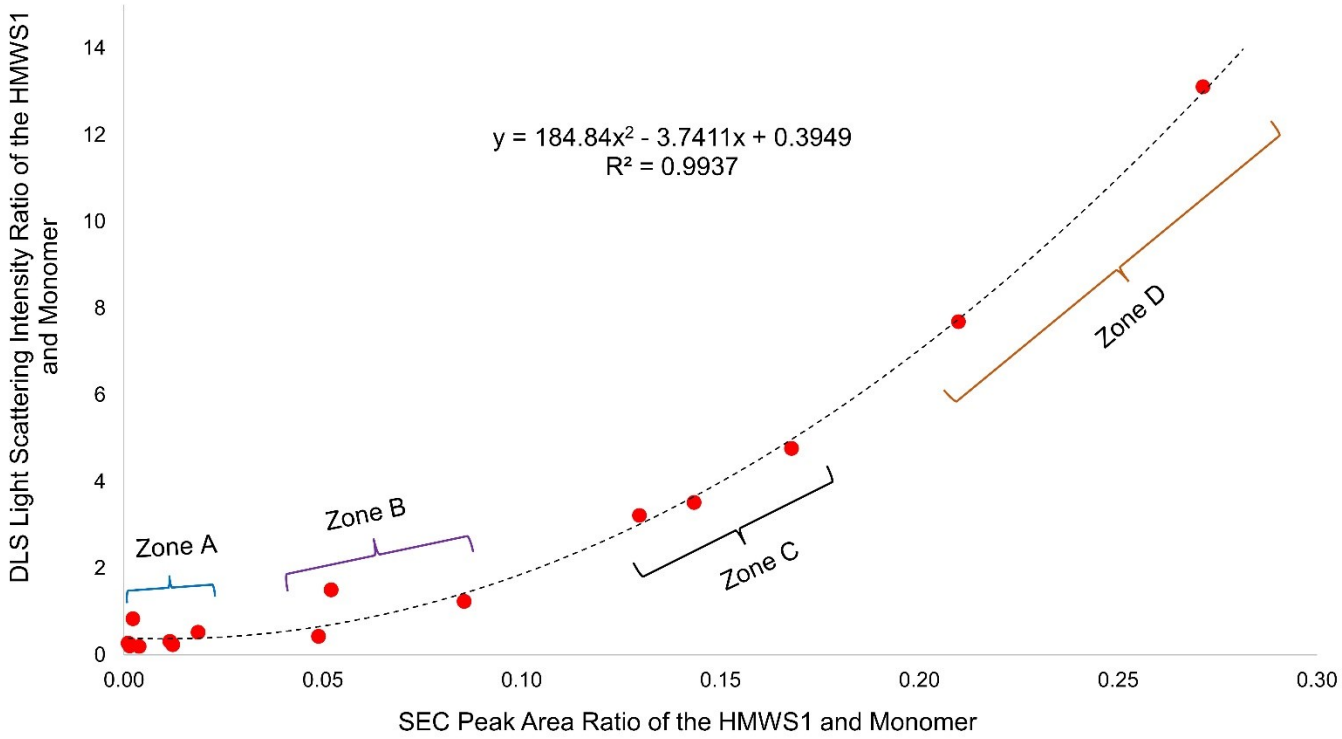

Figure 5.11: A quadratic correlation between the peak area ratios of the HMWS1 and monomer by SEC and the light scattering intensity ratios of the HMWS1 and monomer by MADLS of the enzyme.

Table 5.2: Obtained levels of HMWS1 in the enzyme samples.

Zone	Sample	SEC ratio (HMWS1:Monomer)	DLS ratio (HMWS1:Monomer)	Level of HMWS1 (%)
A (Blue)	990:10	0.0123	0.2341	0.1 – 2
	975:25	0.0116	0.3101	
	950:50	0.0187	0.5202	
	Test sample 1	0.0038	0.1922	
	Test sample 2	0.0023	0.8305	
B (Purple)	850:150	0.0521	1.5000	3 – 8
	700:300	0.0489	0.4301	
	500:500	0.0855	1.2344	
C (Black)	300:700	0.1433	3.5180	10 – 14
	150:850	0.1679	4.7630	
	Test sample 3	0.1296	3.2161	
D (Orange)	Test sample 4	0.2098	7.6852	15 – 20
	Test sample 5	0.2714	13.1030	

5.4 Discussion

5.4.1 Protein Size

The observed hydrodynamic diameter of BSA was in agreement with the reported values (Jachimska *et al.*, 2008; Anton Paar, 2018), whereas the hydrodynamic diameters of the mAb and enzyme were consistent within the operational concentration range. In the case of the mAb, lowering of particle size at high concentrations of 150 mg/mL and 75 mg/mL occurred as a result of multiple scattering. At high concentration, multiple scattering results in a decrease in the particle size (Malvern Panalytical, 2014; Austin *et al.*, 2020; Ragheb and Nobbmann, 2020). The phenomenon of multiple scattering occurs wherein the probability of re-scattering of the scattered photon increases, thereby, decreasing the accuracy of particle size measurements. Moreover, an increase in the decay time in the correlation coefficient at higher concentrations explained the diffusion behaviour of the mAb particles at higher viscosities (Figure 5.3 (b)). In the case of the enzyme, while the accuracy of size measurements of multimodal distributions decreases due to multiple scattering as well as molecular crowding and restricted diffusion, an RSD of ≤ 10 % was achieved for the size measurements of all the multimodal peaks of the enzyme showing reduced peak widths, improved resolution and reproducibility compared to single-angle DLS measurements as shown in Figure A5.1 of the Appendix.

5.4.2 Particle Number Concentration

In terms of the particle concentration measurements, an R^2 of > 0.95 achieved between UV-Vis spectroscopy and MADLS defined the operating particle concentration range for all the proteins which was verified by the DCR. The increase in the uncertainty of particle concentration measurements for all the proteins at low and high concentrations is attributed to particle number fluctuations and multiple scattering, respectively, which was also reported for gold, silica and polystyrene nanoparticles (Austin *et al.*, 2020). This represents the lower and upper limit of the

operating particle concentration range of the nanoparticle (Bhattacharjee, 2016; Austin *et al.*, 2020). Particle number fluctuations arises due to an insufficient number of particles present in the scattering volume wherein the amplitude distribution of the scattered particles does not follow a Gaussian distribution (Hopcraft *et al.*, 2005). Moreover, a change in the dynamic equilibrium between the buffer molecules adsorbed at the surface of the protein and those dispersed in the solution may contribute to the increase in the RSD of the particle number measurements (Austin *et al.*, 2020). Authors have reported an RSD of 80 % in the particle concentration measurements of agglomerated SiO_2 nanoparticles at high concentration and an RSD of up to 30 % at low concentration (Austin *et al.*, 2020) which is consistent with the results shown in section 5.3.1. As evident from the case of the enzyme, it is important to note that many protein solutions are not completely monodisperse as they may contain low concentrations of dimers/oligomers in dynamic equilibrium with monomers, which also play a role in increasing the uncertainty in measurements. Additionally, other factors such as restricted diffusion, electrostatic repulsion and reversible self-associations must also be considered to account for the error in particle size and concentration measurements (Malvern Panalytical, 2014).

Overall, the concentration calibration curve can be employed for the rapid screening of any deviations in both the product concentration and particle size in-lieu of conventional techniques such as UV-Vis spectroscopy.

5.4.3 Protein Aggregation

The ability of MADLS to detect and resolve protein aggregates in heat-treated samples of BSA, the mAb and the enzyme was selective and dependent on the size ratio, nature and the relative concentrations of the monomer and the aggregates in the solution. In the case of BSA, a significant shift in the peak size from 7.5 nm to 20.8 nm of the heat-treated samples (Figure 5.7 (b - c)) indicated the presence of dimers and/or HMWS, but a resolution of the monomer, dimer, trimer was not observed distinctly as achieved by SEC (Sahin *et al.*, 2016). A bimodal distribution of peaks was only

observed in the mixtures with HMWS > 10 % by volume (Figure 5.7 (d - e)). Similarly, in the case of the mAb, a shift in the monomodal peak from 9.65 nm to 22.38 nm (Figure 5.8 (a - c)) indicated the presence of HMWS, but bimodal distributions were observed in only 2 heat-treated samples at 150 mg/mL with poor resolution, reproducibility and accuracy (Figure 5.8 (d) and (e)). The skewed particle sizes of the bimodal distributions of BSA and the mAb are attributed to multiple scattering by the presence of multiple species. Also, the absence of the monomer peak in both heat-treated BSA and mAb suggest that the monomer peak was masked by the signals from the HMWS peak. Moreover, the absence of HMWS peaks in the mixtures could suggest the dissociation of HMWS into monomers at low concentration (Al-Ghobashy *et al.*, 2017). Nonetheless, SEC is required to determine the complete aggregation profile of the two proteins. Therefore, the poor resolution and reproducibility of the multimodal measurements for these cases show that MADLS would not be the most appropriate method for the analyses of aggregation of BSA and the mAb but can be employed as a rapid screening tool to detect any changes in the native PSD of these proteins.

In the case of the heat-treated enzyme, improved resolution and reproducibility was achieved between the monomer and the aggregates for the samples containing aggregates < 50 % by volume (Figure 5.9 (a – f)). At higher aggregate concentration, the light scattering signals from the aggregates dominated the monomer peak and so, MADLS struggled to completely resolve the conjoining peaks (Figure 5.9 (g – h)). Conversely, a resolution between 20 nm and < 200 nm particles could not be achieved by single-angle DLS (Panchal *et al.*, 2014). A reduction in particle size of the 10.9 nm peak to 7.9 nm (referred to as the monomer peak) may be due to the conversion of dimers to higher order aggregates. A reduction in particle was a result of multiple scattering due to increased viscosity and polydispersity of the aggregated sample, thereby, decreasing the accuracy of particle size measurements. DLS is fundamentally not a high-resolution technique, and as such cannot distinguish between monomers and dimers. In some cases, the peak attributed to monomers also comprises of dimers, resulting in the peak mean being skewed towards a larger particle size (Austin *et al.*, 2020). These dimers may subsequently form higher order aggregates, removing them from this population

mode in the distribution. Upon the formation of these aggregates, the peak corresponding to monomers moved back towards smaller particle size, resulting in both a decrease in particle size for this mode, and a reduction in light scattering intensity. Additionally, localised changes in viscosity can be a result of crosslinking or mesh-like network formation of HMWS (von Bülow *et al.*, 2019). Localised changes in viscosity can result in phenomena such as hindered or restricted diffusion. These effects can result in particles being measured as larger than they would be expected to be due to reduced Brownian motion as a consequence of being in localised high viscosity areas. It is important to note that MADLS could not resolve monomer-dimer species of the selected protein nanoparticles in this study, and therefore, unless an alternative analysis procedure is used, the technique is unlikely to be useful in resolving monomer-dimer species in pharmaceutical-grade formulations, which typically have dimer levels ≤ 8 %.

The presence of a quadratic correlation between MADLS and SEC for the enzyme indicated that MADLS dominated the data as the intensity of scattered light is proportional to the sixth power of the particle diameter and inversely proportional to the fourth power of the wavelength (Zhu *et al.*, 2014). As the concentration of large aggregates increases, more light is scattered by DLS compared to the light absorbed by the aggregates during SEC. Such a correlation was not observed for BSA and the mAb due to low resolution of the size ratio and concentration of the monomer and HMWS by MADLS.

5.4.4 Practical relevance

Typically, SEC is a batch release method and DLS is a characterization method in the early stage of development, scale-up and technology transfer of drug products. Development and scale-up activities for biopharmaceutical drug products require several characterization tests with limited product material and time constraints. While DLS by itself may not provide all the information as obtained by SEC and other analytical tests, it is employed as a batch to batch comparability method in tandem

with other tests. Through this study, we suggest that this approach can be employed for rapid screening of the particle size, concentration and the estimation of the level of aggregation in biopharmaceutical formulations provided the aggregates of the biologic are stable, well resolved, and reproducible during MADLS measurements. Moreover, the screening of these CQAs by MADLS during early-phase biopharmaceutical development can help in selecting samples for further analysis by SEC and other QC tests, thereby, reducing the number of samples and experiments required for testing and analysis.

5.5 Conclusion

This study was able to assess the 3-in-1 capability of MADLS technology for the measurement of particle size, particle concentration, and aggregation for 3 different protein modalities in tandem with UV-Vis spectroscopy and SEC. It was observed that the accuracy, resolution, and reproducibility of MADLS measurements are dependent on the nature of the protein nanoparticle. Despite the different levels of polydispersity in the 3 protein solutions, a good calibration curve with an R^2 of > 0.95 was obtained between the particle number concentration by MADLS and protein concentration by UV-Vis spectroscopy. In terms of the accuracy and precision of the measurements, key factors such as multiple scattering and particle number fluctuations are responsible for defining the operating particle concentration range. Additionally, restricted diffusion, electrostatic repulsion, and reversible self-associations can also play a role in increasing the uncertainty in MADLS measurements. In terms of evaluating protein aggregation, MADLS provided better resolution and reproducibility for the multimodal distribution by the intensity of the enzyme. The observed quadratic correlation (R^2 = 0.9938) between MADLS and SEC for the enzyme and the approach provided in this study to assess the 3 CQAs. Overall, MADLS is a promising analytical technique that can be employed as an early-stage screening method for the analysis of different formulations and products prior to other analytical tests. While it may not qualify as a standalone QC release test, it can provide analysts and regulators with additional orthogonal data to complement traditional methods.

Chapter 6:

Conclusion and Future Work

6.1 Conclusion

This thesis has summarized and demonstrated some of the potential process and analytical technologies to produce and characterize dry powder-based biopharmaceuticals as a novel alternative to conventional freeze-drying technology. To combat the drawbacks associated with lyophilization, the effects of freeze-drying and spray-drying on the CQAs of lysozyme and the effects of Active-freeze-drying and spray-drying on the CQAs of Enzyme 'A' were evaluated using several orthogonal techniques. Through both drying processes, comparable RMC was achieved as per the product's specifications.

In terms of the processing time, spray-drying showed a significant reduction in the total drying time. The total drying time for Enzyme 'A' was significantly lower during spray-drying (1 L in 1.1 days at the rate of 0.9 L/day or 4 h for 150 mL) compared to a 55 h freeze-drying cycle (1 L in 2.3 days at the rate of 0.065 L/day). Similar drying times were recorded for lysozyme. These processing times only represent laboratory-scale equipment studies and cannot be compared to commercial-scale manufacturing equipments, however, they do demonstrate considerable potential. While the total Active-freeze-drying time for Enzyme 'A' was 70 h (2.9 days), the length of the drying cycle can be optimized further by installing a condenser, by using a tube of a larger diameter connecting to the drying vessel and the vacuum pump and by increasing the surface area of the filter to improve the removal of water vapour.

As shown in Chapters 2 and 3, lysozyme was observed to be robust post freeze-drying and spray-drying. In the presence of trehalose and sucrose, the enzyme activity of lysozyme was enhanced post drying, while the enzyme activity was preserved in the presence of mannitol. These results were consistent with the molecular dynamics simulations for lysozyme showing that the enzyme was stable by itself and in the presence of mannitol while the increased efficacy of the dried lysozyme formulations containing trehalose and sucrose was attributed to a conformational change (without unfolding) allowing more access to its active sites. However, the limitations of DLS and SEC in

elucidating protein aggregation of lysozyme would require alternative analytics and method optimization. Moreover, the correlation observed between FMS and KF for the determination of vial headspace moisture content and cake moisture, respectively, in lysozyme formulations can be exploited to develop moisture maps and may also be employed as a potential PAT for freeze-drying.

Furthermore, chapter 4 assessed the feasibility of drying a therapeutic enzyme using two alternative drying technologies. The reconstitution properties of Active-freeze-dried and spray-dried Enzyme 'A' were poor. It was found that dehydration via spray-drying significantly impacted the CQAs of the enzyme rather than shear alone. The inclusion of Arg-HCl significantly improved the reconstitution characteristics of spray-dried Enzyme 'A', with a 63 % reduction in the reconstitution time and an 83 % decrease in the optical density, even though the loss of monomer was 5 % higher showing that arginine played a duel role of stabilizing as well as destabilizing the enzyme. However, the destabilizing effect was minuscule as compared to its stabilizing effect. These results were supported by molecular dynamics simulations showing that Enzyme 'A' was better stabilized in the presence of Arg-HCl in terms of RMSD, RMSF, native contacts and secondary structure prediction.

Finally, chapter 5 demonstrated the 3-in-1 capabilities of multi-angle DLS for the evaluation and screening of biopharmaceutical CQAs, namely, particle size, product concentration and protein aggregation. Improved resolution and precision was achieved by MADLS compared to single-angle DLS. Through this study, a good calibration (R^2 of > 0.95) was achieved for the particle number concentration measurements of BSA, a high concentration mAb and a low concentration enzyme, and an excellent correlation (R^2 = 0.9938) was achieved between MADLS and SEC for the quantitative estimation of protein aggregation in the enzyme. While this chapter discuss the advantages as well as limitations of MADLS, the approach provided in this chapter can be employed for early-stage biopharmaceutical formulation development and screening of samples prior to further analysis by other orthogonal tests.

Overall, batch freeze-drying is a well-established drying technology for the majority of biopharmaceutical products. Many of the alternative drying technologies have increasingly shown promising prospects for manufacturing solid biopharmaceuticals without compromising on the safety, quality and efficacy of biopharmaceutical products. These potential drying technologies are significant to the biopharmaceutical industry as they will not only reduce time, energy consumption and associated costs with the manufacturing of life-saving drugs, but also help in mitigating any risks with the supply of drugs during pandemics such as Covid-19. While some of the alternative methods offer continuous manufacturing at reduced operational costs, the impact of CPPs such as temperature, shear, etc. on product CQAs is the fundamental requirement for the selection of drying technologies. Although drying technologies, namely, Spin-freeze-drying, Spray-freeze-drying, Spray-drying, PRINT® and Microglassification™ have shown positive results on the stability of some proteins and inhaled biopharmaceuticals, their impact on a wide range of parenteral biopharmaceuticals is yet to be studied. Through product-specific research, sufficient stability data is required to move from conventional freeze-drying to continuous manufacturing. Along with CPPs, the choice of formulation components with respect to the drying process and the product is crucial to ensure product stability. Moreover, the molecular mechanism of interaction of biopharmaceuticals with specific excipients in the solid-state is poorly understood. Some of the advanced characterization techniques and PATs in tandem can offer faster and in-depth analysis in understanding and evaluating the product-process relationship. While most of the alternative drying methods can offer significant benefits with the usage of PATs, their feasibility at commercial scale requires further exploration. In terms of scale-up, packaging and validation aspects, some of the alternative drying processes offer a greater advantage in reducing the complexities associated with the validation of multiple fill finish unit operations. The commercial scale operation for some alternative drying technologies has been demonstrated with proven potential in the biopharmaceutical industry though some scale-up challenges are yet to be addressed.

This thesis has demonstrated some promising technologies with vast potential for the future of the biopharmaceutical industry while also contributing experimental insights on the stability and behaviour of different generic and therapeutic proteins. The research presented in this body of work opens avenues for further research and innovation to address some of the gaps discussed in future work.

6.2 Future Work

With respect to the body of work shown in this thesis, recommendations for future work are enlisted in the following areas:

1. To optimize the SEC method coupled with a light scattering detector or a mass spectrometer along with the evaluation of alterative analytics such as AUC to address the limitations of DLS and SEC (with a UV-Vis detector) for the analysis of aggregation in lysozyme. Moreover, increasing the scope of advanced analytical techniques such as ssHDX-MS, ssPL-MS, NMR, neutron scattering and Raman Spectroscopy to study protein-matrix interactions, aggregation and structural conformations including secondary and tertiary structure of proteins.

2. To assess the polymorphs of mannitol formed post drying using XRD to understand the stabilizing and/or destabilizing of behaviour of mannitol crystallization on lysozyme along with the inclusion of other solid-state analytical techniques such as dynamic vapor sorption (DVS), scanning electron microscopy (SEM), laser diffraction, ssNMR etc. that can provide further information on dry particle characteristics that impact the reconstitution time and protein-matrix interactions of parenteral products.

3. Optimization of the formulation of Enzyme 'A' with Arg-HCl along with the incorporation of suitable surfactants to achieve best results post spray-drying. Moreover, a design of experiments (DoE) is a useful statistical tool to evaluate process parameters significantly contributing to protein aggregation and denaturation during the atomization and drying phase. Additionally, to determine the T_g of alternative formulations of Enzyme 'A' to assess its long-term stability in the dried state.

4. Investigating the CPPs impacting the CQAs of Active-freeze-dried Enzyme ‘A’ along with the optimization of the Active-freeze-drying cycle in terms of the total drying time to produce bulk dry powder.

5. Investigating the feasibility of other drying technologies including Spray-freeze-drying, Electrostatic Spray-drying, Spin-freeze-drying, PRINT® Technology, etc. for manufacturing biopharmaceuticals.

6. Studying the stability of other biologics such as monoclonal antibodies, nanobodies, fusion proteins, hormones, gene therapy products, etc. using the above mentioned technologies along with the incorporation of appropriate formulation excipients with respect to the product and process.

7. Lastly, developing coarse-grained models using molecular dynamics simulations to understand aggregation pathways and mechanisms of protein-excipient and protein-protein interactions of lysozyme, Enzyme ‘A’ and other biologics.

References

Abdel-Mageed, H. M., Fouad, S. A., Teaima, M. H., Abdel-Aty, A. M., Fahmy, A. S., Shaker, D. S. and Mohamed, S. A. (2019) 'Optimization of nano spray drying parameters for production of α-amylase nanopowder for biotheraputic applications using factorial design', *Drying Technology*. Taylor and Francis Inc., 37(16), pp. 2152–2160. doi: 10.1080/07373937.2019.1565576.

Abdul-Fattah, A. M., Lechuga-Ballesteros, D., Kalonia, D. S. and Pikal, M. J. (2008) 'The impact of drying method and formulation on the physical properties and stability of methionyl human growth hormone in the amorphous solid state', *Journal of Pharmaceutical Sciences*. John Wiley and Sons Inc., 97(1), pp. 163–184. doi: 10.1002/jps.21085.

Abdul-Fattah, A. M., Oeschger, R., Roehl, H., Bauer Dauphin, I., Worgull, M., Kallmeyer, G. and Mahler, H. C. (2013) 'Investigating factors leading to fogging of glass vials in lyophilized drug products', in *European Journal of Pharmaceutics and Biopharmaceutics*. Elsevier, pp. 314–326. doi: 10.1016/j.ejpb.2013.06.007.

Abdul-Fattah, A. M., Truong-Le, V., Yee, L., Nguyen, L., Kalonia, D. S., Cicerone, M. T. and Pikal, M. J. (2007) 'Drying-induced variations in physico-chemical properties of amorphous pharmaceuticals and their impact on stability (I): Stability of a monoclonal antibody', *Journal of Pharmaceutical Sciences*. John Wiley and Sons Inc., 96(8), pp. 1983–2008. doi: 10.1002/jps.20859.

Abdul-Gader, A., Miles, A. J. and Wallace, B. A. (2011) 'A reference dataset for the analyses of membrane protein secondary structures and transmembrane residues using circular dichroism spectroscopy', 27(12), pp. 1630–1636. doi: 10.1093/bioinformatics/btr234.

Abraham, A., Elkassabany, O., Krause, M. E. and Ott, A. (2019) 'A nondestructive and noninvasive method to determine water content in lyophilized proteins using low-field time-domain NMR', *Magnetic Resonance in Chemistry*. John Wiley and Sons Ltd, 57(10), pp. 873–877. doi: 10.1002/mrc.4864.

Abraham, I., Ali Elkordy, E., Haj Ahmad, R., Ahmad, Z. and Ali Elkordy, A. (2019) 'Effect of Spray-Drying and Electrospraying as Drying Techniques on Lysozyme Characterisation', in *Electrospinning and Electrospraying - Techniques and Applications*. IntechOpen. doi: 10.5772/intechopen.86237.

Adali, M. B., Barresi, A. A., Boccardo, G. and Pisano, R. (2020) 'Spray freeze-drying as a solution to continuous manufacturing of pharmaceutical products in bulk', *Processes*. MDPI AG, p. 709. doi: 10.3390/PR8060709.

Affleck, R. P., Khamar, D., Lowerre, K. M., Adler, N., Cullen, S., Yang, M. and McCoy, T. R. (2021) 'Near Infrared and Frequency Modulated Spectroscopy as Non-Invasive Methods for Moisture Assessment of Freeze-Dried Biologics', *Journal of Pharmaceutical Sciences*. Elsevier, 110(10), pp. 3395–3402. doi: 10.1016/J.XPHS.2021.06.016.

Ahern, T. J., Casal, J. I., Petsko, G. A. and Klibanov, A. M. (1987) 'Control of oligomeric enzyme thermostability by protein engineering.', *Proceedings of the National Academy of Sciences of the United States of America*, 84(3), pp. 675–9. Available at: http://www.ncbi.nlm.nih.gov/pubmed/3543933 (Accessed: 26 February 2018).

Ahmed, M., Akter, M. S., Lee, J. C. and Eun, J. B. (2010) 'Encapsulation by spray drying of bioactive components, physicochemical and morphological properties from purple sweet potato', *LWT - Food Science and Technology*. Academic Press, 43(9), pp. 1307–1312. doi:

10.1016/j.lwt.2010.05.014.

Ajmera, A. and Scherließ, R. (2014) 'Stabilisation of proteins via mixtures of amino acids during spray drying', *International Journal of Pharmaceutics*, 463, pp. 98–107. doi: 10.1016/j.ijpharm.2014.01.002.

Al-Ghobashy, M. A., Mostafa, M. M., Abed, H. S., Fathalla, F. A. and Salem, M. Y. (2017) 'Correlation between Dynamic Light Scattering and Size Exclusion High Performance Liquid Chromatography for Monitoring the Effect of pH on Stability of Biopharmaceuticals', *Journal of Chromatography B: Analytical Technologies in the Biomedical and Life Sciences*. Elsevier B.V., 1060, pp. 1–9. doi: 10.1016/j.jchromb.2017.05.029.

Al-Hakim, K., Wigley, G. and Stapley, A. G. F. (2006) 'Phase Doppler Anemometry Studies of Spray Freezing', *Chemical Engineering Research and Design*. Elsevier, 84(12), pp. 1142–1151. doi: 10.1205/CHERD06014.

Al-hussein, A. and Gieseler, H. (2013) 'Investigation of histidine stabilizing effects on LDH during freeze-drying', *Journal of Pharmaceutical Sciences*. John Wiley and Sons Inc., 102(3), pp. 813–826. doi: 10.1002/jps.23427.

Al-Hussein, A. and Gieseler, H. (2012) 'The effect of mannitol crystallization in mannitol-sucrose systems on LDH stability during freeze-drying', *Journal of Pharmaceutical Sciences*. doi: 10.1002/jps.23173.

Albasarah, Y. Y., Somavarapu, S. and Taylor, K. M. G. (2010) 'Stabilizing protein formulations during air-jet nebulization', *International Journal of Pharmaceutics*. Elsevier, 402(1–2), pp. 140–145. doi: 10.1016/j.ijpharm.2010.09.042.

Alhajj, N., O'Reilly, N. J. and Cathcart, H. (2021) 'Designing enhanced spray dried particles for inhalation: A review of the impact of excipients and processing parameters on particle properties', *Powder Technology*. Elsevier, 384, pp. 313–331. doi: 10.1016/j.powtec.2021.02.031.

Ali, M. E. and Lamprecht, A. (2014) 'Spray freeze drying for dry powder inhalation of nanoparticles', *European Journal of Pharmaceutics and Biopharmaceutics*. Elsevier, 87(3), pp. 510–517. doi: 10.1016/J.EJPB.2014.03.009.

Allison, S. D., Chang, B., Randolph, T. W. and Carpenter, J. F. (1999) *Hydrogen Bonding between Sugar and Protein Is Responsible for Inhibition of Dehydration-Induced Protein Unfolding*. Available at: http://www.idealibrary.com.

Almeida, N. L., Oliveira, C. L. P., Torriani, I. L. and Loh, W. (2004) 'Calorimetric and structural investigation of the interaction of lysozyme and bovine serum albumin with poly(ethylene oxide) and its copolymers', *Colloids and Surfaces B: Biointerfaces*. Elsevier, 38(1–2), pp. 67–76. doi: 10.1016/j.colsurfb.2004.08.004.

Amara, C. Ben, Eghbal, N., Degraeve, P. and Gharsallaoui, A. (2016) 'Using complex coacervation for lysozyme encapsulation by spray-drying', *Journal of Food Engineering*. Elsevier Ltd, 183, pp. 50–57. doi: 10.1016/j.jfoodeng.2016.03.016.

Amara, C. Ben, Kim, L., Oulahal, N., Degraeve, P. and Gharsallaoui, A. (2017) 'Using complexation for the microencapsulation of nisin in biopolymer matrices by spray-drying', *Food Chemistry*. Elsevier Ltd, 236, pp. 32–40. doi: 10.1016/j.foodchem.2017.04.168.

Amaro, M. I., Tajber, L., Corrigan, O. I. and Healy, A. M. (2011) 'Optimisation of spray drying process conditions for sugar nanoporous microparticles (NPMPs) intended for inhalation', *International Journal of Pharmaceutics*. Elsevier, 421(1), pp. 99–109. doi: 10.1016/j.ijpharm.2011.09.021.

Andrews, J. M., Weiss IV, W. F. and Roberts, C. J. (2008) 'Nucleation, growth, and activation energies for seeded and unseeded aggregation of α-chymotrypsinogen A', *Biochemistry*. American Chemical Society , 47(8), pp. 2397–2403. doi: 10.1021/bi7019244.

Andya, J. D., Maa, Y., Costantino, H. R., Nguyen, P., Dasovich, N., Sweeney, T. D., Hsu, C. C. and Shire, S. J. (1999) 'The Effect of Formulation Excipients on Protein Stability and Aerosol Performance of Spray-Dried Powders of a Recombinant Humanized Anti-IgE Monoclonal Antibody1', *Pharmaceutical Research*. Kluwer Academic Publishers-Plenum Publishers, 16(3), pp. 350–358. doi: 10.1023/A:1018805232453.

Andya, J. D., Maa, Y. F., Costantino, H. R., Nguyen, P. A., Dasovich, N., Sweeney, T. D., Hsu, C. C. and Shire, S. J. (1999a) 'The effect of formulation excipients on protein stability and aerosol performance of spray-dried powders of a recombinant humanized anti-IgE monoclonal antibody', *Pharmaceutical Research*. Kluwer Academic/Plenum Publishers, 16(3), pp. 350–358. doi: 10.1023/A:1018805232453.

Andya, J. D., Maa, Y. F., Costantino, H. R., Nguyen, P. A., Dasovich, N., Sweeney, T. D., Hsu, C. C. and Shire, S. J. (1999b) 'The effect of formulation excipients on protein stability and aerosol performance of spray-dried powders of a recombinant humanized anti-IgE monoclonal antibody', *Pharmaceutical Research*. Kluwer Academic/Plenum Publishers, 16(3), pp. 350–358. doi: 10.1023/A:1018805232453.

Aniket, Gaul, D. A., Bitterfield, D. L., Su, J. T., Li, V. M., Singh, I., Morton, J. and Needham, D. (2015) 'Enzyme dehydration using microglassification™ preserves the Protein's structure and function', *Journal of Pharmaceutical Sciences*. John Wiley and Sons Inc., 104(2), pp. 640–651. doi: 10.1002/jps.24279.

Aniket, Gaul, D. A., Rickard, D. L. and Needham, D. (2014) 'MicroglassificationTM: A novel technique for protein dehydration', *Journal of Pharmaceutical Sciences*. John Wiley and Sons Inc., 103(3), pp. 810–820. doi: 10.1002/jps.23847.

Aniket, Tang, N., Rosenberg, J., Chilkoti, A. and Needham, D. (2015) 'Elastin-like Polypeptide Microspheres: A Stimuli-Responsive Vehicle for Controlled Drug Delivery', in *Society for Biomaterials*. Charlotte, North Caroline. Available at: https://www.researchgate.net/publication/282504946_Elastin-like_Polypeptide_Microspheres_A_Stimuli-Responsive_Vehicle_for_Controlled_Drug_Delivery (Accessed: 31 January 2021).

Anton Paar (2018) 'Dimerization of Bovine Serum Albumin As Evidenced By Particle Size and Molecular Mass Measurement'. Available at: https://s3-eu-central-1.amazonaws.com/centaur-wp/theengineer/prod/content/uploads/2018/04/05161827/Bovine-serum-albumin-testing.pdf (Accessed: 23 February 2022).

Arakawa, T., Ejima, D., Tsumoto, K., Obeyama, N., Tanaka, Y., Kita, Y. and Timasheff, S. N. (2007) 'Suppression of protein interactions by arginine: A proposed mechanism of the arginine effects', *Biophysical Chemistry*. Elsevier, 127(1–2), pp. 1–8. doi: 10.1016/J.BPC.2006.12.007.

Arakawa, T., Prestrelski, S. J., Kenney, W. C. and Carpenter, J. F. (2001) 'Factors affecting short-term and long-term stabilities of proteins', *Advanced Drug Delivery Reviews*. doi: 10.1016/S0169-409X(00)00144-7.

Arakawa, T. and Timasheff, S. N. (1982) 'Stabilization of Protein Structure by Sugars', *Biochemistry*, 21(25), pp. 6536–6544. doi: 10.1021/bi00268a033.

Arsiccio, A. and Pisano, R. (2018) 'Surfactants as stabilizers for biopharmaceuticals: An insight into the molecular mechanisms for inhibition of protein aggregation', *European Journal of Pharmaceutics and Biopharmaceutics*, 128. doi: 10.1016/j.ejpb.2018.04.005.

Ashton, L., Dusting, J., Imomoh, E., Balabani, S. and Blanch, E. W. (2009) 'Shear-induced unfolding of lysozyme monitored in situ', *Biophysical Journal*. Biophysical Society, 96(10), pp. 4231–4236. doi: 10.1016/j.bpj.2009.02.024.

Aulton, M. E. (2007) 'Drying', in *Aulton's pharmaceutics : The design and manufacture of medicines*. 3rd edn. Churchill Livingstone, pp. 425–440. Available at: https://books.google.ie/books/about/Aulton_s_Pharmaceutics.html?id=2zlQSwAACAAJ&redir_esc=y (Accessed: 12 March 2018).

Auritec Pharmaceuticals (2016) *Plexis*. Available at: http://www.auritecpharma.com/plexis/ (Accessed: 2 August 2021).

Austin, J., Minelli, C., Hamilton, D., Wywijas, M. and Jones, H. J. (2020) 'Nanoparticle number concentration measurements by multi-angle dynamic light scattering', *Journal of Nanoparticle Research*. Springer, 22(5). doi: 10.1007/s11051-020-04840-8.

Authelin, J. R., Rodrigues, M. A., Tchessalov, S., Singh, S. K., McCoy, T., Wang, S. and Shalaev, E. (2020) 'Freezing of Biologicals Revisited: Scale, Stability, Excipients, and Degradation Stresses', *Journal of Pharmaceutical Sciences*. Elsevier B.V., 109(1), pp. 44–61. doi: 10.1016/j.xphs.2019.10.062.

Auvray, F., Dennetiere, D., Giuliani, A., Jamme, F., Wien, F., Nay, B., Zirah, S., Polack, F., Menneglier, C., Lagarde, B., *et al.* (2019) 'Time resolved transient circular dichroism spectroscopy using synchrotron natural polarization', *Structural Dynamics*. American Crystallographic Association, 6(5), p. 054307. doi: 10.1063/1.5120346.

Awotwe-Otoo, D., Agarabi, C., Read, E. K., Lute, S., Brorson, K. A., Khan, M. A. and Shah, R. B. (2013) 'Impact of controlled ice nucleation on process performance and quality attributes of a lyophilized monoclonal antibody', *International Journal of Pharmaceutics*. Elsevier, 450(1–2), pp. 70–78. doi: 10.1016/j.ijpharm.2013.04.041.

Barfuss, H. (2014) 'Qualitätsüberwachung in pharmazeutischen Gefriertrocknungsanlagen', *Vakuum in Forschung und Praxis*. John Wiley & Sons, Ltd, 26(1), pp. 35–38. doi: 10.1002/vipr.201400543.

Barley, J. (2020) *Basic Principles of Freeze Drying*, *SP Scientific*. Available at: https://www.spscientific.com/freeze-drying-lyophilization-basics/ (Accessed: 22 April 2020).

Batens, M., Massant, J., Teodorescu, B. and Van den Mooter, G. (2018) 'Formulating monoclonal antibodies as powders for reconstitution at high concentration using spray drying: Models and pitfalls', *European Journal of Pharmaceutics and Biopharmaceutics*. Elsevier B.V., 127, pp. 407–422. doi: 10.1016/j.ejpb.2018.02.002.

Baynes, B. M. and Trout, B. L. (2004) 'Rational Design of Solution Additives for the Prevention of Protein Aggregation', *Biophysical Journal*. Cell Press, 87(3), pp. 1631–1639. doi: 10.1529/BIOPHYSJ.104.042473.

Baynes, B. M., Wang, D. I. C. and Trout, B. L. (2005) 'Role of arginine in the stabilization of proteins against aggregation', *Biochemistry*. American Chemical Society , 44(12), pp. 4919–4925. doi: 10.1021/BI047528R/ASSET/IMAGES/MEDIUM/BI047528RN00001.GIF.

Becker, W. (1957) 'Gefriertrocknungsverfahren'.

Bee, J. S., Stevenson, J. L., Mehta, B., Svitel, J., Pollastrini, J., Platz, R., Freund, E., Carpenter, J. F. and Randolph, T. W. (2009) 'Response of a concentrated monoclonal antibody formulation to high shear', *Biotechnology and Bioengineering*, 103(5), pp. 936–943. doi: 10.1002/bit.22336.

Bee, J. S., Chiu, D., Sawicki, S., Stevenson, J. L., Chatterjee, K., Freund, E., Carpenter, J. F. and

Randolph, T. W. (2009) 'Monoclonal antibody interactions with micro- and nanoparticles: Adsorption, aggregation, and accelerated stress studies', *Journal of Pharmaceutical Sciences*. John Wiley and Sons Inc., 98(9), pp. 3218–3238. doi: 10.1002/jps.21768.

De Beer, T. R. M., Vercruysse, P., Burggraeve, A., Quinten, T., Ouyang, J., Zhang, X., Vervaet, C., Remon, J. P. and Baeyens, W. R. G. (2009) 'In-line and real-time process monitoring of a freeze drying process using Raman and NIR spectroscopy as complementary process analytical technology (PAT) tools', *Journal of Pharmaceutical Sciences*. doi: 10.1002/jps.21633.

Bekard, I. B., Barnham, K. J., White, L. R. and Dunstan, D. E. (2011) 'α-Helix unfolding in simple shear flow', in *Soft Matter*. Royal Society of Chemistry, pp. 203–210. doi: 10.1039/c0sm00692k.

Bezemer, J. M., Grijpma, D. W., Dijkstra, P. J., Van Blitterswijk, C. A. and Feijen, J. (1999) 'A controlled release system for proteins based on poly(ether ester) block-copolymers: Polymer network characterization', *Journal of Controlled Release*. Elsevier, 62(3), pp. 393–405. doi: 10.1016/S0168-3659(99)00170-4.

Bhambhani, A., Stanbro, J., Roth, D., Sullivan, E., Jones, M., Evans, R. and Blue, J. (2021) 'Evaluation of Microwave Vacuum Drying as an Alternative to Freeze-Drying of Biologics and Vaccines: the Power of Simple Modeling to Identify a Mechanism for Faster Drying Times Achieved with Microwave', *AAPS PharmSciTech*. Springer Science and Business Media Deutschland GmbH, 22(1), pp. 1–16. doi: 10.1208/s12249-020-01912-9.

Bhatnagar, B., Zakharov, B., Fisyuk, A., Wen, X., Karim, F., Lee, K., Seryotkin, Y., Mogodi, M., Fitch, A., Boldyreva, E., *et al.* (2019) 'Protein/Ice Interaction: High-Resolution Synchrotron X-ray Diffraction Differentiates Pharmaceutical Proteins from Lysozyme', *The Journal of Physical Chemistry B*. American Chemical Society, 123(27), pp. 5690–5699. doi: 10.1021/acs.jpcb.9b02443.

Bhattacharjee, S. (2016) 'DLS and zeta potential – What they are and what they are not?', *Journal of Controlled Release*, 235, pp. 337–351. doi: 10.1016/j.jconrel.2016.06.017.

Bhirde, A., Chikkaveeraiah, B. V., Venna, R., Carley, R., Brorson, K. and Agarabi, C. (2020) 'High Performance Size Exclusion Chromatography and High-Throughput Dynamic Light Scattering as Orthogonal Methods to Screen for Aggregation and Stability of Monoclonal Antibody Drug Products', *Journal of Pharmaceutical Sciences*. Elsevier B.V., 109(11), pp. 3330–3339. doi: 10.1016/j.xphs.2020.08.013.

Bjelošević, M., Zvonar Pobirk, A., Planinšek, O. and Ahlin Grabnar, P. (2020) 'Excipients in freeze-dried biopharmaceuticals: Contributions toward formulation stability and lyophilisation cycle optimisation', *International Journal of Pharmaceutics*. Elsevier B.V. doi: 10.1016/j.ijpharm.2020.119029.

Blumlein, A. and McManus, J. J. (2013) 'Reversible and non-reversible thermal denaturation of lysozyme with varying pH at low ionic strength', *Biochimica et Biophysica Acta - Proteins and Proteomics*. Elsevier B.V., 1834(10), pp. 2064–2070. doi: 10.1016/j.bbapap.2013.06.001.

Bodier-Montagutelli, E., Respaud, R., Perret, G., Baptista, L., Duquenne, P., Heuzé-Vourc'h, N. and Vecellio, L. (2020) 'Protein stability during nebulization: Mind the collection step!', *European Journal of Pharmaceutics and Biopharmaceutics*. Elsevier B.V., 152, pp. 23–34. doi: 10.1016/j.ejpb.2020.04.006.

Bouchard, A., Jovanović, N., Jiskoot, W., Mendes, E., Witkamp, G. J., Crommelin, D. J. A. and Hofland, G. W. (2007) 'Lysozyme particle formation during supercritical fluid drying: Particle morphology and molecular integrity', *Journal of Supercritical Fluids*, 40(2), pp. 293–307. doi: 10.1016/j.supflu.2006.07.005.

Bowen, M., Turok, R. and Maa, Y. F. (2013) 'Spray Drying of Monoclonal Antibodies: Investigating Powder-Based Biologic Drug Substance Bulk Storage', *Drying Technology*, 31(13–14), pp. 1441–1450. doi: 10.1080/07373937.2013.796968.

Bradford, M. M. (1976) 'A rapid and sensitive method for the quantitation of microgram quantities of protein utilizing the principle of protein-dye binding', *Analytical Biochemistry*. Academic Press, 72(1–2), pp. 248–254. doi: 10.1016/0003-2697(76)90527-3.

Brady, J., Dürig, T., Lee, P. I. and Li, J.-X. (2017) 'Chapter 7 - Polymer Properties and Characterization', in Qiu, Y., Chen, Y., Zhang, G. G. Z., Yu, L., and Mantri, R. V (eds) *Developing Solid Oral Dosage Forms (Second Edition)*. Second Edi. Boston: Academic Press, pp. 181–223. doi: https://doi.org/10.1016/B978-0-12-802447-8.00007-8.

Branchu, S., Forbes, R. T., York, P., Petrén, S., Nyqvist, H. and Camber, O. (1999) 'Hydroxypropyl-β-cyclodextrin inhibits spray-drying-induced inactivation of β-galactosidase', *Journal of Pharmaceutical Sciences*. American Chemical Society, 88(9), pp. 905–911. doi: 10.1021/js9804819.

Brems, D. N., Plaisted, S. M., Havel, H. A., Kauffman, E. W., Stodola, J. D., Eaton, L. C. and White, R. D. (1985) 'Equilibrium denaturation of pituitary- and recombinant-derived bovine growth hormone', *Biochemistry*, 24(26), pp. 7662–7668. doi: 10.1021/bi00347a025.

Broadhead, J., Rouan, S. K. E., Hau, I. and Rhodes, C. T. (1993) 'The Effect of Process and Formulation Variables on the Properties of Spray-dried β-Galactosidase', *Journal of Pharmacy and Pharmacology*. John Wiley & Sons, Ltd, 46(6), pp. 458–467. doi: 10.1111/j.2042-7158.1994.tb03828.x.

Broadwin, S. M. (1965) 'Centrifugal freeze drying apparatus'. USA. Available at: https://patents.google.com/patent/US3203108A/en.

Brouckaert, D., De Meyer, L., Vanbillemont, B., Van Bockstal, P. J., Lammens, J., Mortier, S., Corver, J., Vervaet, C., Nopens, I. and De Beer, T. (2018) 'Potential of Near-Infrared Chemical Imaging as Process Analytical Technology Tool for Continuous Freeze-Drying', *Analytical Chemistry*. American Chemical Society, 90(7), pp. 4354–4362. doi: 10.1021/acs.analchem.7b03647.

Bryant, G., Abeynayake, C. and Thomas, J. C. (1996) 'Improved Particle Size Distribution Measurements Using Multiangle Dynamic Light Scattering. 2. Refinements and Applications', *Langmuir*. American Chemical Society , 12(26), pp. 6224–6228. doi: 10.1021/LA960224O.

Bryant, G. and Thomas, J. C. (1995) 'Improved Particle Size Distribution Measurements Using Multiangle Dynamic Light Scattering', *Langmuir*. American Chemical Society, 11(7), pp. 2480–2485. doi: 10.1021/LA00007A028/ASSET/LA00007A028.FP.PNG_V03.

Büchi Labortechnik AG (2002) 'Training Papers Spray Drying', *Training papers*, pp. 1–19. Available at: https://static1.buchi.com/sites/default/files/downloads/Set_3_Training_Papers_Spray_Drying_en_01.pdf?996b2db24007502bd69c913b675467cfc63880ba.

Buijs, J., Ramström, M., Danfelter, M., Larsericsdotter, H., Håkansson, P. and Oscarsson, S. (2003) 'Localized changes in the structural stability of myoglobin upon adsorption onto silica particles, as studied with hydrogen/deuterium exchange mass spectrometry', *Journal of Colloid and Interface Science*. Academic Press Inc., 263(2), pp. 441–448. doi: 10.1016/S0021-9797(03)00401-6.

Buijs, J., Speidel, M. and Oscarsson, S. (2000) 'The stability of lysozyme adsorbed on silica and gallium arsenide surfaces: Preferential destabilization of part of the lysozyme structure by

gallium arsenide', *Journal of Colloid and Interface Science*. Academic Press Inc., 226(2), pp. 237–245. doi: 10.1006/jcis.2000.6818.

Buijs, J., Vera, C. C., Ayala, E., Steensma, E., Håkansson, P. and Oscarsson, S. (1999) 'Conformational stability of adsorbed insulin studied with mass spectrometry and hydrogen exchange', *Analytical Chemistry*. American Chemical Society , 71(15), pp. 3219–3225. doi: 10.1021/ac9809433.

Bulheller, B. M., Rodger, A. and Hirst, J. D. (2007) 'Circular and linear dichroism of proteins', *Physical Chemistry Chemical Physics*. The Royal Society of Chemistry, pp. 2020–2035. doi: 10.1039/b615870f.

von Bülow, S., Siggel, M., Linke, M. and Hummer, G. (2019) 'Dynamic cluster formation determines viscosity and diffusion in dense protein solutions', *Proceedings of the National Academy of Sciences of the United States of America*. National Academy of Sciences, 116(20), pp. 9843–9852. doi: 10.1073/PNAS.1817564116/SUPPL_FILE/PNAS.1817564116.SM01.AVI.

Bussi, G., Donadio, D. and Parrinello, M. (2007) 'Canonical sampling through velocity rescaling', *The Journal of Chemical Physics*. American Institute of PhysicsAIP, 126(1), p. 014101. doi: 10.1063/1.2408420.

Cao, W., Krishnan, S., Ricci, M. S. pee., Shih, L. Y., Liu, D., Gu, J. H. u. and Jameel, F. (2013) 'Rational design of lyophilized high concentration protein formulations-mitigating the challenge of slow reconstitution with multidisciplinary strategies', *European journal of pharmaceutics and biopharmaceutics : official journal of Arbeitsgemeinschaft für Pharmazeutische Verfahrenstechnik e.V*, 85(2), pp. 287–293. doi: 10.1016/j.ejpb.2013.05.001.

Capozzi, L. C., Trout, B. L. and Pisano, R. (2019) 'From Batch to Continuous: Freeze-Drying of Suspended Vials for Pharmaceuticals in Unit-Doses', *Industrial and Engineering Chemistry Research*. American Chemical Society, 58(4), pp. 1635–1649. doi: 10.1021/acs.iecr.8b02886.

Carfagna, M., Rosa, M., Lucke, M., Hawe, A. and Frieß, W. (2020) 'Heat flux sensor to create a design space for freeze-drying development', *European Journal of Pharmaceutics and Biopharmaceutics*. Elsevier B.V., 153, pp. 84–94. doi: 10.1016/j.ejpb.2020.05.028.

Carpenter, J. and Chang, B. (1996) 'Lyophilization of Protein Pharmaceuticals', in Avisand, K. and Wu, V. (eds) *Biotechnology and Biopharmaceutical Manufacturing, Processing, and Preservation*, pp. 199–263.

Carpenter, J. F., Prestrelski, S. J., Anchordoguy, T. J. and Arakawa, T. (1994) 'Interactions of Stabilizers with Proteins During Freezing and Drying', in Cleland, J. L. and Langer, R. (eds) *Formulation and Delivery of Proteins and Peptides*. American Chemical Society (ACS), pp. 134–147. doi: 10.1021/bk-1994-0567.ch009.

Carpenter, John F, Chang, B. S., Garzon-Rodriguez, W. and Randolph, T. W. (2002) 'Rationale design of stable lyophilized protein formulations: Theory and Practice.', in Carpenter, J.F. and Manning, M. C. (eds) *Rational Design of stable protein formulations - theory and practice*. New York: Kluwer Academic Publishers-Plenum Publishers, pp. 109–133.

Cegielska-Radziejewska, R., Lesnierowski, G., Szablewski, T. and Kijowski, J. (2010) 'Physico-chemical properties and antibacterial activity of modified egg white-lysozyme', *European Food Research and Technology*. Springer, 231(6), pp. 959–964. doi: 10.1007/s00217-010-1347-y.

Celik, M. and Wendell, S. C. (2010) 'Spray Drying and Pharmaceutical Applications', in Parikh, D. M. (ed.) *Handbook of Pharmaceutical Granulation Technology*. 3rd edn. Taylor and Francis,

pp. 98–125. doi: 10.1201/9780849354953.ch5.

Chan, J. G. Y., Chan, H. K., Prestidge, C. A., Denman, J. A., Young, P. M. and Traini, D. (2013) 'A novel dry powder inhalable formulation incorporating three first-line anti-tubercular antibiotics', *European Journal of Pharmaceutics and Biopharmaceutics*. Elsevier, 83(2), pp. 285–292. doi: 10.1016/j.ejpb.2012.08.007.

Chan, L. W., Tan, L. H. and Heng, P. W. S. (2008) 'Process Analytical Technology: Application to Particle Sizing in Spray Drying', *AAPS PharmSciTech*, 9(1), pp. 259–266. doi: 10.1208/s12249-007-9011-y.

Chandrapala, J. and Vasiljevic, T. (2017) 'Properties of spray dried lactose powders influenced by presence of lactic acid and calcium', *Journal of Food Engineering*. Elsevier Ltd, 198, pp. 63–71. doi: 10.1016/j.jfoodeng.2016.11.017.

Chang, B. S., Kendrick, B. S. and Carpenter, J. F. (1996) 'Surface-induced denaturation of proteins during freezing and its inhibition by surfactants', *Journal of Pharmaceutical Sciences*. John Wiley and Sons Inc., 85(12), pp. 1325–1330. doi: 10.1021/js960080y.

Chang, L., Shepherd, D., Sun, J., Ouellette, D., Grant, K. L., Tang, X. and Pikal, M. J. (2005) 'Mechanism of protein stabilization by sugars during freeze-drying and storage: Native structure preservation, specific interaction, and/or immobilization in a glassy matrix?', *Journal of Pharmaceutical Sciences*. John Wiley and Sons Inc., 94(7), pp. 1427–1444. doi: 10.1002/jps.20364.

Chang, L., Shepherd, D., Sun, J., Tang, X. and Pikal, M. J. (2005) 'Effect of sorbitol and residual moisture on the stability of lyophilized antibodies: Implications for the mechanism of protein stabilization in the solid state', *Journal of Pharmaceutical Sciences*. John Wiley and Sons Inc., 94(7), pp. 1445–1455. doi: 10.1002/jps.20363.

Charm, S. E. and Wong, B. L. (1981) 'Shear effects on enzymes', *Enzyme and Microbial Technology*. Elsevier, 3(2), pp. 111–118. doi: 10.1016/0141-0229(81)90068-5.

Chatterjee, K., Shalaev, E. Y. and Suryanarayanan, R. (2005a) 'Partially crystalline systems in lyophilization: I. Use of ternary state diagrams to determine extent of crystallization of bulking agent', *Journal of Pharmaceutical Sciences*. John Wiley and Sons Inc., 94(4), pp. 798–808. doi: 10.1002/jps.20303.

Chatterjee, K., Shalaev, E. Y. and Suryanarayanan, R. (2005b) 'Partially crystalline systems in lyophilization: II. Withstanding collapse at high primary drying temperatures and impact on protein activity recovery', *Journal of Pharmaceutical Sciences*. John Wiley and Sons Inc., 94(4), pp. 809–820. doi: 10.1002/jps.20304.

Chaurasiya, B. and Zhao, Y.-Y. (2020) 'Dry Powder for Pulmonary Delivery: A Comprehensive Review', *Pharmaceutics*. MDPI AG, 13(1), p. 31. doi: 10.3390/pharmaceutics13010031.

Chen, Y., Ling, J., Li, M., Su, Y., Arte, K. S., Mutukuri, T. T., Taylor, L. S., Munson, E. J., Topp, E. M. and Zhou, Q. T. (2021) 'Understanding the Impact of Protein-Excipient Interactions on Physical Stability of Spray-Dried Protein Solids', *Molecular Pharmaceutics*. American Chemical Society, 18(7), pp. 2657–2668. doi: 10.1021/ACS.MOLPHARMACEUT.1C00189/SUPPL_FILE/MP1C00189_SI_001.PDF.

Chen, Y., Mutukuri, T. T., Wilson, N. E. and Zhou, Q. (Tony) (2021) 'Pharmaceutical protein solids: Drying technology, solid-state characterization and stability', *Advanced Drug Delivery Reviews*. Elsevier BV, 172, pp. 211–233. doi: 10.1016/j.addr.2021.02.016.

Cheow, W. S., Ng, M. L. L., Kho, K. and Hadinoto, K. (2011) 'Spray-freeze-drying production of thermally sensitive polymeric nanoparticle aggregates for inhaled drug delivery: Effect of

freeze-drying adjuvants', *International Journal of Pharmaceutics*. Elsevier, 404(1–2), pp. 289–300. doi: 10.1016/J.IJPHARM.2010.11.021.

Chernysheva, M. G., Badun, G. A., Shnitko, A. V., Petrova, V. I. and Ksenofontov, A. L. (2018) 'Lysozyme-surfactant adsorption at the aqueous-air and aqueous-organic liquid interfaces as studied by tritium probe', *Colloids and Surfaces A: Physicochemical and Engineering Aspects*. Elsevier B.V., 537, pp. 351–360. doi: 10.1016/j.colsurfa.2017.10.048.

Chew, N. Y. K. and Chan, H. K. (1999) 'Influence of particle size, air flow, and inhaler device on the dispersion of mannitol powders as aerosols', *Pharmaceutical Research*. Springer, 16(7), pp. 1098–1103. doi: 10.1023/A:1018952203687.

Chi, E. Y., Krishnan, S., Randolph, T. W. and Carpenter, J. F. (2003) 'Physical stability of proteins in aqueous solution: Mechanism and driving forces in nonnative protein aggregation', *Pharmaceutical Research*. Springer, pp. 1325–1336. doi: 10.1023/A:1025771421906.

Cicerone, M. T., Pikal, M. J. and Qian, K. K. (2015) 'Stabilization of proteins in solid form', *Advanced Drug Delivery Reviews*, 93, pp. 14–24. doi: 10.1016/j.addr.2015.05.006.

Cicerone, M. T. and Soles, C. L. (2004) 'Fast dynamics and stabilization of proteins: Binary glasses of trehalose and glycerol', *Biophysical Journal*. Biophysical Society, 86(6), pp. 3836–3845. doi: 10.1529/biophysj.103.035519.

Claussen, I. C., Ustad, T. S., Strommen, I. and Walde, P. M. (2007) 'Atmospheric Freeze Drying—A Review', *Drying Technology*. Taylor & Francis Group, 25(6), pp. 947–957. doi: 10.1080/07373930701394845.

Cole, L., Fernandes, D., Hussain, M. T., Kaszuba, M., Stenson, J. and Markova, N. (2021) 'Characterization of Recombinant Adeno-Associated Viruses (rAAVs) for Gene Therapy Using Orthogonal Techniques', *Pharmaceutics 2021, Vol. 13, Page 586*. Multidisciplinary Digital Publishing Institute, 13(4), p. 586. doi: 10.3390/PHARMACEUTICS13040586.

Connelly, J. P. and Welch, J. V. (1993) 'Monitor Lyophilization with Mass Spectrometer Gas Analysis', *PDA Journal of Pharmaceutical Science and Technology*, 47(2), pp. 70–75. Available at: https://journal.pda.org/content/47/2/70 (Accessed: 8 February 2021).

Conner, J., Wuchterl, D., Lopez, M., Minshall, B., Prusti, R., Boclair, D., Peterson, J. and Allen, C. (2014) 'The Biomanufacturing of Biotechnology Products', in *Biotechnology Entrepreneurship: Starting, Managing, and Leading Biotech Companies*. Elsevier, pp. 351–385. doi: 10.1016/B978-0-12-404730-3.00026-9.

Cook, I. (2003) 'Why , What and How ? Understanding the freeze drying process', *Biopharma Technology Ltd*, pp. 1–3.

Cook, I. A. and Ward, K. R. (2011a) 'Applications of Headspace Moisture Analysis for Investigating the Water Dynamics within a Sealed Vial Containing Freeze-dried Material', *PDA Journal of Pharmaceutical Science and Technology*, 65(1), pp. 2–11. Available at: https://journal.pda.org/content/65/1/2 (Accessed: 12 April 2021).

Cook, I. A. and Ward, K. R. (2011b) 'Headspace moisture mapping and the information that can be gained about freeze-dried materials and processes', *PDA Journal of Pharmaceutical Science and Technology*. Parenteral Drug Association (PDA), 65(5), pp. 457–467. doi: 10.5731/pdajpst.2011.00760.

Cooper, A. (1999) 'Thermodynamic analysis of biomolecular interactions', *Current Opinion in Chemical Biology*. Current Biology Ltd, pp. 557–563. doi: 10.1016/S1367-5931(99)00008-3.

Corbett, D., Bye, J. W. and Curtis, R. A. (2019) 'Measuring Nonspecific Protein-Protein

Interactions by Dynamic Light Scattering', in McManus, J. J. (ed.) *Protein Self-Assembly*. Kildare, Ireland: Humana Press, pp. 3–22. Available at: https://www.roma1.infn.it/~sciortif/PDF/2019/protein.pdf.

Corver, J. A. W. M. (2012) 'Method and System For Freeze-Drying Injectable Compositions, In Particular Pharmaceutical Compositions'. USA.

Corver, J., Bockstal, P.-J. Van and Beer, T. De (2018) *A continuous and controlled pharmaceutical freeze-drying technology for unit doses*, *European Pharmaceutical Review*. Available at: https://www.europeanpharmaceuticalreview.com/article/70823/continuous-controlled-pharmaceutical-freeze-drying-technology-unit-doses/ (Accessed: 27 February 2021).

Costa-Silva, T. A., Souza, C. R. F., Oliveira, W. P. and Said, S. (2014) 'Characterization and spray drying of lipase produced by the endophytic fungus Cercospora kikuchii', *Brazilian Journal of Chemical Engineering*. Assoc. Brasiliera de Eng. Quimica / Braz. Soc. Chem. Eng., 31(4), pp. 849–858. doi: 10.1590/0104-6632.20140314s00002880.

Costantino, H. R., Firouzabadian, L., Hogeland, K., Wu, C., Beganski, C., Carrasquillo, K. G., Có, M., Griebenow, K., Zale, S. E. and Tracy, M. A. (2000) 'Protein Spray-Freeze Drying. Effect of Atomization Conditions on Particle Size and Stability', *Pharmaceutical Research*, 17(11), pp. 1374–1383.

Costantino, H. R., Andya, J. D., Nguyen, P.-A., Dasovich, N., Sweeney, T. D., Shire, S. J., Hsu, C. C. and Maa, Y.-F. (1998) 'Effect of Mannitol Crystallization on the Stability and Aerosol Performance of a Spray-Dried Pharmaceutical Protein, Recombinant Humanized anti-IgE Monoclonal Antibody', *Journal of Pharmaceutical Sciences*. Wiley-Blackwell, 87(11), pp. 1406–1411. doi: 10.1021/js9800679.

Costantino, H. R., Langer, R. and Klibanov, A. M. (1994) 'Solid-Phase Aggregation of Proteins under Pharmaceutically Relevant Conditions†', *Journal of Pharmaceutical Sciences*. John Wiley & Sons, Ltd, 83(12), pp. 1662–1669. doi: 10.1002/jps.2600831205.

Craig, D. Q., Royall, P. G., Kett, V. L. and Hopton, M. L. (1999) 'The relevance of the amorphous state to pharmaceutical dosage forms: glassy drugs and freeze dried systems.', *International journal of pharmaceutics*, 179(2), pp. 179–207. Available at: http://www.ncbi.nlm.nih.gov/pubmed/10053213 (Accessed: 14 February 2018).

Crommelin, D. J. A., Storm, G., Verrijk, R., De Leede, L., Jiskoot, W. and Hennink, W. E. (2003) 'Shifting paradigms: Biopharmaceuticals versus low molecular weight drugs', *International Journal of Pharmaceutics*. Elsevier, 266(1–2), pp. 3–16. doi: 10.1016/S0378-5173(03)00376-4.

Cullen, S., Walsh, E., Gervasi, V., Khamar, D. and McCoy, T. R. (2022) 'Technical transfer and commercialisation of lyophilised biopharmaceuticals — application of lyophiliser characterisation and comparability', *AAPS Open 2022 8:1*. SpringerOpen, 8(1), pp. 1–20. doi: 10.1186/S41120-022-00059-0.

Cuvelier, B., Eloy, P., Loira-Pastoriza, C., Ucakar, B., Sanogo, A. A., Dupont-Gillain, C. and Vanbever, R. (2015) 'Minimal amounts of dipalmitoylphosphatidylcholine improve aerosol performance of spray-dried temocillin powders for inhalation', *International Journal of Pharmaceutics*. Elsevier, 495(2), pp. 981–990. doi: 10.1016/j.ijpharm.2015.10.019.

D'Addio, S. M., Chan, J. G. Y., Kwok, P. C. L., Prud'Homme, R. K. and Chan, H. K. (2012) 'Constant size, variable density aerosol particles by ultrasonic spray freeze drying', *International Journal of Pharmaceutics*, 427(2), pp. 185–191. doi: 10.1016/j.ijpharm.2012.01.048.

Dani, B., Platz, R. and Tzannis, S. T. (2007) 'High concentration formulation feasibility of human immunoglubulin G for subcutaneous administration', *Journal of Pharmaceutical Sciences*. John Wiley and Sons Inc., 96(6), pp. 1504–1517. doi: 10.1002/jps.20508.

Darden, T., York, D. and Pedersen, L. (1998) 'Particle mesh Ewald: An N·log(N) method for Ewald sums in large systems', *The Journal of Chemical Physics*. American Institute of PhysicsAIP, 98(12), p. 10089. doi: 10.1063/1.464397.

Das, U., Hariprasad, G., Ethayathulla, A. S., Manral, P., Das, T. K., Pasha, S., Mann, A., Ganguli, M., Verma, A. K., Bhat, R., *et al.* 'Inhibition of Protein Aggregation: Supramolecular Assemblies of Arginine Hold the Key'. doi: 10.1371/journal.pone.0001176.

Declerck, P. J. (2012) 'Biologicals and biosimilars: a review of the science and its implications', *Generics and Biosimilars Initiative Journal*, 1(1), pp. 13–16. doi: 10.5639/gabij.2012.0101.005.

DeMarco, F. and Renzi, E. (2015) 'Bulk Freeze Drying Using Spray Freezing and Stirred Drying'. USA.

Depaz, R. A., Pansare, S. and Patel, S. M. (2016) 'Freeze-Drying above the Glass Transition Temperature in Amorphous Protein Formulations while Maintaining Product Quality and Improving Process Efficiency', *Journal of Pharmaceutical Sciences*. Elsevier B.V., 105(1), pp. 40–49. doi: 10.1002/jps.24705.

Desai, K. G. H. and Park, H. J. (2005) 'Recent developments in microencapsulation of food ingredients', *Drying Technology*, pp. 1361–1394. doi: 10.1081/DRT-200063478.

DeSimone, J. M. (2016) 'Co-opting Moore's law: Therapeutics, vaccines and interfacially active particles manufactured via PRINT®', *Journal of Controlled Release*. Elsevier B.V., 240, pp. 541–543. doi: 10.1016/j.jconrel.2016.07.019.

Dixon, D., Tchessalov, S., Barry, A. and Warne, N. (2009) 'The Impact of Protein Concentration on Mannitol and Sodium Chloride Crystallinity and Polymorphism Upon Lyophilization', *Journal of Pharmaceutical Sciences*. John Wiley and Sons Inc., 98(9), pp. 3419–3429. doi: 10.1002/jps.21537.

Domján, J., Vass, P., Hirsch, E., Szabó, E., Pantea, E., Andersen, S. K., Vigh, T., Verreck, G., Marosi, G. and Nagy, Z. K. (2020) 'Monoclonal antibody formulation manufactured by high-speed electrospinning', *International Journal of Pharmaceutics*. Elsevier B.V., 591, p. 120042. doi: 10.1016/j.ijpharm.2020.120042.

Dong, A., Huang, P. and Caughey, W. S. (1990) 'Protein Secondary Structures in Water from Second-Derivative Amide I Infrared Spectra', *Biochemistry*. American Chemical Society, 29(13), pp. 3303–3308. doi: 10.1021/bi00465a022.

Dong, A., Huang, P. and Caughey, W. S. (1992) 'Redox-Dependent Changes in. ^{2}-extended Chain and Turn Structures of Cytochrome C in Water Solution Determined by Second Derivative Amide I Infrared Spectra', *Biochemistry*. American Chemical Society, 31(1), pp. 182–189. doi: 10.1021/bi00116a027.

Dong, A., Prestrelski, S. J., Allison, D. and Carpenter, J. F. (1994) *Infrared Spectroscopic Studies of Lyophi I izat ion-and Temperat u re4 nd uced Protein Aggregation*.

Dormer, N., Berkland, C. and Orbis Biosciences Inc. (2016) 'Biodegradable polymer microsphere compositions for parenteral administration'. Available at: https://patents.google.com/patent/WO2017189645A1/en (Accessed: 2 August 2021).

Drake, A. C., Lee, Y., Burgess, E. M., Karlsson, J. O. M., Eroglu, A. and Higgins, A. Z. (2018)

'Effect of water content on the glass transition temperature of mixtures of sugars, polymers, and penetrating cryoprotectants in physiological buffer', *PLoS ONE*. Public Library of Science, 13(1). doi: 10.1371/journal.pone.0190713.

Drusch, S. (2007) 'Sugar beet pectin: A novel emulsifying wall component for microencapsulation of lipophilic food ingredients by spray-drying', *Food Hydrocolloids*, 21(7), pp. 1223–1228. doi: 10.1016/j.foodhyd.2006.08.007.

Duerkop, M., Berger, E., Dürauer, A. and Jungbauer, A. (2018) 'Impact of Cavitation, High Shear Stress and Air/Liquid Interfaces on Protein Aggregation', *Biotechnology Journal*. Wiley-VCH Verlag, 13(7), p. 1800062. doi: 10.1002/biot.201800062.

Dumont, E. F., Oliver, A. J., Ioannou, C., Billiard, J., Dennison, J., Van Den Berg, F., Yang, S., Chandrasekaran, V., Young, G. C., Lahiry, A., *et al.* (2020) 'A novel inhaled dry-powder formulation of ribavirin allows for efficient lung delivery in healthy participants and those with chronic obstructive pulmonary disease in a phase 1 study', *Antimicrobial Agents and Chemotherapy*. American Society for Microbiology, 64(5). doi: 10.1128/AAC.02267-19.

Duran, T., Minatovicz, B., Bai, J., Shin, D., Mohammadiarani, H. and Chaudhuri, B. (2021) 'Molecular Dynamics Simulation to Uncover the Mechanisms of Protein Instability During Freezing', *Journal of Pharmaceutical Sciences*. Elsevier, 110(6), pp. 2457–2471. doi: 10.1016/J.XPHS.2021.01.002.

Durance, T., Noorbakhsh, R., Sandberg, G. and Sáenz-Garza, N. (2020) 'Microwave Drying of Pharmaceuticals', in Ohtake, S., Izutsu, K., and Lechuga-Ballesteros, D. (eds) *Drying Technologies for Biotechnology and Pharmaceutical Applications*. Wiley, pp. 239–255. doi: 10.1002/9783527802104.ch9.

Durocher, Y. and Butler, M. (2009) 'Expression systems for therapeutic glycoprotein production', *Current Opinion in Biotechnology*, 20(6), pp. 700–707. doi: 10.1016/j.copbio.2009.10.008.

Dziezak, J. D. (1988) 'Microencapsulation and Encapsulation Ingredients', *Food Technology*, 2(4), pp. 136–151. Available at: https://www.scirp.org/(S(351jmbntvnsjt1aadkposzje))/reference/ReferencesPapers.aspx?ReferenceID=601155.

E. W. Flosdorf and Mudd, S. (1935) 'Procedure and Apparatus for Preservation in " Lyophile " Form of Serum and Other Biological Substances.', *Journal of Immunology*, 29, pp. 389–425. Available at: https://www.cabdirect.org/cabdirect/abstract/19362700898# (Accessed: 19 March 2018).

Ecker, D. M., Jones, S. D. and Levine, H. L. (2015) 'The therapeutic monoclonal antibody market.', *mAbs*. Taylor & Francis, 7(1), pp. 9–14. doi: 10.4161/19420862.2015.989042.

Eckhardt, B. M., Oeswein, J. Q., Yeung, D. A., Milby, T. D. and Bewley, T. A. (1994) 'A turbidimetric method to determine visual appearance of protein solutions', *PDA Journal of Pharmaceutical Science and Technology*. Parenteral Drug Association (PDA), 48(2), pp. 64–70.

ElKassas, K., Chullipalliyalil, K., McAuliffe, M., Vucen, S. and Crean, A. (2021) 'Fluorescence spectroscopy for the determination of reconstitution time of an in-vial lyophilised product', *International Journal of Pharmaceutics*. Elsevier BV, 597, p. 120368. doi: 10.1016/j.ijpharm.2021.120368.

Elkordy, A. A., Forbes, R. T. and Barry, B. W. (2002) 'Integrity of crystalline lysozyme exceeds that of a spray-dried form', *International Journal of Pharmaceutics*, 247(1–2), pp. 79–90. doi: 10.1016/S0378-5173(02)00379-4.

Ellab (2020) *TrackSense® Pro Wireless Data Loggers*. Available at: https://www.ellab.com/solutions/wireless-data-loggers/tracksense-pro-data-logger (Accessed: 10 October 2020).

Elversson, J. and Millqvist-Fureby, A. (2005) 'Aqueous two-phase systems as a formulation concept for spray-dried protein', *International Journal of Pharmaceutics*. Elsevier, 294(1–2), pp. 73–87. doi: 10.1016/j.ijpharm.2005.01.015.

Emami, F., Keihan Shokooh, M. and Mostafavi Yazdi, S. J. (2022) 'Recent progress in drying technologies for improving the stability and delivery efficiency of biopharmaceuticals', *Journal of Pharmaceutical Investigation 2022 53:1*. Springer, 53(1), pp. 35–57. doi: 10.1007/S40005-022-00610-X.

Emami, F., Vatanara, A., Park, E. J. and Na, D. H. (2018) 'Drying technologies for the stability and bioavailability of biopharmaceuticals', *Pharmaceutics*, 10(3), pp. 1–22. doi: 10.3390/pharmaceutics10030131.

Den Engelsman, J., Garidel, P., Smulders, R., Koll, H., Smith, B., Bassarab, S., Seidl, A., Hainzl, O. and Jiskoot, W. (2011) 'Strategies for the assessment of protein aggregates in pharmaceutical biotech product development', *Pharmaceutical Research*, pp. 920–933. doi: 10.1007/s11095-010-0297-1.

EnWave (2021) *Merck cites EnWave's REV™ Technology as a Faster, Viable Drying Alternative to Vial-Based Lyophilization for Vaccines and Biologics*. Available at: https://www.enwave.net/merck-cites-enwaves-rev-technology-as-a-faster-viable-drying-alternative-to-vial-based-lyophilization-for-vaccines-and-biologics (Accessed: 1 April 2021).

Esfandiary, R., Gattu, S. K., Stewart, J. M. and Patel, S. M. (2016) 'Effect of Freezing on Lyophilization Process Performance and Drug Product Cake Appearance', *Journal of Pharmaceutical Sciences*. Elsevier Ltd, 105(4), pp. 1427–1433. doi: 10.1016/j.xphs.2016.02.003.

Estevinho, B. N., Carlan, I., Blaga, A. and Rocha, F. (2016) 'Soluble vitamins (vitamin B12 and vitamin C) microencapsulated with different biopolymers by a spray drying process', *Powder Technology*. Elsevier, 289, pp. 71–78. doi: 10.1016/j.powtec.2015.11.019.

Euliss, L. E., DuPont, J. A., Gratton, S. and DeSimone, J. (2006) 'Imparting size, shape, and composition control of materials for nanomedicine', *Chemical Society Reviews*. Chem Soc Rev, 35(11), pp. 1095–1104. doi: 10.1039/b600913c.

Evonik (2015) *Evonik issued U.S. Patent for Groundbreaking Microencapsulation Process - Evonik Industries*. Available at: https://healthcare.evonik.com/en/evonik-issued-us-patent-for-groundbreaking-microencapsulation-process-103039.html (Accessed: 2 August 2021).

Fan, J., Cooper, E. I. and Angell, C. A. (1994) 'Glasses with strong calorimetric β-glass transitions and the relation to the protein glass transition problem', *Journal of Physical Chemistry*, 98(37), pp. 9345–9349. doi: 10.1021/j100088a041.

Farinha, S., Sá, J. V., Lino, P. R., Galésio, M., Pires, J., Rodrigues, M. Â. and Henriques, J. (2022) 'Spray Freeze Drying of Biologics: A Review and Applications for Inhalation Delivery', *Pharmaceutical Research 2022*. Springer, pp. 1–26. doi: 10.1007/S11095-022-03442-4.

Farrell, A., Bones, J. and Cook, K. (2016) *The importance of correct UHPLC instrument setup for protein aggregate analysis by size-exclusion chromatography*. Available at: https://www.separatedbyexperience.com/documents/AN-21602-LC-SEC-mAbs-Instrument-Setup-AN21602-EN.pdf (Accessed: 22 March 2020).

FDA (2006) *NDA 21-868 / EXUBERA® US Package Insert*. Available at:

https://www.accessdata.fda.gov/drugsatfda_docs/label/2006/021868lbl.pdf (Accessed: 27 June 2020).

FDA (2010a) *FABRAZYME® (agalsidase beta) Injection, powder, lyophilized for solution for intravenous use*. Available at: https://www.accessdata.fda.gov/drugsatfda_docs/label/2010/103979s5135lbl.pdf (Accessed: 16 March 2021).

FDA (2010b) *Guidance for Industry Drug Substance Chemistry, Manufacturing, and Controls Information*. Available at: https://www.fda.gov/media/69923/download (Accessed: 22 September 2022).

FDA (2014a) *ALPROLIX® [coagulation factor IX (recombinant), Fc fusion protein], lyophilized powder for solution, for intravenous injection*. Available at: https://www.fda.gov/media/88119/download (Accessed: 16 March 2021).

FDA (2014b) *ELOCTATE® [Antihemophilic Factor (Recombinant), Fc Fusion Protein] Lyophilized Powder for Solution for Intravenous Injection*. Available at: https://www.fda.gov/media/88746/download (Accessed: 16 March 2021).

FDA (2014c) *Lyophilization of Parenteral (7/93) - Inspection guides lyophilization of parenteral.* Available at: https://www.fda.gov/inspections-compliance-enforcement-and-criminal-investigations/inspection-guides/lyophilization-parenteral-793 (Accessed: 5 March 2020).

FDA (2015) *RAPLIXA® (Fibrin Sealant Human)*. Available at: https://www.fda.gov/media/91418/download (Accessed: 29 March 2020).

FDA (2022) *U.S. Food and Drug Administration*. Available at: https://www.fda.gov/ (Accessed: 29 December 2022).

FDA (a) *Cimzia® (certolizumab pegol), For injection, subcutaneous. UCB, Inc.* Available at: https://www.accessdata.fda.gov/drugsatfda_docs/label/2017/125160s270lbl.pdf (Accessed: 23 February 2020).

FDA (b) *Cosentyx® (secukinumab), For injection, subcutaneous. Novartis Pharmaceuticals Corporation*. Available at: https://www.accessdata.fda.gov/drugsatfda_docs/label/2015/125504s000lbl.pdf (Accessed: 23 February 2020).

FDA (c) *Ilaris® (canakinumab), For injection, subcutaneous. Novartis Pharmaceuticals Corporation.* Available at: https://www.accessdata.fda.gov/drugsatfda_docs/label/2016/BLA125319_858687lbl.pdf (Accessed: 23 February 2020).

FDA (d) *Nucala® (mepolizumab), For injection, subcutaneous. GlaxoSmithKline LLC*. Available at: https://www.accessdata.fda.gov/drugsatfda_docs/label/2015/125526Orig1s000Lbl.pdf (Accessed: 23 February 2020).

FDA (e) *RAPTIVA ® [efalizumab] For injection, subcutaneous. Genentech, Inc.* Available at: https://www.fda.gov/media/75713/download (Accessed: 23 February 2020).

FDA (f) *XOLAIR® (omalizumab), For Subcutaneous Use*. Available at: https://www.accessdata.fda.gov/drugsatfda_docs/label/2007/103976s5102lbl.pdf (Accessed: 23 February 2020).

Fedorov, M. V., Goodman, J. M., Nerukh, D. and Schumm, S. (2011) 'Self-assembly of trehalose molecules on a lysozyme surface: The broken glass hypothesis', *Physical Chemistry Chemical Physics*, 13(6), pp. 2294–2299. doi: 10.1039/c0cp01705a.

Fekete, S., Beck, A., Veuthey, J. L. and Guillarme, D. (2014) 'Theory and practice of size exclusion chromatography for the analysis of protein aggregates', *Journal of Pharmaceutical and Biomedical Analysis*. Elsevier, 101, pp. 161–173. doi: 10.1016/J.JPBA.2014.04.011.

Fellows, P. (Peter) (2009) 'Processing by Heat Removal', in *Food processing technology : principles and practice*. 3rd edn. CRC Press, p. 913.

Fiedler, D., Hartl, S., Gerlza, T., Trojacher, C., Kungl, A., Khinast, J. and Roblegg, E. (2021) 'Comparing freeze drying and spray drying of interleukins using model protein CXCL8 and its variants', *European Journal of Pharmaceutics and Biopharmaceutics*. Elsevier, 168, pp. 152–165. doi: 10.1016/J.EJPB.2021.08.006.

Filipe, V., Hawe, A. and Jiskoot, W. (2010) 'Critical evaluation of nanoparticle tracking analysis (NTA) by NanoSight for the measurement of nanoparticles and protein aggregates', *Pharmaceutical Research*. Springer, 27(5), pp. 796–810. doi: 10.1007/s11095-010-0073-2.

Filkova, I., Huang, L. X. and Mujumdar, A. S. (2007) 'Industrial Spray Drying Systems', in A. S. Majumdar (ed.) *Handbook of industrial drying*. 3rd edn. CRC/Taylor & Francis, pp. 215–256. Available at: https://books.google.ie/books?hl=en&lr=&id=oT36AwAAQBAJ&oi=fnd&pg=PA191&dq=Filkov+a,+I.,+Huang,+L.+X.,+%26+Mujumdar,+A.+S.+(2007).+Industrial+Spray+drying+systems.+In+A.+S.+Mujumdar+(Ed.),+Handbook+of+industrial+drying&ots=80UwCrbPBO&sig=9SXZDbf1SuHPJ0I74 (Accessed: 31 March 2018).

Fissore, D., Pisano, R. and Barresi, A. A. (2018) 'Process analytical technology for monitoring pharmaceuticals freeze-drying–A comprehensive review', *Drying Technology*. Taylor and Francis Inc., 36(15), pp. 1839–1865. doi: 10.1080/07373937.2018.1440590.

Flosdorf, E. W. and Mudd, S. (1935) 'Procedure and Apparatus for Preservation in "Lyophile" form of Serum and Other Biological Substances', *The Journal of Immunology*, 29(5).

Flosdorf, E. W. and Mudd, S. (1938) 'An Improved Procedure and Apparatus for Preservation of Sera, Microörganisms and Other Substances—The Cryochem-Process', *The Journal of Immunology*, 34(6).

Forbes, R. T., Barry, B. W. and Elkordy, A. A. (2007) 'Preparation and characterisation of spray-dried and crystallised trypsin: FT-Raman study to detect protein denaturation after thermal stress', *European Journal of Pharmaceutical Sciences*. Elsevier, 30(3–4), pp. 315–323. doi: 10.1016/j.ejps.2006.11.019.

Fröhlich, E. and Salar-Behzadi, S. (2021) 'Oral inhalation for delivery of proteins and peptides to the lungs', *European Journal of Pharmaceutics and Biopharmaceutics*. Elsevier, 163, pp. 198–211. doi: 10.1016/J.EJPB.2021.04.003.

Gaiani, C., Schuck, P., Scher, J., Desobry, S. and Banon, S. (2007) 'Dairy powder rehydration: Influence of protein state, incorporation mode, and agglomeration', *Journal of Dairy Science*. American Dairy Science Association, 90(2), pp. 570–581. doi: 10.3168/jds.S0022-0302(07)71540-0.

Galloway, A. L., Murphy, A., DeSimone, J. M., Di, J., Herrmann, J. P., Hunter, M. E., Kindig, J. P., Malinoski, F. J., Rumley, M. A., Stoltz, D. M., *et al.* (2013) 'Development of a nanoparticle-based influenza vaccine using the PRINT® technology', *Nanomedicine: Nanotechnology, Biology, and Medicine*. Elsevier, 9(4), pp. 523–531. doi: 10.1016/j.nano.2012.11.001.

Ganderton, D., Morton, D. A. V. and Lucas, P. (1999) 'Powders'. US. Available at: https://patents.google.com/patent/US6989155B1/en (Accessed: 22 February 2021).

Ganguly, A., Stewart, J., Rhoden, A., Volny, M. and Saad, N. (2018) 'Mass spectrometry in freeze-

drying: Motivations for using a bespoke PAT for laboratory and production environment', *European Journal of Pharmaceutics and Biopharmaceutics*. Elsevier, 127(December 2017), pp. 298–308. doi: 10.1016/j.ejpb.2018.02.036.

Garcia, A., Mack, P., Williams, S., Fromen, C., Shen, T., Tully, J., Pillai, J., Kuehl, P., Napier, M., Desimone, J. M., *et al.* (2012) 'Microfabricated Engineered Particle Systems for Respiratory Drug Delivery and Other Pharmaceutical Applications', *Journal of Drug Delivery*. Hindawi Publishing Corporation, 2012. doi: 10.1155/2012/941243.

GE (2014) *Cross Flow Filtration Method Handbook*. Sweden. Available at: http://www.processdevelopmentforum.com/files/articles/Cross-Flow_Filtration_Handbook.pdf (Accessed: 16 March 2021).

GEA Pharma Systems (2018) 'GEA spray drying', *GEA Process Engineering A/S*. Denmark.

Gervasi, V., Cullen, S., McCoy, T., Crean, A. and Vucen, S. (2019) 'Application of a mixture DOE for the prediction of formulation critical temperatures during lyophilisation process optimisation', *International Journal of Pharmaceutics*. Elsevier B.V., 572. doi: 10.1016/j.ijpharm.2019.118807.

Gervasi, V., Dall Agnol, R., Cullen, S., McCoy, T., Vucen, S. and Crean, A. (2018) 'Parenteral protein formulations: An overview of approved products within the European Union', *European Journal of Pharmaceutics and Biopharmaceutics*, 131, pp. 8–24. doi: 10.1016/j.ejpb.2018.07.011.

Ghandi, A., Powell, I. B., Howes, T., Chen, X. D. and Adhikari, B. (2012) 'Effect of shear rate and oxygen stresses on the survival of Lactococcus lactis during the atomization and drying stages of spray drying: A laboratory and pilot scale study', *Journal of Food Engineering*. Elsevier, 113(2), pp. 194–200. doi: 10.1016/j.jfoodeng.2012.06.005.

Gharsallaoui, A., Roudaut, G., Chambin, O., Voilley, A. and Saurel, R. (2007) 'Applications of spray-drying in microencapsulation of food ingredients: An overview', *Food Research International*. Elsevier, 40(9), pp. 1107–1121. doi: 10.1016/J.FOODRES.2007.07.004.

Giancola, C., De Sena, C., Fessas, D., Graziano, G. and Barone, G. (1997) 'DSC studies on bovine serum albumin denaturation effects of ionic strength and SDS concentration', *International Journal of Biological Macromolecules*. Elsevier, 20(3), pp. 193–204. doi: 10.1016/S0141-8130(97)01159-8.

Gibbs, B. F., Kermasha, S., Alli, I. and Mulligan, C. N. (1999) 'Encapsulation in the food industry: A review', *International Journal of Food Sciences and Nutrition*. Carfax Publishing Company, 50(3), pp. 213–224. doi: 10.1080/096374899101256.

Gieseler, H., Kessler, W. J., Finson, M., Davis, S. J., Mulhall, P. A., Bons, V., Debo, D. J. and Pikal, M. J. (2007) 'Evaluation of tunable diode laser absorption spectroscopy for in-process water vapor mass flux measurements during freeze drying', *Journal of Pharmaceutical Sciences*. John Wiley and Sons Inc., 96(7), pp. 1776–1793. doi: 10.1002/jps.20827.

Gikanga, B., Turok, R., Hui, A., Bowen, M., Stauch, O. B. and Maa, Y.-F. (2015) 'Manufacturing of High-Concentration Monoclonal Antibody Formulations via Spray Drying - the Road to Manufacturing Scale', *PDA Journal of Pharmaceutical Science and Technology*, 69, pp. 59–73. doi: 10.5731/pdajpst.2015.01003.

Gilbert, A. T. B. and Hirst, J. D. (2004) 'Charge-transfer transitions in protein circular dichroism spectra', *Journal of Molecular Structure: THEOCHEM*. Elsevier, 675(1–3), pp. 53–60. doi: 10.1016/j.theochem.2003.12.038.

Gitter, J. H., Geidobler, R., Presser, I. and Winter, G. (2018) 'Significant Drying Time Reduction

Using Microwave-Assisted Freeze-Drying for a Monoclonal Antibody', *Journal of Pharmaceutical Sciences*, 107(10), pp. 1–6. doi: 10.1016/j.xphs.2018.05.023.

Gitter, J. H., Geidobler, R., Presser, I. and Winter, G. (2019) 'Microwave-Assisted Freeze-Drying of Monoclonal Antibodies: Product Quality Aspects and Storage Stability', *Pharmaceutics*. MDPI AG, 11(12), p. 674. doi: 10.3390/pharmaceutics11120674.

Giurleo, J. T., He, X. and Talaga, D. S. (2008) 'β-Lactoglobulin Assembles into Amyloid through Sequential Aggregated Intermediates', *Journal of Molecular Biology*. Academic Press, 381(5), pp. 1332–1348. doi: 10.1016/j.jmb.2008.06.043.

Goethals, W., Vanbillemont, B., Lammens, J., De Beer, T., Vervaet, C. and Boone, M. N. (2020) 'In-Situ X-ray Imaging Of Sublimating Spin-Frozen Solutions', *Materials*. MDPI AG, 13(13), p. 2953. doi: 10.3390/ma13132953.

Gohel, M. C. and Jogani, P. D. (2005) 'A review of co-processed directly compressible excipients', *Journal of Pharmacy and Pharmaceutical Sciences*, 8(1), pp. 76–93.

Golovanov, A. P., Hautbergue, G. M., Wilson, S. A. and Lian, L. Y. (2004) 'A simple method for improving protein solubility and long-term stability', *Journal of the American Chemical Society*. American Chemical Society , 126(29), pp. 8933–8939. doi: 10.1021/JA049297H/ASSET/IMAGES/MEDIUM/JA049297HN00001.GIF.

Gomme, P. T., Hunt, B. M., Tatford, O. C., Johnston, A. and Bertolini, J. (2006) 'Effect of lobe pumping on human albumin: investigating the underlying mechanisms of aggregate formation1', *Biotechnology and Applied Biochemistry*. Wiley, 43(2), p. 103. doi: 10.1042/ba20050147.

Gouin, S. (2004) 'Microencapsulation: Industrial appraisal of existing technologies and trends', in *Trends in Food Science and Technology*, pp. 330–347. doi: 10.1016/j.tifs.2003.10.005.

Grasmeijer, N., Tiraboschi, V., Woerdenbag, H. J., Frijlink, H. W. and Hinrichs, W. L. J. (2019) 'Identifying critical process steps to protein stability during spray drying using a vibrating mesh or a two-fluid nozzle', *European Journal of Pharmaceutical Sciences*. Elsevier, 128, pp. 152–157. doi: 10.1016/J.EJPS.2018.11.027.

Gratton, S. E. A., Pohlhaus, P. D., Lee, J., Guo, J., Cho, M. J. and DeSimone, J. M. (2007) 'Nanofabricated particles for engineered drug therapies: A preliminary biodistribution study of PRINT^{TM} nanoparticles', *Journal of Controlled Release*. Elsevier, 121(1–2), pp. 10–18. doi: 10.1016/j.jconrel.2007.05.027.

Greaves, R. I. N. (1946) 'preservation of proteins by drying'. H.M. Stationery Off.

Green, J. L. and Angell, C. A. (1989) 'Phase relations and vitrification in saccharide-water solutions and the trehalose anomaly', *The Journal of Physical Chemistry*. American Chemical Society, 93(8), pp. 2880–2882. doi: 10.1021/j100345a006.

Green, J. L., Fan, J. and Angell, C. A. (1994) 'The protein-glass analogy: Some insights from homopeptide comparisons', *Journal of Physical Chemistry*, 98(51), pp. 13780–13790. doi: 10.1021/j100102a052.

Grisso, R., Hipkins, P., Askew, S. D., Hipkins, L. and Mccall, D. (2013) 'Nozzles: selection and sizing', *Publication 442-032*, 2015. doi: doi: http://pubs.ext.vt.edu/442/442-032/442-032_pdf.pdf.

Grohganz, H., Lee, Y.-Y., Rantanen, J. and Yang, M. (2013) 'The influence of lysozyme on mannitol polymorphism in freeze-dried and spray-dried formulations depends on the selection of the drying process', *International Journal of Pharmaceutics*, 447, pp. 224–230. doi:

10.1016/j.ijpharm.2013.03.003.

Guvench, O., Mallajosyula, S. S., Raman, E. P., Hatcher, E., Vanommeslaeghe, K., Foster, T. J., Jamison, F. W. and MacKerell, A. D. (2011) 'CHARMM additive all-atom force field for carbohydrate derivatives and its utility in polysaccharide and carbohydrate-protein modeling', *Journal of Chemical Theory and Computation*. American Chemical Society, 7(10), pp. 3162–3180. doi: 10.1021/CT200328P/SUPPL_FILE/CT200328P_SI_001.PDF.

Haeuser, C., Goldbach, P., Huwyler, J., Friess, W. and Allmendinger, A. (2018) 'Imaging Techniques to Characterize Cake Appearance of Freeze-Dried Products', *Journal of Pharmaceutical Sciences*. Elsevier B.V., 107(11), pp. 2810–2822. doi: 10.1016/j.xphs.2018.06.025.

Harguindeguy, M. and Fissore, D. (2021) 'Temperature/end point monitoring and modelling of a batch freeze-drying process using an infrared camera', *European Journal of Pharmaceutics and Biopharmaceutics*. Elsevier B.V., 158, pp. 113–122. doi: 10.1016/j.ejpb.2020.10.023.

Harrison, R. G. (1994) *Protein purification process engineering*. Edited by R. G. Harrison. M. Dekker Inc. Available at: https://books.google.ie/books?id=bFwlV7_JopIC&printsec=frontcover#v=onepage&q&f=false.

Hatley, R. H. (1992) 'The effective use of differential scanning calorimetry in the optimisation of freeze-drying processes and formulations.', *Developments in biological standardization*, 74, pp. 105–19; discussion 119-22. Available at: http://www.ncbi.nlm.nih.gov/pubmed/1592162 (Accessed: 12 February 2018).

Hawe, A. and Frieß, W. (2006) 'Impact of freezing procedure and annealing on the physico-chemical properties and the formation of mannitol hydrate in mannitol-sucrose-NaCl formulations', *European Journal of Pharmaceutics and Biopharmaceutics*. Elsevier, 64(3), pp. 316–325. doi: 10.1016/j.ejpb.2006.06.002.

Hawe, A., Hulse, W. L., Jiskoot, W. and Forbes, R. T. (2011) 'Taylor dispersion analysis compared to dynamic light scattering for the size analysis of therapeutic peptides and proteins and their aggregates', *Pharmaceutical Research*. Springer, 28(9), pp. 2302–2310. doi: 10.1007/s11095-011-0460-3.

Hebbink, G. A. and Dickhoff, B. H. J. (2019) 'Application of lactose in the pharmaceutical industry', in *Lactose: Evolutionary Role, Health Effects, and Applications*. Elsevier, pp. 175–229. doi: 10.1016/B978-0-12-811720-0.00005-2.

Hede, P. D., Bach, P. and Jensen, A. D. (2008) 'Two-fluid spray atomisation and pneumatic nozzles for fluid bed coating/agglomeration purposes: A review', *Chemical Engineering Science*. Pergamon, pp. 3821–3842. doi: 10.1016/j.ces.2008.04.014.

Hedoux, A., Paccou, L., Achir, S. and Guinet, Y. (2013) 'Mechanism of protein stabilization by trehalose during freeze-drying analyzed by in situ micro-raman spectroscopy', *Journal of Pharmaceutical Sciences*. John Wiley and Sons Inc., 102(8), pp. 2484–2494. doi: 10.1002/jps.23638.

Helal, R. and Melzig, M. F. (2008) 'Determination of lysozyme activity by a fluorescence technique in comparison with the classical turbidity assay', *Pharmazie*, 63(6), pp. 415–419. doi: 10.1691/ph.2008.7846.

Hertel, S. P., Winter, G. and Friess, W. (2015) 'Protein stability in pulmonary drug delivery via nebulization', *Advanced Drug Delivery Reviews*. Elsevier, pp. 79–94. doi: 10.1016/j.addr.2014.10.003.

Hess, B. (2007) 'P-LINCS: A Parallel Linear Constraint Solver for Molecular Simulation', *Journal of Chemical Theory and Computation*. American Chemical Society , 4(1), pp. 116–122. doi: 10.1021/CT700200B.

Heumann, W. (1997) *Industrial Air Pollution Control Systems*. New York: McGraw-Hill, USA.

Hindmarsh, J. ., Russell, A. . and Chen, X. . (2003) 'Experimental and numerical analysis of the temperature transition of a suspended freezing water droplet', *International Journal of Heat and Mass Transfer*. Pergamon, 46(7), pp. 1199–1213. doi: 10.1016/S0017-9310(02)00399-X.

Hindmarsh, J. P., Russell, A. B. and Chen, X. D. (2007) 'Fundamentals of the spray freezing of foods—microstructure of frozen droplets', *Journal of Food Engineering*. Elsevier, 78(1), pp. 136–150. doi: 10.1016/J.JFOODENG.2005.09.011.

Hinrichs, W. L. J., Prinsen, M. G. and Frijlink, H. W. (2001) 'Inulin glasses for the stabilization of therapeutic proteins', *International Journal of Pharmaceutics*. Elsevier, 215(1–2), pp. 163–174. doi: 10.1016/S0378-5173(00)00677-3.

Hirai, M., Arai, S., Iwase, H. and Takizawa, T. (1998) 'Small-angle X-ray scattering and calorimetric studies of thermal conformational change of lysozyme depending on pH', *Journal of Physical Chemistry B*. American Chemical Society , 102(7), pp. 1308–1313. doi: 10.1021/jp9713367.

Hockney, R. W., Goel, S. P. and Eastwood, J. W. (1974) 'Quiet high-resolution computer models of a plasma', *Journal of Computational Physics*. Academic Press, 14(2), pp. 148–158. doi: 10.1016/0021-9991(74)90010-2.

Hoffer, T. E. (1961) 'A LABORATORY INVESTIGATION OF DROPLET FREEZING', *Journal of Meteorology*, 18(6), pp. 766–778. doi: 10.1175/1520-0469(1961)018<0766:ALIODF>2.0.CO;2.

Hofmann, C. L., Savage, J. R., Folk, D., Sprague, J. J., Kalluri, P., Leming, R., Jain, P., Colborn, A., Santos, L. and Hird, G. (2019) *PRINT® Particle Design Improves Skin Penetration in a Topical Formulation*. Available at: https://liquidia.com/products-and-pipeline/publications (Accessed: 27 September 2020).

Hopcraft, K., Chang, P., Jakeman, E. and Walker, J. (2005) 'Polarization fluctuation spectroscopy', in Videen, G., Yatskiv, Y., and Mishchenko, M. (eds) *Photopolarimetry in remote sensing*. Netherlands: Springer, pp. 137–174. Available at: https://doi.org/10.1007/1-4020-2368-5_6.

Horn, J. and Friess, W. (2018) 'Detection of collapse and crystallization of saccharide, protein, and mannitol formulations by optical fibers in lyophilization', *Frontiers in Chemistry*. Frontiers Media S. A, 6(JAN). doi: 10.3389/fchem.2018.00004.

Horn, J., Mahler, H. and Friess, W. (2020) 'Drying for Stabilization of Protein Formulations', in Ohtake, S., Izutsu, K., and Lechuga-Ballesteros, D. (eds) *Drying Technologies for Biotechnology and Pharmaceutical Applications*. Wiley, pp. 91–119. doi: 10.1002/9783527802104.ch4.

Horn, J., Schanda, J. and Friess, W. (2018) 'Impact of fast and conservative freeze-drying on product quality of protein-mannitol-sucrose-glycerol lyophilizates', *European Journal of Pharmaceutics and Biopharmaceutics*. Elsevier B.V., 127, pp. 342–354. doi: 10.1016/j.ejpb.2018.03.003.

Hosokawa Micron B.V. (2019) *Active Freeze Dryer*. Available at: https://www.hosokawa-micron-bv.com/technologies/industrial-dryers/batch-drying-technologies/active-freeze-dryer.html (Accessed: 2 November 2019).

Hosokawa U.K. (2019) *Active Freeze Drying*. Available at: https://www.hosokawa.co.uk/products/active-freeze-drying/ (Accessed: 2 November 2019).

Houde, D., Berkowitz, S. A. and Engen, J. R. (2011) 'The utility of hydrogen/deuterium exchange mass spectrometry in biopharmaceutical comparability studies', *Journal of Pharmaceutical Sciences*. John Wiley and Sons Inc., 100(6), pp. 2071–2086. doi: 10.1002/jps.22432.

Huang, J., Rauscher, S., Nawrocki, G., Ran, T., Feig, M., De Groot, B. L., Grubmüller, H. and MacKerell, A. D. (2016) 'CHARMM36m: an improved force field for folded and intrinsically disordered proteins', *Nature Methods 2016 14:1*. Nature Publishing Group, 14(1), pp. 71–73. doi: 10.1038/nmeth.4067.

Hulse, W. L., Forbes, R. T., Bonner, M. C. and Getrost, M. (2008) 'Do co-spray dried excipients offer better lysozyme stabilisation than single excipients?', *European Journal of Pharmaceutical Sciences*, 33(3), pp. 294–305. doi: 10.1016/j.ejps.2007.12.007.

Hulse, W. L., Forbes, R. T., Bonner, M. C. and Getrost, M. (2009) 'Influence of protein on mannitol polymorphic form produced during co-spray drying', *International Journal of Pharmaceutics*. doi: 10.1016/j.ijpharm.2009.08.007.

Hussain, R., Longo, E. and Siligardi, G. (2018) 'UV-Denaturation Assay to Assess Protein Photostability and Ligand-Binding Interactions Using the High Photon Flux of Diamond B23 Beamline for SRCD', *Molecules*. MDPI AG, 23(8), p. 1906. doi: 10.3390/molecules23081906.

ICH (2000) 'ICH Q7 - GMP', (November).

ICH (2004) *Comparability Of Biotechnological/Biological Products Subject To Changes In Their Manufacturing Process Q5E*, *International Conference On Harmonisation*. Available at: https://database.ich.org/sites/default/files/Q5E Guideline.pdf (Accessed: 12 April 2021).

ICH (2009) *Pharmaceutical Development Q8(R2)*, *International Conference On Harmonisation*. Available at: https://database.ich.org/sites/default/files/Q8_R2_Guideline.pdf (Accessed: 13 February 2021).

ICH (2019) *Technical and Regulatory Considerations For Pharmaceutical Product Lifecycle Management Q12*, *International Conference On Harmonisation*. Available at: https://database.ich.org/sites/default/files/Q12_Guideline_Step4_2019_1119.pdf (Accessed: 12 April 2021).

IMA Life (2019a) *Continuous Aseptic Spray Freeze Drying*. IMA Life. Available at: https://ima.it/pharma/paper/lynfinity-continuous-aseptic-spray-freeze-drying-process-technology-and-product-characterization/.

IMA Life (2019b) *LYNFINITY: Continuous Aseptic Spray Freeze Drying. Process, Technology and Product Characterization.* Available at: https://ima.it/pharma/paper/lynfinity-continuous-aseptic-spray-freeze-drying-process-technology-and-product-characterization/ (Accessed: 1 April 2020).

IMA Life (2019c) *Lynfinity is just a drop away*. Available at: https://ima.it/pharma/lab4life/publications/.

Inoue, N., Takai, E., Arakawa, T. and Shiraki, K. (2014) 'Specific decrease in solution viscosity of antibodies by arginine for therapeutic formulations', *Molecular Pharmaceutics*. American Chemical Society, 11(6), pp. 1889–1896. doi: 10.1021/mp5000218.

Ishibashi, M., Tsumoto, K., Tokunaga, M., Ejima, D., Kita, Y. and Arakawa, T. (2005) 'Is arginine a protein-denaturant?', *Protein Expression and Purification*. Academic Press, 42(1), pp. 1–6. doi: 10.1016/J.PEP.2005.03.028.

Ishwarya, S. P., Anandharamakrishnan, C. and Stapley, A. G. F. (2015) 'Spray-freeze-drying: A novel process for the drying of foods and bioproducts', *Trends in Food Science and Technology*. doi: 10.1016/j.tifs.2014.10.008.

Iwashita, K., Handa, A. and Shiraki, K. (2017) 'Co-aggregation of ovalbumin and lysozyme', *Food Hydrocolloids*. Elsevier B.V., 67, pp. 206–215. doi: 10.1016/j.foodhyd.2017.01.014.

Iyer, L. K., Moorthy, B. S. and Topp, E. M. (2013) 'Photolytic labeling to probe molecular interactions in lyophilized powders', *Molecular Pharmaceutics*. American Chemical Society, 10(12), pp. 4629–4639. doi: 10.1021/mp4004332.

Iyer, L. K., Sacha, G. A., Moorthy, B. S., Nail, S. L. and Topp, E. M. (2016) 'Process and Formulation Effects on Protein Structure in Lyophilized Solids Using Mass Spectrometric Methods', *Journal of Pharmaceutical Sciences*. Elsevier B.V., 105(5), pp. 1684–1692. doi: 10.1016/j.xphs.2016.02.033.

Jachimska, B., Wasilewska, M. and Adamczyk, Z. (2008) 'Characterization of Globular Protein Solutions by Dynamic Light Scattering, Electrophoretic Mobility, and Viscosity Measurements', *Langmuir*. American Chemical Society, 24(13), pp. 6867–6872. doi: 10.1021/LA800548P.

Jadhav, N. R., Gaikwad, V. L., Nair, K. J. and Kadam, H. M. (2014) 'Glass transition temperature: Basics and application in pharmaceutical sector', *Asian Journal of Pharmaceutics (AJP): Free full text articles from Asian J Pharm*, 3(2). doi: 10.22377/AJP.V3I2.246.

Jain, A. K., Sood, V., Bora, M., Vasita, R. and Katti, D. S. (2014) 'Electrosprayed inulin microparticles for microbiota triggered targeting of colon', *Carbohydrate Polymers*. Elsevier Ltd, 112, pp. 225–234. doi: 10.1016/j.carbpol.2014.05.087.

Jain, M., Ganesh, L., Manoj, B., Randhir, C., Shashikant, B. and Chirag, S. (2012) 'Spray Drying in Pharmaceutical Industry', *Pharmaceutical Dosage Forms and Technology*, 4(2), pp. 74–79.

Jenke, D. R. (2014) 'Extractables and leachables considerations for prefilled syringes', *Expert Opinion on Drug Delivery*, 11(10), pp. 1591–1600. doi: 10.1517/17425247.2014.928281.

De Jesus, S. S. and Maciel Filho, R. (2014) 'Drying of α-amylase by spray drying and freeze-drying - A comparative study', *Brazilian Journal of Chemical Engineering*. Assoc. Brasiliera de Eng. Quimica / Braz. Soc. Chem. Eng., 31(3), pp. 625–631. doi: 10.1590/0104-6632.20140313s00002642.

Ji, C., Sun, M., Yu, J., Wang, Y., Zheng, Y., Wang, H. and Niu, R. (2009) 'Trehalose and tween 80 improve the stability of marine lysozyme during freeze-drying', *Biotechnology and Biotechnological Equipment*. Taylor & Francis, 23(3), pp. 1351–1354. doi: 10.1080/13102818.2009.10817668.

Ji, S., Thulstrup, P. W., Mu, H., Hansen, S. H., van de Weert, M., Rantanen, J. and Yang, M. (2016) 'Effect of ethanol as a co-solvent on the aerosol performance and stability of spray-dried lysozyme', *International Journal of Pharmaceutics*. doi: 10.1016/j.ijpharm.2016.09.025.

Ji, S., Thulstrup, P. W., Mu, H., Hansen, S. H., van de Weert, M., Rantanen, J. and Yang, M. (2017) 'Investigation of factors affecting the stability of lysozyme spray dried from ethanol-water solutions', *International Journal of Pharmaceutics*. Elsevier B.V., 534(1–2), pp. 263–271. doi: 10.1016/j.ijpharm.2017.10.021.

Jirgensons, B. (1962) 'Natural organic macromolecules'. Pergamon Press.

Johnson, R. E., Kirchhoff, C. F. and Gaud, H. T. (2002) 'Mannitol-sucrose mixtures - Versatile formulations for protein lyophilization', *Journal of Pharmaceutical Sciences*. John Wiley and

Sons Inc., 91(4), pp. 914–922. doi: 10.1002/jps.10094.

Jonas, J. (1997) 'Cold Denaturation of Proteins', *ACS Symposium Series*, 676, pp. 310–323. doi: 10.3109/10409239009090612.

Jordi Palau (2018) *Freeze Drying Technology*. Available at: http://www.freezedryingtech.com/en/lyophilizator-components.aspx (Accessed: 24 February 2018).

Jovanović, N., Bouchard, A., Hofland, G. W., Witkamp, G. J., Crommelin, D. J. A. and Jiskoot, W. (2004) 'Stabilization of proteins in dry powder formulations using supercritical fluid technology', *Pharmaceutical Research*, pp. 1955–1969. doi: 10.1023/B:PHAM.0000048185.09483.e7.

Jovanović, N., Bouchard, A., Hofland, G. W., Witkamp, G. J., Crommelin, D. J. A. and Jiskoot, W. (2008) 'Stabilization of IgG by supercritical fluid drying: Optimization of formulation and process parameters', *European Journal of Pharmaceutics and Biopharmaceutics*, 68(2), pp. 183–190. doi: 10.1016/j.ejpb.2007.05.001.

Jovanović, N., Bouchard, A., Sutter, M., Van Speybroeck, M., Hofland, G. W., Witkamp, G. J., Crommelin, D. J. A. and Jiskoot, W. (2008) 'Stable sugar-based protein formulations by supercritical fluid drying', *International Journal of Pharmaceutics*, 346(1–2), pp. 102–108. doi: 10.1016/j.ijpharm.2007.06.013.

Jozala, A. F., Geraldes, D. C., Tundisi, L. L., Feitosa, V. de A., Breyer, C. A., Cardoso, S. L., Mazzola, P. G., de Oliveira-Nascimento, L., Rangel-Yagui, C. de O., Magalhães, P. de O., *et al.* (2016) 'Biopharmaceuticals from microorganisms: from production to purification', *Brazilian Journal of Microbiology*. Sociedade Brasileira de Microbiologia, 47, pp. 51–63. doi: 10.1016/j.bjm.2016.10.007.

Junod, S. W. (2007) 'Celebrating a Milestone: FDA's Approval of First Genetically-Engineered Product', *Food and Drug Law Institute*. Available at: www.fda.gov (Accessed: 22 January 2020).

Kaialy, W., Martin, G. P., Ticehurst, M. D., Momin, M. N. and Nokhodchi, A. (2010) 'The enhanced aerosol performance of salbutamol from dry powders containing engineered mannitol as excipient', *International Journal of Pharmaceutics*. Elsevier, 392(1–2), pp. 178–188. doi: 10.1016/j.ijpharm.2010.03.057.

Kammari, R. and Topp, E. M. (2020) 'Effects of Secondary Structure on Solid-State Hydrogen-Deuterium Exchange in Model α-Helix and β-Sheet Peptides', *Molecular pharmaceutics*. NLM (Medline), 17(9), pp. 3501–3512. doi: 10.1021/acs.molpharmaceut.0c00521.

Kaneko, Y., Nimmerjahn, F. and Ravetch, J. V. (2006) 'Anti-Inflammatory Activity of Immunoglobulin G Resulting from Fc Sialylation', *Science*, 313(5787). Available at: http://science.sciencemag.org/content/313/5787/670 (Accessed: 13 August 2017).

Karthikeyan, K., Krishnaswamy, V. R., Lakra, R., Kiran, M. S. and Korrapati, P. S. (2015) 'Fabrication of electrospun zein nanofibers for the sustained delivery of siRNA', *Journal of Materials Science: Materials in Medicine*. Springer Nature, 26(2), pp. 1–8. doi: 10.1007/s10856-015-5439-x.

Kasper, J. C., Wiggenhorn, M., Resch, M. and Friess, W. (2013) 'Implementation and evaluation of an optical fiber system as novel process monitoring tool during lyophilization', *European Journal of Pharmaceutics and Biopharmaceutics*, 83(3), pp. 449–459. doi: 10.1016/j.ejpb.2012.10.009.

Kaszuba, M., McKnight, D., Connah, M. T., McNeil-Watson, F. K. and Nobbmann, U. (2008)

'Measuring sub nanometre sizes using dynamic light scattering', *Journal of Nanoparticle Research*. Springer, 10(5), pp. 823–829. doi: 10.1007/s11051-007-9317-4.

Ke, E. W., Fosdorf, U. and Darby, F. J. (1942) 'Packaging and preserving dried biologicals, pharmaceuticals, and the like'. USA: United States.

Ke, Y., Wang, Y., Ding, W., Leng, Y., Lv, Q., Yang, H., Wang, X. and Ding, B. (2020) 'Effects of inulin on protein in frozen dough during frozen storage', *Food and Function*. Royal Society of Chemistry, 11(9), pp. 7775–7783. doi: 10.1039/d0fo00461h.

Kelly, J. Y. and DeSimone, J. M. (2008) 'Shape-specific, monodisperse nano-molding of protein particles', *Journal of the American Chemical Society*. American Chemical Society, 130(16), pp. 5438–5439. doi: 10.1021/ja8014428.

Kelly, S. M., Jess, T. J. and Price, N. C. (2005) 'How to study proteins by circular dichroism', *Biochimica et Biophysica Acta - Proteins and Proteomics*, 1751(2), pp. 119–139. doi: 10.1016/j.bbapap.2005.06.005.

Kessler, W., Davis, S., Mulhall, P. and Finson, M. (2006) 'System for monitoring a drying process'. United States. Available at: https://patents.google.com/patent/US20060208191A1/en (Accessed: 13 October 2020).

Khairnar, S., Kini, R., Harwalkar, M., salunkhe, K. and Khairnar, S. A. (2013) 'A Review on Freeze Drying Process of Pharmaceuticals TABLE OF CONTENT', *Int. J. Res. Pharm. Sc. International Journal of Research in Int. J. Res. Pharm. Sc*, 4(41), pp. 76–94.

Kho, K., Cheow, W. S., Lie, R. H. and Hadinoto, K. (2010) 'Aqueous re-dispersibility of spray-dried antibiotic-loaded polycaprolactone nanoparticle aggregates for inhaled anti-biofilm therapy', *Powder Technology*. Elsevier, 203(3), pp. 432–439. doi: 10.1016/j.powtec.2010.06.003.

Kim, N. A., Hada, S., Thapa, R. and Jeong, S. H. (2016) 'Arginine as a protein stabilizer and destabilizer in liquid formulations', *International journal of pharmaceutics*. Int J Pharm, 513(1–2), pp. 26–37. doi: 10.1016/J.IJPHARM.2016.09.003.

King, A. H. (1995) 'Encapsulation of Food Ingredients', in, pp. 26–39. doi: 10.1021/bk-1995-0590.ch003.

Kita, Y., Arakawa, T., Lin, T. yin and Timasheff, S. N. (1994) 'Contribution of the Surface Free Energy Perturbation to Protein-Solvent Interactions', *Biochemistry*. American Chemical Society, 33(50), pp. 15178–15189. doi: 10.1021/BI00254A029/ASSET/BI00254A029.FP.PNG_V03.

Knight, M. I. and Chambers, P. J. (2003) 'Problems associated with determining protein concentration: a comparison of techniques for protein estimations', *Molecular biotechnology*. Mol Biotechnol, 23(1), pp. 19–28. doi: 10.1385/MB:23:1:19.

Kobata, A. (2008) 'The N-Linked sugar chains of human immunoglobulin G: Their unique pattern, and their functional roles', *Biochimica et Biophysica Acta (BBA) - General Subjects*, 1780(3), pp. 472–478. doi: 10.1016/j.bbagen.2007.06.012.

Kochs, M., Körber, C., Nunner, B. and Heschel, I. (1991) 'The influence of the freezing process on vapour transport during sublimation in vacuum-freeze-drying', *International Journal of Heat and Mass Transfer*. Pergamon, 34(9), pp. 2395–2408. doi: 10.1016/0017-9310(91)90064-L.

Kolhe, P., Amend, E. and K. Singh, S. (2009) 'Impact of freezing on pH of buffered solutions and consequences for monoclonal antibody aggregation', *Biotechnology Progress*. American Chemical Society (ACS), 26(3), pp. 727–733. doi: 10.1002/btpr.377.

Kong, J. and Yu, S. (2007) 'Fourier Transform Infrared Spectroscopic Analysis of Protein Secondary Structures', *Acta Biochimica et Biophysica Sinica*, 39(8), pp. 549–559. doi: 10.1111/j.1745-7270.2007.00320.x.

Korey, D. J. and Schwartz, J. B. (1989) 'Effects of excipients on the crystallization of pharmaceutical compounds during lyophilization.', *Journal of parenteral science and technology : a publication of the Parenteral Drug Association*, 43(2), pp. 80–3. Available at: http://www.ncbi.nlm.nih.gov/pubmed/2709239 (Accessed: 19 February 2018).

Koshari, S. H. S., Ross, J. L., Nayak, P. K., Zarraga, I. E., Rajagopal, K., Wagner, N. J. and Lenhoff, A. M. (2017) 'Characterization of protein-excipient microheterogeneity in biopharmaceutical solid-state formulations by confocal fluorescence microscopy', *Molecular Pharmaceutics*. American Chemical Society, 14(2), pp. 546–553. doi: 10.1021/acs.molpharmaceut.6b00940.

Kreilgaard, L., Frokjaer, S., Flink, J. M., Randolph, T. W. and Carpenter, J. F. (1999) 'Effects of Additives on the Stability of Humicola Lanuginosa Lipase During Freeze-Drying and Storage in the Dried Solid', *Journal of Pharmaceutical Sciences*. American Chemical Society, 88(3), pp. 281–290. doi: 10.1021/js980399d.

Krimm, S. and Bandekar, J. (1986) 'Vibrational spectroscopy and conformation of peptides, polypeptides, and proteins', *Advances in Protein Chemistry*. Academic Press, 38(C), pp. 181–364. doi: 10.1016/S0065-3233(08)60528-8.

Krittanai, C. and Johnson, W. C. (1997) 'Correcting the circular dichroism spectra of peptides for contributions of absorbing side chains', *Analytical Biochemistry*. Academic Press Inc., 253(1), pp. 57–64. doi: 10.1006/abio.1997.2366.

Kulkarni, S. S., Suryanarayanan, R., Rinella, J. V. and Bogner, R. H. (2018) 'Mechanisms by which crystalline mannitol improves the reconstitution time of high concentration lyophilized protein formulations', *European Journal of Pharmaceutics and Biopharmaceutics*. doi: 10.1016/j.ejpb.2018.07.022.

Kumar, V., Sharma, V. K. and Kalonia, D. S. (2009) 'In situ precipitation and vacuum drying of interferon alpha-2a: Development of a single-step process for obtaining dry, stable protein formulation', *International Journal of Pharmaceutics*. Elsevier, 366(1–2), pp. 88–98. doi: 10.1016/j.ijpharm.2008.09.001.

Kunugi, S. and Tanaka, N. (2002) 'Cold denaturation of proteins under high pressure', *Biochimica et Biophysica Acta - Protein Structure and Molecular Enzymology*, pp. 329–344. doi: 10.1016/S0167-4838(01)00354-5.

Kureha (2019) *KUREHA Microsphere* . Available at: https://www.kureha.co.jp/en/business/material/microspheres.html (Accessed: 2 August 2021).

Kuu, W. Y., Nail, S. L. and Sacha, G. (2009) 'Rapid determination of vial heat transfer parameters using tunable diode laser absorption spectroscopy (TDLAS) in response to step-changes in pressure set-point during freeze-drying', *Journal of Pharmaceutical Sciences*. John Wiley and Sons Inc., 98(3), pp. 1136–1154. doi: 10.1002/jps.21478.

Kuu, W. Y., Obryan, K. R., Hardwick, L. M. and Paul, T. W. (2011) 'Product mass transfer resistance directly determined during freeze-drying cycle runs using tunable diode laser absorption spectroscopy (TDLAS) and pore diffusion model', *Pharmaceutical Development and Technology*. Taylor & Francis, 16(4), pp. 343–357. doi: 10.3109/10837451003739263.

Lam, P. and Patapoff, T. W. (2011) 'An improved method for visualizing the morphology of lyophilized product cakes', *PDA Journal of Pharmaceutical Science and Technology*, 65(4),

pp. 425–430. doi: 10.5731/pdajpst.2011.00749.

Lammens, J., Mortier, S. T. F. C., De Meyer, L., Vanbillemont, B., Van Bockstal, P. J., Van Herck, S., Corver, J., Nopens, I., Vanhoorne, V., De Geest, B. G., *et al.* (2018) 'The relevance of shear, sedimentation and diffusion during spin freezing, as potential first step of a continuous freeze-drying process for unit doses', *International Journal of Pharmaceutics*. doi: 10.1016/j.ijpharm.2018.01.009.

Langford, A., Bhatnagar, B., Walters, R., Tchessalov, S. and Ohtake, S. (2017) 'Drying of biopharmaceuticals: Recent developments, new technologies and future direction', *Drying Technology*. Taylor & Francis, 19(1), pp. 15–25. doi: 10.11301/jsfe.18514.

Larrain, R., Tagle, L. H. and Diaz, F. R. (1981) 'Glass transition temperature-molecular weight relation for poly(hexamethylene perchloroterephthalamide)', *Polymer Bulletin*. Springer-Verlag, 4(8), pp. 487–490. doi: 10.1007/BF00255705.

Leach, S. J. and Scheraga, H. A. (1960) 'Effect of Light Scattering on Ultraviolet Difference Spectra', *Journal of the American Chemical Society*. American Chemical Society, 82(18), pp. 4790–4792. doi: 10.1021/ja01503a008.

Lechuga-Ballesteros, D., Charan, C., Stults, C. L. M., Stevenson, C. L., Miller, D. P., Vehring, R., Tep, V. and Kuo, M. C. (2008) 'Trileucine improves aerosol performance and stability of spray-dried powders for inhalation', *Journal of Pharmaceutical Sciences*. Elsevier Masson SAS, 97(1), pp. 287–302. doi: 10.1002/jps.21078.

Lee, G. (2002) 'Spray-drying of proteins.', in Carpenter, J. F. and Manning, M. C. (eds) *Rational Design of Stable Protein Formulations*. 1st edn. Springer US, pp. 135–158. doi: 10.1007/978-1-4615-0557-0_6.

Lee, J. H., Kim, M. J., Yoon, H., Shim, C. R., Ko, H. A., Cho, S. A., Lee, D. and Khang, G. (2013) 'Enhanced dissolution rate of celecoxib using PVP and/or HPMC-based solid dispersions prepared by spray drying method', *Journal of Pharmaceutical Investigation*. Springer, 43(3), pp. 205–213. doi: 10.1007/s40005-013-0067-2.

Lerbret, A., Affouard, F., Bordat, P., Hédoux, A., Guinet, Y. and Descamps, M. (2008) 'Molecular dynamics simulations of lysozyme in water/sugar solutions', *Chemical Physics*. North-Holland, 345(2–3), pp. 267–274. doi: 10.1016/j.chemphys.2007.09.011.

Leuenberger, H. (2002) 'Spray Freeze-drying – The Process of Choice for Low Water Soluble Drugs?', *Journal of Nanoparticle Research*. Kluwer Academic Publishers, 4(1/2), pp. 111–119. doi: 10.1023/A:1020135603052.

Levitt, M. and Greer, J. (1977) 'Automatic identification of secondary structure in globular proteins', *Journal of Molecular Biology*. Academic Press, 114(2), pp. 181–239. doi: 10.1016/0022-2836(77)90207-8.

Lewis, L. M., Johnson, R. E., Oldroyd, M. E., Ahmed, S. S., Joseph, L., Saracovan, I. and Sinha, S. (2010) 'Characterizing the Freeze–Drying Behavior of Model Protein Formulations', *AAPS PharmSciTech*, II(4), pp. 1580–1590. doi: 10.1208/s12249-010-9530-9.

Li, E. (2015) 'Biologic, Biosimilar, and Interchangeable Biologic Drug Products. Background Paper Prepared for the 2015–2016 APhA Policy Committee.' Available at: https://www.pharmacist.com/sites/default/files/files/Biosimilar Policy Background Paper - FINAL.PDF (Accessed: 23 June 2017).

Li, J., Garg, M., Shah, D. and Rajagopalan, R. (2010) 'Solubilization of aromatic and hydrophobic moieties by arginine in aqueous solutions', *The Journal of Chemical Physics*. American Institute of PhysicsAIP, 133(5), p. 054902. doi: 10.1063/1.3469790.

Liao, X., Krishnamurthy, R. and Suryanarayanan, R. (2007) 'Influence of processing conditions on the physical state of mannitol - Implications in freeze-drying', *Pharmaceutical Research*. Springer, 24(2), pp. 370–376. doi: 10.1007/s11095-006-9158-3.

Liao, Y.-H., Brown, M. B., Quader, A. and Martin, G. P. (2003) 'Investigation of the physical properties of spray-dried stabilised lysozyme particles', *Journal of Pharmacy and Pharmacology*. Wiley-Blackwell, 55(9), pp. 1213–1221. doi: 10.1211/0022357021611.

Liao, Y. H., Brown, M. B. and Martin, G. P. (2004) 'Investigation of the stabilisation of freeze-dried lysozyme and the physical properties of the formulations', *European Journal of Pharmaceutics and Biopharmaceutics*, 58(1), pp. 15–24. doi: 10.1016/j.ejpb.2004.03.020.

Liao, Y. H., Brown, M. B., Nazir, T., Quader, A. and Martin, G. P. (2002) 'Effects of sucrose and trehalose on the preservation of the native structure of spray-dried lysozyme', *Pharmaceutical Research*, 19(12), pp. 1847–1853. doi: 10.1023/A:1021445608807.

Liapis, A. I. and Bruttini, R. (2008) 'Exergy analysis of freeze drying of pharmaceuticals in vials on trays', *International Journal of Heat and Mass Transfer*, 51(15–16), pp. 3854–3868. doi: 10.1016/j.ijheatmasstransfer.2007.11.048.

LightHouse Instruments (2018) *FMS Pressure/Moisture Headspace Analysis* . Available at: https://www.lighthouseinstruments.com/fms-pressure-moisture-headspace-analysis (Accessed: 7 April 2020).

Lin, T. P. and Hsu, C. C. (2002) 'Determination of Residual Moisture in Lyophilized Protein Pharmaceuticals Using a Rapid and Non-Invasive Method: Near Infrared Spectroscopy', *PDA Journal of Pharmaceutical Science and Technology*, 56(4), pp. 196–205. Available at: https://journal.pda.org/content/56/4/196 (Accessed: 12 February 2021).

Liquidia Corporation (2021) *PRINT® Technology*. Available at: https://liquidia.com/print-technology/ (Accessed: 20 September 2020).

Liu, Y., Zhao, Y. and Feng, X. (2008) 'Exergy analysis for a freeze-drying process', *Applied Thermal Engineering*, 28(7), pp. 675–690. doi: 10.1016/j.applthermaleng.2007.06.004.

Liu, Z. Q., Zhou, J. H., Zeng, Y. L. and Ouyang, X. L. (2004) 'The enhancement and encapsulation of Agaricus bisporus flavor', *Journal of Food Engineering*, 65(3), pp. 391–396. doi: 10.1016/j.jfoodeng.2004.01.038.

Long, B., Ryan, K. M. and Padrela, L. (2019) 'From batch to continuous — New opportunities for supercritical CO2 technology in pharmaceutical manufacturing', *European Journal of Pharmaceutical Sciences*. Elsevier B.V., 137, p. 104971. doi: 10.1016/j.ejps.2019.104971.

Lovalenti, P. M. and Truong-Le, V. (2020) 'Foam Drying', in Ohtake, S., Iztutsu, K.-I., and Lechuga-Ballesteros, D. (eds) *Drying Technologies for Biotechnology and Pharmaceutical Applications*. Wiley, pp. 257–282. doi: 10.1002/9783527802104.ch10.

Lowe, D., Mehta, M., Govindan, G. and Gupta, K. (2018) *Spray Freeze-Drying Technology: Enabling Flexibility of Supply Chain and Drug-Product Presentation for Biologics - BioProcess InternationalBioProcess International*, *BioProcess International*. Available at: https://bioprocessintl.com/manufacturing/supply-chain/spray-freeze-drying-technology-enabling-flexibility-of-supply-chain-and-drug-product-presentation-for-biologics/ (Accessed: 29 January 2021).

Lowry, O. H., Rosebrough, N. J., FARR, A. L. and RANDALL, R. J. (1951) 'Protein measurement with the Folin phenol reagent.', *The Journal of biological chemistry*, 193(1), pp. 265–275. doi: 10.1016/0922-338X(96)89160-4.

Lu, X. and Pikal, M. J. (2004) 'Freeze-Drying of Mannitol-Trehalose-Sodium Chloride-Based Formulations: The Impact of Annealing on Dry Layer Resistance to Mass Transfer and Cake Structure', *Pharmaceutical Development and Technology*. Taylor & Francis, 9(1), pp. 85–95. doi: 10.1081/PDT-120027421.

Lueckel, B., Bodmer, D., Helk, B. and Leuenberger, H. (1998) 'Formulations of sugars with amino acids or mannitol - Influence of concentration ratio on the properties of the freeze-concentrate and the lyophilizate', *Pharmaceutical Development and Technology*. Marcel Dekker Inc., 3(3), pp. 325–336. doi: 10.3109/10837459809009860.

Luo, S., Huang, C. Y. F., McClelland, J. F. and Graves, D. J. (1994) 'A study of protein secondary structure by Fourier transform infrared/photoacoustic spectroscopy and its application for recombinant proteins', *Analytical Biochemistry*. Academic Press, 216(1), pp. 67–76. doi: 10.1006/abio.1994.1009.

Luy, B., Plitzko, M. and Struschka, M. (2018) 'Process line for the production of freeze-dried particles'. USA.

Luy, B. and Stamato, H. (2020) 'Spray Freeze Drying', in Ohtake, S., Iztutsu, K.-I., and Lechuga-Ballesteros, D. (eds) *Drying Technologies for Biotechnology and Pharmaceutical Applications*. Wiley, pp. 217–237. doi: 10.1002/9783527802104.ch8.

LyophilizationWorld (2020) *The Lyophilization Basics*. Available at: https://www.lyophilizationworld.com/post/2020/03/19/the-lyophilization-process (Accessed: 18 March 2021).

Maa, Y.-F. and Hsu, C. C. (1997) *Protein Denaturation by Combined Effect of Shear and Air-Liquid Interface*.

Maa, Y.-F., Nguyen, P.-A. T. and Hsu, S. W. (1998) 'Spray-Drying of Air–Liquid Interface Sensitive Recombinant Human Growth Hormone', *Journal of Pharmaceutical Sciences*. Wiley-Blackwell, 87(2), pp. 152–159. doi: 10.1021/js970308x.

Maa, Y. F., Costantino, H. R., Nguyen, P. A. and Hsu, C. C. (1997) 'The effect of operating and formulation variables on the morphology of spray-dried protein particles', *Pharmaceutical Development and Technology*. Informa Healthcare, 2(3), pp. 213–223. doi: 10.3109/10837459709031441.

Maa, Y. F. and Hsu, C. C. (1997) 'Protein denaturation by combined effect of shear and air-liquid interface', *Biotechnology and Bioengineering*. John Wiley & Sons Inc, 54(6), pp. 503–512. doi: 10.1002/(SICI)1097-0290(19970620)54:6<503::AID-BIT1>3.0.CO;2-N.

Maa, Y. F., Nguyen, P. A. T. and Hsu, S. W. (1998) 'Spray-drying of air-liquid interface sensitive recombinant human growth hormone', *Journal of Pharmaceutical Sciences*. John Wiley and Sons Inc., 87(2), pp. 152–159. doi: 10.1021/js970308x.

MacLeod, C. S., McKittrick, J. A., Hindmarsh, J. P., Johns, M. L. and Wilson, D. I. (2006) 'Fundamentals of spray freezing of instant coffee', *Journal of Food Engineering*. Elsevier, 74(4), pp. 451–461. doi: 10.1016/J.JFOODENG.2005.03.034.

Mahler, H. C., Friess, W., Grauschopf, U. and Kiese, S. (2009) 'Protein aggregation: Pathways, induction factors and analysis', *Journal of Pharmaceutical Sciences*. John Wiley and Sons Inc., pp. 2909–2934. doi: 10.1002/jps.21566.

Mahler, H. C., Müller, R., Frieß, W., Delille, A. and Matheus, S. (2005) 'Induction and analysis of aggregates in a liquid IgG1-antibody formulation', *European Journal of Pharmaceutics and Biopharmaceutics*. Elsevier, 59(3), pp. 407–417. doi: 10.1016/j.ejpb.2004.12.004.

Malvern Panalytical (2011) ‘Dynamic Light Scattering’, *Inform White Paper*, pp. 1–6.

Malvern Panalytical (2014) *Influence of Concentration Effects and Particle Interactions on DLS Analysis of Bioformulations*, *News Medical Life Sciences*. Available at: https://www.news-medical.net/whitepaper/20141218/Influence-of-Concentration-Effects-and-Particle-Interactions-on-DLS-Analysis-of-Bioformulations.aspx (Accessed: 18 July 2022).

Malvern Panalytical (2018) *Multi-angle Dynamic Light Scattering (MADLS) on the Zetasizer Ultra – How it Works | Malvern Panalytical*. Available at: https://www.malvernpanalytical.com/en/learn/knowledge-center/technical-notes/TN180719HowItWorksMADLS.html (Accessed: 22 June 2022).

Malvern Panalytical (2022) *Zetasizer Ultra*. Available at: https://www.malvernpanalytical.com/en/products/product-range/zetasizer-range/zetasizer-ultra (Accessed: 7 April 2022).

Malzert, A., Boury, F., Renard, D., Robert, P., Proust, J. E. and Benoît, J. P. (2002) ‘Influence of some formulation parameters on lysozyme adsorption and on its stability in solution’, *International Journal of Pharmaceutics*. Elsevier, 242(1–2), pp. 405–409. doi: 10.1016/S0378-5173(02)00226-0.

Mann, K. (2007) ‘The chicken egg white proteome’, *Proteomics*, 7(19), pp. 3558–3568. doi: 10.1002/pmic.200700397.

Marianayagam, N. J., Sunde, M. and Matthews, J. M. (2004) ‘The power of two: protein dimerization in biology’. doi: 10.1016/j.tibs.2004.09.006.

Markova, N., Cairns, S., Jankevics-Jones, H., Kaszuba, M., Caputo, F. and Parot, J. (2021) ‘Biophysical Characterization of Viral and Lipid-Based Vectors for Vaccines and Therapeutics with Light Scattering and Calorimetric Techniques’, *Vaccines 2022, Vol. 10, Page 49*. Multidisciplinary Digital Publishing Institute, 10(1), p. 49. doi: 10.3390/VACCINES10010049.

Martins, E., Cnossen, D. C., Silva, C. R. J., Vakarelova, M. and Carvalho, A. F. (2019) ‘Short communication: Effect of lactose on the spray drying of Lactococcus lactis in dairy matrices’, *Journal of Dairy Science*. Elsevier Inc., 102(11), pp. 9763–9766. doi: 10.3168/jds.2019-16939.

Massant, J., Fleurime, S., Batens, M., Vanhaerents, H. and Van den Mooter, G. (2020) ‘Formulating monoclonal antibodies as powders for reconstitution at high concentration using spray-drying: Trehalose/amino acid combinations as reconstitution time reducing and stability improving formulations’, *European Journal of Pharmaceutics and Biopharmaceutics*. Elsevier B.V., 156, pp. 131–142. doi: 10.1016/j.ejpb.2020.08.019.

Masters, K. (1985) *Spray drying handbook.* 4th edn, *Spray drying handbook.* 4th edn. George Godwin Ltd. Available at: https://www.cabdirect.org/cabdirect/abstract/19880428422 (Accessed: 12 March 2018).

Masters, K (1991) *The spray drying Handbook (pp. 329-556)*. 5th edn. Edited by Keith Masters. Longman Scientific & Technical, 1991. Available at: https://books.google.ie/books/about/Spray_Drying_Handbook.html?id=kLtTAAAAMAAJ&redir_esc=y (Accessed: 3 May 2020).

Matsuo, K., Sakurada, Y., Yonehara, R., Kataoka, M. and Gekko, K. (2007) ‘Secondary-structure analysis of denatured proteins by vacuum-ultraviolet circular dichroism spectroscopy’, *Biophysical Journal*. Biophysical Society, 92(11), pp. 4088–4096. doi: 10.1529/biophysj.106.103515.

Matveev, Y. I., Grinberg, V. Y., Sochava, I. V. and Tolstoguzov, V. B. (1997) ‘Glass transition

temperature of proteins. Calculation based on the additive contribution method and experimental data', *Food Hydrocolloids*. doi: 10.1016/S0268-005X(97)80020-3.

Maury, M., Murphy, K., Kumar, S., Mauerer, A. and Lee, G. (2005) 'Spray-drying of proteins: Effects of sorbitol and trehalose on aggregation and FT-IR amide I spectrum of an immunoglobulin G', *European Journal of Pharmaceutics and Biopharmaceutics*. doi: 10.1016/j.ejpb.2004.07.010.

Mehta, D. B., Corbo, D. C. and Iqbal, K. (1996) 'Spray dried erythropoietin'. United States. Available at: https://patents.google.com/patent/US6001800A/en (Accessed: 4 May 2020).

Meister, E. and Gieseler, H. (2009) 'Freeze-dry microscopy of protein/sugar mixtures: Drying behavior, interpretation of collapse temperatures and a comparison to corresponding glass transition data', *Journal of Pharmaceutical Sciences*. John Wiley and Sons Inc., 98(9), pp. 3072–3087. doi: 10.1002/jps.21586.

Meister, E., Šašić, S. and Gieseler, H. (2009) 'Freeze-dry microscopy: Impact of nucleation temperature and excipient concentration on collapse temperature data', *AAPS PharmSciTech*. AAPS PharmSciTech, 10(2), pp. 582–588. doi: 10.1208/s12249-009-9245-y.

Mensink, M. A., Van Bockstal, P. J., Pieters, S., De Meyer, L., Frijlink, H. W., Van Der Voort Maarschalk, K., Hinrichs, W. L. J. and De Beer, T. (2015) 'In-line near infrared spectroscopy during freeze-drying as a tool to measure efficiency of hydrogen bond formation between protein and sugar, predictive of protein storage stability', *International Journal of Pharmaceutics*. Elsevier B.V., 496(2), pp. 792–800. doi: 10.1016/j.ijpharm.2015.11.030.

Mensink, M. A., Frijlink, H. W., van der Voort Maarschalk, K. and Hinrichs, W. L. J. (2017a) 'How sugars protect proteins in the solid state and during drying (review): Mechanisms of stabilization in relation to stress conditions', *European Journal of Pharmaceutics and Biopharmaceutics*. Elsevier B.V., pp. 288–295. doi: 10.1016/j.ejpb.2017.01.024.

Mensink, M. A., Frijlink, H. W., van der Voort Maarschalk, K. and Hinrichs, W. L. J. (2017b) 'How sugars protect proteins in the solid state and during drying (review): Mechanisms of stabilization in relation to stress conditions', *European Journal of Pharmaceutics and Biopharmaceutics*. Elsevier B.V., pp. 288–295. doi: 10.1016/j.ejpb.2017.01.024.

Mensink, M. A., Nethercott, M. J., Hinrichs, W. L. J., van der Voort Maarschalk, K., Frijlink, H. W., Munson, E. J. and Pikal, M. J. (2016) 'Influence of Miscibility of Protein-Sugar Lyophilizates on Their Storage Stability', *AAPS Journal*. Springer New York LLC, 18(5), pp. 1225–1232. doi: 10.1208/s12248-016-9937-7.

De Meyer, L., Van Bockstal, P. J., Corver, J., Vervaet, C., Remon, J. P. and De Beer, T. (2015) 'Evaluation of spin freezing versus conventional freezing as part of a continuous pharmaceutical freeze-drying concept for unit doses', *International Journal of Pharmaceutics*. Elsevier B.V., 496(1), pp. 75–85. doi: 10.1016/j.ijpharm.2015.05.025.

Mezhericher, M. (2011) *Theoretical modelling of spray drying processes : Volume 1 ; Drying kinetics, two and three dimensional CFD modelling*. Lambert Academic Publ. Available at: https://www.researchgate.net/publication/283317044_Theoretical_modelling_of_spray_drying_processes_Drying_kinetics_two_and_three_dimensional_CFD_modelling (Accessed: 22 March 2018).

Midatech Pharma (2021) *Midatech's Q-Sphera technology*. Available at: https://www.midatechpharma.com/technology (Accessed: 2 August 2021).

Miles, A. J., Janes, R. W., Brown, A., Clarke, D. T., Sutherland, J. C., Tao, Y., Wallace, B. A. and Hoffmann, S. V. (2008) 'Light flux density threshold at which protein denaturation is induced

by synchrotron radiation circular dichroism beamlines', *Journal of Synchrotron Radiation*. International Union of Crystallography, 15(4), pp. 420–422. doi: 10.1107/S0909049508009606.

Miles, A. J. and Wallace, B. A. (2006) 'Synchrotron radiation circular dichroism spectroscopy of proteins and applications in structural and functional genomics', *Chemical Society Reviews*. Royal Society of Chemistry, pp. 39–51. doi: 10.1039/b316168b.

Miles, A. J. and Wallace, B. A. (2020) 'Biopharmaceutical applications of protein characterisation by circular dichroism spectroscopy', in *Biophysical Characterization of Proteins in Developing Biopharmaceuticals*. Elsevier, pp. 123–152. doi: 10.1016/b978-0-444-64173-1.00006-8.

Miller, D. P., Tan, T., Tarara, T. E., Nakamura, J., Malcolmson, R. J. and Weers, J. G. (2015) 'Physical Characterization of Tobramycin Inhalation Powder: I. Rational Design of a Stable Engineered-Particle Formulation for Delivery to the Lungs', *Molecular Pharmaceutics*. American Chemical Society, 12(8), pp. 2582–2593. doi: 10.1021/acs.molpharmaceut.5b00147.

Milne, J. (2016) 'Biopharmaceutical Industry Regulation and Management. Introduction to the Course.'

Mishra, M. (2015) 'Handbook of encapsulation and controlled release', *CRC Press*.

Moeller, E. H. and Jorgensen, L. (2008) 'Alternative routes of administration for systemic delivery of protein pharmaceuticals', *Drug Discovery Today: Technologies*. Elsevier, 5(2–3), pp. e89–e94. doi: 10.1016/J.DDTEC.2008.11.005.

Molina, C., Kaialy, W. and Nokhodchi, A. (2019) 'The crucial role of leucine concentration on spray dried mannitol-leucine as a single carrier to enhance the aerosolization performance of Albuterol sulfate', *Journal of Drug Delivery Science and Technology*. Editions de Sante, 49, pp. 97–106. doi: 10.1016/j.jddst.2018.11.007.

Mönckedieck, M., Kamplade, J., Fakner, P., Urbanetz, N. A., Walzel, P., Steckel, H. and Scherließ, R. (2017) 'Spray drying of mannitol carrier particles with defined morphology and flow characteristics for dry powder inhalation', *Drying Technology*. Taylor and Francis Inc., 35(15), pp. 1843–1857. doi: 10.1080/07373937.2017.1281291.

Montserrat, S. and Colomer, P. (1984) 'The effect of the molecular weight on the glass transition temperature in amorphous poly(ethylene terephthalate)', *Polymer Bulletin*. Springer-Verlag, 12(2), pp. 173–180. doi: 10.1007/BF00263341.

Moorthy, B. S., Schultz, S. G., Kim, S. G. and Topp, E. M. (2014) 'Predicting protein aggregation during storage in lyophilized solids using solid state amide hydrogen/deuterium exchange with mass spectrometric analysis (ssHDX-MS)', *Molecular Pharmaceutics*. American Chemical Society, 11(6), pp. 1869–1879. doi: 10.1021/mp500005v.

Moorthy, B. S., Zarraga, I. E., Kumar, L., Walters, B. T., Goldbach, P., Topp, E. M. and Allmendinger, A. (2018) 'Solid-State Hydrogen-Deuterium Exchange Mass Spectrometry: Correlation of Deuterium Uptake and Long-Term Stability of Lyophilized Monoclonal Antibody Formulations', *Molecular Pharmaceutics*. American Chemical Society, 15(1), pp. 1–11. doi: 10.1021/acs.molpharmaceut.7b00504.

Moreau, D. L. and Rosenberg, M. (1996) 'Oxidative Stability of Anhydrous Milkfat Microencapsulated in Whey Proteins', *Journal of Food Science*, 61(1), pp. 39–43. doi: 10.1111/j.1365-2621.1996.tb14721.x.

Morgan, B. A., Manser, M., Jeyanathan, M., Xing, Z., Cranston, E. D. and Thompson, M. R. (2020) 'Effect of Shear Stresses on Adenovirus Activity and Aggregation during Atomization to

Produce Thermally Stable Vaccines by Spray Drying', *ACS Biomaterials Science and Engineering*. American Chemical Society, 6(7), pp. 4304–4313. doi: 10.1021/acsbiomaterials.0c00317.

Mörsky, P. (1983) 'Turbidimetric determination of lysozyme with Micrococcus lysodeikticus cells: Reexamination of reaction conditions', *Analytical Biochemistry*, 128(1), pp. 77–85. doi: 10.1016/0003-2697(83)90347-0.

Morton, S. W., Herlihy, K. P., Shopsowitz, K. E., Deng, Z. J., Chu, K. S., Bowerman, C. J., Desimone, J. M. and Hammond, P. T. (2013) 'Scalable manufacture of built-to-order nanomedicine: Spray-assisted layer-by-layer functionalization of PRINT nanoparticles', *Advanced Materials*, 25(34), pp. 4707–4713. doi: 10.1002/adma.201302025.

Moussa, E. M., Panchal, J. P., Moorthy, B. S., Blum, J. S., Joubert, M. K., Narhi, L. O. and Topp, E. M. (2016) 'Immunogenicity of Therapeutic Protein Aggregates', *Journal of Pharmaceutical Sciences*. Elsevier B.V., pp. 417–430. doi: 10.1016/j.xphs.2015.11.002.

Mozhaev, V. V. (1993) 'Mechanism-based strategies for protein thermostabilization', *Trends in Biotechnology*, 11(3), pp. 88–95. doi: 10.1016/0167-7799(93)90057-G.

Mukherjee, S., Chowdhury, P. and Gai, F. (2009) 'Effect of dehydration on the aggregation kinetics of two amyloid peptides', *Journal of Physical Chemistry B*. American Chemical Society, 113(2), pp. 531–535. doi: 10.1021/jp809817s.

Mumenthaler, M., Hsu, C. C. and Pearlman, R. (1994) 'Feasibility Study on Spray-Drying Protein Pharmaceuticals: Recombinant Human Growth Hormone and Tissue-Type Plasminogen Activator', *Pharmaceutical Research: An Official Journal of the American Association of Pharmaceutical Scientists*, 11(1), pp. 12–20. doi: 10.1023/A:1018929224005.

Munir, M., Jena, L., Kett, V. L., Dunne, N. J. and McCarthy, H. O. (2022) 'Spray drying: Inhalable powders for pulmonary gene therapy', *Biomaterials Advances*. Elsevier, 133, p. 112601. doi: 10.1016/J.MSEC.2021.112601.

Mutukuri, T. T., Wilson, N. E., Taylor, L. S., Topp, E. M. and Zhou, Q. T. (2021) 'Effects of drying method and excipient on the structure and physical stability of protein solids: Freeze drying vs. spray freeze drying', *International Journal of Pharmaceutics*. Elsevier, 594, p. 120169. doi: 10.1016/j.ijpharm.2020.120169.

Naiim, M., Boualem, A., Ferre, C., Jabloun, M., Jalocha, A. and Ravier, P. (2015) 'Multiangle dynamic light scattering for the improvement of multimodal particle size distribution measurements', *Soft Matter*. Royal Society of Chemistry, 11(1), pp. 28–32. doi: 10.1039/c4sm01995d.

Nail, S., Tchessalov, S., Shalaev, E., Ganguly, A., Renzi, E., Dimarco, F., Wegiel, L., Ferris, S., Kessler, W., Pikal, M., *et al.* (2017) 'Recommended Best Practices for Process Monitoring Instrumentation in Pharmaceutical Freeze Drying—2017', *AAPS PharmSciTech*. Springer New York LLC, 18(7), pp. 2379–2393. doi: 10.1208/s12249-017-0733-1.

Nail, S. L. and Gatin, L. A. (1993) 'Freeze-drying: principles and practice.', in Avis, K. E., Lieberman, H. A., and Lechman, L. (eds) *Pharmaceutical Dosage Forms: Parenteral Medications*. 2nd edn. New York, pp. 163–233.

Nail, S. L. and Johnson, W. (1992) 'Methodology for in-process determination of residual water in freeze-dried products.', *Developments in Biological Standardization*. Available at: https://pubmed.ncbi.nlm.nih.gov/1592164/ (Accessed: 10 October 2020).

Nail, S. L. and Searles, J. A. (2008) *Elements of Quality by Design in Development and Scale-Up of Freeze-Dried Parenterals*, *BioPharma International*. Available at:

https://www.baxterbiopharmasolutions.com/pdf/publications/ElementsofQualitybyDesign.pdf (Accessed: 31 March 2021).

Namaldi, A., Çalik, P. and Uludag, Y. (2006) 'Effects of spray drying temperature and additives on the stability of serine alkaline protease powders', *Drying Technology*. Taylor & Francis Group , 24(11), pp. 1495–1500. doi: 10.1080/07373930600961108.

Nasser, S., Hédoux, A., Giuliani, A., Le Floch-Fouéré, C., Santé-Lhoutellier, V., de Waele, I. and Delaplace, G. (2018) 'Investigation of secondary structure evolution of micellar casein powder upon aging by FTIR and SRCD: consequences on solubility', *Journal of the Science of Food and Agriculture*. John Wiley and Sons Ltd, 98(6), pp. 2243–2250. doi: 10.1002/jsfa.8711.

NCT03626714 (2019) *Safety and Pharmacokinetics of Sustained-release Depot Tacrolimus: A First-in-human*. Available at: https://clinicaltrials.gov/ct2/show/NCT03626714?term=auritec&rank=1 (Accessed: 2 August 2021).

Nelson, D. L. and Cox, M. M. (2012) 'Amino Acids, Peptides and Proteins', in *Lehninger Principles of Biochemistry*, pp. 75–115.

Nemzer, L. R., Flanders, B. N., Schmit, J. D., Chakrabarti, A. and Sorensen, C. M. (2013) 'Ethanol shock and lysozyme aggregation', *Soft Matter*. Royal Society of Chemistry, 9(7), pp. 2187–2196. doi: 10.1039/c2sm27124a.

Nguyen, T. Van, Pham, N. Van, Mai, H. H., Duong, D. C., Le, H. H., Sapienza, R. and Ta, V. D. (2019) 'Protein-based microsphere biolasers fabricated by dehydration', *Soft Matter*. Royal Society of Chemistry, 15(47), pp. 9721–9726. doi: 10.1039/c9sm01610d.

Nguyen, T. Van and Ta, V. D. (2020) 'High-quality factor, biological microsphere and microhemisphere lasers fabricated by a single solution process', *Optics Communications*. Elsevier B.V., 465, p. 125647. doi: 10.1016/j.optcom.2020.125647.

Nireesha, G., Divya, L., Sowmya, C., Venkateshan, N., Niranjan Babu, M. and Lavakumar, V. (2013) 'Lyophilization/Freeze Drying -An Review', *Ijntps*, 3(4), pp. 87–98.

Nitika, N., Chhabra, H. and Rathore, A. S. (2021) 'Raman spectroscopy for in situ, real time monitoring of protein aggregation in lyophilized biotherapeutic products', *International Journal of Biological Macromolecules*. Elsevier, 179, pp. 309–313. doi: 10.1016/j.ijbiomac.2021.02.214.

Niven, R. W., Ip, A. Y., Mittelman, S., Prestrelski, S. J. and Arakawa, T. (1995) 'Some Factors Associated with the Ultrasonic Nebulization of Proteins', *Pharmaceutical Research: An Official Journal of the American Association of Pharmaceutical Scientists*. Springer, 12(1), pp. 53–59. doi: 10.1023/A:1016282502954.

Niven, R. W., Prestrelski, S. J., Treuheit, M. J., Ip, A. Y. and Arakawa, T. (1996) 'Protein nebulization II. Stabilization of G-CSF to air-jet nebulization and the role of protectants', *International Journal of Pharmaceutics*. Elsevier B.V., 127(2), pp. 191–201. doi: 10.1016/0378-5173(95)04209-1.

Noble, J. E. and Bailey, M. J. A. (2009) 'Chapter 8 Quantitation of Protein', in *Methods in Enzymology*. Academic Press Inc., pp. 73–95. doi: 10.1016/S0076-6879(09)63008-1.

Ohori, R., Akita, T. and Yamashita, C. (2021) 'Scale-up/tech transfer issues of the lyophilization cycle for biopharmaceuticals and recently emerging technologies and approaches', *https://doi.org/10.1080/07373937.2021.2015372*. Taylor & Francis. doi: 10.1080/07373937.2021.2015372.

Ohori, R. and Yamashita, C. (2017) 'Effects of temperature ramp rate during the primary drying process on the properties of amorphous-based lyophilized cake, Part 1: Cake characterization, collapse temperature and drying behavior', *Journal of Drug Delivery Science and Technology*. Editions de Sante, 39, pp. 131–139. doi: 10.1016/j.jddst.2017.03.013.

Ohtake, S., Martin, R., Saxena, A., Pham, B., Chiueh, G., Osorio, M., Kopecko, D., Xu, D. Q., Lechuga-Ballesteros, D. and Truong-Le, V. (2011) 'Room temperature stabilization of oral, live attenuated Salmonella enterica serovar Typhi-vectored vaccines', *Vaccine*, 29(15), pp. 2761–2771. doi: 10.1016/j.vaccine.2011.01.093.

Ohtake, S., Martin, R. A., Saxena, A., Lechuga-ballesteros, D., Santiago, A. E., Barry, E. M. and Truong-Le, V. (2011) 'Formulation and stabilization of Francisella tularensis Live Vaccine Strain', *Journal of Pharmaceutical Sciences*. John Wiley and Sons Inc., 100(8), pp. 3076–3087. doi: 10.1002/jps.22563.

Oliveira, A. and Poco, J. G. R. (2013) 'Nano spray drying as an innovative technology for encapsulating hydrophilic active pharmaceutical ingredients (API) Design o Chemical Processes View project Síntese e aplicação de Resinas Poliméricas View project', *Article in Journal of Nanomedicine & Nanotechnology*. doi: 10.4172/2157-7439.1000186.

Olson, B. J. S. C. and Markwell, J. (2007) 'Assays for Determination of Protein Concentration', *Current Protocols in Pharmacology*. John Wiley & Sons, Ltd, 38(1), p. A.3A.1-A.3A.29. doi: 10.1002/0471141755.PHA03AS38.

Onuma, K. and Inaka, K. (2008) 'Lysozyme dimer association: Similarities and differences compared with lysozyme monomer association', *Journal of Crystal Growth*. North-Holland, 310(6), pp. 1174–1181. doi: 10.1016/j.jcrysgro.2007.12.029.

Oughton, D. M. ., Smith, P. R. . and MacMichael D.B.A (1999) 'Freeze-drying process and apparatus'.

Owczarz, M. and Arosio, P. (2014) 'Sulfate anion delays the self-assembly of human insulin by modifying the aggregation pathway', *Biophysical Journal*. Biophysical Society, 107(1), pp. 197–207. doi: 10.1016/j.bpj.2014.05.030.

Pan, H. W., Seow, H. C., Lo, J. C. K., Guo, J., Zhu, L., Leung, S. W. S., Zhang, C. and Lam, J. K. W. (2022) 'Spray-Dried and Spray-Freeze-Dried Powder Formulations of an Anti-Interleukin-4Rα Antibody for Pulmonary Delivery', *Pharmaceutical Research*. Springer, 39(9), pp. 2291–2304. doi: 10.1007/S11095-022-03331-W.

Panchal, J., Kotarek, J., Marszal, E. and Topp, E. M. (2014) 'Analyzing subvisible particles in protein drug products: A comparison of Dynamic Light Scattering (DLS) and Resonant Mass Measurement (RMM)', *AAPS Journal*. Springer New York LLC, 16(3), pp. 440–451. doi: 10.1208/s12248-014-9579-6.

Paptoff, T. W. and Overcashier, D. E. (2002) *The Importance of Freezing on Lyophilization Cycle Development*. Available at: https://pdfs.semanticscholar.org/9e7a/d73a74ef66067b72c924491f4077dcfe05c1.pdf (Accessed: 7 April 2020).

Pardeshi, S., More, M., Patil, P., Pardeshi, C., Deshmukh, P., Mujumdar, A. and Naik, J. (2021) 'A meticulous overview on drying-based (spray-, freeze-, and spray-freeze) particle engineering approaches for pharmaceutical technologies', *Drying Technology*. Taylor & Francis, 39(11), pp. 1447–1491. doi: 10.1080/07373937.2021.1893330.

Park, C. W., Li, X., Vogt, F. G., Hayes, D., Zwischenberger, J. B., Park, E. S. and Mansour, H. M. (2013) 'Advanced spray-dried design, physicochemical characterization, and aerosol

dispersion performance of vancomycin and clarithromycin multifunctional controlled release particles for targeted respiratory delivery as dry powder inhalation aerosols', *International Journal of Pharmaceutics*. Elsevier B.V., 455(1–2), pp. 374–392. doi: 10.1016/j.ijpharm.2013.06.047.

Parlati, C., Colombo, P., Buttini, F., Young, P. M., Adi, H., Ammit, A. J. and Traini, D. (2009) 'Pulmonary Spray Dried Powders of Tobramycin Containing Sodium Stearate to Improve Aerosolization Efficiency', *Pharmaceutical Research*. Springer, 26(5), pp. 1084–1092. doi: 10.1007/s11095-009-9825-2.

Partridge, T. A., Ahmed, M., Choudhary, S. B., van der Walle, C. F., Patel, S. M., Bishop, S. M. and Mantle, M. D. (2019) 'Application of Magnetic Resonance to Assess Lyophilized Drug Product Reconstitution', *Pharmaceutical Research*. Springer New York LLC, 36(5), pp. 1–21. doi: 10.1007/s11095-019-2591-x.

Patel, B. A., Gospodarek, A., Larkin, M., Kenrick, S. A., Haverick, M. A., Tugcu, N., Brower, M. A. and Richardson, D. D. (2018) 'Multi-angle light scattering as a process analytical technology measuring real-time molecular weight for downstream process control', *mAbs*. Taylor and Francis Inc., 10(7), pp. 1–6. doi: 10.1080/19420862.2018.1505178.

Patel, S. M., Chaudhuri, S. and Pikal, M. J. (2010) 'Choked flow and importance of Mach I in freeze-drying process design', *Chemical Engineering Science*, 65(21), pp. 5716–5727. doi: 10.1016/j.ces.2010.07.024.

Patel, S. M., Doen, T. and Pikal, M. J. (2010) 'Determination of end point of primary drying in freeze-drying process control', *AAPS PharmSciTech*, 11(1), pp. 73–84. doi: 10.1208/s12249-009-9362-7.

Patel, S. M., Nail, S. L., Pikal, M. J., Geidobler, R., Winter, G., Hawe, A., Davagnino, J. and Rambhatla Gupta, S. (2017) 'Lyophilized Drug Product Cake Appearance: What Is Acceptable?', *Journal of Pharmaceutical Sciences*. Elsevier B.V., pp. 1706–1721. doi: 10.1016/j.xphs.2017.03.014.

Patel, S. M. and Pikal, M. J. (2011) 'Emerging freeze-drying process development and scale-up issues', *AAPS PharmSciTech*, pp. 372–378. doi: 10.1208/s12249-011-9599-9.

Paudel, A., Worku, Z. A., Meeus, J., Guns, S. and Van Den Mooter, G. (2013) 'Manufacturing of solid dispersions of poorly water soluble drugs by spray drying: Formulation and process considerations', *International Journal of Pharmaceutics*. Elsevier B.V., pp. 253–284. doi: 10.1016/j.ijpharm.2012.07.015.

Percy SR (1872) 'Improvement in drying and concentrating liquid substances by atomizing'. Available at: https://patents.google.com/patent/US125406A/en (Accessed: 12 March 2018).

Perez, A. S. and Oliveira, C. L. P. (2017) 'Thermal-Induced Denaturation and Aggregation Behavior of Lysozyme and Bovine Serum Albumin: a Thermodynamic and Structural Study', *Brazilian Journal of Physics*. Springer New York LLC, 47(5), pp. 524–531. doi: 10.1007/s13538-017-0520-1.

Peters, B. H., Staels, L., Rantanen, J., Molnár, F., De Beer, T., Lehto, V. P. and Ketolainen, J. (2016) 'Effects of cooling rate in microscale and pilot scale freeze-drying – Variations in excipient polymorphs and protein secondary structure', *European Journal of Pharmaceutical Sciences*. Elsevier B.V., 95, pp. 72–81. doi: 10.1016/j.ejps.2016.05.020.

Petrak, D., Eckardt, G., Dietrich, S., Köhler, M., Wiegel, D., Wolf, B., Priese, F. and Jacob, M. (2018) 'In-line measurement of layer thickness, agglomerate fraction and spray drying during pellet coating in the fluidized bed Use of an in-line particle probe as PAT instrument for real-

time monitoring', *Pharm. Ind.*, pp. 262–270. Available at: https://www.parsum.de/wp-content/uploads/2019/02/Reprint-Petrak-et-al-In-line-measurement-of-layer-thickness.pdf (Accessed: 8 February 2021).

Pieters, S., De Beer, T., Kasper, J. C., Boulpaep, D., Waszkiewicz, O., Goodarzi, M., Tistaert, C., Friess, W., Remon, J. P., Vervaet, C., *et al.* (2012) 'Near-infrared spectroscopy for in-line monitoring of protein unfolding and its interactions with lyoprotectants during freeze-drying', *Analytical Chemistry*. UTC, 84(2), pp. 947–955. doi: 10.1021/ac2022184.

Pieters, S., Vander Heyden, Y., Roger, J. M., D'Hondt, M., Hansen, L., Palagos, B., De Spiegeleer, B., Remon, J. P., Vervaet, C. and De Beer, T. (2013) 'Raman spectroscopy and multivariate analysis for the rapid discrimination between native-like and non-native states in freeze-dried protein formulations', in *European Journal of Pharmaceutics and Biopharmaceutics*. Elsevier, pp. 263–271. doi: 10.1016/j.ejpb.2013.03.035.

Pikal, M. (2004) 'Mechanisms of Protein Stabilization during Freeze-Drying and Storage', in Rey, L. (ed.) *Freeze-Drying/Lyophilization of Biological Products*. 3rd edn. doi: 10.1201/9780203021323.ch3.

Pikal, M. J., Rigsbee, D. R. and Roy, M. L. (2007) 'Solid State Chemistry of Proteins: I. Glass Transition Behavior in Freeze Dried Disaccharide Formulations of Human Growth Hormone (HGH)', *Journal of Pharmaceutical Sciences*. John Wiley and Sons Inc., 96(10), pp. 2765–2776. doi: 10.1002/jps.20960.

Pilcer, G., Wauthoz, N. and Amighi, K. (2012) 'Lactose characteristics and the generation of the aerosol', *Advanced Drug Delivery Reviews*. Elsevier, pp. 233–256. doi: 10.1016/j.addr.2011.05.003.

Pinal, R. (2008) 'Entropy of Mixing and the Glass Transition of Amorphous Mixtures', *Entropy*. MDPI AG, 10(3), pp. 207–223. doi: 10.3390/entropy-e10030207.

Pinto, J. T., Faulhammer, E., Dieplinger, J., Dekner, M., Makert, C., Nieder, M. and Paudel, A. (2021) 'Progress in spray-drying of protein pharmaceuticals: Literature analysis of trends in formulation and process attributes', *Drying Technology*. Taylor & Francis, pp. 1–32. doi: 10.1080/07373937.2021.1903032.

Pisano, R. (2020) *Continuous Manufacturing of Lyophilized Products: Why and How to Make it Happen | American Pharmaceutical Review - The Review of American Pharmaceutical Business & Technology*. Available at: https://www.americanpharmaceuticalreview.com/Featured-Articles/563771-Continuous-Manufacturing-of-Lyophilized-Products-Why-and-How-to-Make-it-Happen/ (Accessed: 7 August 2021).

Pisano, R., Adali, M. B. and Stratta, L. (2022) 'Modernizing Manufacturing of Parenteral Products : From Batch to Continuous Lyophilization', in Narang, A. S. and Dubey, A. (eds) *Continuous Pharmaceutical Processing and Process Analytical Technology*. Boca Raton: CRC Press, pp. 285–307. doi: 10.1201/9781003149835-11.

Pisano, R., Arsiccio, A., Capozzi, L. C. and Trout, B. L. (2019) 'Achieving continuous manufacturing in lyophilization: Technologies and approaches', *European Journal of Pharmaceutics and Biopharmaceutics*. Elsevier B.V., pp. 265–279. doi: 10.1016/j.ejpb.2019.06.027.

Planinc, A., Bones, J., Dejaegher, B., Van Antwerpen, P. and Delporte, C. (2016) 'Glycan characterization of biopharmaceuticals: Updates and perspectives', *Analytica Chimica Acta*, 921, pp. 13–27. doi: 10.1016/j.aca.2016.03.049.

Poole, P. L. and Finney, J. L. (1983) 'Sequential hydration of a dry globular protein', *Biopolymers*. Wiley Subscription Services, Inc., A Wiley Company, 22(1), pp. 255–260. doi: 10.1002/bip.360220135.

Poon, Z., Chang, D., Zhao, X. and Hammond, P. T. (2011) 'Layer-by-layer nanoparticles with a pH-sheddable layer for in vivo targeting of tumor hypoxia', *ACS Nano*. American Chemical Society, 5(6), pp. 4284–4292. doi: 10.1021/nn200876f.

Poon, Z., Lee, J. B., Morton, S. W. and Hammond, P. T. (2011) 'Controlling in vivo stability and biodistribution in electrostatically assembled nanoparticles for systemic delivery', *Nano Letters*. American Chemical Society, 11(5), pp. 2096–2103. doi: 10.1021/nl200636r.

Protein Data Bank 1DPX *RCSB PDB - 1DPX:Structure of Hen Egg-White Lysozyme*. Available at: https://www.rcsb.org/structure/1DPX (Accessed: 9 March 2020).

Protein Data Bank 3T6U *RCSB PDB - 3T6U: Crystal Structure of Lysozyme in 40% sucrose*. Available at: http://www.rcsb.org/structure/3T6U (Accessed: 9 March 2020).

Pu, Y.-(Elaine), Li, Y. and Xiang, D. (2022) 'Noninvasive Moisture Detection in Lyophilized Drug Product Using NIR Spectrometer and Headspace Moisture Analyzer', *Journal of Pharmaceutical Sciences*. Elsevier. doi: 10.1016/J.XPHS.2022.11.009.

Pulmatrix (2021) *PULMATRiX*. Available at: https://ir.pulmatrix.com/Zacks-Initiates-on-Pulmatrix-NASDAQ-PULM (Accessed: 4 August 2021).

Ragheb, R. and Nobbmann, U. (2020) 'Multiple scattering effects on intercept, size, polydispersity index, and intensity for parallel (VV) and perpendicular (VH) polarization detection in photon correlation spectroscopy', *Scientific Reports 2020 10:1*. Nature Publishing Group, 10(1), pp. 1–9. doi: 10.1038/s41598-020-78872-4.

Rajan, R., Ahmed, S., Sharma, N., Kumar, N., Debas, A. and Matsumura, K. (2021) 'Review of the current state of protein aggregation inhibition from a materials chemistry perspective: special focus on polymeric materials', *Materials Advances*. Royal Society of Chemistry, 2(4), pp. 1139–1176. doi: 10.1039/D0MA00760A.

Ramakrishna, A., Prathap, V., Maranholkar, V. and Rathore, A. S. (2022) 'Multi-wavelength UV-based PAT tool for measuring protein concentration', *Journal of Pharmaceutical and Biomedical Analysis*. Elsevier, 207, p. 114394. doi: 10.1016/J.JPBA.2021.114394.

Rambhatla, S., Obert, J. P., Luthra, S., Bhugra, C. and Pikal, M. J. (2005) 'Cake Shrinkage During Freeze Drying: A Combined Experimental and Theoretical Study', *Pharmaceutical Development and Technology*. Informa UK Limited, 10(1), pp. 33–40. doi: 10.1081/pdt-35871.

Rathore, N. and Rajan, R. S. (2008) 'Current Perspectives on Stability of Protein Drug Products during Formulation, Fill and Finish Operations', *Biotechnology Progress*. American Chemical Society (ACS), 24(3), pp. 504–514. doi: 10.1021/bp070462h.

Reimschuessel, H. K. (1978) 'Relationships on the effect of water on glass transition temperature and young's modulus of nylon 6', *Journal of Polymer Science: Polymer Chemistry Edition*. John Wiley & Sons, Ltd, 16(6), pp. 1229–1236. doi: 10.1002/pol.1978.170160606.

Dos Reis, L. G., Chaugule, V., Fletcher, D. F., Young, P. M., Traini, D. and Soria, J. (2021) 'In-vitro and particle image velocimetry studies of dry powder inhalers', *International Journal of Pharmaceutics*. Elsevier B.V., 592, p. 119966. doi: 10.1016/j.ijpharm.2020.119966.

Reslan, M., Demir, Y. K., Trout, B. L., Chan, H. K. and Kayser, V. (2017) 'Lack of a synergistic effect of arginine–glutamic acid on the physical stability of spray-dried bovine serum albumin', *Pharmaceutical Development and Technology*. Taylor and Francis Ltd, 22(6), pp.

785–791. doi: 10.1080/10837450.2016.1185116.

Rey, L. (1935) ‘Glimpses into the Realm of Freeze-Drying: Fundamental Issues’, p. 1010.

Rey, L. and May, J. C. (2004) ‘Glimpses into the Realm of Freeze-Drying: Fundamental Issues’, in Rey, L. (ed.) *Freeze-Drying/Lyophilization of Biological Products of Biological Products*. 3rd edn. Marcel Dekker, pp. 1–32. Available at: papers3://publication/uuid/F3F2E43B-F55D-4FC2-B9B7-267A00EF6D15.

Rolland, J. P., Maynor, B. W., Euliss, L. E., Exner, A. E., Denison, G. M. and DeSimone, J. M. (2005) ‘Direct fabrication and harvesting of monodisperse, shape-specific nanobiomaterials’, *Journal of the American Chemical Society*. American Chemical Society , 127(28), pp. 10096–10100. doi: 10.1021/ja051977c.

Rosenberg, M. and Sheu, T. Y. (1996) ‘Microencapsulation of volatiles by spray-drying in whey protein-based wall systems’, *International Dairy Journal*. Elsevier Ltd, 6(3), pp. 273–284. doi: 10.1016/0958-6946(95)00020-8.

Roser, B. (1991) ‘Trehalose, a new approach to premium dried foods’, *Trends in Food Science and Technology*. Elsevier, 2(C), pp. 166–169. doi: 10.1016/0924-2244(91)90671-5.

Roser, B. (2005) ‘Sterile Spray Drying for Stable Liquid 21st Century Pharmaceuticals’, (19), pp. 50–54.

Roudaut, G., Simatos, D., Champion, D., Contreras-Lopez, E. and Le Meste, M. (2004) ‘Molecular mobility around the glass transition temperature: A mini review’, *Innovative Food Science and Emerging Technologies*. doi: 10.1016/j.ifset.2003.12.003.

Roy, I. and Gupta, M. N. (2004) ‘Freeze-drying of proteins: some emerging concerns’, *Biotechnology and Applied Biochemistry*. doi: 10.1042/BA20030133.

Sahin, Z., Demir, Y. K. and Kayser, V. (2016) ‘Global kinetic analysis of seeded BSA aggregation’, *European Journal of Pharmaceutical Sciences*. Elsevier B.V., 86, pp. 115–124. doi: 10.1016/j.ejps.2016.03.007.

Salnikova, M., Varshney, D. and Shalaev, E. (2015) ‘Heterogeneity of Protein Environments in Frozen Solutions and in the Dried State’, in Varshney, D. and Singh, M. (eds) *Lyophilized Biologics and Vaccines*. USA: Springer, pp. 11–24. doi: 10.1007/978-1-4939-2383-0.

Samborska, K., Witrowa-Rajchert, D. and Gonçalves, A. (2005) ‘Spray-drying of α-amylase - The effect of process variables on the enzyme inactivation’, *Drying Technology*. Taylor and Francis Inc., 23(4), pp. 941–953. doi: 10.1081/DRT-200054243.

Santivarangkna, C., Kulozik, U. and Foerst, P. (2007) ‘Alternative Drying Processes for the Industrial Preservation of Lactic Acid Starter Cultures’, *Biotechnology Progress*. American Chemical Society (ACS), 23(2), pp. 302–315. doi: 10.1021/bp060268f.

Sarti, F., Iqbal, J., Müller, C., Shahnaz, G., Rahmat, D. and Bernkop-Schnürch, A. (2012) ‘Poly(acrylic acid)-cysteine for oral vitamin B12 delivery’, *Analytical Biochemistry*. Academic Press, 420(1), pp. 13–19. doi: 10.1016/j.ab.2011.08.039.

Saß, A. and Lee, G. (2014) ‘Evaluation of some water-miscible organic solvents for spray-drying enzymes and carbohydrates’, *Drug Development and Industrial Pharmacy*. Informa Healthcare, 40(6), pp. 749–757. doi: 10.3109/03639045.2013.782554.

Schaefer, J. and Lee, G. (2015a) ‘Arrhenius activation energy of damage to catalase during spray-drying’, *International Journal of Pharmaceutics*. Elsevier, 489(1–2), pp. 124–130. doi: 10.1016/j.ijpharm.2015.04.078.

Schaefer, J. and Lee, G. (2015b) 'Post-chamber inactivation of catalase powder during spray drying in bench-top machines', *Powder Technology*. Elsevier, 277, pp. 231–236. doi: 10.1016/j.powtec.2015.03.008.

Schersch, K., Betz, O., Garidel, P., Muehlau, S., Bassarab, S. and Winter, G. (2010) 'Systematic investigation of the effect of lyophilizate collapse on pharmaceutically relevant proteins I: Stability after freeze-drying', *Journal of Pharmaceutical Sciences*. John Wiley and Sons Inc., 99(5), pp. 2256–2278. doi: 10.1002/jps.22000.

Schersch, K., Betz, O., Garidel, P., Muehlau, S., Bassarab, S. and Winter, G. (2012) 'Systematic investigation of the effect of lyophilizate collapse on pharmaceutically relevant proteins, part 2: Stability during storage at elevated temperatures', *Journal of Pharmaceutical Sciences*. John Wiley and Sons Inc., 101(7), pp. 2288–2306. doi: 10.1002/jps.23121.

Schneid, S. C., Gieseler, H., Kessler, W. J., Luthra, S. A. and Pikal, M. J. (2011) 'Optimization of the secondary drying step in freeze drying using TDLAS technology', *AAPS PharmSciTech*. Springer, 12(1), pp. 379–387. doi: 10.1208/s12249-011-9600-7.

Schneid, S. C., Gieseler, H., Kessler, W. J. and Pikal, M. J. (2009) 'Non-invasive product temperature determination during primary drying using tunable diode laser absorption spectroscopy', *Journal of Pharmaceutical Sciences*. John Wiley and Sons Inc., 98(9), pp. 3406–3418. doi: 10.1002/jps.21522.

Schneid, S. and Gieseler, H. (2008) 'Evaluation of a new wireless temperature remote interrogation system (TEMPRIS) to measure product temperature during freeze drying', *AAPS PharmSciTech*, 9(3), pp. 729–739. doi: 10.1208/s12249-008-9099-8.

Schneider, C. P. and Trout, B. L. (2009) 'Investigation of Cosolute−Protein Preferential Interaction Coefficients: New Insight into the Mechanism by Which Arginine Inhibits Aggregation', *Journal of Physical Chemistry B*. American Chemical Society, 113(7), pp. 2050–2058. doi: 10.1021/JP808042W.

Schott *SCHOTT Vials* . Available at: https://www.schott.com/d/pharmaceutical_packaging/33243f84-657e-49f9-97b4-06180b08ac7e/1.6/schott-brochure-schott-vials-english-20092017.pdf (Accessed: 6 March 2020).

Schüle, S., Schulz-Fademrecht, T., Garidel, P., Bechtold-Peters, K. and Frieß, W. (2008) 'Stabilization of IgG1 in spray-dried powders for inhalation', *European Journal of Pharmaceutics and Biopharmaceutics*. Elsevier, 69(3), pp. 793–807. doi: 10.1016/J.EJPB.2008.02.010.

Scientific, S. (2018) *Basic Principles of Freeze Drying*. Available at: https://www.spscientific.com/freeze-drying-lyophilization-basics/ (Accessed: 23 February 2018).

Seaman, P., Damment, S., Bamsey, K., Dryja, A. and Cook, C. (2019) 'SAT-432 MTD201 Has a Favourable 28-Day Sustained Release Profile Compared to Sandostatin LAR in Healthy Subjects', *Journal of the Endocrine Society*. Oxford Academic, 3(Supplement_1). doi: 10.1210/JS.2019-SAT-432.

Searles, J. A., Carpenter, J. F. and Randolph, T. W. (2001) 'The ice nucleation temperature determines the primary drying rate of lyophilization for samples frozen on a temperature-controlled shelf', *Journal of Pharmaceutical Sciences*. Elsevier, 90(7), pp. 860–871. doi: 10.1002/jps.1039.

Sebastião, I. B., Bhatnagar, B., Tchessalov, S., Ohtake, S., Plitzko, M., Luy, B. and Alexeenko, A.

(2019) ‘Bulk Dynamic Spray Freeze-Drying Part 1: Modeling of Droplet Cooling and Phase Change’, *Journal of Pharmaceutical Sciences*. Elsevier B.V., 108(6), pp. 2063–2074. doi: 10.1016/j.xphs.2019.01.009.

Sellers, S. P., Clark, G. S., Sievers, R. E. and Carpenter, J. F. (2001) ‘Dry powders of stable protein formulations from aqueous solutions prepared using supercritical CO2-assisted aerosolization’, *Journal of Pharmaceutical Sciences*. John Wiley and Sons Inc., 90(6), pp. 785–797. doi: 10.1002/jps.1032.

Seo, J. A., Kim, S. J., Kwon, H. J., Yang, Y. S., Kim, H. K. and Hwang, Y. H. (2006) ‘The glass transition temperatures of sugar mixtures’, *Carbohydrate Research*. Elsevier Ltd, 341(15), pp. 2516–2520. doi: 10.1016/j.carres.2006.08.014.

Serno, T., Carpenter, J. F., Randolph, T. W. and Winter, G. (2010) ‘Inhibition of agitation-induced aggregation of an IgG-antibody by hydroxypropyl-β-cyclodextrin’, *Journal of Pharmaceutical Sciences*. John Wiley and Sons Inc., 99(3), pp. 1193–1206. doi: 10.1002/jps.21931.

Seville, P. C., Learoyd, T. P., Li, H. Y., Williamson, I. J. and Birchall, J. C. (2007) ‘Amino acid-modified spray-dried powders with enhanced aerosolisation properties for pulmonary drug delivery’, *Powder Technology*. Elsevier, 178(1), pp. 40–50. doi: 10.1016/j.powtec.2007.03.046.

Shah, D., Li, J., Shaikh, A. R. and Rajagopalan, R. (2012) ‘Arginine-aromatic interactions and their effects on arginine-induced solubilization of aromatic solutes and suppression of protein aggregation’, *Biotechnology Progress*. American Chemical Society (ACS), 28(1), pp. 223–231. doi: 10.1002/btpr.710.

Shahidi, F. and Han, X. Q. (1993) ‘Encapsulation of Food Ingredients’, *Critical Reviews in Food Science and Nutrition*, 33(6), pp. 501–547. doi: 10.1080/10408399309527645.

Shalaev, E., Gatlin, L. A., Auffret, T. and Speaker, S. M. (2008) *Freeze-drying concepts: the basics*.

Shamblin, S. L., Taylor, L. S. and Zografi, G. (1998) ‘Mixing Behavior of Colyophilized Binary Systems’, *Journal of Pharmaceutical Sciences*. John Wiley and Sons Inc., 87(6), pp. 694–701. doi: 10.1021/JS9704801.

Sharma, A., Khamar, D., Cullen, S., Hayden, A. and Hughes, H. (2021) ‘Innovative Drying Technologies for Biopharmaceuticals’, *International Journal of Pharmaceutics*. Elsevier, p. 121115. doi: https://doi.org/10.1016/j.ijpharm.2021.121115.

Sharma, P., Kessler, W. J., Bogner, R., Thakur, M. and Pikal, M. J. (2019) ‘Applications of the Tunable Diode Laser Absorption Spectroscopy: In-Process Estimation of Primary Drying Heterogeneity and Product Temperature During Lyophilization’, *Journal of Pharmaceutical Sciences*, 108(1). doi: 10.1016/j.xphs.2018.07.031.

Shepard, K. B., Vodak, D. T., Kuehl, P. J., Revelli, D., Zhou, Y., Pluntze, A. M., Adam, M. S., Oddo, J. C., Switala, L., Cape, J. L., *et al.* (2021) ‘Local Treatment of Non-small Cell Lung Cancer with a Spray-Dried Bevacizumab Formulation’, *AAPS PharmSciTech*. Springer Science and Business Media Deutschland GmbH, 22(7), pp. 1–11. doi: 10.1208/S12249-021-02095-7/FIGURES/5.

Shepard, K. B., Pluntze, A. M. and Vodak, D. T. (2022) ‘Simultaneous Spray Drying for Combination Dry Powder Inhaler Formulations’, *Pharmaceutics 2022, Vol. 14, Page 1130*. Multidisciplinary Digital Publishing Institute, 14(6), p. 1130. doi: 10.3390/PHARMACEUTICS14061130.

Shukla, D. and Trout, B. L. (2010) ‘Interaction of arginine with proteins and the mechanism by

which it inhibits aggregation', *Journal of Physical Chemistry B*. American Chemical Society, 114(42), pp. 13426–13438. doi: 10.1021/JP108399G/SUPPL_FILE/JP108399G_SI_001.PDF.

Shukla, D. and Trout, B. L. (2011a) 'Preferential interaction coefficients of proteins in aqueous arginine solutions and their molecular origins', *Journal of Physical Chemistry B*. American Chemical Society, 115(5), pp. 1243–1253. doi: 10.1021/JP108586B/ASSET/IMAGES/MEDIUM/JP-2010-08586B_0011.GIF.

Shukla, D. and Trout, B. L. (2011b) 'Understanding the synergistic effect of arginine and glutamic acid mixtures on protein solubility', *Journal of Physical Chemistry B*. American Chemical Society, 115(41), pp. 11831–11839. doi: 10.1021/jp204462t.

Siddhanta, S., Barman, I. and Narayana, C. (2015) 'Revealing the trehalose mediated inhibition of protein aggregation through lysozyme-silver nanoparticle interaction', *Soft Matter*. Royal Society of Chemistry, 11(37), pp. 7241–7249. doi: 10.1039/c5sm01896j.

Sigma *Lysozyme from chicken egg white for Molecular Biology*.

Sigma Aldrich (2017) 'Lysozyme Detection Kit - Product Information'. Sigma Aldrich. Available at: https://www.sigmaaldrich.com/content/dam/sigma-aldrich/docs/Sigma/Bulletin/1/ly0100bul.pdf.

Silva, A. F. T., Burggraeve, A., Denon, Q., Van Der Meeren, P., Sandler, N., Van Den Kerkhof, T., Hellings, M., Vervaet, C., Remon, J. P., Lopes, J. A., *et al.* (2013) 'Particle sizing measurements in pharmaceutical applications: Comparison of in-process methods versus off-line methods', *European Journal of Pharmaceutics and Biopharmaceutics*. Elsevier B.V., 85(3 PART B), pp. 1006–1018. doi: 10.1016/j.ejpb.2013.03.032.

Simperler, A., Kornherr, A., Chopra, R., Bonnet, P. A., Jones, W., Motherwell, W. D. S. and Zifferer, G. (2006) 'Glass transition temperature of glucose, sucrose, and trehalose: An experimental and in silico study', *Journal of Physical Chemistry B*, 110(39), pp. 19678–19684. doi: 10.1021/jp063134t.

Singh, S. K. (2018) 'Sucrose and Trehalose in Therapeutic Protein Formulations', in Warne, N. W. and Mahler, H.-C. (eds) *Challenges in Protein Product Development*. Springer, Cham, pp. 63–95. doi: 10.1007/978-3-319-90603-4_3.

Singh, S. K., Kolhe, P., Mehta, A. P., Chico, S. C., Lary, A. L. and Huang, M. (2011) 'Frozen State Storage Instability of a Monoclonal Antibody: Aggregation as a Consequence of Trehalose Crystallization and Protein Unfolding', *Pharmaceutical Research 2011 28:4*. Springer, 28(4), pp. 873–885. doi: 10.1007/S11095-010-0343-Z.

Singh, S. and Singh, J. (2003) 'Effect of Polyols on the Conformational Stability and Biological Activity of a Model Protein Lysozyme', *AAPS PharmSciTech*, 4(3), p. 42. Available at: http://www.pharmscitech.org (Accessed: 30 October 2021).

Siow, C. R. S., Heng, P. W. S. and Chan, L. W. (2018) 'Bulk Freeze-Drying Milling: a Versatile Method of Developing Highly Porous Cushioning Excipients for Compacted Multiple-Unit Pellet Systems (MUPS)', *AAPS PharmSciTech*. Springer New York LLC, 19(2), pp. 845–857. doi: 10.1208/s12249-017-0899-6.

Smith, G., Arshad, M. S., Polygalov, E., Ermolina, I., McCoy, T. R. and Matejtschuk, P. (2017) 'Process Understanding in Freeze-Drying Cycle Development: Applications for Through-Vial Impedance Spectroscopy (TVIS) in Mini-pilot Studies', *Journal of Pharmaceutical Innovation*. doi: 10.1007/s12247-016-9266-5.

Smith, P. K., Krohn, R. I., Hermanson, G. T., Mallia, A. K., Gartner, F. H., Provenzano, M. D., Fujimoto, E. K., Goeke, N. M., Olson, B. J. and Klenk, D. C. (1985) 'Measurement of protein

using bicinchoninic acid', *Analytical Biochemistry*. Academic Press, 150(1), pp. 76–85. doi: 10.1016/0003-2697(85)90442-7.

Smith, R., Shah, U. V., Parambil, J. V., Burnett, D. J., Thielmann, F. and Heng, J. Y. Y. (2017) 'The Effect of Polymorphism on Surface Energetics of D-Mannitol Polymorphs', *AAPS Journal*. Springer New York LLC, 19(1), pp. 103–109. doi: 10.1208/S12248-016-9978-Y/METRICS.

Snyder, H. (2012) 'Pharmaceutical spray drying: solid-dose process technology platform for the 21st century', *Therapeutic Delivery*, 3(7), pp. 901–912. doi: 10.4155/tde.12.64.

Snyder, H. E. and Lechuga-Ballesteros, D. (2008) *Spray Drying: Theory and Pharmaceutical Applications*. 3rd edn, *Pharmaceutical dosage forms - Tablets*. 3rd edn. Available at: https://books.google.com.br/books?hl=pt-BR&lr=&id=JP_LBQAAQBAJ&oi=fnd&pg=PP1&dq=modified+release+forms&ots=dX5budkSJl&sig=P3KmnaT87qEIpUQEnSPD9qRKeWw#v=onepage&q=spray drying&f=false (Accessed: 25 March 2018).

Sonje, J., Fleagle Chisholm, C. and Suryanarayanan, R. (2023) 'Frozen storage of proteins: Use of mannitol to generate a homogenous freeze-concentrate', *International Journal of Pharmaceutics*. Elsevier, 630, p. 121995. doi: 10.1016/J.IJPHARM.2022.121995.

Sonje, J., Thakral, S., Mayhugh, B., Sacha, G., Nail, S., Srinivasan, J. and Suryanarayanan, R. (2022) 'Mannitol hemihydrate in lyophilized protein formulations: Impact of its dehydration during storage on sucrose crystallinity and protein stability', *International Journal of Pharmaceutics*. Elsevier, 624, p. 121974. doi: 10.1016/J.IJPHARM.2022.121974.

Van Der Spoel, D., Lindahl, E., Hess, B., Groenhof, G., Mark, A. E. and Berendsen, H. J. C. (2005) 'GROMACS: Fast, flexible, and free', *Journal of Computational Chemistry*. John Wiley & Sons, Ltd, 26(16), pp. 1701–1718. doi: 10.1002/JCC.20291.

Sreerama, N. (2003) 'Structural composition of betaI- and betaII-proteins', *Protein Science*. Wiley, 12(2), pp. 384–388. doi: 10.1110/ps.0235003.

Staniforth, J. N., Morton, D. A. V., Gill, R., Brambilla, G., Musa, R. and Ferrarini, L. (2001) 'Pharmaceutical formulations for dry powder inhalers'. WIPO. Available at: https://patents.google.com/patent/WO2001078695A2/en (Accessed: 22 February 2021).

Starciuc, T., Guinet, Y., Paccou, L. and Hedoux, A. (2017) 'Influence of a Small Amount of Glycerol on the Trehalose Bioprotective Action Analyzed In Situ During Freeze-Drying of Lyzozyme Formulations by Micro-Raman Spectroscopy', *Journal of Pharmaceutical Sciences*. Elsevier B.V., 106(10), pp. 2988–2997. doi: 10.1016/j.xphs.2017.05.040.

Starciuc, T., Malfait, B., Danede, F., Paccou, L., Guinet, Y., Correia, N. T. and Hedoux, A. (2020) 'Trehalose or Sucrose: Which of the Two Should be Used for Stabilizing Proteins in the Solid State? A Dilemma Investigated by In Situ Micro-Raman and Dielectric Relaxation Spectroscopies During and After Freeze-Drying', *Journal of Pharmaceutical Sciences*. Elsevier B.V., 109(1), pp. 496–504. doi: 10.1016/j.xphs.2019.10.055.

Stärtzel, P. (2018) 'Arginine as an Excipient for Protein Freeze-Drying: A Mini Review', *Journal of Pharmaceutical Sciences*. doi: 10.1016/j.xphs.2017.11.015.

Stärtzel, P., Gieseler, H., Gieseler, M., Abdul-Fattah, A. M., Adler, M., Mahler, H. C. and Goldbach, P. (2015) 'Freeze Drying of l -Arginine/Sucrose-Based Protein Formulations, Part I: Influence of Formulation and Arginine Counter Ion on the Critical Formulation Temperature, Product Performance and Protein Stability', *Journal of Pharmaceutical Sciences*. doi: 10.1002/jps.24501.

Stroev, P. V., Hoskins, P. R. and Easson, W. J. (2007) 'Distribution of wall shear rate throughout the arterial tree: A case study', *Atherosclerosis*, 191(2), pp. 276–280. doi: 10.1016/j.atherosclerosis.2006.05.029.

Struschka, M., Plitzko, M., Gebhard, T. and Luy, B. (2016) 'Rotary drum for use in a vacuum freeze-dryer'. USA.

Su, J. T., Duncan, P. B., Momaya, A., Jutila, A. and Needham, D. (2010) 'The effect of hydrogen bonding on the diffusion of water in n -alkanes and n -alcohols measured with a novel single microdroplet method', *Journal of Chemical Physics*, 132(4). doi: 10.1063/1.3298857.

Sudrik, C. M., Cloutier, T., Mody, N., Sathish, H. A. and Trout, B. L. (2019) 'Understanding the Role of Preferential Exclusion of Sugars and Polyols from Native State IgG1 Monoclonal Antibodies and its Effect on Aggregation and Reversible Self-Association', *Pharmaceutical Research 2019 36:8*. Springer, 36(8), pp. 1–12. doi: 10.1007/S11095-019-2642-3.

Sun, M.-F., Liao, J.-N., Jing, Z.-Y., Gao, H., Shen, B.-B., Xu, Y.-F. and Fang, W.-J. (2022) 'Effects of polyol excipient stability during storage and use on the quality of biopharmaceutical formulations', *Journal of Pharmaceutical Analysis*. Elsevier. doi: 10.1016/J.JPHA.2022.03.003.

Sun, W. Q. and Davidson, P. (1998) 'Protein inactivation in amorphous sucrose and trehalose matrices: effects of phase separation and crystallization.', *Biochimica et biophysica acta*, 1425(1), pp. 235–44. Available at: http://www.ncbi.nlm.nih.gov/pubmed/9813347 (Accessed: 12 February 2018).

Sun, Y., Filho, P. L. O., Bozelli, J. C., Carvalho, J., Schreier, S. and Oliveira, C. L. P. (2015) 'Unfolding and folding pathway of lysozyme induced by sodium dodecyl sulfate', *Soft Matter*. Royal Society of Chemistry, 11(39), pp. 7769–7777. doi: 10.1039/c5sm01231g.

Susi, H. and Byler, D. M. (1986) '[13] Resolution-Enhanced Fourier Transform Infrared Spectroscopy of Enzymes', *Methods in Enzymology*. Academic Press, 130(C), pp. 290–311. doi: 10.1016/0076-6879(86)30015-6.

Sweeney, L. G., Wang, Z., Loebenberg, R., Wong, J. P., Lange, C. F. and Finlay, W. H. (2005) 'Spray-freeze-dried liposomal ciprofloxacin powder for inhaled aerosol drug delivery', *International Journal of Pharmaceutics*. Elsevier, 305(1–2), pp. 180–185. doi: 10.1016/J.IJPHARM.2005.09.010.

Tang, X. and Pikal, Michael J (2004) 'Design of freeze-drying processes for pharmaceuticals: practical advice.', *Pharmaceutical research*, 21(2), pp. 191–200.

Tang, X. and Pikal, Michael J. (2004) 'Design of Freeze-Drying Processes for Pharmaceuticals: Practical Advice', *Pharmaceutical Research*. doi: 10.1023/B:PHAM.0000016234.73023.75.

TaPrime Consulting 'Tg′ Values of Common Materials', *taPrime Consulting*, 30, p. 1.

Tejasvi Mutukuri, T., Maa, Y.-F., Gikanga, B., Sakhnovsky, R. and Tony Zhou, Q. (2021) 'Electrostatic Spray Drying for Monoclonal Antibody Formulation', *International Journal of Pharmaceutics*. Elsevier, p. 120942. doi: 10.1016/J.IJPHARM.2021.120942.

Tewes, F., Ehrhardt, C. and Healy, A. M. (2014) 'Superparamagnetic iron oxide nanoparticles (SPIONs)-loaded Trojan microparticles for targeted aerosol delivery to the lung', *European Journal of Pharmaceutics and Biopharmaceutics*. Elsevier, 86(1), pp. 98–104. doi: 10.1016/j.ejpb.2013.09.004.

Thakral, S., Sonje, J., Munjal, B., Bhatnagar, B. and Suryanarayanan, R. (2023) 'Mannitol as an Excipient for Lyophilized Injectable Formulations', *Journal of Pharmaceutical Sciences*.

Elsevier, 112(1), pp. 19–35. doi: 10.1016/J.XPHS.2022.08.029.

Thomas, B. R., Vekilov, P. G. and Rosenberger, F. (1996) 'Heterogeneity determination and purification of commercial hen egg-white lysozyme', *Acta Crystallographica Section D: Biological Crystallography*. Blackwell Publishing Ltd, 52(4), pp. 776–784. doi: 10.1107/S090744499600279X.

Thorat, B. N., Sett, A. and Mujumdar, A. S. (2020) 'Drying of Vaccines and Biomolecules', *Drying Technology*. Bellwether Publishing, Ltd. doi: 10.1080/07373937.2020.1825293.

Tian, F., Middaugh, C. R., Offerdahl, T., Munson, E., Sane, S. and Rytting, J. H. (2007) 'Spectroscopic evaluation of the stabilization of humanized monoclonal antibodies in amino acid formulations', *International Journal of Pharmaceutics*. Elsevier, 335(1–2), pp. 20–31. doi: 10.1016/j.ijpharm.2006.10.037.

Touzet, A., Pfefferlé, F., der Wel, P. van, Lamprecht, A. and Pellequer, Y. (2018) 'Active freeze drying for production of nanocrystal-based powder: A pilot study', *International Journal of Pharmaceutics*. Elsevier B.V., 536(1), pp. 222–230. doi: 10.1016/j.ijpharm.2017.11.050.

Tsumoto, K., Ejima, D., Kita, Y. and Arakawa, T. (2005) 'Review: Why is arginine effective in suppressing aggregation?', *Protein and peptide letters*. Protein Pept Lett, 12(7), pp. 613–619. doi: 10.2174/0929866054696109.

Tsumoto, K., Umetsu, M., Kumagai, I., Ejima, D., Philo, J. S. and Arakawa, T. (2004) 'Role of Arginine in Protein Refolding, Solubilization, and Purification', *Biotechnology Progress*. American Chemical Society, 20(5), pp. 1301–1308. doi: 10.1021/bp0498793.

Tsutsui, Y. and Wintrode, P. (2007) 'Hydrogen/Deuterium Exchange-Mass Spectrometry: A Powerful Tool for Probing Protein Structure, Dynamics and Interactions', *Current Medicinal Chemistry*. Bentham Science Publishers Ltd., 14(22), pp. 2344–2358. doi: 10.2174/092986707781745596.

Tzannis, S. T. and Prestrelski, S. J. (1999) 'Activity–stability considerations of trypsinogen during spray drying: Effects of sucrose', *Journal of Pharmaceutical Sciences*. American Chemical Society, 88(3), pp. 351–359. doi: 10.1021/js980011e.

Uddin, D., Ruetti, D. P., Meuri, M. and John, P. (2021) *Spray Drying Inhalable Particles*. Available at: https://static1.buchi.com/sites/default/files/downloads/Set_3_Poster_Spray-Drying_Inhalable_Particles_en_01.pdf?89288b48e0981a628593201f305b1f10a573188d (Accessed: 9 February 2021).

Uddin, M. S., Hawlader, M. N. A. and Zhu, H. J. (2001) 'Microencapsulation of ascorbic acid: Effect of process variables on product characteristics', *Journal of Microencapsulation*. Taylor & Francis, 18(2), pp. 199–209. doi: 10.1080/02652040010000352.

Ullrich, S., Seyferth, S. and Lee, G. (2015a) 'Measurement of shrinkage and cracking in lyophilized amorphous cakes, Part 3: Hydrophobic vials and the question of adhesion', *Journal of Pharmaceutical Sciences*. John Wiley and Sons Inc., 104(6), pp. 2040–2046. doi: 10.1002/jps.24441.

Ullrich, S., Seyferth, S. and Lee, G. (2015b) 'Measurement of shrinkage and cracking in lyophilized amorphous cakes. Part I: Final-product assessment', *Journal of Pharmaceutical Sciences*. John Wiley and Sons Inc., 104(1), pp. 155–164. doi: 10.1002/jps.24284.

Ullrich, S., Seyferth, S. and Lee, G. (2015c) 'Measurement of shrinkage and cracking in lyophilized amorphous cakes. Part IV: Effects of freezing protocol', *International Journal of Pharmaceutics*. Elsevier B.V., 495(1), pp. 52–57. doi: 10.1016/j.ijpharm.2015.08.091.

Utsumi, M., Horiuchi, H. and Okutsu, T. (2017) 'Photo sensitization reaction-induced crystallization of lysozyme', *Journal of Photochemistry and Photobiology A: Chemistry*. Elsevier B.V., 344, pp. 223–227. doi: 10.1016/j.jphotochem.2017.05.027.

Valderrama-Rincon, J. D., Fisher, A. C., Merritt, J. H., Fan, Y.-Y., Reading, C. A., Chhiba, K., Heiss, C., Azadi, P., Aebi, M. and DeLisa, M. P. (2012) 'An engineered eukaryotic protein glycosylation pathway in Escherichia coli.', *Nature chemical biology*. Nature Publishing Group, 8(5), pp. 434–6. doi: 10.1038/nchembio.921.

Valstar, A., Brown, W. and Almgren, M. (1999) 'Lysozyme-sodium dodecyl sulfate system studied by dynamic and static light scattering', *Langmuir*. ACS, 15(7), pp. 2366–2374. doi: 10.1021/la981234n.

Vanbillemont, B., Carpenter, J. F., Probst, C. and De Beer, T. (2020) 'The Impact of Formulation Composition and Process Settings of Traditional Batch Versus Continuous Freeze-Drying On Protein Aggregation', *Journal of Pharmaceutical Sciences*. Elsevier B.V., 109(11), pp. 3308–3318. doi: 10.1016/j.xphs.2020.07.023.

Vanbillemont, B., Lammens, J., Goethals, W., Vervaet, C., Boone, M. N. and De Beer, T. (2020) '4D Micro-Computed X-ray Tomography as a Tool to Determine Critical Process and Product Information of Spin Freeze-Dried Unit Doses', *Pharmaceutics*. MDPI AG, 12(5), p. 430. doi: 10.3390/pharmaceutics12050430.

Varshney, D. B., Kumar, S., Shalaev, E. Y., Sundaramurthi, P., Kang, S. W., Gatlin, L. A. and Suryanarayanan, R. (2007) 'Glycine crystallization in frozen and freeze-dried systems: Effect of pH and buffer concentration', *Pharmaceutical Research*. Springer New York, 24(3), pp. 593–604. doi: 10.1007/s11095-006-9178-z.

Varshney, D. and Singh, M. (2015) *Lyophilised Biologics and Vaccines*. Edited by D. Varshney and M. Singh. Springer US. doi: 10.1007/978-1-4939-2383-0.

Vass, P., Démuth, B., Hirsch, E., Nagy, B., Andersen, S. K., Vigh, T., Verreck, G., Csontos, I., Nagy, Z. K. and Marosi, G. (2019a) 'Drying technology strategies for colon-targeted oral delivery of biopharmaceuticals', *Journal of Controlled Release*. doi: 10.1016/j.jconrel.2019.01.023.

Vass, P., Démuth, B., Hirsch, E., Nagy, B., Andersen, S. K., Vigh, T., Verreck, G., Csontos, I., Nagy, Z. K. and Marosi, G. (2019b) 'Drying technology strategies for colon-targeted oral delivery of biopharmaceuticals', *Journal of Controlled Release*. Elsevier B.V., pp. 162–178. doi: 10.1016/j.jconrel.2019.01.023.

Vehring, R. (2008) 'Pharmaceutical particle engineering via spray drying', *Pharmaceutical Research*, pp. 999–1022. doi: 10.1007/s11095-007-9475-1.

Vehring, R., Snyder, H. and Lechuga-Ballesteros, D. (2020) 'Spray Drying', in *Drying Technologies for Biotechnology and Pharmaceutical Applications*. Wiley, pp. 179–216. doi: 10.1002/9783527802104.ch7.

Verlet, L. (1967) 'Computer "Experiments" on Classical Fluids. I. Thermodynamical Properties of Lennard-Jones Molecules', *Physical Review*. American Physical Society, 159(1), p. 98. doi: 10.1103/PhysRev.159.98.

Vhora, I., Bardoliwala, D., Ranamalla, S. R. and Javia, A. (2019) 'Parenteral controlled and prolonged drug delivery systems: Therapeutic needs and formulation strategies', *Novel Drug Delivery Technologies: Innovative Strategies for Drug Re-positioning*. Springer Singapore, pp. 183–260. doi: 10.1007/978-981-13-3642-3_7.

Victor, K. G., Levac, L., Timmins, M. and Veale, J. (2017) 'Method development for container

closure integrity evaluation via headspace gas ingress by using frequency modulation spectroscopy', *PDA Journal of Pharmaceutical Science and Technology*. Parenteral Drug Association Inc., 71(6), pp. 429–453. doi: 10.5731/pdajpst.2017.007518.

Vo, C. L.-N., Park, C. and Lee, B.-J. (2013) 'Current trends and future perspectives of solid dispersions containing poorly water-soluble drugs', *European Journal of Pharmaceutics and Biopharmaceutics*. Elsevier, 85(3), pp. 799–813. doi: 10.1016/J.EJPB.2013.09.007.

Voets, I. K., Cruz, W. A., Moitzi, C., Lindner, P., Arêas, E. P. G. and Schurtenberger, P. (2010) 'DMSO-induced denaturation of hen egg white lysozyme', *Journal of Physical Chemistry B*. American Chemical Society, 114(36), pp. 11875–11883. doi: 10.1021/jp103515b.

Vogel, R., Savage, J., Muzard, J., Camera, G. Della, Vella, G., Law, A., Marchioni, M., Mehn, D., Geiss, O., Peacock, B., *et al.* (2021) 'Measuring particle concentration of multimodal synthetic reference materials and extracellular vesicles with orthogonal techniques: Who is up to the challenge?', *Journal of Extracellular Vesicles*. Wiley-Blackwell, 10(3). doi: 10.1002/JEV2.12052.

Wagner, I., Nagy, Z. K., Vass, P., Fehér, C., Barta, Z., Vigh, T., Sóti, P. L., Harasztos, A. H., Pataki, H., Balogh, A., *et al.* (2015) 'Stable formulation of protein-type drug in electrospun polymeric fiber followed by tableting and scaling-up experiments', *Polymers for Advanced Technologies*. John Wiley and Sons Ltd, 26(12), pp. 1461–1467. doi: 10.1002/pat.3569.

Wales, T. E. and Engen, J. R. (2006) 'Hydrogen exchange mass spectrometry for the analysis of protein dynamics', *Mass Spectrometry Reviews*. John Wiley & Sons, Ltd, 25(1), pp. 158–170. doi: 10.1002/mas.20064.

Wallace, B. A. (2009) 'Protein characterisation by synchrotron radiation circular dichroism spectroscopy', *Quarterly Reviews of Biophysics*, 42(4), pp. 317–370. doi: 10.1017/S003358351000003X.

Wallace, B. A. (2019) 'The role of circular dichroism spectroscopy in the era of integrative structural biology', *Current Opinion in Structural Biology*. Elsevier Ltd, 58, pp. 191–196. doi: 10.1016/j.sbi.2019.04.001.

Wallace, B. A. (2020) *DichroWeb - Online Circular Dichroism Analysis*. Available at: http://dichroweb.cryst.bbk.ac.uk/html/home.shtml (Accessed: 27 June 2020).

Wallace, B. A., Wien, F., Miles, A. J., Lees, J. G., Vronning Hoffmann, S., Evans, P., Wistow, G. J. and Slingsby, C. (2004) 'Biomedical applications of synchrotron radiation circular dichroism spectroscopy: Identification of mutant proteins associated with disease and development of a reference database for fold motifs', *Faraday Discussions*. The Royal Society of Chemistry, 126(1), pp. 237–243. doi: 10.1039/b306055c.

Walsh, G. (2010) 'Biopharmaceutical benchmarks 2010', *Nature Biotechnology*, 28(9), pp. 917–924. doi: 10.1038/nbt0910-917.

Walters H., R., Bhatnagar, B., Tchessalov, S., Iztutsu, K.-I., Tsumoto, K. and Ohtake, S. (2014) 'Next-Generation Drying Technologies for Pharmaceutical Applications', *Journal of pharmaceutical sciences*, 44(1), pp. 91–93. doi: 10.1002/jps.23998.

Wang, C., Zhong, X., Ruffner, D. B., Stutt, A., Philips, L. A., Ward, M. D. and Grier, D. G. (2016) 'Holographic Characterization of Protein Aggregates', *Journal of Pharmaceutical Sciences*. Elsevier B.V., 105(3), pp. 1074–1085. doi: 10.1016/j.xphs.2015.12.018.

Wang, D. Q., Hey, J. M. and Nail, S. L. (2004) 'Effect of Collapse on the Stability of Freeze-Dried Recombinant Factor VIII and α-Amylase', *Journal of Pharmaceutical Sciences*. John Wiley and Sons Inc., 93(5), pp. 1253–1263. doi: 10.1002/jps.20065.

Wang, W. (1999) 'Instability, stabilization, and formulation of liquid protein pharmaceuticals', *International Journal of Pharmaceutics*. Elsevier, pp. 129–188. doi: 10.1016/S0378-5173(99)00152-0.

Wang, W. (2000) 'Lyophilization and development of solid protein pharmaceuticals', *International Journal of Pharmaceutics*. doi: 10.1016/S0378-5173(00)00423-3.

Wang, W., Nema, S. and Teagarden, D. (2010) 'Protein aggregation-Pathways and influencing factors', *International Journal of Pharmaceutics*, pp. 89–99. doi: 10.1016/j.ijpharm.2010.02.025.

Wang, W. and Roberts, C. J. (2010) *Aggregation of Therapeutic Proteins*, *Aggregation of Therapeutic Proteins*. Edited by W. Wang and C. J. Roberts. Hoboken, NJ, USA: John Wiley and Sons. doi: 10.1002/9780470769829.

Wang, W. and Roberts, C. J. (2018) 'Protein aggregation – Mechanisms, detection, and control', *International Journal of Pharmaceutics*, 550(1–2), pp. 251–268. doi: 10.1016/j.ijpharm.2018.08.043.

Wang, W., Singh, S., Zeng, D. L., King, K. and Nema, S. (2007) 'Antibody Structure, Instability, and Formulation', *Journal of Pharmaceutical Sciences*. John Wiley and Sons Inc., 96(1), pp. 1–26. doi: 10.1002/jps.20727.

Wang, X., Esquerre, C., Downey, G., Henihan, L., O'Callaghan, D. and O'Donnell, C. (2018) 'Assessment of infant formula quality and composition using Vis-NIR, MIR and Raman process analytical technologies', *Talanta*. Elsevier B.V., 183, pp. 320–328. doi: 10.1016/j.talanta.2018.02.080.

Wang, Y., Kho, K., Cheow, W. S. and Hadinoto, K. (2012) 'A comparison between spray drying and spray freeze drying for dry powder inhaler formulation of drug-loaded lipid–polymer hybrid nanoparticles', *International Journal of Pharmaceutics*. Elsevier, 424(1–2), pp. 98–106. doi: 10.1016/J.IJPHARM.2011.12.045.

Wanning, S., Süverkrüp, R. and Lamprecht, A. (2015) 'Pharmaceutical spray freeze drying', *International Journal of Pharmaceutics*. doi: 10.1016/j.ijpharm.2015.04.053.

Waters, P. (1993) *Procedure for Salvage of Water Damaged Library Materials*. Available at: https://www.archives.gov/preservation/conservation/library-materials-01.html (Accessed: 7 March 2018).

Weers, J. and Tarara, T. (2014) 'The PulmoSphere™ platform for pulmonary drug delivery', *Therapeutic Delivery*. Future Science Ltd London, UK, 5(3), pp. 277–295. doi: 10.4155/tde.14.3.

Wei, Y., Wang, C., Jiang, B., Sun, C. C. and Middaugh, C. R. (2019) 'Developing Biologics Tablets: The Effects of Compression on the Structure and Stability of Bovine Serum Albumin and Lysozyme', *Molecular Pharmaceutics*. American Chemical Society, 16(3), pp. 1119–1131. doi: 10.1021/acs.molpharmaceut.8b01118.

Weinbuch, D., Cheung, J. K., Ketelaars, J., Filipe, V., Hawe, A., Den Engelsman, J. and Jiskoot, W. (2015) 'Nanoparticulate impurities in pharmaceutical-grade sugars and their interference with light scattering-based analysis of protein formulations', *Pharmaceutical Research*. Springer New York LLC, 32(7), pp. 2419–2427. doi: 10.1007/s11095-015-1634-1.

Van Der Wel, P. G. (2012) 'Stirred freeze drying'. European Patent Office.

Weng, L., Vijayaraghavan, R., MacFarlane, D. R. and Elliott, G. D. (2014) 'Application of the Kwei equation to model the Tg behavior of binary blends of sugars and salts', *Cryobiology*.

Academic Press, 68(1), pp. 155–158. doi: 10.1016/j.cryobiol.2013.12.005.

Werly, E. F. and Bauman, E. K. (1964) 'Production of Submicronic Powder by Spray-Freezing', *Archives of Environmental Health: An International Journal*. Taylor & Francis Group , 9(5), pp. 567–571. doi: 10.1080/00039896.1964.10663881.

Whitaker, J. R. and Tannenbaum, S. R. (1977) 'Food proteins.', *Food proteins.* AVI Publishing Co. Inc.

White, S., Bennett, D. B., Cheu, S., Conley, P. W., Guzek, D. B., Gray, S., Howard, J., Malcolmson, R., Parker, J. M., Roberts, P., *et al.* (2005) 'EXUBERA®: Pharmaceutical Development of a Novel Product for Pulmonary Delivery of Insulin', *Diabetes Technology & Therapeutics*. Mary Ann Liebert, Inc. 2 Madison Avenue Larchmont, NY 10538 USA , 7(6), pp. 896–906. doi: 10.1089/dia.2005.7.896.

Whitmore, L. and Wallace, B. A. (2004) 'DICHROWEB, an online server for protein secondary structure analyses from circular dichroism spectroscopic data'. doi: 10.1093/nar/gkh371.

Whitmore, L. and Wallace, B. A. (2007) 'Protein Secondary Structure Analyses from Circular Dichroism Spectroscopy: Methods and Reference Databases'. doi: 10.1002/bip.20853.

Wien, F., Geinguenaud, F., Grange, W. and Arluison, V. (2021) 'SRCD and FTIR Spectroscopies to Monitor Protein-Induced Nucleic Acid Remodeling', in *Methods in Molecular Biology*. Humana Press Inc., pp. 87–108. doi: 10.1007/978-1-0716-0935-4_6.

Williams, N. A., Lee, Y., Polli, G. P. and Jennings, T. A. (1986) 'The effects of cooling rate on solid phase transitions and associated vial breakage occurring in frozen mannitol solutions.', *Journal of parenteral science and technology : a publication of the Parenteral Drug Association*. Parenteral Drug Association (PDA), 40(4), pp. 135–41. Available at: http://www.ncbi.nlm.nih.gov/pubmed/3095527 (Accessed: 6 March 2020).

Wilson, E. M., Luft, J. C. and DeSimone, J. M. (2018) 'Formulation of High-Performance Dry Powder Aerosols for Pulmonary Protein Delivery', *Pharmaceutical Research*. Springer New York LLC, 35(10), pp. 1–11. doi: 10.1007/s11095-018-2452-z.

Wilson, N. E., Topp, E. M. and Zhou, Q. T. (2019) 'Effects of drying method and excipient on structure and stability of protein solids using solid-state hydrogen/deuterium exchange mass spectrometry (ssHDX-MS)', *International Journal of Pharmaceutics*. Elsevier B.V., 567. doi: 10.1016/j.ijpharm.2019.118470.

Wisniewski, R. (2015) 'Spray Drying Technology Review', in *45th International Conference on Environmental Systems*. Washington, pp. 1–223.

Wittaya-Areekul, S., Needham, G. F., Milton, N., Roy, M. L. and Nail, S. L. (2002) 'Freeze-drying of tert-butanol/water cosolvent systems: A case report on formation of a friable freeze-dried powder of tobramycin sulfate', *Journal of Pharmaceutical Sciences*. Elsevier, 91(4), pp. 1147–1155. doi: 10.1002/jps.10113.

Woody, R. W. (1995) 'Circular Dichroism', *Methods in Enzymology*. Academic Press, 246(C), pp. 34–71. doi: 10.1016/0076-6879(95)46006-3.

Wu, C., Shamblin, S., Varshney, D. and Shalaev, E. (2015) 'Advance Understanding of Buffer Behavior during Lyophilization', in *Lyophilized Biologics and Vaccines*. Springer New York, pp. 25–41. doi: 10.1007/978-1-4939-2383-0_3.

Wu, J., Wu, L., Wan, F., Rantanen, J., Cun, D. and Yang, M. (2019) 'Effect of thermal and shear stresses in the spray drying process on the stability of siRNA dry powders', *International Journal of Pharmaceutics*. Elsevier B.V., 566, pp. 32–39. doi: 10.1016/j.ijpharm.2019.05.019.

Wu, L., Zhao, W., Yang, R. and Yan, W. (2015) 'Pulsed electric field (PEF)-induced aggregation between lysozyme, ovalbumin and ovotransferrin in multi-protein system', *Food Chemistry*. Elsevier Ltd, 175, pp. 115–120. doi: 10.1016/j.foodchem.2014.11.136.

Xu, J., Wang, J., Luft, J. C., Tian, S., Owens, G., Pandya, A. A., Berglund, P., Pohlhaus, P., Maynor, B. W., Smith, J., *et al.* (2012) 'Rendering protein-based particles transiently insoluble for therapeutic applications', *Journal of the American Chemical Society*, 134(21), pp. 8774–8777. doi: 10.1021/ja302363r.

Xu, J., Wong, D. H. C., Byrne, J. D., Chen, K., Bowerman, C. and DeSimone, J. M. (2013) 'Future of the Particle Replication in Nonwetting Templates (PRINT) Technology', *Angewandte Chemie International Edition*. John Wiley & Sons, Ltd, 52(26), pp. 6580–6589. doi: 10.1002/anie.201209145.

Yamaguchi, K. I., Kamatari, Y. O., Fukuoka, M., Miyaji, R. and Kuwata, K. (2013) 'Nearly reversible conformational change of amyloid fibrils as revealed by ph-jump experiments', *Biochemistry*. American Chemical Society, 52(39), pp. 6797–6806. doi: 10.1021/bi400698u.

Yang, H., Yang, S., Kong, J., Dong, A. and Yu, S. (2015) 'Obtaining information about protein secondary structures in aqueous solution using Fourier transform IR spectroscopy', *Nature Protocols*. Nature Publishing Group, 10(3), pp. 382–396. doi: 10.1038/nprot.2015.024.

Ye, P. and Byron, T. (2008) 'Characterization of d-mannitol by thermal analysis, FTIR, and raman spectroscopy', *American Laboratory*.

Ying, D., Sun, J., Sanguansri, L., Weerakkody, R. and Augustin, M. A. (2012) 'Enhanced survival of spray-dried microencapsulated Lactobacillus rhamnosus GG in the presence of glucose', *Journal of Food Engineering*. Elsevier, 109(3), pp. 597–602. doi: 10.1016/j.jfoodeng.2011.10.017.

Yoshioka, S., Forney, K. M., Aso, Y. and Pikal, M. J. (2011) 'Effect of sugars on the molecular motion of freeze-dried protein formulations reflected by NMR relaxation times', *Pharmaceutical Research*. Springer, 28(12), pp. 3237–3247. doi: 10.1007/s11095-011-0512-8.

Yu, J., Romeo, M. C., Cavallaro, A. A. and Chan, H. K. (2018) 'Protective effect of sodium stearate on the moisture-induced deterioration of hygroscopic spray-dried powders', *International Journal of Pharmaceutics*. Elsevier B.V., 541(1–2), pp. 11–18. doi: 10.1016/j.ijpharm.2018.02.018.

Yu, Z., Garcia, A. S., Johnston, K. P. and Williams, R. O. (2004) 'Spray freezing into liquid nitrogen for highly stable protein nanostructured microparticles', *European Journal of Pharmaceutics and Biopharmaceutics*. Elsevier, 58(3), pp. 529–537. doi: 10.1016/J.EJPB.2004.04.018.

Yu, Z., Johnston, K. P. and Williams, R. O. (2006) 'Spray freezing into liquid versus spray-freeze drying: Influence of atomization on protein aggregation and biological activity', *European Journal of Pharmaceutical Sciences*. Elsevier, 27(1), pp. 9–18. doi: 10.1016/j.ejps.2005.08.010.

Zakarian, J. A. and King, C. J. (1982) 'Volatiles loss in the nozzle zone during spray drying of emulsions', *Industrial & Engineering Chemistry Process Design and Development*, 21(1), pp. 107–113. doi: 10.1021/i200016a019.

Zawaira, A., Pooran, A., Barichievy, S. and Chopera, D. (2012) 'A Discussion of Molecular Biology Methods for Protein Engineering', *Molecular Biotechnology*. Humana Press Inc, 51(1), pp. 67–102. doi: 10.1007/s12033-011-9448-9.

Zeng, X. M., Martin, G. P. and Marriott, C. (2001) 'Effects of molecular weight of

polyvinylpyrrolidone on the glass transition and crystallization of co-lyophilized sucrose', *International Journal of Pharmaceutics*. doi: 10.1016/S0378-5173(01)00613-5.

Zhang, A., Qi, W., Singh, S. K. and Fernandez, E. J. (2011) 'A new approach to explore the impact of freeze-thaw cycling on protein structure: Hydrogen/deuterium exchange mass spectrometry (HX-MS)', *Pharmaceutical Research*. Springer, 28(5), pp. 1179–1193. doi: 10.1007/s11095-011-0383-z.

Zhang, A., Singh, S. K., Shirts, M. R., Kumar, S. and Fernandez, E. J. (2012) 'Distinct aggregation mechanisms of monoclonal antibody under thermal and freeze-thaw stresses revealed by hydrogen exchange', *Pharmaceutical Research*. Springer, 29(1), pp. 236–250. doi: 10.1007/s11095-011-0538-y.

Zhang, Y. and Cremer, P. S. (2009) 'The inverse and direct Hofmeister series for lysozyme', *Proceedings of the National Academy of Sciences of the United States of America*. National Academy of Sciences, 106(36), pp. 15249–15253. doi: 10.1073/pnas.0907616106.

Zhang, Y., Farrell, E., Mankiewicz, D. and Weiner, Z. (2020) *Study of Protein Hydrodynamics with Light Scatter-ing: Size and Charge of Lysozyme*.

Zhang, Z. and Smith, D. L. (1993) 'Determination of amide hydrogen exchange by mass spectrometry: A new tool for protein structure elucidation', *Protein Science*. John Wiley & Sons, Ltd, 2(4), pp. 522–531. doi: 10.1002/pro.5560020404.

Zhao, Z., Huang, Z., Zhang, X., Huang, Y., Cui, Y., Ma, C., Wang, G., Freeman, T., Lu, X. yun, Pan, X., *et al.* (2018) 'Low density, good flowability cyclodextrin-raffinose binary carrier for dry powder inhaler: anti-hygroscopicity and aerosolization performance enhancement', *Expert Opinion on Drug Delivery*. Taylor and Francis Ltd, 15(5), pp. 443–457. doi: 10.1080/17425247.2018.1450865.

Zhu, S., Ma, L., Wang, S., Chen, C., Zhang, W., Yang, L., Hang, W., Nolan, J. P., Wu, L. and Yan, X. (2014) 'Light-Scattering Detection below the Level of Single Fluorescent Molecules for High-Resolution Characterization of Functional Nanoparticles'. doi: 10.1021/nn505162u.

Ziaee, A., Albadarin, A. B., Padrela, L., Femmer, T., O'Reilly, E. and Walker, G. (2019) 'Spray drying of pharmaceuticals and biopharmaceuticals: Critical parameters and experimental process optimization approaches', *European Journal of Pharmaceutical Sciences*. Elsevier B.V., pp. 300–318. doi: 10.1016/j.ejps.2018.10.026.

Ziaee, A., Albadarin, A. B., Padrela, L., Ung, M.-T., Femmer, T., Walker, G. and O'Reilly, E. (2020) 'A rational approach towards spray drying of biopharmaceuticals: The case of lysozyme', *Powder Technology*, 366, pp. 206–215. doi: 10.1016/j.powtec.2020.02.057.

Zillen, D., Beugeling, M., Hinrichs, W. L. J., Frijlink, H. W. and Grasmeijer, F. (2021) 'Natural and bioinspired excipients for dry powder inhalation formulations', *Current Opinion in Colloid & Interface Science*. Elsevier, 56, p. 101497. doi: 10.1016/J.COCIS.2021.101497.

Zölls, S., Tantipolphan, R., Wiggenhorn, M., Winter, G., Jiskoot, W., Friess, W. and Hawe, A. (2012) 'Particles in Therapeutic Protein Formulations, Part 1: Overview of Analytical Methods', *Journal of Pharmaceutical Sciences*. Elsevier, 101(3), pp. 914–935. doi: 10.1002/JPS.23001.

Appendix

Supplementary Information for Chapter 2

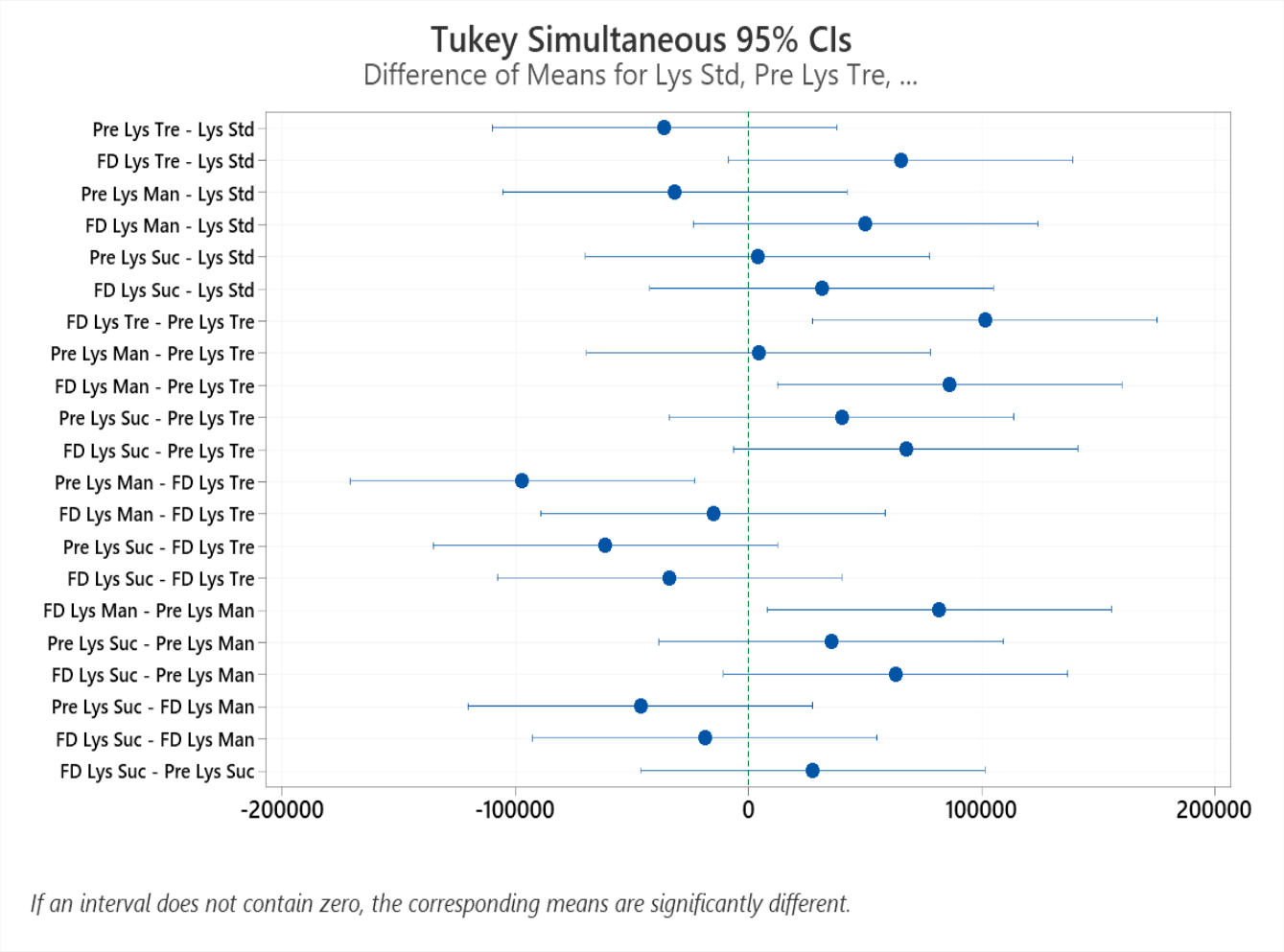

Figure A2.1: Statistical significance for the bioactivity of pre-dried and freeze-dried lysozyme formulations using one-way ANOVA – Tukey's post-hoc test (n = 3).

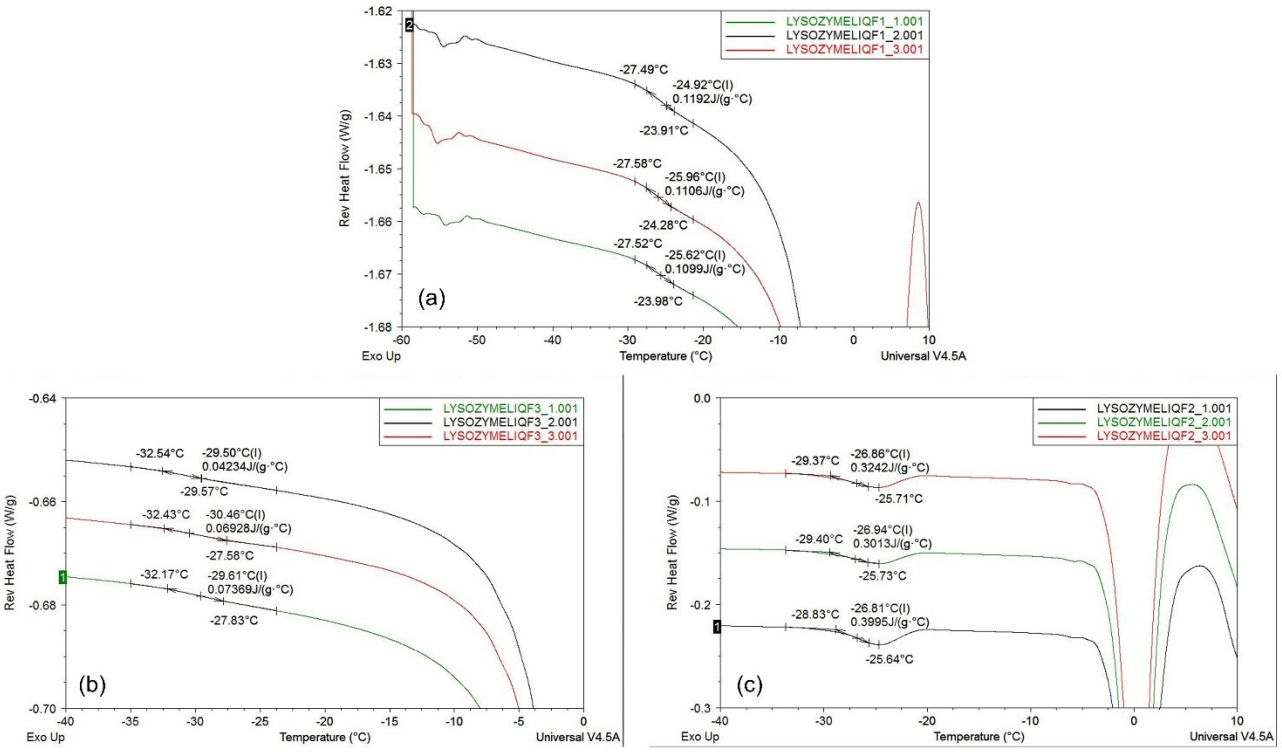

Figure A2.2: Frozen-state DSC thermograms of (a) lysozyme trehalose, (b) lysozyme mannitol, (c) lysozyme sucrose.

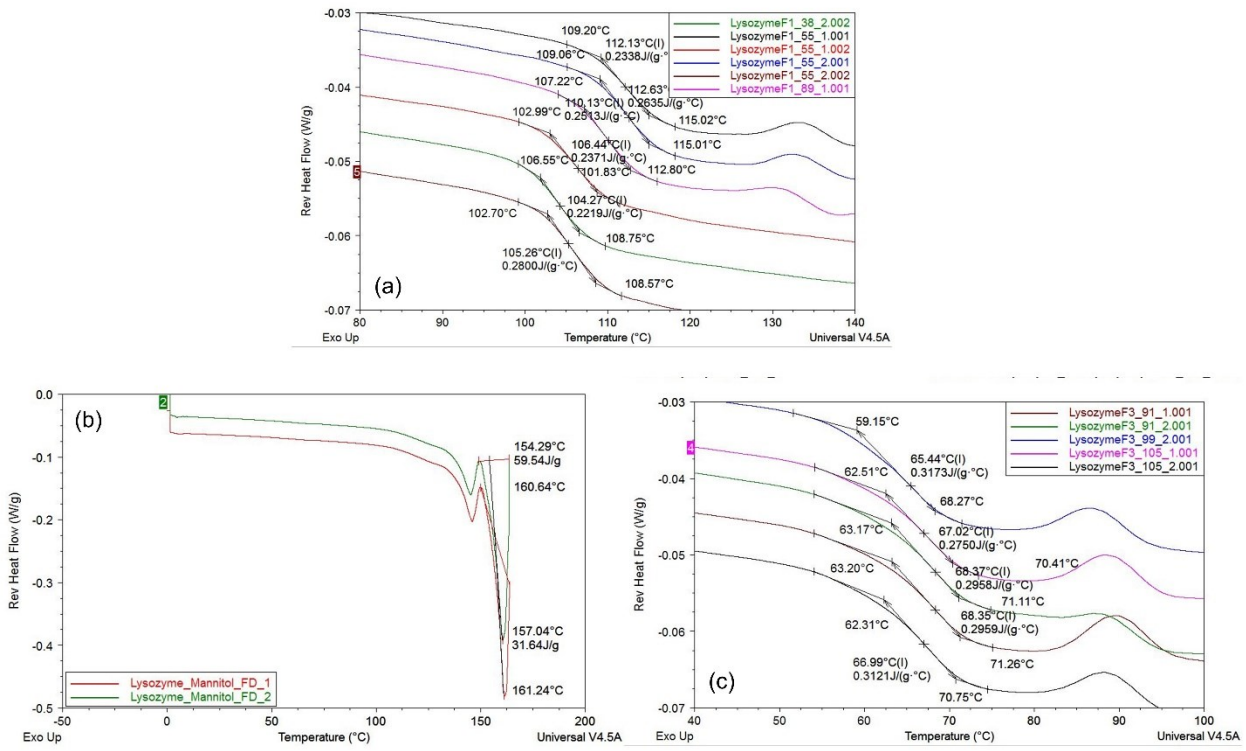

Figure A2.3: DSC thermograms of (a) freeze-dried lysozyme trehalose, (b) freeze-dried lysozyme mannitol, (c) freeze-dried lysozyme sucrose.

Supplementary Information for Chapter 3

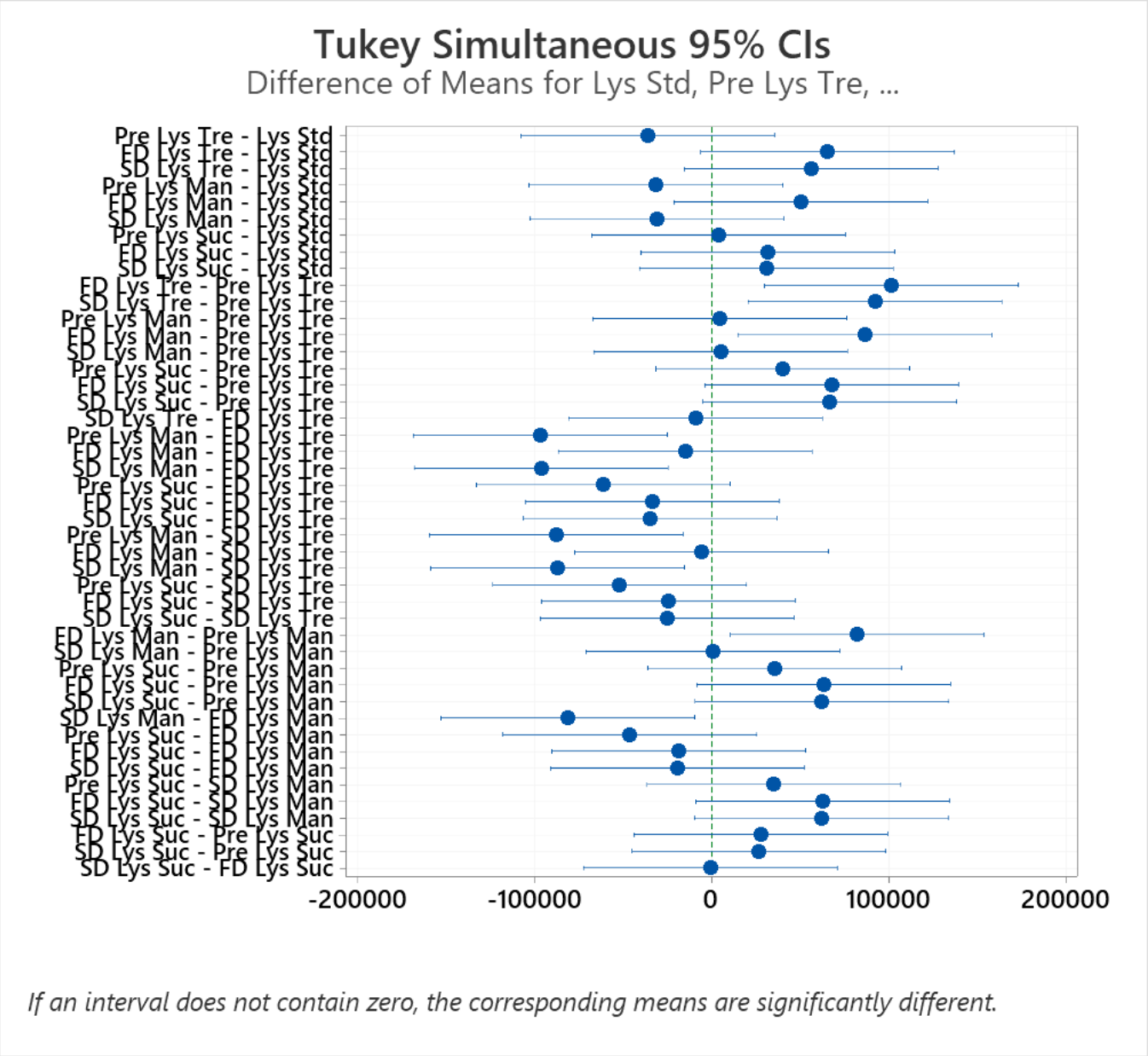

Figure A3.1: Statistical significance for the bioactivity of pre-dried, freeze-dried and spray-dried lysozyme formulations using one-way ANOVA – Tukey's post-hoc test (n = 3).

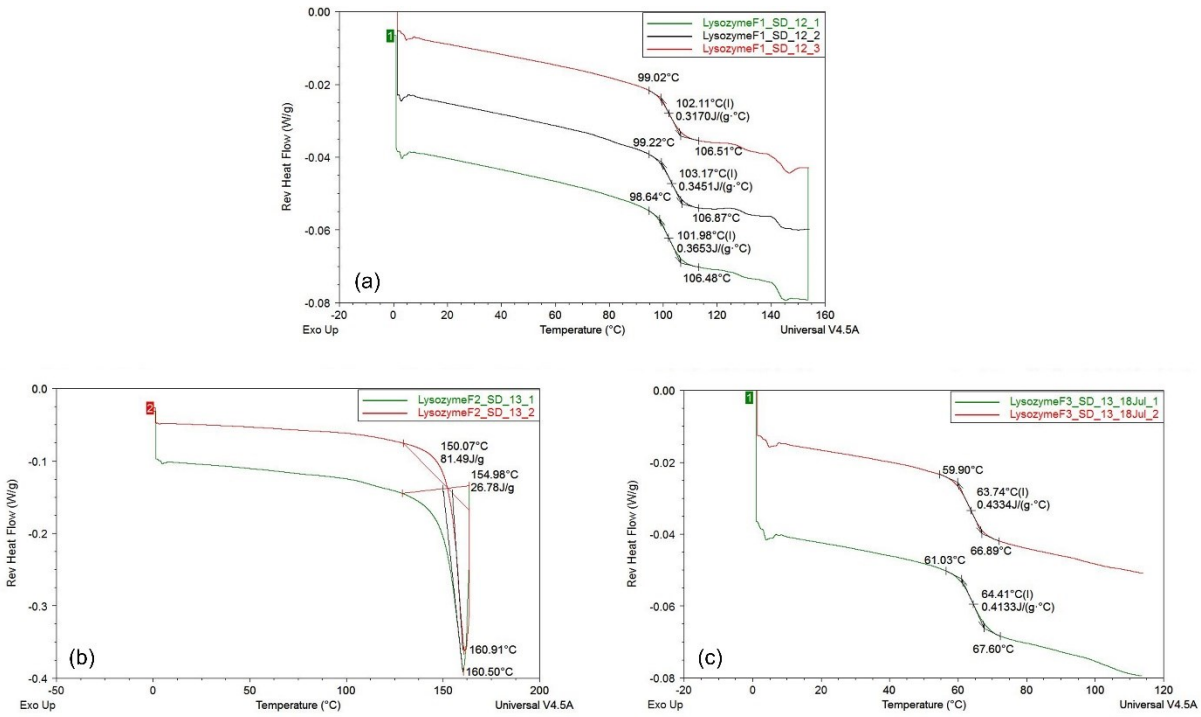

Figure A3.2: DSC thermograms: (a) spray-dried lysozyme trehalose, (b) spray-dried lysozyme mannitol, (c) spray-dried lysozyme sucrose.

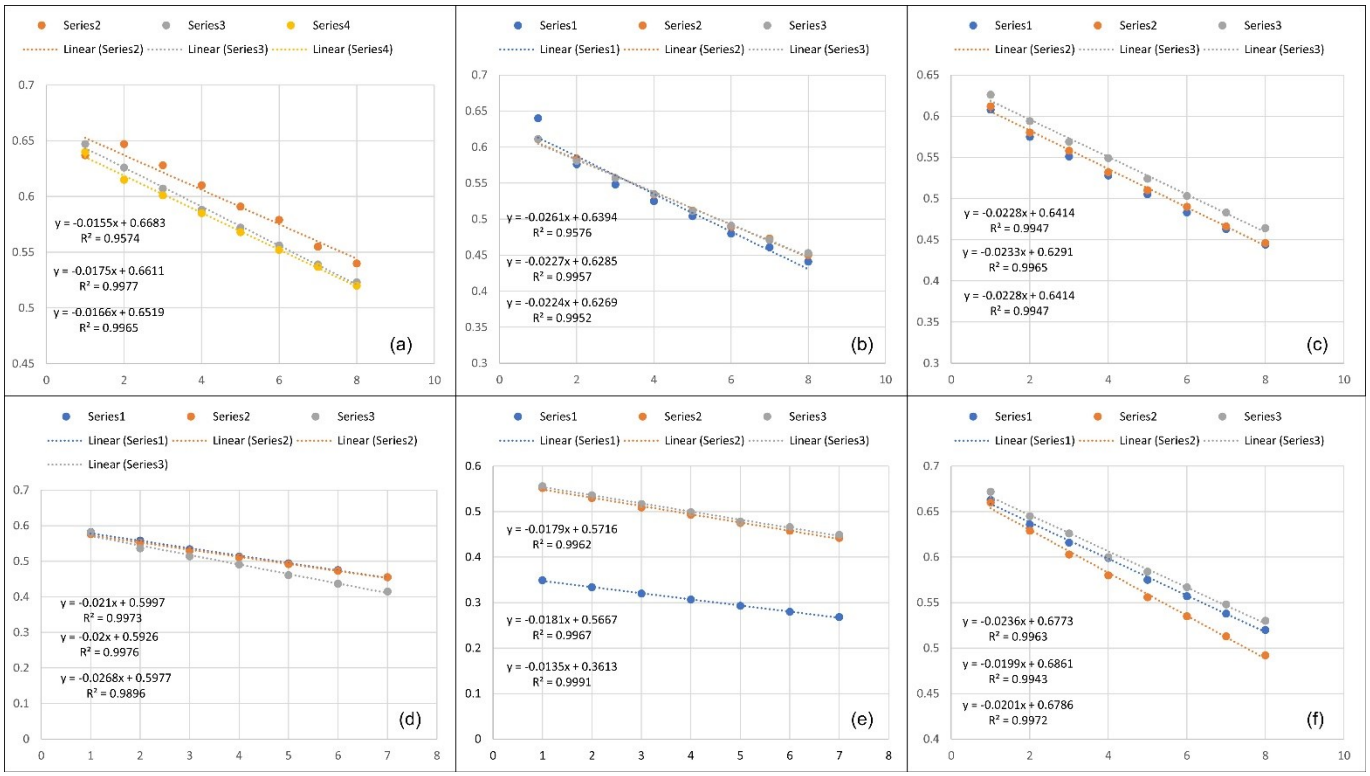

Figure A3.3: Enzyme activity of lysozyme as a function of decrease in absorbance at 450 nm: (a) control, (b) freeze-dried lysozyme trehalose, (c) spray-dried lysozyme trehalose, (d) freeze-dried lysozyme mannitol, (e) spray-dried lysozyme mannitol, (f) freeze-dried lysozyme sucrose. X-axis represents time in min and Y-axis represents absorbance at 450 nm.

Supplementary Information for Chapter 4

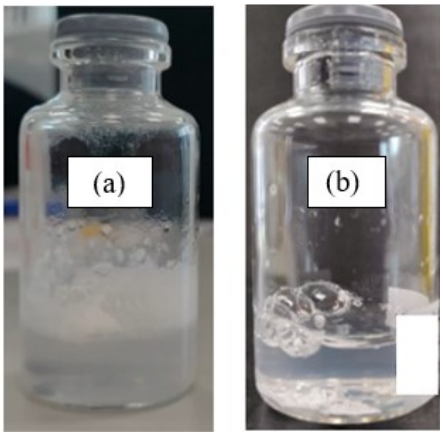

Figure A4.1: Rehydration behaviour of (a) Active-freeze-dried and (b) Spray-dried Enzyme 'A'.

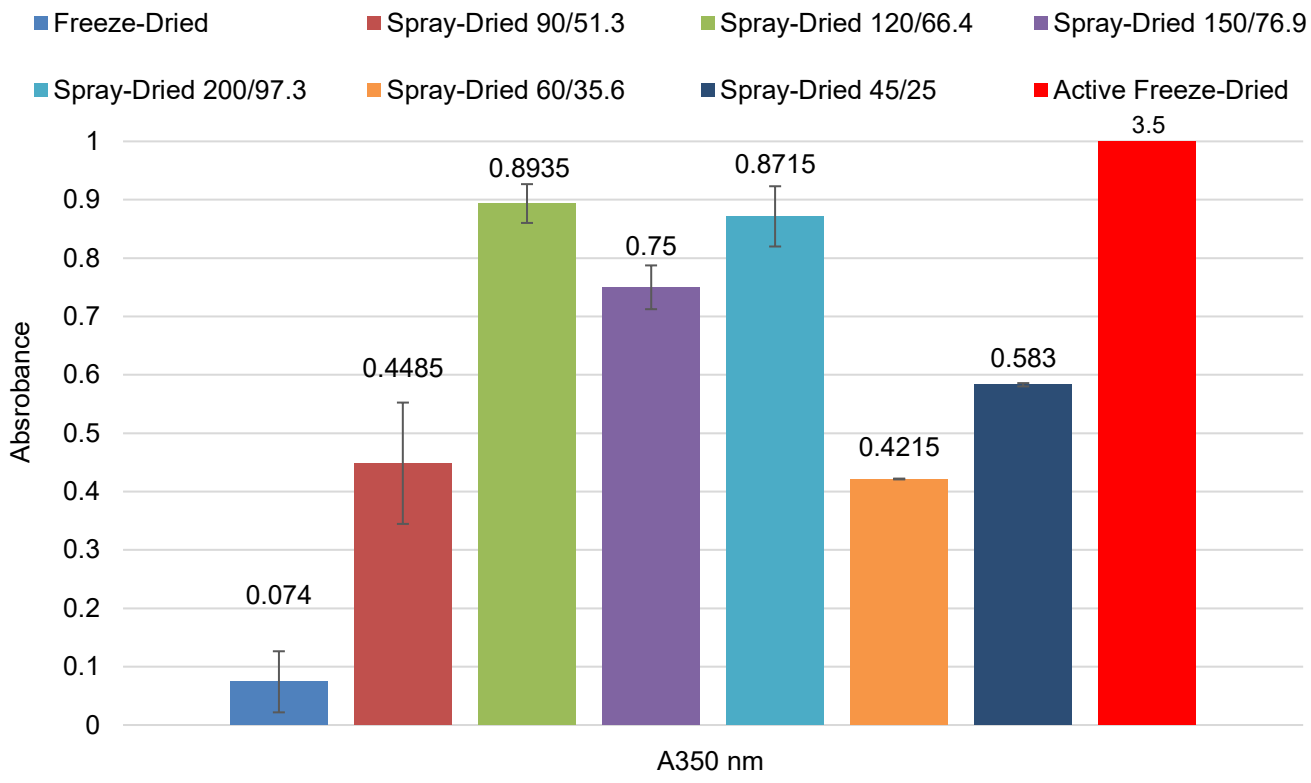

Figure A4.2: Optical Density of reconstituted Freeze-dried, Active-freeze-dried and Spray-dried Enzyme 'A' at 350 nm. The Spray-dried values are represented as Inlet/Outlet temperatures.

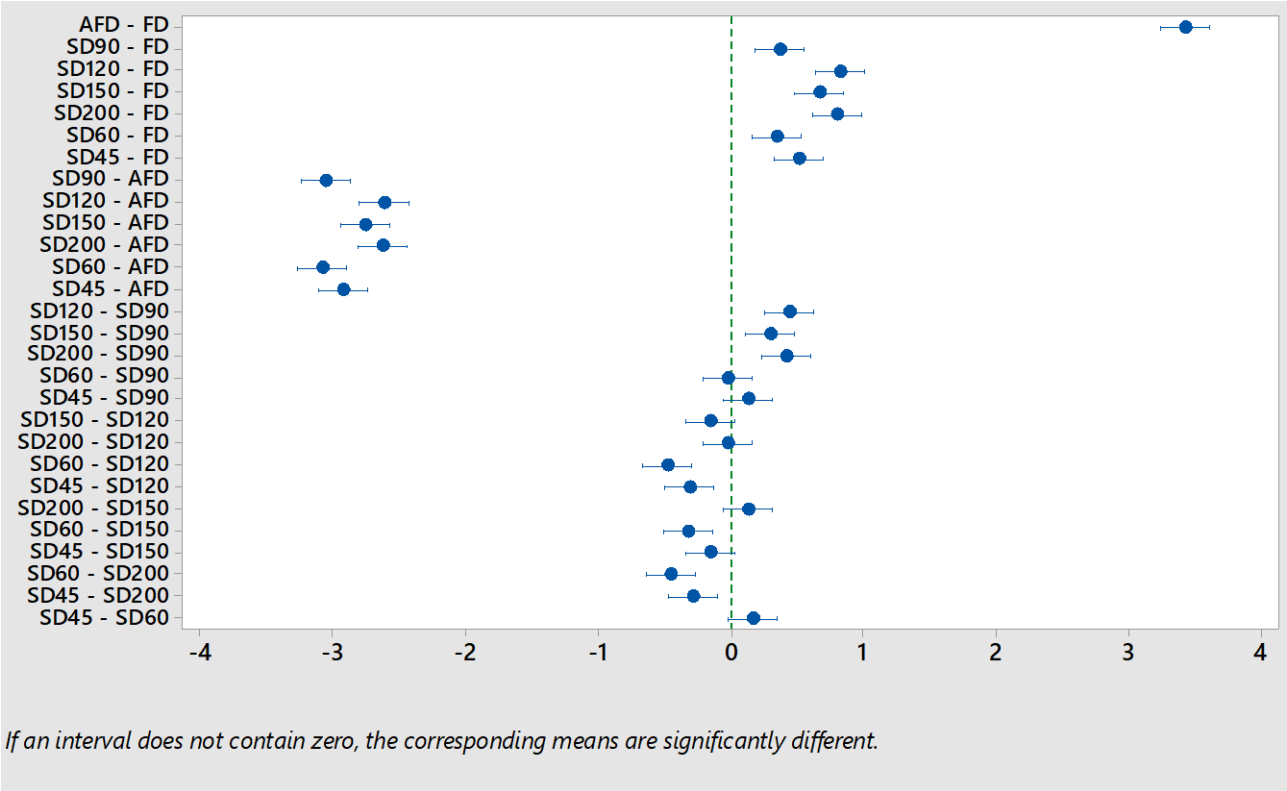

Figure A4.3: Statistical significance for differences in the turbidity of rehydrated Freeze-dried, Active-freeze-dried and Spray-dried Enzyme 'A'. The x-axis represents the confidence interval.

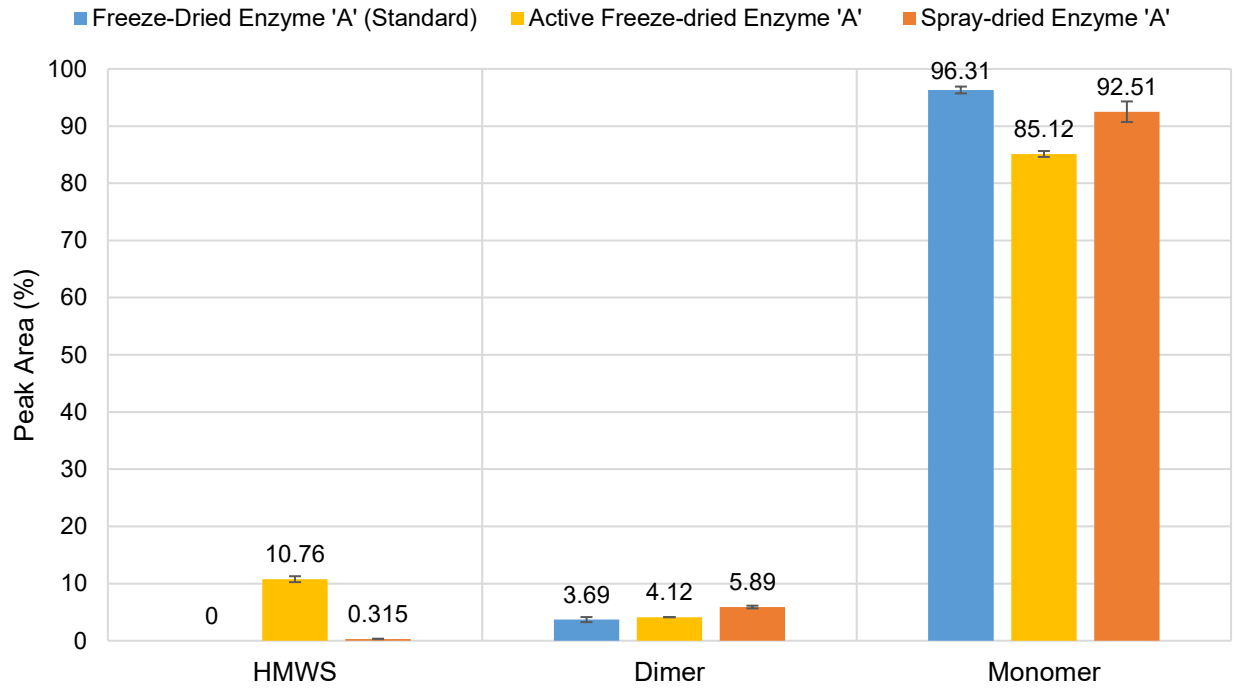

Figure A4.4: Aggregation profile of Freeze-dried, Active-freeze-fried and Spray-dried Enzyme 'A' represented as monomers, dimers and high molecular weight species (HMWS).

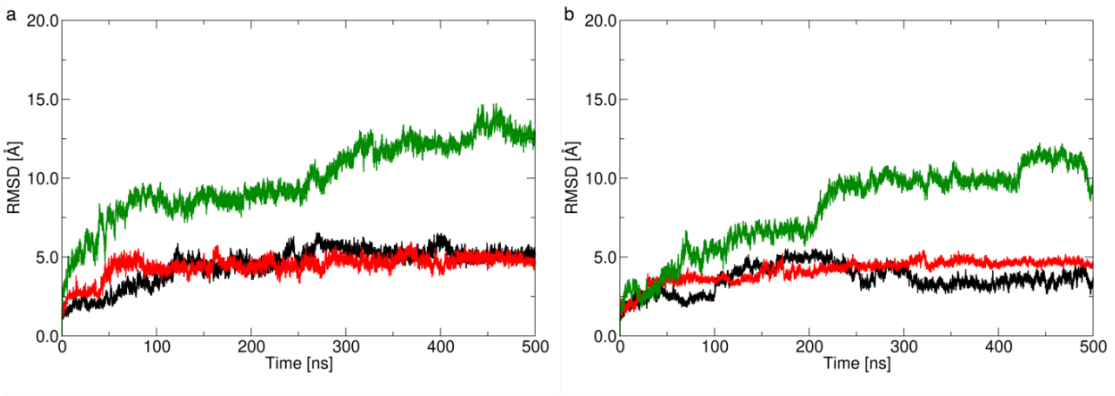

Figure A4.5: RMSD of Enzyme 'A' in 1X concentration (left) and 10X concentration (right) at 300K (black), 340K (red) and 380K (green).

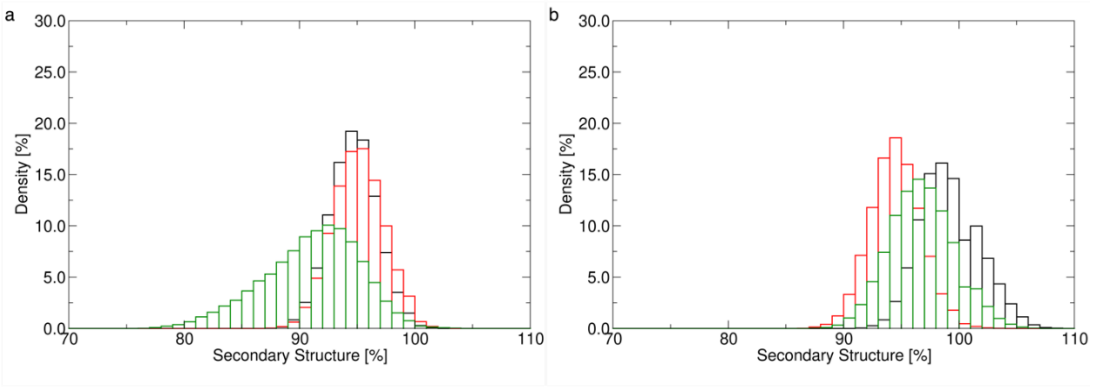

Figure A4.6: Secondary structure prediction of Enzyme 'A' for 1X concentration (left) and 10X concentration (right) of Enzyme 'A' at 300K (black), 340K (red) and 380K (green).

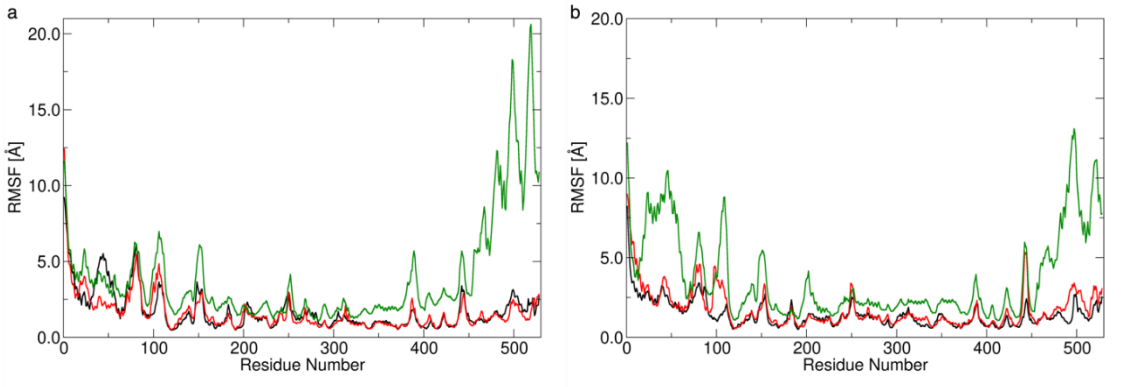

Figure A4.7: Root mean-square fluctuations of Enzyme 'A' for 1X concentration (left) and 10X concentration (right) of Enzyme 'A' at 300K (black), 340K (red) and 380K (green).

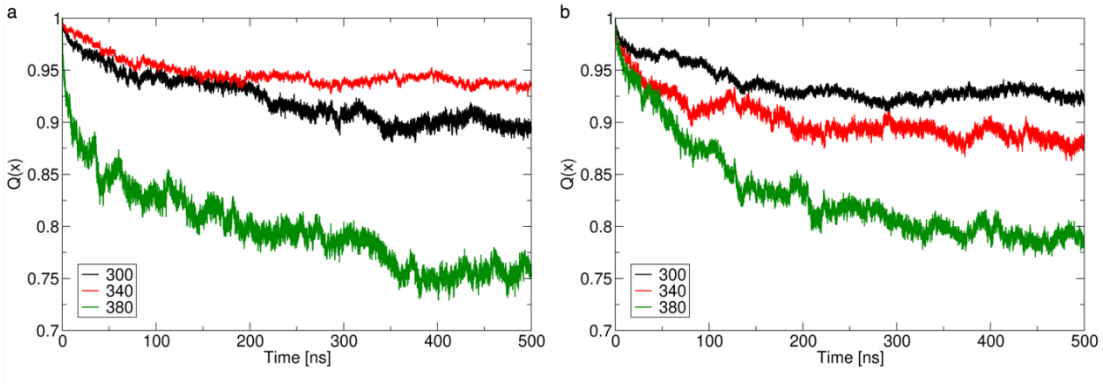

Figure A4.8: Fraction of native contacts of Enzyme 'A' for 1X concentration (left) and 10X concentration (right) of Enzyme 'A' at 300K (black), 340K (red) and 380K (green).

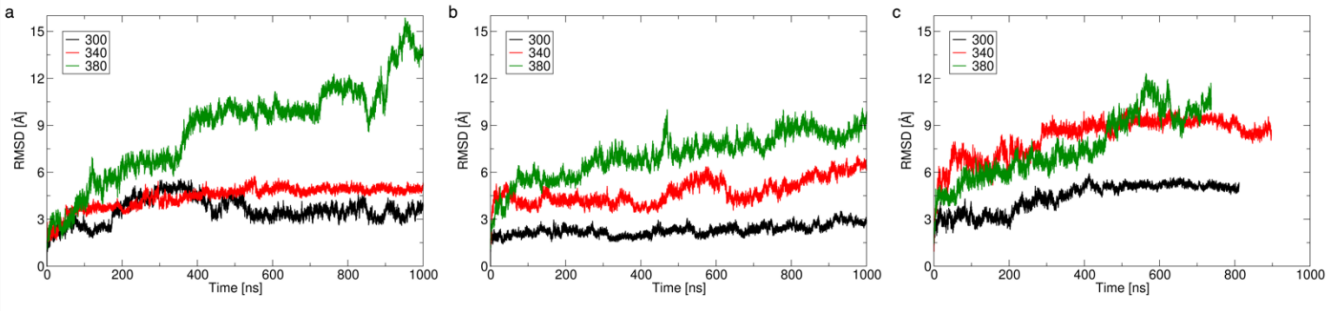

Figure A4.9: Plot of the RMSD of Enzyme 'A' with 10x concentration of (a) Sucrose, (b) Sucrose/Arg-HCl and (c) Sucrose/Trehalose.

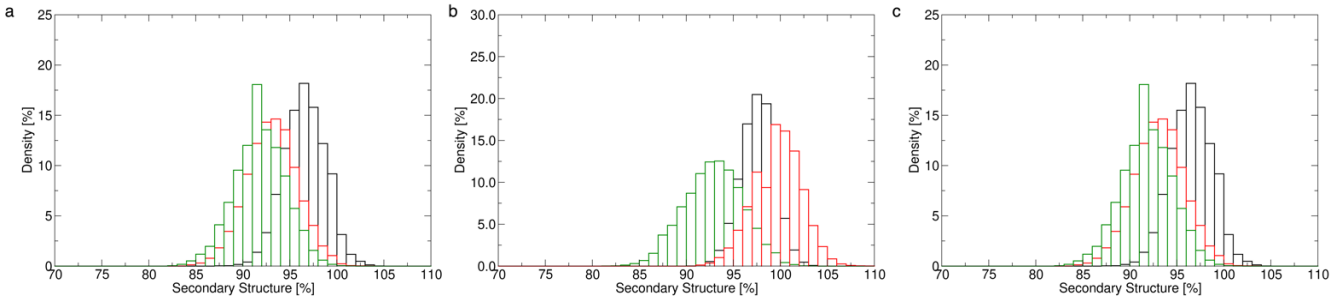

Figure A4.10: Plot of the secondary structure distribution of Enzyme 'A' with 10x concentration of (a) sucrose, (b) sucrose/Arg-HCl and (c) sucrose/trehalose.

Supplementary Information for Chapter 5

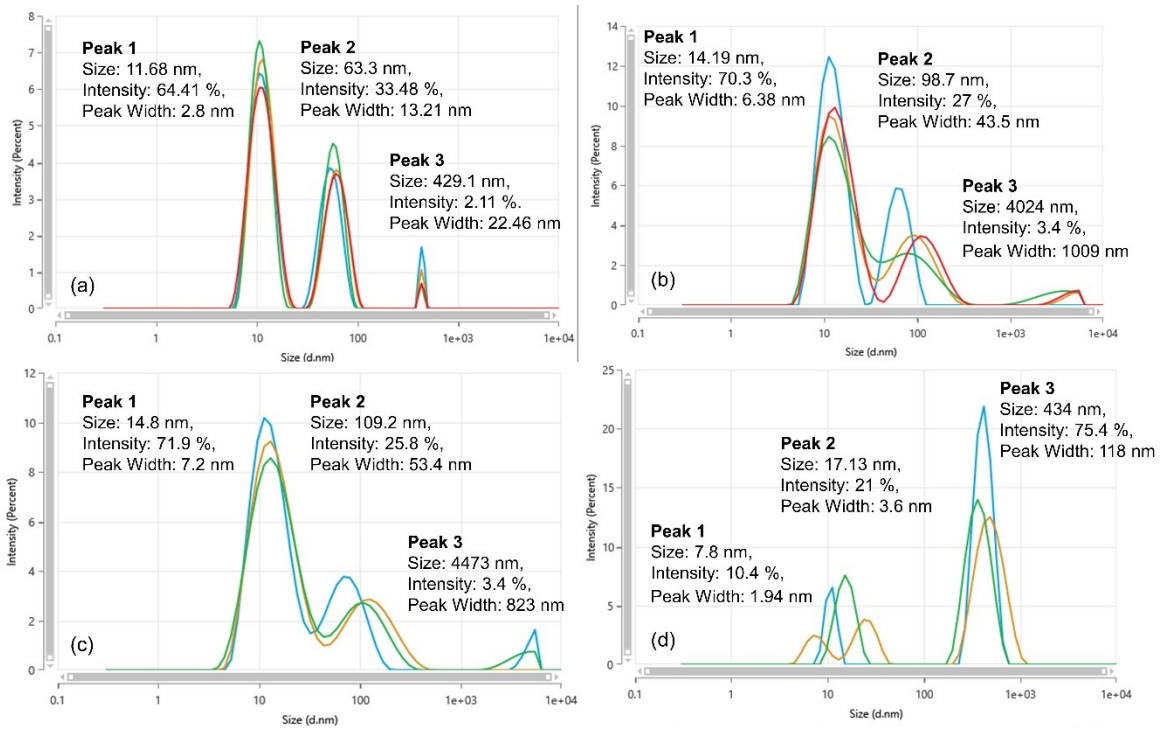

Figure A5.1: (a) MADLS, (b) Back Scatter, (c) Side Scatter and (d) Forward scatter measurements of the enzyme.